PB-239 869

AN EXPERIMENTAL HIGH ASH PAPERMILL SLUDGE LANDFILL

MICHIGAN STATE UNIVERSITY

PREPARED FOR
NATIONAL ENVIRONMENTAL RESEARCH CENTER

DECEMBER 1974

DISTRIBUTED BY:
NTIS
National Technical Information Service
U. S. DEPARTMENT OF COMMERCE

TECHNICAL REPORT DATA
(Please read Instructions on the reverse before completing)

1. REPORT NO. EPA-670/2-74-076a	2.	3. PB 239 869
4. TITLE AND SUBTITLE AN EXPERIMENTAL HIGH ASH PAPERMILL SLUDGE LANDFILL: First Annual Report		5. REPORT DATE December 1974-Issuing Dat 6. PERFORMING ORGANIZATION CODE
7. AUTHOR(S) O. B. Andersland, Robert P. Vallee, and Timothy A. Armstrong		8. PERFORMING ORGANIZATION REPORT NO.
9. PERFORMING ORGANIZATION NAME AND ADDRESS Division of Engineering Research Michigan State University East Lansing, Michigan 48824		10. PROGRAM ELEMENT NO. 1DB064 ROAP 24ALH Task 02 11. CONTRACT/GRANT NO. R-801282
12. SPONSORING AGENCY NAME AND ADDRESS National Environmental Research Center Office of Research and Development U.S. Environmental Protection Agency Cincinnati, Ohio 45268		13. TYPE OF REPORT AND PERIOD COVERED First Annual Report 14. SPONSORING AGENCY CODE

15. SUPPLEMENTARY NOTES

See "AN EXPERIMENTAL HIGH ASH PAPERMILL SLUDGE LANDFILL: Second Annual Report," EPA-670/2-74-076b.

16. ABSTRACT

An experimental papermill sludge landfill was constructed and monitored to obtain engineering information essential to the development of guidelines and recommendations for the design and operation of solid papermill waste landfills. The experimental landfill consisted of two sludge layers, with sand drainage blankets, an earth dike for lateral confinement and a natural soil cover. The landfill was instrumented for settlement, water pressure, vertical and lateral earth pressure, temperature, sludge unit weights, specific gravity, and water contents. Laboratory work was also conducted. A detailed description of the field behavior is given in the report along with predictions based on laboratory results and soil mechanics theory. Sampling of leachate from the sludge landfill at weekly intervals and laboratory analysis according to standard methods for the examination of water and waste water provided documentation as to leachate composition. A lysimeter study provides information on changes in quality of the leachate when passed through selected natural soils.

Reproduced by
NATIONAL TECHNICAL
INFORMATION SERVICE
US Department of Commerce
Springfield, VA. 22151

17. KEY WORDS AND DOCUMENT ANALYSIS

a. DESCRIPTORS	b. IDENTIFIERS/OPEN ENDED TERMS	c. COSATI Field/Group
Lysimeters Sludge Leaching Papermills Soils Soil mechanics	Sludge landfill Solid waste management Landfill	13B

PRICES SUBJECT TO CHANGE

18. DISTRIBUTION STATEMENT Released to public	19. SECURITY CLASS *(This Report)* Unclassified	21. NO. OF PAGES 200
	20. SECURITY CLASS *(This page)* Unclassified	22. PRICE 7.00 - 2.25

EPA Form 2220-1 (9-73)

REVIEW NOTICE

The National Environmental Research Center--Cincinnati has reviewed this report and approved its publication. Approval does not signify that the contents necessarily reflect the views and policies of the U.S. Environmental Protection Agency, nor does mention of trade names or commercial products constitute endorsement or recommendation for use.

FOREWORD

Man and his environment must be protected from the adverse effects of pesticides, radiation, noise and other forms of pollution, and the unwise management of solid waste. Efforts to protect the environment require a focus that recognizes the interplay between the components of our physical environment--air, water, and land. The National Environmental Research Centers provide this multidisciplinary focus through programs engaged in

- studies on the effects of environmental contaminants on man and the biosphere, and
- a search for ways to prevent contamination and to recycle valuable resources.

This research work was supported by EPA to obtain engineering information essential to the development of guidelines and recommendations for the design and operation of papermill waste landfills.

A. W. Breidenbach, Ph.D.
Director
National Environmental
Research Center, Cincinnati

ABSTRACT

An experimental papermill sludge landfill was constructed and monitored to obtain engineering information essential to the development of guidelines and recommendations for the design and operation of solid papermill waste landfills. The experimental landfill consisted of 2 sludge layers, each initially 10 ft thick, with sand drainage blankets at the top, middle, and bottom. An earth dike provided lateral confinement of the soft sludge both during and after construction. A surface load, consisting of 3 ft of natural soil, was placed immediately after construction. The landfill was instrumented with 32 settlement plates, 16 piezometers, 3 total pressure cells, and 10 thermistors. Field data obtained during the first year included settlements, pore water pressures, vertical and lateral earth pressures, temperature, sludge unit weights, specific gravity, and water contents. Laboratory work included consistency limits, ash contents, and consolidation tests. A detailed description of the field behavior is given in the report along with predictions based on laboratory results and soil mechanics theory. Sampling of leachate from the sludge landfill at weekly intervals and laboratory analysis according to standard methods for the examination of water and wastewater provided documentation as to leachate composition. A lysimeter study provides information on changes in quality of the leachate when passed through selected natural soils.

It is shown that soil mechanics theory can be used to accurately model the sludge consolidation behavior for different conditions of loading. Ultimate primary settlements can be reasonably estimated if appropriate pore pressure changes and void ratio considerations are included in the settlement analysis. Secondary compression is difficult to predict from laboratory parameters. The time-rate of settlement is accurately modeled by Terzaghi's (1943) theory when a representative value for the coefficient of consolidation is used. Laboratory consolidation tests underestimated this parameter by a factor of about four. Consolidation theory can be used to predict pore pressures up to about 70 percent dissipation. Residual pore pressures were observed in the sludge at the completion of primary compression. Pore pressures generated during construction were in general agreement with predicted values based on Gibson's (1958) theory. The coefficient of lateral stress decreased from an initial value close to

0.65 immediately after sludge placement to about 0.32 for the final stages of consolidation. The lysimeter study showed that passage of leachate through a minimal depth of soil should render the percolate innocuous.

PREFACE

This annual report covers phase I of an experimental high ash papermill sludge landfill project. The work described was made possible by Research Grant R-EP00685-01 from the U.S. Environmental Protection Agency, under agreement with Michigan State University.

Robert P. Vallee, research assistant in soil mechanics, was responsible for the supervision of construction at the site, instrumentation, and monitoring of the landfill, and carried out experimental laboratory work in the Soil Mechanics Laboratory of the Department of Civil Engineering at Michigan State University. Timothy A. Armstrong, Research Engineer for the National Council of the Paper Industry for Air and Stream Improvement, Inc., performed the leachate analysis and lysimeter study. Dr. O. B. Andersland, Professor of Civil Engineering, supervised the research and the preparation of this report. The landfill site and dewatered sludge were furnished by the Kimberly Clark Corporation-Morraine Mill, West Carrollton, Ohio. The B. G. Danis Co., Dayton, Ohio, carried out the construction of the landfill.

The opinions, findings and conclusions expressed in this publication are those of the authors and not necessarily those of the U.S. Environmental Protection Agency.

TABLE OF CONTENTS

Page
ABSTRACT iv
PREFACE vi
LIST OF TABLES ix
LIST OF FIGURES xi
LIST OF SYMBOLS xv

Chapter I. INTRODUCTION 1

Need for study 1
Objectives of study 2
Research plan 3

Chapter II. PAPERMILL SLUDGE LANDFILLS-- 5
LITERATURE REVIEW 5

Current practice 5
Settlement 6
Groundwater protection 12

Chapter III. EVALUATION OF SLUDGE ENGINEERING CHARACTERISTICS 15

Physical properties 15
- Water content 15
- Unit weight 16
- Specific gravity 17
- Ash content, organic content 17
- Consistency limits 18

Stress-deformation characteristics 18
- Consolidation behavior 18
- Undrained shear strength 20

Chapter IV. CONSTRUCTION, INSTRUMENTATION AND MONITORING 25

Construction of the experimental landfill 25
- Site preparation and dike construction 25
- Sludge placement 26
- Drainage blanket placement 27
- Earth surcharge placement 28

Instrumentation and monitoring 28
- Settlement plates 28
- Piezometers 29
- Total pressure cells 30
- Temperature sensors 31
- Vane shear tests 31
- Leachate sampling, analysis, and lysimeter study 32

Page
Chapter V. EXPERIMENTAL RESULTS 45

Physical properties of the papermill sludge 45

Stress-deformation behavior of the sludge 45
  Laboratory consolidation 45
  In-place vane shear tests 46

Field monitoring 47
  Settlement 47
  Pore water pressures 48
  Temperature 48
  Lateral sludge pressures 48

Leachate analysis and lysimeter study 49

Chapter VI. DISCUSSION AND INTERPRETATION OF RESULTS 101

Sludge placement 101

Engineering characteristics of the papermill sludge 102
  Physical properties 102
  Consolidation behavior 102
  Undrained shear strength 104
  Stress state in the sludge 105
  Temperature 106

Settlement behavior of the landfill 106
  Upper sludge layer 106
    Loading and field observations 106
    Ultimate settlement 108
    Time-rate of settlement 112
    Pore pressure dissipation 114
  Lower sludge layer 117
    Loading and field observations 117
    Ultimate settlement 118
    Time-rate of settlement 119
    Pore pressure dissipation 121

Leachate analysis and lysimeter study 140

Chapter VII. SUMMARY AND CONCLUSIONS 145

Field consolidation 145
  Settlement 145
  Pore pressures 146
  Stress and temperature conditions 147

Leachate analysis and lysimeter study 147

REFERENCES 149

LIST OF TABLES

Table		Page
5.1	Physical properties of the papermill sludge	51
5.2	Sludge placement water contents	52
5.3	Summary of consolidation characteristics	53
6.1	Comparison of actual and calculated settlements	123
A-1	Settlement plate elevations at the bottom sand blanket	155
A-2	Settlement plate elevations at the midpoints of the lower and upper sludge layers	156
A-3	Settlement plate elevations at the middle sand blanket	157
A-4	Settlement plate elevations at the top sand blanket	157
B-1	Pore water pressures for the bottom sand blanket and upper sludge layer	158
B-2	Pore water pressures for the middle sand blanket and upper sludge layer	159
C-1	Total pressure cell data	160
D-1	Temperature data for the papermill sludge landfill	161
E-1	Undisturbed vane shear strengths	162
E-2	Remolded vane shear strengths	163
F-1 to 7	Conventional consolidation data	164-170
F-8 to 12	Bishop consolidation data	171-175
F-13 to 14	Single increment Bishop consolidation data	176-177
G-1	Well leachate (WL) data	178
G-2	Pipe leachate (PL) data	180
H-1	Organic loam column, well leachate (WL)	182
H-2	Sand column, pipe leachate (PS)	183
H-3	Organic loam column, aerobic, pipe leachate (PTA)	184
H-4	Organic loam column, anaerobic, pipe leachate (PTAN)	185
H-5	Clay column, pipe leachate (PC)	186
H-6	Organic loam column, double dose, pipe leachate (DPT)	187

APPENDICES Page 153

A. Settlement data 155
B. Piezometer data 158
C. Pressure cell data 160
D. Temperature data 161
E. Vane shear strength data 162
F. Consolidation data 164
G. Leachate analysis 178
H. Lysimeter study 182
I. Computer program for load increasing linearly with time followed by an instantaneous surcharge application 188

LIST OF FIGURES

Figure Page

2.1 The settlement problem. (a) Section through a sludge landfill. (b) Volume-void ratio relationships. 8

3.1 Time-compression curves. (a) Primary and secondary compression. (b) Definitions. 21

3.2 (a) Consolidation machine and recorder. (b) Fixed ring consolidation unit and sludge sample. 22

3.3 Vane shear apparatus. 23

4.1 Pre-construction map of existing gravel pit area including dike layout. 34

4.2 Experimental landfill and instrument group locations, plan view. 35

4.3 Section of landfill (typical), north dike at end of construction. 36

4.4 Sludge placement. (a) Dragline operation. (b) Dumping over the dike sides. 37

4.5 Experimental sludge landfill during placement of the lower sludge layer. 38

4.6 Settlement plate. (a) Installation in a sand blanket. (b) Placement in the sludge, carpenters level shown on the plate. 39

4.7 Distribution of settlement plates, piezometers, and total pressure cells in the instrument groups. 40

4.8 Piezometer. (a) Pore pressure transducer. (b) Installation in a small sand pocket in the sludge. 41

4.9 Diagram of lysimeter. (a) Aerobic. (b) Anaerobic. 42

4.10 Schematic of analyses conducted on leachate and lysimeter percolates. 43

5.1 Consolidation characteristics for sludge sample U-5. (a) Void ratio. (b) Coefficient of consolidation, c_v. (c) Primary compression ratio, r. 56

5.2 Compression dial reading versus logarithm of time. (a) Load increment 0.1-0.2 kg/cm^2. (b) Load increment 0.4-0.8 kg/cm^2. 57-57

5.3 Coefficient of secondary compression, C_α. (a) C_α versus log p. (b) $C_\alpha/\Delta p$ versus log p. 58

5.4 Vane shear strengths after completion of each sludge layer and after partial consolidation. 59

5.5 Settlement-time curves. (a) Group 1. (b) Group 2. (c) Group 3. (d) Group 4. (e) Group 5. (f) Group 6. (g) Group 7. (h) Group 8. 60-67

Figure List of Figures (cont.) Page

5.6 Settlement versus square root of time curves, upper sludge layer. (a) Groups 1 through 4. (b) Group 5 through 8. 68-69

5.7 Settlement-logarithm of time curves, upper sludge layer. (a) Groups 1 through 3 and 7. (b) Groups 4 through 6 and 8. 70-71

5.8 Settlement-logarithm of time curves, lower sludge layer after surcharge placement. (a) Groups 1, 2, 3, and 4. (b) Groups 5, 6, 7, and 8. 72-73

5.9 Pore pressure versus time curves. (a) Group 5, piezometers 3 and 6. (b) Group 5, piezometers 2 and 7. (c) Group 5, piezometers 4 and 8. (d) Group 6. (e) Group 7, piezometers 3 and 6. (f) Group 7, piezometers 4 and 7. (g) Group 5, piezometers 5. 74-80

5.10 Temperature versus time. (a) Thermistors 1, 3, 5, 7, and 9. (b) Thermistors 2, 4, 6, 8, and 0. 81-82

5.11 Horizontal and vertical total stresses, lower sludge layer. 83

5.12 COD versus time for pipe leachate (PL) and well leachate (WL). 84

5.13 BOD versus time for pipe leachate (PL) and well leachate (WL). 85

5.14 Specific conductance versus time for pipe leachate (PL) well leachate (WL). 86

5.15 Turbidity versus time for pipe leachate (PL) and well leachate (WL). 86

5.16 Total solids versus time for pipe leachate (PL) and well leachate (WL). 87

5.17 Dissolved solids versus time for pipe leachate (PL) and well leachate (WL). 88

5.18 Suspended solids versus time for pipe leachate (PL) and well leachate (WL). 88

5.19 COD versus time for organic loam column-well leachate (WT) and organic loam column-aerobic-pipe leachate (PTA). 89

5.20 COD versus time for sand column-pipe leachate (PS) and clay column-pipe leachate (PC). 89

5.21 COD versus time for organic loam column-anaerobic-pipe leachate (PTAN). 90

5.22 BOD versus time for organic loam column-well leachate (WT) and organic loam column-aerobic-pipe leachate (PTA). 90

5.23 BOD versus time for sand column-pipe leachate (PS) and clay column-pipe leachate (PC). 91

Figure List of Figures (cont.) Page

5.24 BOD versus time for organic loam column-anaerobic-pipe leachate (PTAN) and organic loam column-double dose-pipe leachate (DPT). 91

5.25 Specific conductance versus time for organic loam column-well leachate (WT) and organic loam column-aerobic-pipe leachate (PTA). 92

5.26 Specific conductance versus time for sand column-pipe leachate (PS) and clay column-pipe leachate (PC). 93

5.27 Specific conductance versus time for organic loam column-anaerobic-pipe leachate (PTAN) and organic loam column-double dose-pipe leachate (DPT). 94

5.28 Total solids versus time for organic loam column-well leachate (WT) and organic loam column-aerobic-pipe leachate (PTA). 94

5.29 Total solids versus time for sand column-pipe leachate (PS) and clay column-pipe leachate (PC). 95

5.30 Total solids versus time for organic loam column-anaerobic-pipe leachate (PTAN) and organic loam column-double dose-pipe leachate (DPT). 96

5.31 Dissolved solids versus time for organic loam column-well leachate (WT) and organic loam column-aerobic-pipe leachate (PTA). 97

5.32 Dissolved solids versus time for sand column-pipe leachate (PS) and clay column-pipe leachate (PC). 97

5.33 Dissolved solids versus time for organic loam column-anaerobic-pipe leachate (PTAN) and organic loam column-double dose-pipe leachate (DPT). 98

5.34 Suspended solids versus time for organic loam column-well leachate (WT) and organic loam column-aerobic-pipe leachate (PTA). 98

5.35 Suspended solids versus time for sand column-pipe leachate (PS) and clay column pipe leachate (PC). 99

5.36 Suspended solids versus time for organic loam column-anaerobic-pipe leachate (PTAN) and organic loam column-double dose-pipe leachate (DPT). 99

6.1 Comparison between the measured leachate flow rate and the flow rate calculated from time-settlement curves. 124

6.2 Estimated effective stress changes and strain distribution in the upper sludge layer. (a) Initial stresses. (b) Final stresses. (c) Strain distribution. 125

6.3 Mathematical model of the soil skeleton (Gibson and Lo, 1961). 126

6.4 Parameter determination for the method of Gibson and Lo. 126

Figure List of Figures (cont.) Page

6.5 Measured residual excess pore pressures versus depth. 127

6.6 Comparison of actual and predicted time-settlement curves, upper sludge layer. (a) Settlement versus time. (b) Settlement versus logarithm of time. 128-129

6.7 Pore pressure increase due to application of the upper sand blanket and surcharge. (a) Group 5, upper layer. (b) Groups 6 and 7, upper layer. (c) Group 5, lower layer. (d) Groups 6 and 7, lower layer. 130

6.8 Comparison of measured and predicted initial pore pressures, upper sludge layer. 131

6.9 Comparison of measured and predicted pore pressure midpoint of upper sludge layer. 132

6.10 Theoretical final pore pressure distribution at the end of consolidation if a threshold gradient exists. 133

6.11 Comparison of initial, maximum, and residual pore pressures, upper sludge layer. 133

6.12 Estimated effective stress changes and strain distribution in the lower sludge layer. (a) Initial stresses. (b) Final stresses. (c) Strain distribution. 134

6.13 Load increasing linearly with time followed by an instantaneous surcharge application. 135

6.14 Estimates of ultimate settlement of the lower sludge layer for different elevations of the upper sludge layer. 136

6.15 Comparison between the predicted and measured time-settlement curves, lower sludge layer. 137

6.16 Comparison between predicted and measured pore pressures at the midpoint of the lower sludge layer. 138

6.17 Measured and estimated initial excess pore pressures in the lower sludge layer. 139

LIST OF SYMBOLS

a = primary compressibility of the soil skeleton

a_v = coefficient of compressibility

b = secondary compressibility of the soil skeleton

c = distance to the midpoint of a doubly drained clay layer at $t = 0$

C_c = compression index

c_v = coefficient of consolidation

C_α = coefficient of secondary compression

C_F = $(1 + e_o)/(1 + e) \times c_v$

D = total oedometer compression for an increment of load

d_i = initial compression in oedometer for an increment of load

d_p = primary compression in oedometer for an increment of load

d_s = secondary compression in oedometer for an increment of load

e = void ratio

G_s = specific gravity of the soil solids

H = thickness of sludge layer or sample

i = hydraulic gradient

i_o = threshold hydraulic gradient

k = coefficient of permeability

L_w = liquid limit

p = pressure

$\overline{p}$ = effective pressure

p_w = plastic limit

q_o = applied surface load

Q = leachate flow rate from drain pipe

r = primary compression ratio, d_p/D

$S(t)$ = settlement as a function of time

t = time

t_p = time assumed for the end of primary compression

t_s = time of surcharge application

T_v = time factor

u = excess hydrostatic pore pressure

U = percent consolidation

u_r = residual excess pore pressure

v_o = nominal flow rate of pore fluid

V = volume

w water content

z = depth to a point in a soil layer

γ_w = unit weight of water

γ_d = dry unit weight

Δ = increment

δ_1 = settlement at time t_1

δ_2 = settlement at time t_2

ϵ = strain at a point

$\overline{\sigma}$ = effective normal stress

$1/\lambda$ = viscosity of the soil structure

AN EXPERIMENTAL HIGH ASH PAPERMILL SLUDGE LANDFILL
First Annual Report

O. B. Andersland,[+] Robert P. Vallee,[+] and Timothy A. Armstrong[*]

CHAPTER I. INTRODUCTION

Need for Study

Solid wastes resulting from the pulp or paper making process are removed from effluent streams by treatment devices designed to protect the nation's surface water resources. An estimated 2,500,000 dry tons of solid residue are removed annually (Gillespie, Gellman, and Janes, 1970) giving a sludge cake volume close to 200 million cubic yards. The great majority of these sludges are disposed of on land. A survey (Gillespie, 1969) by the National Council of the Paper Industry for Air and Stream Improvement, Inc., indicated that more than 1100 acres of land are in use as sludge depositories. Sludge disposal on land, in most cases, lacks long-range planning, hence disposal is achieved on a temporary rather than a permanent basis. Thorough planning would include the application of sound engineering principles to all stages of site selection, design, operation, and completed use of the landfill.

In order to do this planning, it is essential to have an understanding of the many variables that affect landfill volume change and settlement, slope stability and bearing capacity, drainage of waste material, and potential for pollution of local streams or groundwater supplies. In anticipation of the industry's need for information on satisfactory disposal practices, the National Council of the Paper Industry for Air and Stream Improvement conducted a questionnaire survey of current land disposal practices (Gillespie, 1969) and a core sampling investigation of existing sludge deposits to measure certain soil mechanics related properties

---

[+] Department of Civil Engineering, Michigan State University, East Lansing.
[*] National Council of the Paper Industry for Air and Stream Improvement, Inc.

(Gillespie, Mazzola, and Gellman, 1970). The core sampling program showed that existing water contents were higher than would be expected in clay soils, with large variations in the vertical direction. High water contents suggest that large settlements can be expected for surface loads. In situ vane shear strengths ranged from 0.12 to 0.37 kg/cm,^{2} indicating low sludge stability. Experimental laboratory data (Andersland and Laza, 1971; Andersland and Paloorthekkathil, 1972) demonstrated the influence of a number of variables on shear strength, permeability, and consolidation behavior of papermill sludge. The task remained to verify, with field observations, the accuracy of predictions (based on laboratory data) of settlement, drainage, and stability.

Objectives of Study

The general objective of the study is to contribute--through field observations on an experimental landfill, laboratory work, and analysis--basic information relative to the sludge behavior which is needed for developing guidelines and recommendations for the design and operation of solid papermill waste landfills. It is desirable that the completed sludge landfill be stable and have the potential for a number of uses, including recreational purposes or as a foundation for light construction. Pursuant to this general objective the research program was directed to the consolidation behavior and stability of the landfill, and the potential for contamination of local streams or groundwater supplies. More specific items relative to consolidation behavior and the leachate analysis and lysimeter study include:

1. Dewatered pulp and papermill sludges from different mills may have consistencies which require different placement techniques. Effectiveness of placement methods used at the experimental site will be summarized.
2. Consolidation parameters, which include the compression index, coefficient of consolidation, and coefficient of secondary compression, are useful in prediction of settlement in soils. Comparisons will be made between the observed field behavior and predictions based on these experimental sludge parameters. These predictions have implications relative to landfill capacity, settlement of future structures built on the landfill, and flow rate and volume of drainage effluent.

3. Surcharge loads used in combination with drainage blankets are an effective means for drainage of certain peat and clay soils. Use of this method in the experimental sludge landfill will be evaluated as to future potential for better drainage and increasing sludge shear strength for improved landfill stability.

4. The magnitude of effective lateral stresses has implications relative to stability analyses involving bearing capacity and slope stability. The observed change in lateral stresses during sludge placement, surcharge loading, and consolidation will provide insight as to the actual stress distribution existing in the sludge.

5. The sampling and analysis of leachate from the sludge landfill serves to both document the leachate composition and to help determine its potential for pollution of local streams or ground water supplies.

6. Leachate draining from a sludge landfill will most likely be subjected to a soil filtration process. The lysimeter approach is used to evaluate drainage effluent quality when it is passed through selected natural soils.

The stability of the experimental sludge landfill will be covered during the second year of the study, hence specific items to be considered are omitted in this annual report.

Research Plan

To accomplish the general and specific objectives of the study, the research program was designed to be conducted in two essentially sequential phases: (1) landfill consolidation plus leachate analysis and lysimeter study, and (2) the stability study. The first phase involved construction of the experimental sludge landfill, placement and monitoring of instrumentation, laboratory work for determination of physical properties and certain stress-deformation characteristics of the sludge, and the leachate analysis and lysimeter study. The second phase falls entirely in the second year, hence it is omitted in this report. Personnel involved in both phases include the project director and two research assistants from Michigan State University working on the soil mechanics related portions of the project. The leachate analysis and lysimeter work was carried out by two research engineers with the National Council of the Paper Industry for Air and Stream Improvement, Inc. Consultant services on both phases, at no cost to the project, were available from the technical director of the National Council of the Paper Industry.

The field research site was selected in collaboration with the National Council of the Paper Industry for Air and Stream Improvement, Inc., and the host papermill. The experimental landfill site, the dewatered sludge (including hauling to the site), and field laboratory space were provided by the host papermill. A local contractor constructed the earth dikes and placed the dewatered papermill sludge and sand drainage blankets during the summer and fall of 1971. Staff from Michigan State University supervised construction of the landfill, took initial sludge samples, installed instrumentation, and initiated field monitoring of the landfill. Staff from the Central-Lake States Regional Center, NCASI, took leachate samples and conducted the analysis and lysimeter study on the sludge leachate. Physical properties and certain stress-deformation characteristics of the sludge were obtained using the soils mechanics laboratory facilities at Michigan State University. The annual report for the first year's activities was prepared during the summer of 1972.

CHAPTER II. PAPERMILL SLUDGE LANDFILLS LITERATURE REVIEW

Information directly oriented to the design and operation of pulp and papermill sludge landfills is very limited. Most of the literature concerns the separation and concentration of solids from the pulp and papermill waste, with very limited planning and application of engineering principles to disposal of the sludge cake on land. Current practice depends on land available, haul distance, nuisance condition, and local requirements for sanitary landfills. Settlement data for these sludge landfills is essentially nonexistent except for some laboratory research. Work on slope stability is to be covered in phase II of the project and will be included in the final report. Groundwater protection includes the potential effect of leachate on groundwater quality and changes in the leachate resulting from soil filtration.

Current Practice

Sludge disposal procedures followed at a particular mill are dependent, to some extent, on the quantity and nature of the sludge produced. The clarifier sludge may range from 1 to 15 percent solids by weight, with ash contents as high as 70 percent. This low consistency sludge is in some cases pumped to earthen basins, lagoons, or drying beds for natural dewatering. The earthen basins or drying beds require adjacent soils which are relatively permeable, such as sands or gravels. After dewatering by natural drainage, the sludge cake may be covered with soil and left in place indefinitely, or may be excavated and hauled to some more distant landfill. Gillespie (1969) states that data available for drying beds are too erratic to draw meaningful conclusions on the performance of this type of dewatering. In some cases pipelines have been constructed to transport the more fluid sludge to large abandoned pits, especially when the calculated use period exceeds five years. The life of these pits is usually extended by the construction of dikes to retain more sludge. Very often, odors emanating from the lagoons or drying beds during warm weather become a nuisance to local residents and property owners. This approach is limited to smaller mills where volume of sludge production is small and where land is available. The practice of pumping clarifier sludge to earthen basins, in most instances, lacks long-range planning and solves the disposal problem on a temporary rather than a permanent basis.

Core sampling studies (Gillespie, Mazzola, and Gellman, 1970) showed that in many cases existing sludge deposits contained in situ water contents much greater than the liquid limit. These deposits have the potential for large settlements under surface loads, and have little stability for slopes or building foundations.

More recent developments (Follet and Gehm, 1966) include dewatering of the clarifier sludge by means of centrifugation, vacuum filtration, or mechanical pressing. The resulting sludge cake may have a solids content as high as 40 percent (equivalent to 150 percent water content) for the high ash sludges. The dewatered sludge is hauled to the disposal site, in some cases as far as five miles from the mill. The disposal sites often are abandoned gravel pits, low lying areas, or other such lands depreciated through use. The sludge is dumped at the site and distributed with suitable earth moving equipment. In a few cases, a cell type of landfill with individual compartments separated horizontally and vertically with a porous material has been used. The resulting slow drainage has helped decrease the volume occupied by the residue. Limited information on sludge stability and sludge drainability has hindered the development of this approach to organized landfill operations. This project is intended to provide information relative to sludge consolidation and slope stability which is needed for developing guidelines and recommendations for the design and operation of papermill sludge landfills.

Settlement

Natural drainage of water from sludge deposits results in a decrease in volume with an accompanying settlement of the surface. This volume change may occur almost entirely in the vertical direction, approximating one-dimensional compression. Application of surface loads from additional sludge, soil cover, or construction serves to increase this volume change or settlement. This phenomenon can be readily observed for existing sludge deposits containing high in situ water contents. For organized landfill operations it is desirable to predict this volume change so as to permit estimation of total sludge capacity of a landfill and to predict settlement of any constructed facilities placed on the sludge landfill.

Very little published information is available regarding the settlement of papermill sludge landfills. Accordingly, one goes to related areas, such as soils mechanics, and borrows those theories which appear to describe the sludge behavior. Consolidation theory involves setting up an equation from which pressure and void ratio values may be computed at any point and time in a stratum of consolidating material. From such an equation the change in overall thickness of the strata after any interval of time may be determined by integration or numerical computation. To illustrate the application of certain consolidation concepts, consider a section through a sludge landfill as shown in Figure 2. 1a. If it is assumed that leachate drainage results in one-dimensional compression, i.e. volume change occurs only in the vertical direction as settlement, then the change in sludge layer thickness, ΔH, per unit of original thickness, H_o, equals the change in volume, ΔV, per unit of original volume V_o. It is convenient to work with a small sludge sample, which can be represented as shown in Figure 2. 1b. Volume-void ratio relationships show that $\Delta V/V_o = \Delta e/(1 + e_o)$, where Δe is the change in void ratio and $e_o = V_v/V_s$ is the initial void ratio expressed in terms of the initial void volume, V_v, and the solids volume, V_s. Now it is convenient to compute settlement ΔH as

$$\Delta H = H_o \frac{\Delta e}{1 + e_o} \qquad (2.1)$$

The initial sludge layer thickness, H_o, and the average initial void ratio, e_o, can be determined. The problem now becomes one of determining the relationship between void ratio and effective normal stress (loads) and how effective normal stress changes with drainage of water from the sludge. The theory and procedures needed are given in various references (Lambe and Whitman, 1969; Leonards, 1962; Lambe, 1951).

These procedures are based entirely on Terzaghi's (1943) one-dimensional consolidation theory, and although this theory is widely accepted, it includes certain assumptions that may not apply to papermill sludge. To determine the significance of these assumptions, several theories are reviewed below which include one or several of the assumptions in

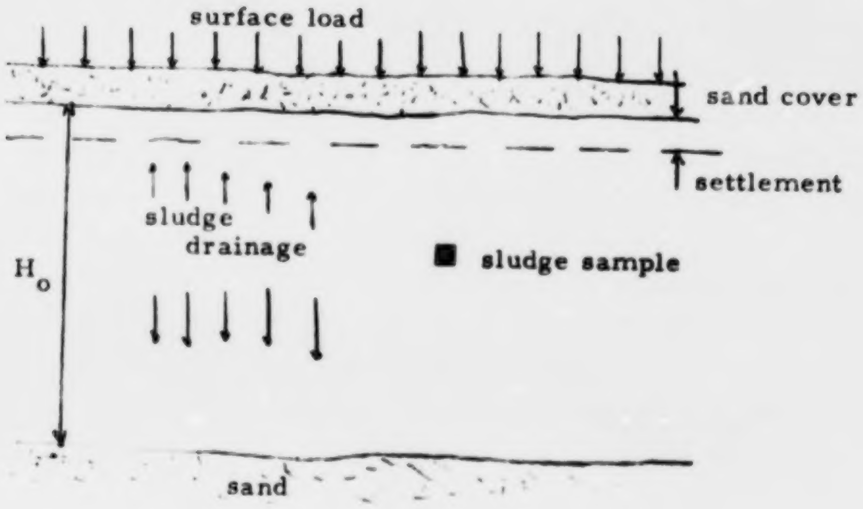
surface load
sand cover
settlement
sludge
drainage
sludge sample
H_o
sand

a) Section through a sludge landfill.

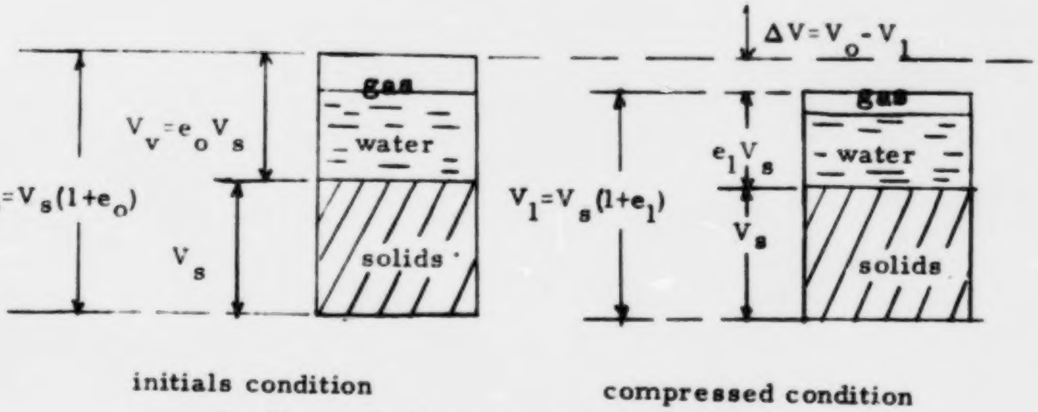
ΔV=V_o-V_1
V_v=e_oV_s
V_o=V_s(1+e_o)
V_s
gas
water
solids
V_1=V_s(1+e_1)
e_1V_s
V_s
gas
water
solids
initials condition
compressed condition

$$\frac{\Delta V}{V_o} = \frac{V_o - V_1}{V_o} = \frac{V_s(1+e_o) - V_s(1+e_1)}{V_s(1+e_o)} = \frac{e_o - e_1}{1+e_o} = \frac{\Delta e}{1+e_o}$$

b. Volumn-void ratio relationships.

Figure 2.1. The settlement problem.

their mathematical formulation. Among the assumptions involved are: (1) the time lag of compression is caused exclusively by the low permeability of the material (ignores secondary compression), (2) constant soil compressibility during the load increment (assumes a linear stress-strain relation), (3) Darcy's law is valid at low hydraulic gradients (no threshold gradient), and (4) small strain theory is valid.

Gibson and Lo (1961) and Garlanger (1972) have formulated theories which include secondary compression throughout the consolidation process. Since Gibson and Lo's theory will be used in estimating the ultimate settlement of the upper sludge layer, its description is referred to in chapter VI. It differs from the other theories described here in that a rheological model is used to mathematically model the soil skeleton. Garlanger (1972) bases his theory on a soil model described by Bjerrum (1967), and replaces the Terzaghi equation

$$\frac{\partial e}{\partial t} = -a_v \frac{\partial \overline{p}}{\partial t} \qquad (2.2)$$

where e is the void ratio, t the time, and $\overline{p}$ the effective normal stress, and a_v the coefficient of compressibility equal to $\partial e/_{\partial \overline{p}}$, a constant which assumes a time-independent linear relationship between void ratio and pressure, with the equation

$$\frac{\partial e}{\partial t} = \frac{\partial e}{\partial \overline{p}} \frac{\partial \overline{p}}{\partial t} + \left(\frac{\partial e}{\partial t}\right)_c \qquad (2.3)$$

In this equation the compressibility, $\frac{\partial e}{\partial \overline{p}}$, and creep rate, $\left(\frac{\partial e}{\partial t}\right)_c$, are assumed to be functions of both void ratio and pressure. To obtain numerical values for these relations, the appropriate coefficients are determined from a plot of logarithm of void ratio versus logarithm of the effective normal stress. Garlanger (1972) solves equation 2.3 simultaneously with two Terzaghi equations, by a numerical process, to give the void ratio-time and the pore pressure-time relationships at every point within the consolidating soil. Both theories mentioned above require the assumption of a value for the coefficient of consolidation, c_v, and as discussed in chapter VI, the time-settlement relation is quite sensitive to this value. Therefore it might be concluded that although these theories more accurately model the consolidating soil, the determination of a proper value for c_v may be a far more important consideration in the settlement analysis.

Janbu (1965) and Davis and Raymond (1965) have included the non-linear stress-strain relation of equation 6.2 into the consolidation development to replace Terzaghi's assumed linear relation. Janbu formulates the differential equation of consolidation in terms of strain, i.e.

$$\frac{\partial \epsilon}{\partial t} = c_v \frac{\partial^2 \epsilon}{\partial z^2} - \frac{\partial v_o}{\partial z} \qquad (2.4)$$

where ϵ is the strain at a point, c_v the coefficient of consolidation, v_o the nominal flow rate associated with a threshold gradient i_o, and solves the equation based on different assumed final strain-depth distributions. Since his model can account for the decrease in strain with depth shown in Figure 6.1c, it allows consolidation to take place more rapidly than it would in a solution obtained on the basis of constant additional stress. Since the laboratory parameters in Terzaghi's theory underestimate the rate of settlement, such a rate increase would be desirable. However, there are problems involved in assuming a proper analytical final strain distribution for use in the theory. As seen above, this theory allows for the formation of a residual pore pressure in the soil based on the concept of a threshold gradient.

Davis and Raymond (1965) use the non-linear relation of equation 6.2 in a different method of formulation, based on continuity and stress conditions, and arrive at the conclusion that Terzaghi's theory accurately predicts the time-rate of settlement but overestimates the rate of pore pressure dissipation. This theory, along with Janbu's (1965), involves the assumption of a value of c_v in its application, and thus is subject to the same explanation given previously on its limitation in predicting time rate of settlement. There are also some contradictions between the conclusions of the two theories, which make it hard to assess which one would be most applicable to papermill sludge.

Gibson et al. (1967) have attempted to take into account the variability of the coefficient of consolidation, and have also eliminated the assumption of small strains. In so doing they have formulated the

the governing differential equation for a thin clay layer subjected to large deformations. The solution is obtained for both a constant C_F and a C_F linearly related to the void ratio, where C_F is a coefficient closely related to the familiar coefficient of consolidation c_v. In the solution of the former case, the linear differential equation is

$$C_F \frac{\partial^2 e}{\partial c^2} = \frac{\partial e}{\partial t} \tag{2.5}$$

where C_F is the term $\frac{(1+e_0)}{(1+e)} c_v$, e the void ratio, and c the distance from the midpoint of a doubly drained clay layer (at $t = 0$). This equation holds without restriction on the form of the relation between effective stress and void ratio. It also assumes only C_F as constant, with no such restrictions being placed on the coefficient of permeability, k, and compressibility, ($^{d\sigma'}/_{de}$), as in Terzaghi's (1943) theory. Upon solution of equation 2.5, the effective stresses can be found by application of a suitable stress strain relation (void ratio vs. effective normal stress) and the pore pressures obtained from the effective stresses (constant total stress). The resulting pore pressures will in general not correspond to those obtained by Terzaghi's theory, however the early part of settlement will, as in the Terzaghi case, behave like $t^{1/2}$. Such a result would indicate that Terzaghi's theory should adequately predict the time-settlement relation for papermill sludge even though it undergoes large deformation.

Applications of consolidation theory to pulp and papermill sludges do have certain limitations, as shown by Andersland and Paloorthekkathil (1972). They conducted a series of one-dimensional compression tests on an integrated pulp and papermill sludge and two secondary fiber mill sludges. Most of their results are relevant to this study. For example, the composition and solids content of the dewatered sludge produced at a given mill will vary from day to day. Since the consolidation parameters are dependent on these factors, the problem arises as to how much sampling and testing is required to obtain representative consolidation data for the sludge being placed into the landfill. Data presented by Andersland and Laza (1972) show the influence of gas bubbles trapped in the sludge on its permeability. Hydraulic pressures existing in most sludge landfills will not be large enough to eliminate this factor, hence the problem of predicting consolidation rates becomes more complicated. Energy released during sludge decomposition will alter the temperature of sludge landfills. Andersland and Paloorthekkathil (1972) show that temperature change alters the equilibrium void ratio as well as the coefficient of consolidation. The observed settlements in the experimental sludge landfill will permit comparisons with predicted settlements based on laboratory data, thereby helping to delineate possible limitations of the application of consolidation theory to papermill sludges.

Groundwater Protection

Dewatered papermill sludges placed in landfills contain liquids of undesirable quality and soluble fractions which constitute a source of potential groundwater pollution. The quantity of fluid leaving a sludge landfill will equal approximately the decrease in volume associated with settlement. The greatest rate of flow will occur during the initial stages of settlement, with subsequent rates approaching zero. The low permeability of sludge (Andersland and Laza, 1972) should minimize groundwater seepage through the sludge. These liquids can be described as a leachate which is high in dissolved solids and in chemical and biological oxygen demand. These components, or products from decomposition, may affect the groundwater quality if the drainage effluent comes in contact with the groundwater body. As leachate migrates through soil it is attenuated by ion exchange, dilution, dispersion, complexing, and filtration. Hughs, et al. (1971) state that fine grained soils have a high capacity for retaining the dissolved solids. Their low permeability permits only a low rate of groundwater movement. Sands and gravels have a lower capacity to retain the dissolved solids and permit higher rates of flow. Recent studies of irrigation and land disposal of pulp and papermill effluents (Blosser and Owens, 1964) deals with changes in characteristics when percolated through different soil types. The work demonstrated that a BOD loading criterion of 200 lb/acre-day did not cause a reduction in soil permeability, yet yielded in excess of 95 percent BOD reduction as effluent percolated through 20-in. of soil. It was further demonstrated that sodium and color bodies present in the mill effluent were partially retained in the soil during the period of effluent application, the degree of retention being dependent on the soil type.

The amount of ion exchange depends on (1) the type of material involved, (2) the ions existing on the surface of clay particles, and (3) other elements in solution and their concentration. Blosser and Owens (1964), in laboratory investigations, observed that effluents with a sodium absorption ratio of 8 or less do not create an adverse reaction for permeable soils. Basic information on ion exchange phenomena in clay minerals is given by Grim (1953, 1962). Data presented by the County of Los Angeles and Engineering-Science, Inc. (1969) show a marked reduction in mineral content, BOD, and COD for leachate passing through 5C ft of soil as compared to leachate samples taken from the test fill.

Leachate reaching the groundwater will be diluted by mixing with adjacent water when it enters a well casing and is pumped out, and by dispersion into adjacent groundwater during flow. The extent of this dilution is dependent on the characteristics of both the leachate and the groundwater body. Dissolved mineral matter entering the groundwater will have its greatest travel in the direction of flow. Vertical diffusion will occur to a limited extent. The lysimeter study, included as a part of this project, will provide information on changes in quality of the leachate when passed through selected natural soils.

Chapter III. EVALUATION OF SLUDGE ENGINEERING CHARACTERISTICS

The physical properties and stress-deformation behavior of the papermill sludge is needed for making predictions for comparison with observed field behavior of the experimental landfill. Methods used for measurement of these engineering characteristics are described below. Reference is made to standard test procedures where possible.

Physical Properties

Physical properties of papermill sludge characterize, to some extent, the quality of the sludge relative to engineering purposes. Those properties important to this project include water content, unit weight, specific gravity, ash (or organic) content, and consistency limits.

Water Content. The water content of a soil or sludge sample is defined as the ratio of the weight of water to the weight of dry soil or dry sludge and is usually expressed as a percentage. Drying temperatures for sludges are the same as used for mineral soils (105 - 110 °C). In order to obtain consistent dry sludge weights, careful control of the oven temperature is required. Care must be exercised so as to obtain a representative sample that avoids local variations. A minimum sample size of at least 10 gm of dry solids is recommended. Lambe (1951) gives additional information on water content of soils.

Fresh papermill sludges contain large amounts of water, hence some prefer to use solids content by weight rather than water content by weight. The solids content is defined as the ratio of the weight of solids to the weight of the wet sample. A simple conversion from solids content to water content is

$$w = 100 \left[\frac{100}{\%\text{dry solids}} - 1 \right] \qquad (3.1)$$

where $w = \frac{W_w}{W_s}(100)$ is water content in percent based on the dry weight of solids, W_s, and the weight of water, W_w.

Water contents of sludge samples taken from the landfill are given in Table 5.2. The lower layer had an average initial water content of

Preceding page blank

261 percent with a range from 210 to 309 percent. The upper layer had an average initial water content of 263 percent and a range from 212 to 290 percent. All water content samples were taken shortly after the sludge had been placed in its final location by the dragline. Variations present are due to: (1) changes in sludge output from the dewatering plant, (2) localized surface wetting and drying as a result of weather changes, and (3) different times of sludge exposure before sampling. It should be noted that after the construction of a sludge layer the water contents toward the bottom were less than those at the top because leachate drained from the sludge into the bottom sand blanket during construction. Application of the surcharge reduced the water content throughout both sludge layers as the leachate was expelled.

Unit Weight. The unit weight of sludge is defined as the weight of the aggregate (sludge plus water) per unit volume. Unit weight of sludge depends on the solids content, unit weight of the solid constituents, and the degree of saturation. The natural unit weight can be determined by careful volume and weight measurements. The unit weight of fluid sludges may approach that of water (62.4 lb/cu ft) whereas the unit weight of dewatered sludges cannot exceed that for the solid constituents. The dry unit weight, γ_d, may be computed as

$$\gamma_d = \frac{G_s}{1 + e} \gamma_w \qquad (3.2)$$

where G_s is the specific gravity of the solids, $e = \frac{V_v}{V_s}$ is the void ratio expressed in terms of the volume of voids, V_v, the volume of solids, V_s, and γ_w is the unit weight of water.

Two procedures were used to determine the total unit weight of the papermill sludge as placed in the landfill. In the first procedure, a truck carrying sludge was weighed both when full and when empty to determine the total weight of the sludge being carried. The volume of the truck box was then determined and divided into the sludge weight to determine the unit weight. This procedures gave a total sludge unit weight of 69.7 lb/cu ft. The second procedure involved packing the sludge by hand into a bucket of known volume (1/10 cu ft), and weighing to determine the quantity of sludge in the bucket. The sludge was placed into the bucket in 5 lifts, and care was exercised to be sure that no air pockets were present. The total unit weight determined from this procedure was 69.0 lb/cu ft. The second procedure is similar to the method used for determination of the unit weight of fresh concrete.

Specific Gravity. The specific gravity of a papermill sludge is the ratio of the weight in air of a given volume of sludge particles to the weight in air of an equal volume of distilled water at a temperature of 4°C. The lower limit for sludge will approximate the specific gravity of the organic material. The higher limit will correspond to the specific gravity of the mineral matter, generally greater than 2. Accurate determination of the specific gravity requires special care because of the presence of small gas bubbles in the sludge sample. This was overcome by application of a vacuum to the pycnometer containing the water and sludge. Details of the test for specific gravity of the sludge solids are given under ASTM designation D 854-58. Oven dry test samples were used for the papermill sludge.

Ash Content, Organic Content. The organic material of sludge, primarily cellulose fibers, is combustible carbonaceous matter, whereas the mineral constituents are incombustible and ash forming. In the manufacture of paper, kaolinite is used in filler and coating operations. In waste paper reclamation this clay is removed from the fiber and becomes a part of the paper sludge. The sludge also contains small amounts of aluminum hydrate, titanium oxide, lime and iron (Gillespie, Gellman, and Janes, 1970).

The ash content of pulp and paper sludge is determined by firing an ovendried sample in a muffle furnace at a temperature of 925 ± 25°C (ASTM test method D 586-63). The ash content A_c is determined from the equation

$$A_c\ (\%) = \frac{\text{weight of ash or residue}}{\text{dry weight of sample}} \times 100. \qquad (3.3)$$

MacFarlane (1969) states that, for peat, it is standard engineering practice to determine the ash content as described above and then to consider the organic content equal to $(100 - A_c)$. Comparative results (Andersland and Laza, 1971; Andersland and Paloorthekkathil, 1972) between the ash content determined from the above method and the organic content determined by the method given in Agronomy No. 9, Sec. 92-3.3 (Black, 1965) support the use of (100 - A_c) for estimating organic content of papermill sludges.

Consistency Limits. The consistency, or Atterberg limits, indicate the range of water contents in which a soil or sludge may be considered as a fluid, plastic, or solid. The liquid limit is the water content at which the soil or sludge has such a small shear strength that it will flow and close a groove of standard width when jarred in a specified manner. The plastic limit is the water content at which the soil or sludge begins to crumble when rolled into threads of a specified size. The amount of water which must be added to change a soil or sludge from its plastic limit to its liquid limit is an indication of the plasticity of the material. The plasticity is measured by the plasticity index, which is equal to the liquid limit minus the plastic limit. Detailed procedures for the consistency limits are given by Lambe (1951). Values for the sludge can be found in Table 5.1.

Papermill sludges containing fibers do not lend themselves to the standard consistency tests. The fibers interfere with the test procedures and probably alter the shear strength of the material adjacent to the standard groove in the liquid limit test. Andersland and Laza (1971) show that both the liquid and plastic limits decrease with a decrease in organic content whereas the plasticity index shows very little change. This behavior suggests that the organic fibers contribute little to the plasticity of the sludge.

Stress Deformation Characteristics

The stress-deformation behavior of papermill sludge will determine its volume change and settlement and will control stability of sludge landfills. The methods used for evaluating the consolidation behavior and the undrained shear strength are given below. Sludge properties measured in the triaxial test will be covered under phase II of the project.

Consolidation Behavior. The process of leachate flow from sludge, involving volume change as a function of time, is called consolidation. When volume change occurs only in the vertical direction, as in a horizontal sludge layer (Figure 2.1a), changes in the surface elevation are labeled settlement. Two forms of volume change in papermill sludges include primary and secondary compression (Figure 3.1). Primary compression involves a transference of load from the pore water to the sludge structure and is accompanied by a change in volume equal to the volume of water drained from the sludge. The rate at which primary compression occurs in sludge is directly related to the sludge permeability (the speed at which pore water can escape). Pore water pressure measurements taken during the settlement study provide information on this rate of consolidation. When the excess hydrostatic pressure associated with primary compression has been dissipated, the change in void ratio generally continues at a reduced rate. This phenomenon is referred to as secondary compression and is often expressed by the slope, C_a, of the final portion of the time-compression curve plotted on semi-log paper (Figure 3.1b).

Laboratory consolidation tests (Lambe, 1951) were used to provide quantitative information on the sludge compressibility. The Wykeham Farrance consolidation test machine shown in Figure 3.2, designed by Professor A.W. Bishop, provided consistent laboratory consolidation test results. The first step required in running a test was to carefully place the sludge, in small amounts, into the 2-1/2 in diameter by 3/4 in high consolidation ring and to knead the mass by hand so that a continuous sample free of large air pockets was obtained. The top and bottom of the sample were carefully smoothed off and trimmed to conform to the right height. The sample was then placed in the cell chamber (with perspex wall) shown in Figure 3.2b and the clamp ring and top pressure pad were situated in their proper location. The cell was then placed in the consolidation machine (Figure 3.2a) and the load increment applied. Drainage from the sample took place through two bauxilite discs, one located on the bottom of the cell and one attached to the top pressure pad. Deformation of the sample was obtained from a displacement transducer attached to the frame of the consolidation machine and connected to a Sargent recorder. Recorder output was verified at the start of testing by comparison to deformations measured with a dial gauge. In a standard, multiple increment test, stresses of 0.1, 0.2, 0.4, 0.8, 1.6, and 3.2 kg/cm^2 were applied for a period of 24 hours to the sample. Special single increment tests were also carried out, usually involving a

24 hour time period. Consolidation characteristics are summarized in Table 5. 3.

Undrained Shear Strength. The undrained shearing resistance of papermill sludge may be determined using a cylindrical compression test (Bishop and Henkel, 1962) or a vane shear test (Terzaghi and Peck, 1967). Information regarding the triaxial test will be covered in phase II of the project. The vane shear test was used to measure the increase in undrained shearing resistance, with consolidation, at various levels in the experimental sludge landfill. The vane shear apparatus consists of a four-bladed vane attached to the bottom of a vertical rod, as shown in Figure 3. 3. The vane and rod can be forced into the soft sludge without appreciable disturbance. The assembly can then be rotated and the shearing resistance computed by using the dimensions of the vane and the observed torque. The sludge fails along a cylindrical surface passing through the outer edges of the vane, as well as along the conical surfaces at the top and bottom of the blades. When the vane is rotated rapidly through several revolutions, the sludge becomes remolded and the shearing strength can again be determined. The ratio of the undisturbed shear strength to the remolded value gives the sensitivity of the sludge. Details on the apparatus and procedures for the vane shear test as used on the project are given in chapter IV.

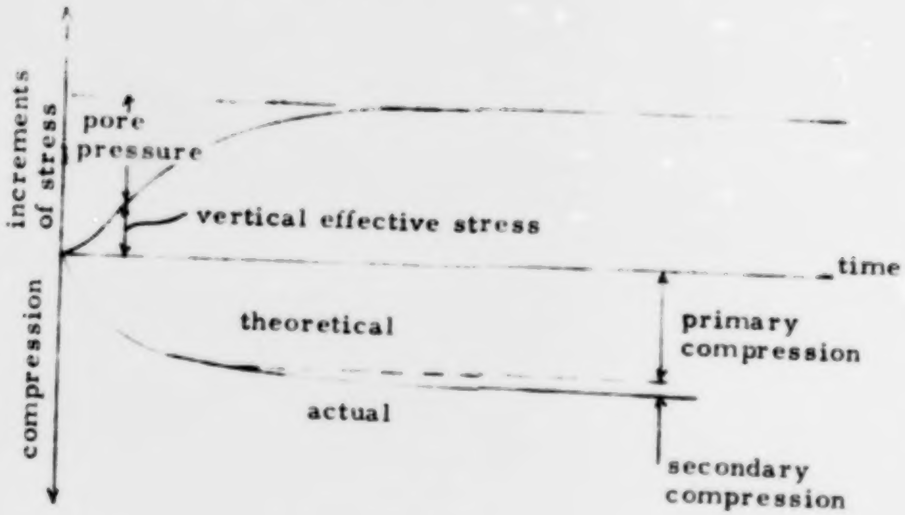
increments of stress
pore pressure
vertical effective stress
time
compression
theoretical
actual
primary compression
secondary compression

a) Primary and secondary compression.

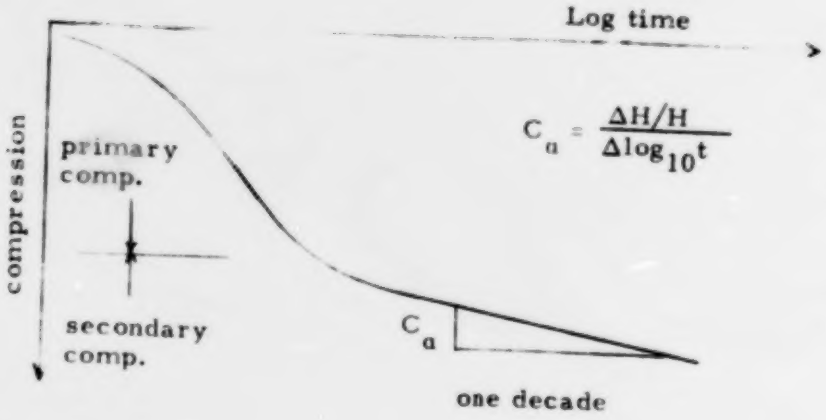
Log time
compression
primary comp.
secondary comp.
$C_\alpha = \frac{\Delta H/H}{\Delta \log_{10} t}$
C_α
one decade

b) Definitions.

Figure 3.1. Time-compression curves.

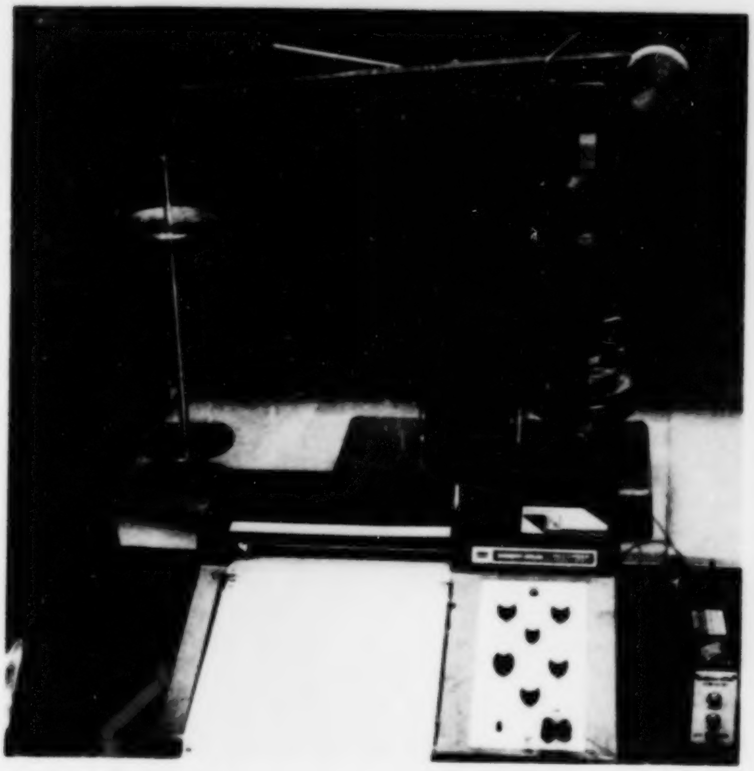

(a)

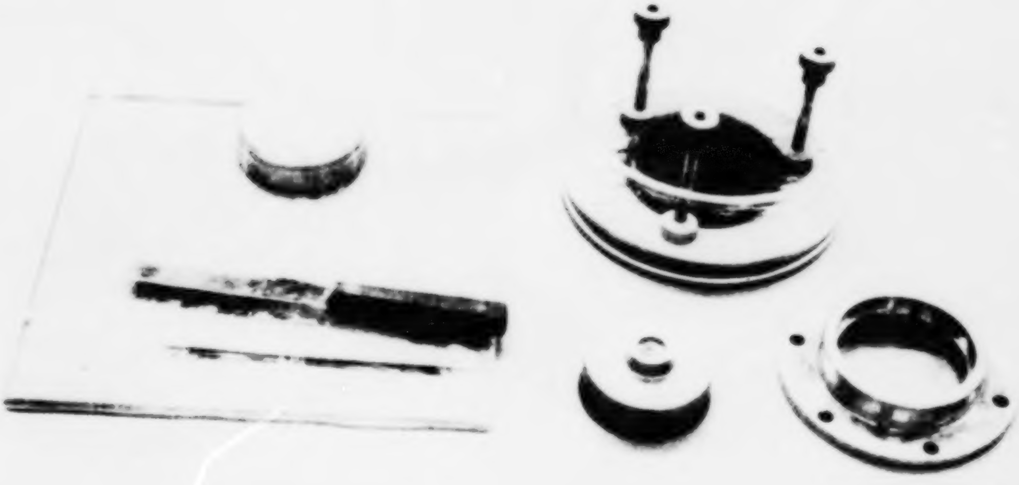

(b)

Figure 3.2. (a) Consolidation machine and recorder. (b) Fixed ring consolidation unit and sludge sample.

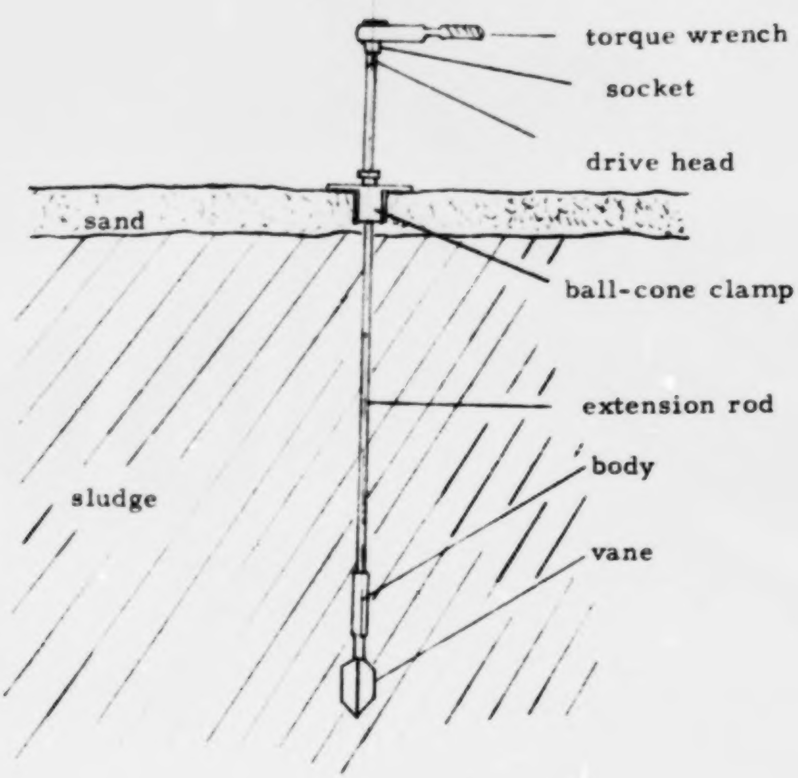
torque wrench
socket
drive head
sand
ball-cone clamp
extension rod
body
sludge
vane

Figure 3.3. Vane shear apparatus.

Blank

Chapter IV. CONSTRUCTION, INSTRUMENTATION AND MONITORING

Construction of the Experimental Landfill

Construction methods employed at the site are summarized here for later reference. They are described in terms of the site preparation and dike construction, sludge placement, drainage blanket placement, and earth surcharge placement. The B.G. Danis Company, Inc., Dayton, Ohio, provided equipment and operators. Coordination of construction operations was handled by Michigan State University personnel working with Mr. Tom Danis, Sr. Field work on the papermill sludge landfill commenced on August 23, 1971.

Site Preparation and Dike Construction. An old gravel pit located close to West Carrollton, Ohio, and within hauling distance of the papermill was selected for the experimental sludge landfill site. A pre-construction map of the immediate gravel pit area and dike layout is shown in Figure 4.1. Other parts of this gravel pit contained large amounts of dewatered papermill sludge. A small pond in the gravel pit, about 400-ft north of the existing slope, provided a reference as to the groundwater elevation. This information indicated that the groundwater level would not be encountered during dike construction. The pond also served as an outlet for the drainage pipe installed in the lower sand blanket. Several bench marks were established and a stadia survey was completed of the immediate gravel pit area, as shown in Figure 4.1. From the stadia survey it was apparent that a maximum dike grade elevation of 95.5 ft would allow the entire west dike and part of the south dike to be shaped from the natural ground. Excavated soil would provide material for the remaining dike areas. The bottom grade elevation of 77.0 ft was about 7 ft above the groundwater level.

Prior to excavation for the dikes, an 8-in. diameter pipe was installed to the pond to provide drainage for the sand drainage blankets. The upper end extended under the north dike and into a gravel pocket in the lower sand blanket (invert elevation 77.0 ft) as shown in Figures 4.2 and 4.3. The lower end (invert elevation 73.6 ft) drained into the pond. The gravel drain surrounding the pipe entrance was continued up the inner dike wall to provide drainage for the middle sand blanket

Preceding page blank

(Figure 4.3). Observations at the pipe outlet both during and after construction indicated that it was functioning properly. Pipe joints were not sealed, hence some seepage to and from adjacent soil could occur.

The top inside corners of the dikes and the required grades were established using results from the stadia survey (Figure 4.1). A one cubic yard 35-ton Link Belt power shovel did the bulk of the excavation work, while a D-6 caterpillar dozer moved the excavated earth and shaped the dikes. Excavation began near corner 1 (Figure 4.1), with the power shovel digging into the existing bank and side casting to the dike area. The dozer would spread soil toward corner 2, gradually building up this dike. As grade was approached, the dozer spread the soil toward corner 3 thus building up the east dike. The excavated material was a well graded till consisting of particles ranging in size from clay to gravel. It was easy to handle and during placement some compaction was achieved from the dozer thus permitting construction of a fairly steep inner dike slope. This slope helped minimize the volume of material required and reduced construction time.

After the power shovel had completed the excavation near the top, it was moved to the bottom area and proceeded to excavate down about 6 ft to final grade at elevation 77.0 ft. The excavated material was used to complete the north and east dikes. Corner 3 was left low until sand for the lower drainage blanket had been dumped inside the dike area. When the bottom of the landfill area had reached grade, the power shovel was converted into a dragline unit and soil for completing the dike was obtained outside the fill area. The dozer spread this soil to complete the dike and leveled the sand dumped for the lower drainage blanket. The gravel surrounding the upper end of the drainage pipe and extending up the slope (Figure 4.3) was placed near the end of the dike construction period. Shaping of this 10-ft wide gravel chimney drain was handled by the dozer.

Sludge Placement. After spreading sand for the lower sand blanket and shaping the gravel chimney drain, sludge was dumped from a truck over the west and south dikes as shown in Figure 4.4b. The sludge exhibited a plastic behavior and would not support the usual construction equipment. The dragline (Figure 4.4a) proved ideal for moving the sludge to other locations in the landfill. A lightweight dozer with extra track width arrived at the site too late for use in spreading the sludge. Current use of this lightweight dozer by the contractor indicates that it is quite effective in moving sludge and that it should be considered for future operations.

Some initial difficulty was encountered when unmonitored sludge dumping was permitted over a weekend. Unusually high sludge production (about 300 cu yd/day) caused more area to be used at the bottom of the landfill than was anticipated, and a sludge flow towards the center of the site occurred. Two settlement plates with vertical rods were shoved out of position and required replacement. Leachate draining from about ten feet of sludge stacked along the west dike saturated the sand blanket. Temporary channels were dug in the sand blanket to the drainage pipe to remove the leachate. After re-leveling of the sand surface and more uniform placement of the sludge with the dragline, dumping was continued with daily monitoring. Shortly thereafter, sludge production dropped to about one-half its normal rate, delaying the landfill construction. The dragline was used for the placement of both sludge layers.

Drainage Blanket Placement. Placement of the lower sand blanket was described in the preceding sections. When the lower sludge layer reached grade it was leveled with the dragline bucket, and then two telephone poles cabled together were dragged over the surface. This reduced variations in the sludge surface to about ± 3 inches. Sand was next dumped along one dike edge and distributed by dragline over the sludge layer. Again the two telephone poles were dragged over the surface to give a reasonably level sand surface. Use of a lightweight dozer for spreading the sand was not attempted because of potential sinkage into the sludge. The surface of the lower sludge layer was 11 ft below the top of the dike, as shown in Figure 4.5. Next, sludge placement was resumed.

When the upper sludge layer reached grade, the surface was leveled with the dragline followed by dragging the pole rig over the surface. Sand was dumped at the dike edge and the lightweight dozer pushed the sand out over the sludge surface. Because the sand acted as a supporting mat, the small dozer was readily able to travel over the landfill while spreading the sand. Placement of the sand with the dozer was considerably faster than with the dragline.

Earth Surcharge Placement. The earth surcharge was constructed of the same soil used to build the dikes. It was obtained outside the dike area by the dragline and dumped onto the landfill surface near instrument group 7. Both the D-6 and lightweight dozers were then used to spread the soil over the required area. Some compaction occurred as the dozers operated over the surcharge. Placement required only 1-1/2 days, hence for analysis purposes the surcharge was placed essentially instantaneously. Lateral dimensions of the surcharge were selected (Figures 4.2 and 4.3) so that one-dimensional consolidation would be approximated at all instrument group locations. Field density determinations using the sand-cone method established a soil unit weight equal to 130.4 pcf for the surcharge material. Preliminary consolidation data indicated that the 3-ft thick soil layer would give time-settlement curves suitable for the project research objectives.

Instrumentation and Monitoring

The instrumentation and monitoring of the experimental sludge landfill provided information both during and after construction on vertical movements, pore water pressures, lateral earth pressures, temperature, and undrained shear strength. Instrument placement and monitoring commenced on September 10, 1971, with the installation of settlement plates in the lower sand blanket. Instrumentation of the landfill continued as construction progressed. Monitoring began with each instrument installation and was continued throughout the year. The frequency of readings was based on relative change in the observed phenomena, with the most frequent readings (2 per week) required in the first few weeks after construction. The following sections describe the settlement plates, piezometers, total pressure cells, temperature sensors, vane shear tests, and the leachate sampling and analyses.

Settlement Plates. A settlement plate consisted of a 2-ft by 2-ft by 1/8-in thick aluminum plate with 3/8-in diameter steel rods of known length attached to the center, as shown in Figure 4.6a. Additional rods of known length were added at each location as sludge placement progressed. To minimize the adhesion from the sludge on the steel rod, a 1-1/2 in O. D. aluminum tube was placed around each rod when installed. Radiator hose (1-1/2 in I. D.) provided a flexible connection for the aluminum tubing. Elevations taken with a surveyor's level (or transit) on the top of each steel rod were referenced to a bench mark outside the fill area.

Installation of the plates in a sand blanket and in the sludge is shown in Figure 4.6. First, a hole 3-ft square by 4 to 6-in deep was excavated in the sand or sludge, the bottom was tamped lightly to densify the material, and the plate was then carefully leveled using a carpenter's level. Next the settlement plate, attached rod, and aluminum tube were installed in the hole, an initial elevation reading taken on the plate, and the hole backfilled. Because the aluminum plates were light, there was no danger of their sinking into the sludge. The sludge consistency was such that a man could walk on its surface.

A total of 32 settlement plates were installed at various levels in 8 instrument groups. The distribution of settlement plates in each group is shown on Figure 4.7. The lower plate was placed at the center of the group, with each higher plate offset by 1-1/2 ft from the center so that no interference could occur between rods and higher plates. Duplicate locations served as insurance in case certain groups were accidentally destroyed during construction, and the additional data served as a check on adjacent groups. Location of each instrument group is shown on Figure 4.2.

Piezometers. Piezometers measure the static pressure or head (elevation to which water will rise in an open standpipe) of the fluid in the pore space between the solid sludge particles. The pneumatic type piezometer (Slope Indicator Company model 51401) used on this project did not require in-place calibration and was not subject to changes in sensitivity. The sensitivity of the transducer approaches 0.5 in of water. Because the sludge has a high degree of saturation, the standard Norton Casagrande type filter with large pore size and low air entry pressure was used. The transducer (Figure 4.8a) converts water pressure into pneumatic pressure which is relayed to the surface reading station by means of twin nylon tubing. Pore pressure readings were taken with the model 51421 (Slope Indicator Company) portable pore pressure indicator.

Installation of the pore pressure transducers first required excavation of a small hole in the sludge as shown in Figure 4.8b. At least

3 inches of sand and water were placed in the hole, followed by the transducer,with ample slack allowed for in the twin nylon tubing. Next, the piezometer was covered with a minimum of 3 inches more of saturated sand followed by a layer of wet sludge. The sand pocket was used because it was unknown how sludge decomposition might influence piezometer readings. The twin nylon tubes were connected to a terminal box housed in a waterproofed wooden box located at the edge of the landfill. The pore pressure measuring system appeared to function well, with no pinched or disconnected lines caused by constructions operations. The observed pore water pressure-time curves indicate that readings are consistent and that they are in agreement with duplicate piezometers.

A total of 16 piezometers were installed as part of instrument groups 5, 6, and 7. Their group identification and relative elevation is shown in Figure 4. 7, with group locations given in Figure 4. 2. Piezometers located at the same level as a settlement plate were offset about 6 to 12 inches from the plate.

Total Pressure Cells. Total pressure cells assist in determining the state of stress in the sludge mass. The model T-9010 (Terra Tec) cell consisted of two 9-inch diameter steel plates welded together at the circumference with the void filled with an incompressible oil. The oil transmits the pressure to a sensing unit consisting of a double bellow assembly. Air pressure from the control unit (Terra Tec model C 1000) is applied through a closed loop system inside the bellows to balance the external pressure. This air pressure is relayed to the surface reading station by means of twin nylon tubing. Calibration charts based on a hydraulic and a sand loading give the limits of possible pressures acting on the cell by the sludge.

Three total pressure cells were installed in the lower sludge layer near group 7 as shown in Figure 4. 7. Two of the cells were installed in the vertical position to measure horizontal stresses. The remaining unit was installed in the horizontal position to measure total vertical stresses. Its installation involved digging a hole 1 foot square by 4 inches deep into which the horizontal cell was placed. An elevation reading was taken and the hole backfilled. The vertical cells were pushed part way into the sludge at the bottom of the hole, with sludge then placed around the cell and tamped until it was firmly imbedded. An elevation reading was taken on the top edge of the cell before backfilling was completed.

Temperature Sensors. The temperature sensors are small YSI precision thermistors which are made of a material whose electrical resistance varies sharply in a known manner with temperature. Given the resistance reading, the thermistor temperature is obtained from a calibration chart. Ten YSI precision thermistors (part #44033) were mounted at 2-ft intervals on a 1-in square wooden pole. The thermistors and wooden pole were installed via a 4-in I. D. hollow core auger using a truck mounted drill rig. Since the augered hole was not expected to remain open without casing, the wooden pole was lowered through the hollow core and the auger carefully pulled up around it. The elevation of the top thermistor equals 95.43 ft, with the additional thermistors located below at 2-ft intervals. Thermistor lead wires followed the pole to the surface and then across the fill to the readout box. Resistance readings were obtained with a model 300 digital passive scalor from Western Electronics, Inc. Data indicated that 9 of the 10 thermistors were functioning properly.

Vane Shear Tests. Vane shear tests were carried out using a Geonor H-70 heavy field inspection vane borer. It is a hand operated unit that comes equipped with a torque wrench, 3 different size vanes, extension rods, and various accessories. The basic unit, as it would be set up in the field, is illustrated in Figure 3.3. Undrained shear strengths up to 12 tons/sq m can be measured with the small vane (55.9 x 111.8 mm).

The test procedure first involves driving, by hand or when needed by a sledge, the vane and claw coupling (lower part) into the sludge to the desired depth. The measurement of shear strength is then carried out in four stages for each depth. The extension-rod friction is measured by turning the torque wrench slowly clockwise through an arc a little less than 180 degrees. The rods are then rotated still further clockwise until the dog-coupling in the lower vane borer engages. The measurement of shear strength is taken by slowly turning the extension rods clockwise until the maximum shear reading is obtained. The difference between the maximum reading and the rod friction reading, with the proper conversion, equals the undrained shear strength of the sludge. The vane is then turned 20 times clockwise in order to remold the sludge adjacent to the vane and rod. The rod is then rotated 1/2 revolution conterclockwise before measuring the rod friction and shear strength of the remolded sludge using the same procedure as before.

Shear strengths were obtained at 3 elevations in the upper sludge layer and at two elevations in the lower sludge layer. Because of augering through the surcharge and upper sand blanket, the upper layer rod friction was low and difficult to read on the torque wrench. Shear strengths were relatively easy to obtain. In the lower sludge layer much greater driving resistance was encountered and rod friction became high. Vane shear strengths were obtained only at the two higher elevations in the lower sludge layer. At the lower elevation the capacity of the torque wrench would have been exceeded using the small vane.

Leachate Sampling, Analysis, and Lysimeter Study. Leachate from the experimental sludge landfill was obtained from the bottom and middle sand drainage blankets. The 8-in iron pipe running from the bottom sand blanket (Figures 4.2 and 4.3) to a pond some 400 ft to the northwest served as the initial source of leachate. Considerable iron contamination of the leachate was observed. This fact, plus dilution of leachate from surface runoff, prompted the installation of a wellpoint in the middle sand drainage blanket.

The mid-depth sample point consisted of a 1-1/2-in diameter galvanized pipe noted on Figure 4.2 and was extended into the middle sand blanket as shown on Figure 4.3. A 12-volt electric marine bilge pump was used to obtain samples from the wellpoint. Samples were shipped in small plastic cubitainers once a week to the NCASI Central-Lake States Regional Center in Kalamazoo, Michigan.

Analyses conducted on the leachate and percolate from the lysimeters are shown in the schematic, Figure 4.10. All analyses were conducted according to Standard Methods for the Examination of Water and Wastewater, 13th edition, except for color. Color determinations were conducted according to the procedures outlined in NCASI Technical Bulletin No. 253, "An Investigation of Improved Procedures for Measurement of Mill Effluent and Receiving Water Color."

Lysimeters were constructed as shown in Figure 4.9 and consisted of 3-ft acrylic tubes (4-in O.D. by 1/8-in wall). A plate was placed in the bottom with a drain hole. Sand was placed in the bottom of the tube and glass wool was placed on top. Columns were then filled with soil.

Six columns were constructed: four containing organic loam, one clay, and one sand. After construction all columns were initially washed with distilled water to moisten the soil and permit some compaction so as to minimize the possibility of channeling. One of the organic loam columns was set up to simulate anaerobic conditions, as shown in Figure 4. 9b. The conditions present under the landfill are not known, so aerobic and anaerobic conditions were required to establish data for the two types of environment. Air was prevented from entering the top of the column by use of a rubber stopper and a glass U-tube. Leachate remains in the U-tube and restricts diffusion of oxygen into the system. The exit tube is maintained submerged at all times to further minimize oxygen diffusion.

Flow rates to the lysimeters were based on dry weather flow rates from the landfill. It was assumed that all of the leachate from the landfill exited by the lower pipe drain. Flow rates obtained from this pipe drain were converted into units of ml/sq in/day using the base area of the landfill and appropriate conversion factors. The area, in square inches, of the lysimeter columns were calculated and application rates determined. All columns but one received 45 ml/day.

It was noted that flow rates from the landfill increased during periods of precipitation. Since this increased the amount of leachate to the ground under the landfill, it was felt a lysimeter column should be set up simulating these higher flow rates. The highest flow rate observed from the landfill was doubled, yielding a flow rate to the lysimeter of 180 ml/day.

Leachate from the pipe source was applied to all columns except one. This procedure was followed because a larger volume of sample could be obtained from the pipe source. At first, the wellpoint for the mid-depth source yielded only a small amount of leachate. As time passed a larger sample volume could be obtained. Around the middle of June, 1972, pipe samples were no longer obtainable since the pond, which had begun to fill due to heavy rainfall, covered the end of the pipe. After June 23 (129th day of the project), only mid-depth samples were applied to the lysimeter columns.

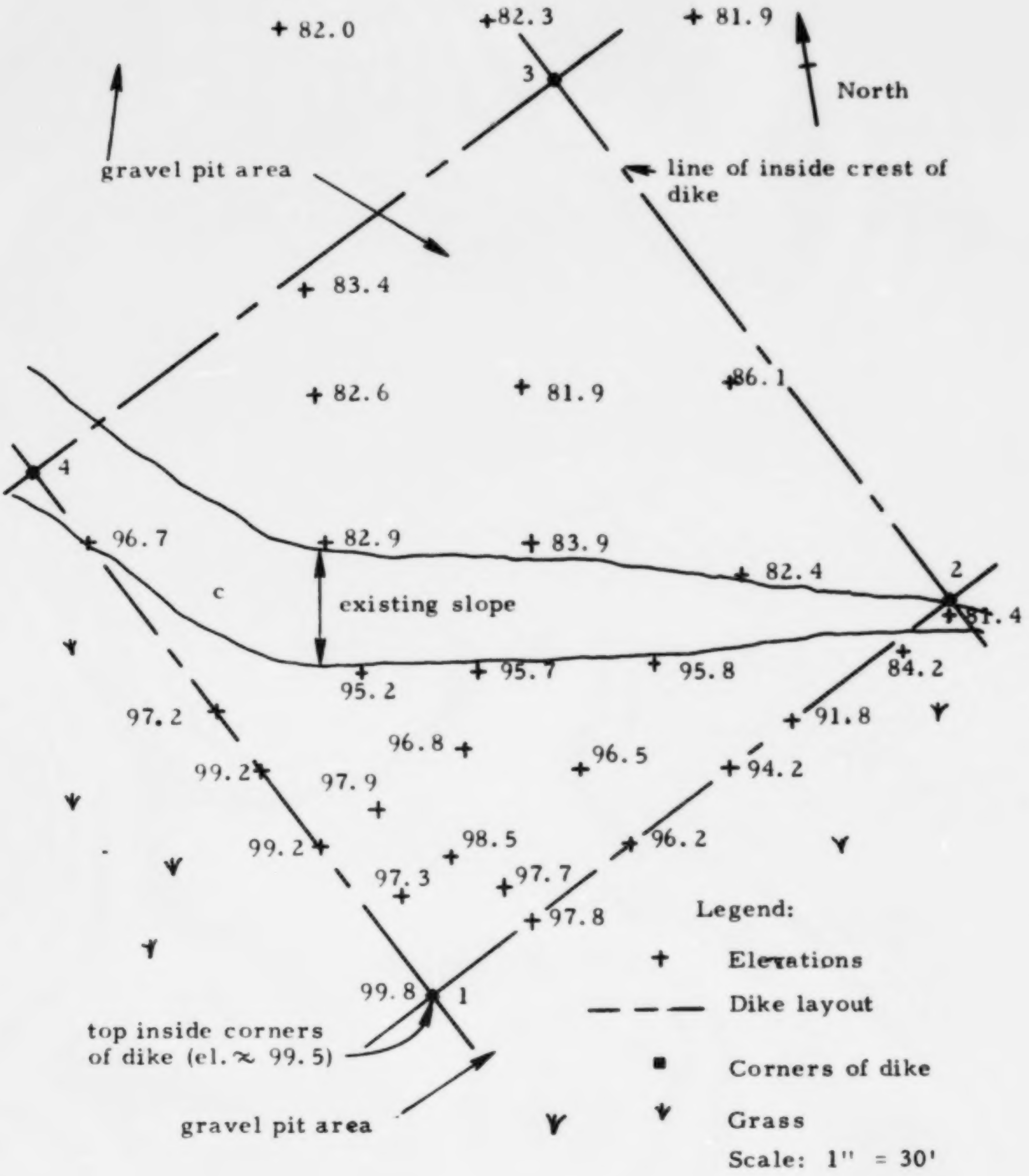
+ 82.0
+82.3
+ 81.9
North
3
gravel pit area
line of inside crest of dike
+ 83.4
+ 82.6
+ 81.9
+86.1
4
+ 96.7
+ 82.9
+ 83.9
+ 82.4
2
c
existing slope
+81.4
+ 95.2
+ 95.7
+ 95.8
+ 84.2
97.2 +
+ 91.8
96.8 +
+ 96.5
+ 94.2
99.2 +
97.9 +
99.2 +
+ 98.5
+ 96.2
97.3 +
+ 97.7
+ 97.8
99.8
1
top inside corners of dike (el. ≈ 99.5)
gravel pit area
Legend:
+ Elevations
— — — Dike layout
■ Corners of dike
Y Grass
Scale: 1" = 30'

Assumed elevation datum top
of gas line marker = 100.00 ft.

4.1. Pre-construction map of existing gravel pit area including dike layout.

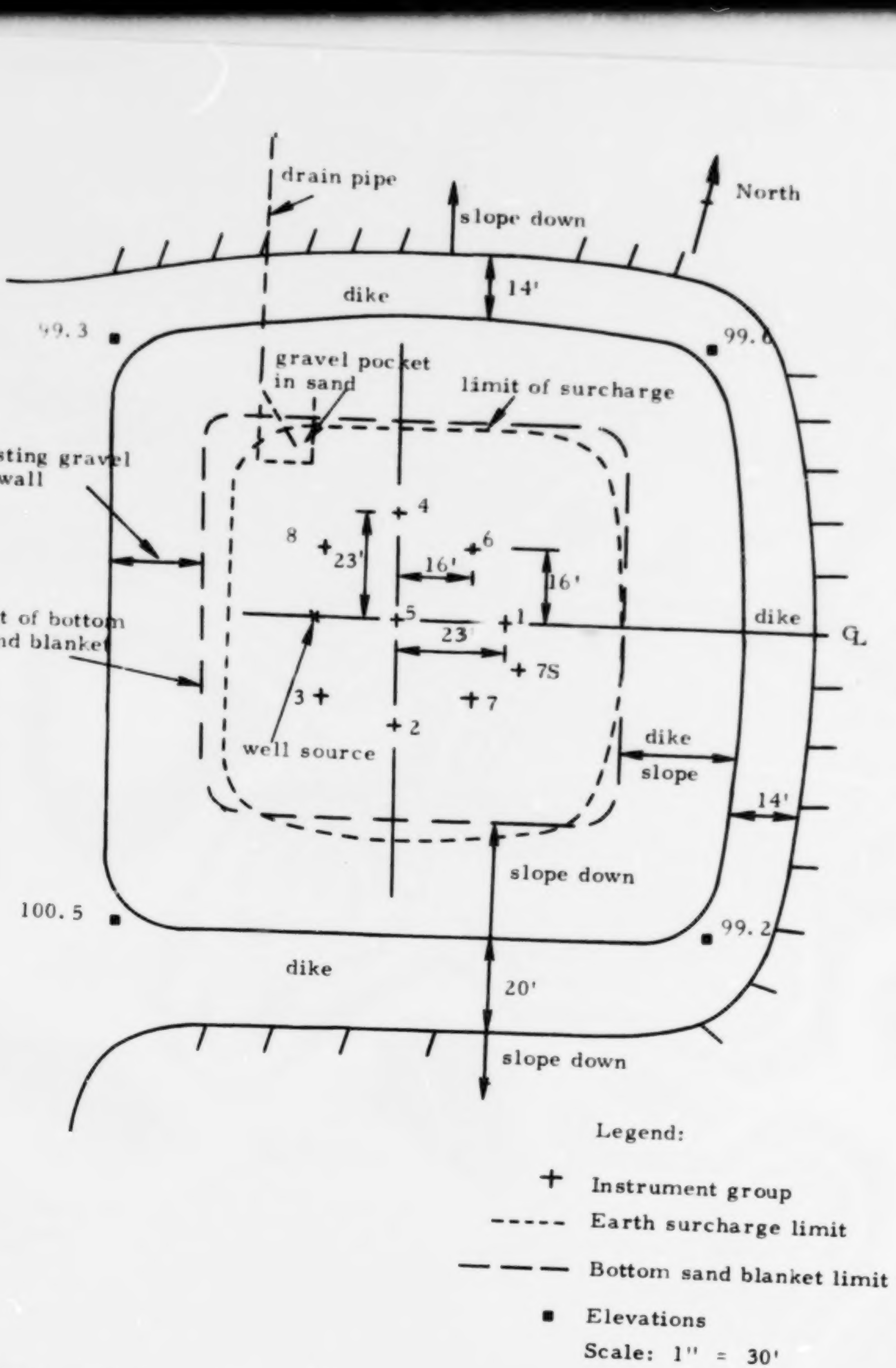
drain pipe
slope down
North
14'
dike
99.3
99.6
gravel pocket
in sand
limit of surcharge
existing gravel
pit wall
4
8
23'
6
16'
16'
limit of bottom
sand blanket
5
1
dike
℄
23'
7S
3
7
2
well source
dike
slope
14'
slope down
100.5
99.2
dike
20'
slope down
Legend:
Instrument group
Earth surcharge limit
Bottom sand blanket limit
Elevations
Scale: 1" = 30'

Figure 4.2. Experimental landfill and instrument group locations, plan view.

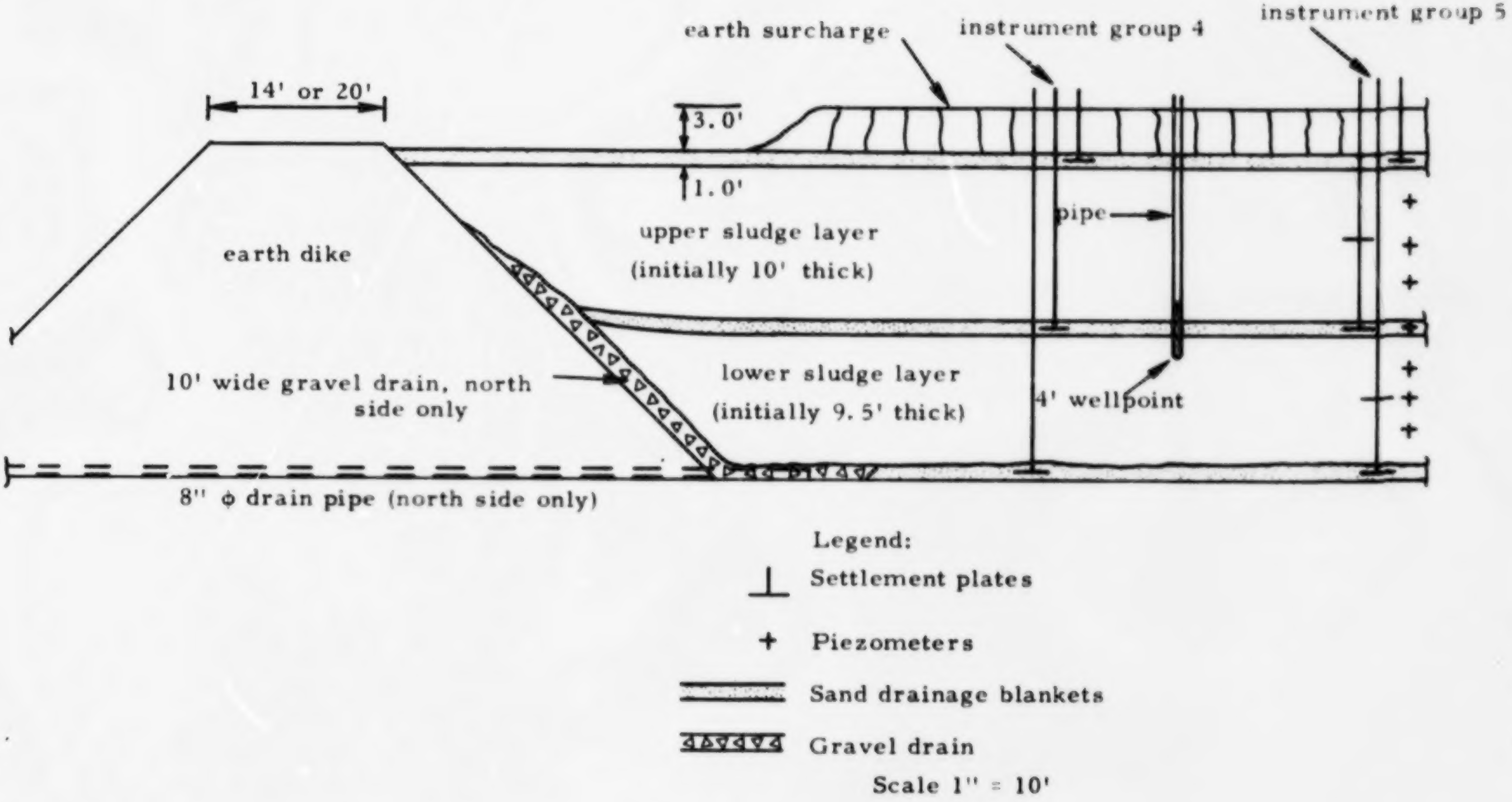
earth surcharge
instrument group 4
instrument group 5
14' or 20'
3.0'
1.0'
pipe
earth dike
upper sludge layer
(initially 10' thick)
10' wide gravel drain, north side only
lower sludge layer
(initially 9.5' thick)
4' wellpoint
8" ϕ drain pipe (north side only)
Legend:
⊥ Settlement plates
+ Piezometers
Sand drainage blankets
Gravel drain
Scale 1" = 10'

Figure 4.3. Section of landfill (typical), north dike at end of construction.

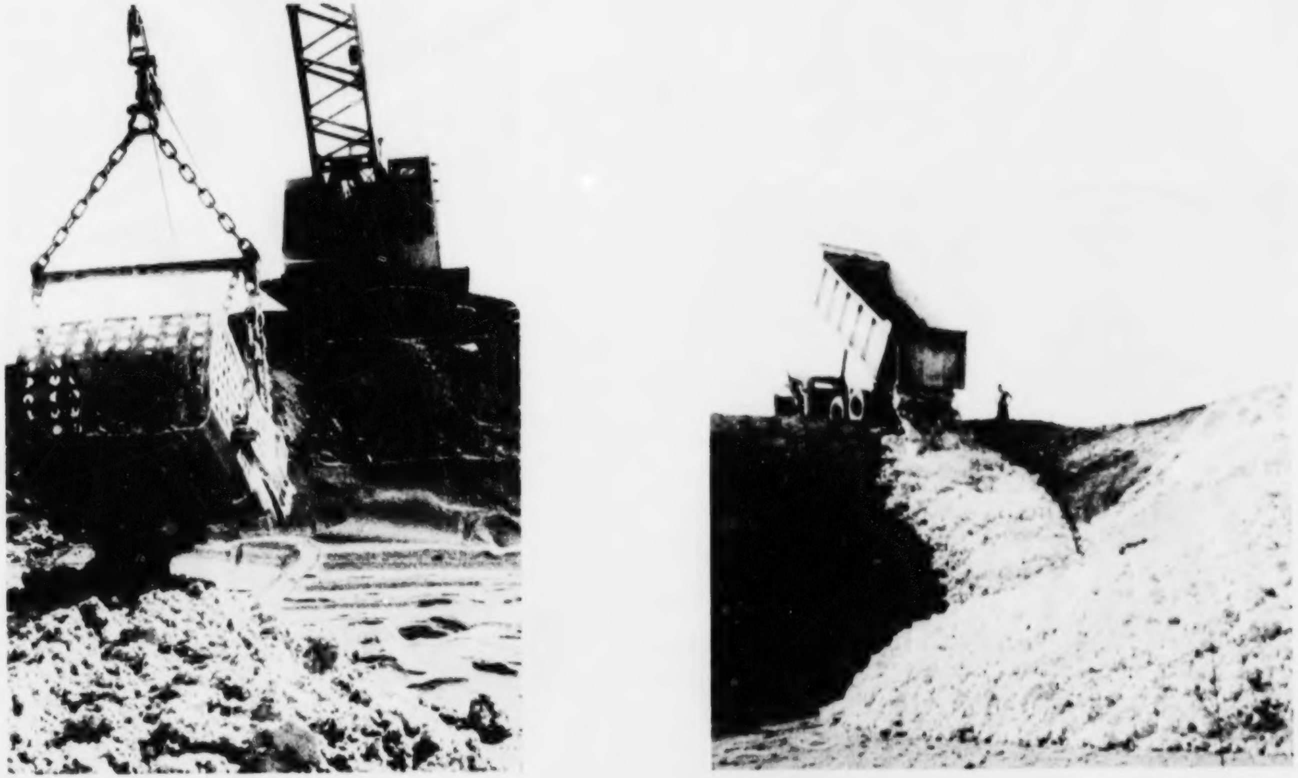

(a) Dragline operation.

(b) Dumping over the dike sides.

Figure 4. 4. Sludge placement.

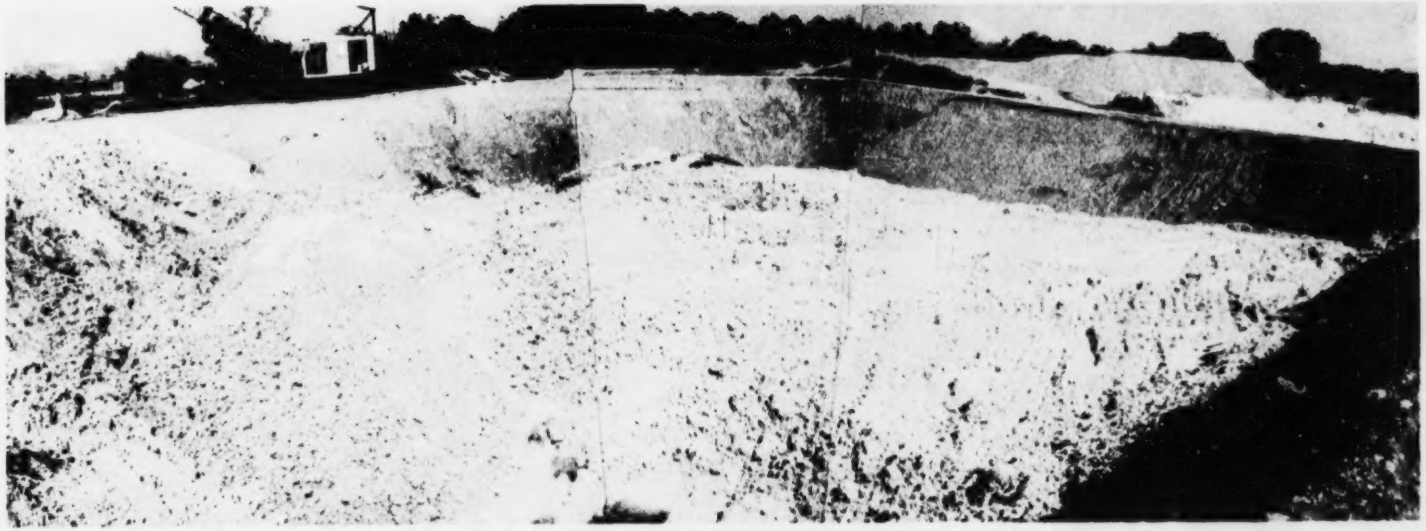

Figure 4.5. Experimental sludge landfill during placement of the lower sludge layer.

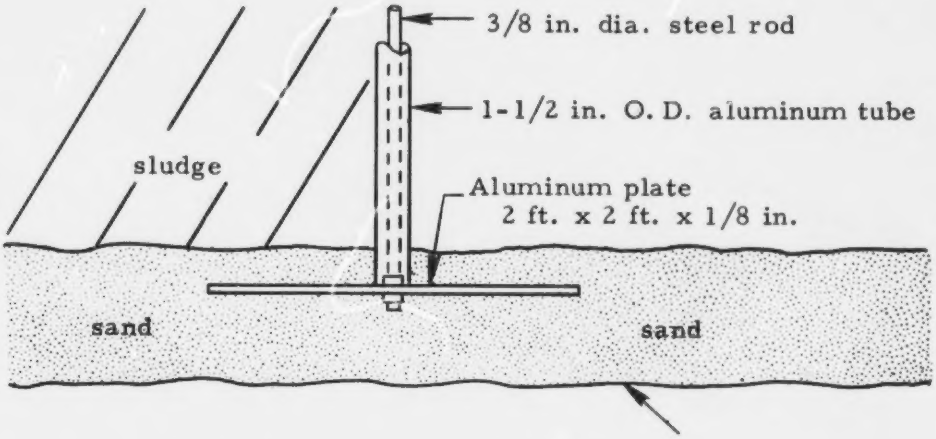
3/8 in. dia. steel rod
1-1/2 in. O.D. aluminum tube
sludge
Aluminum plate
2 ft. x 2 ft. x 1/8 in.
sand
sand

(a) Installation in a sand blanket.

(b) Placement in the sludge, carpenters level shown on the plate.

Figure 4.6. Settlement plate.

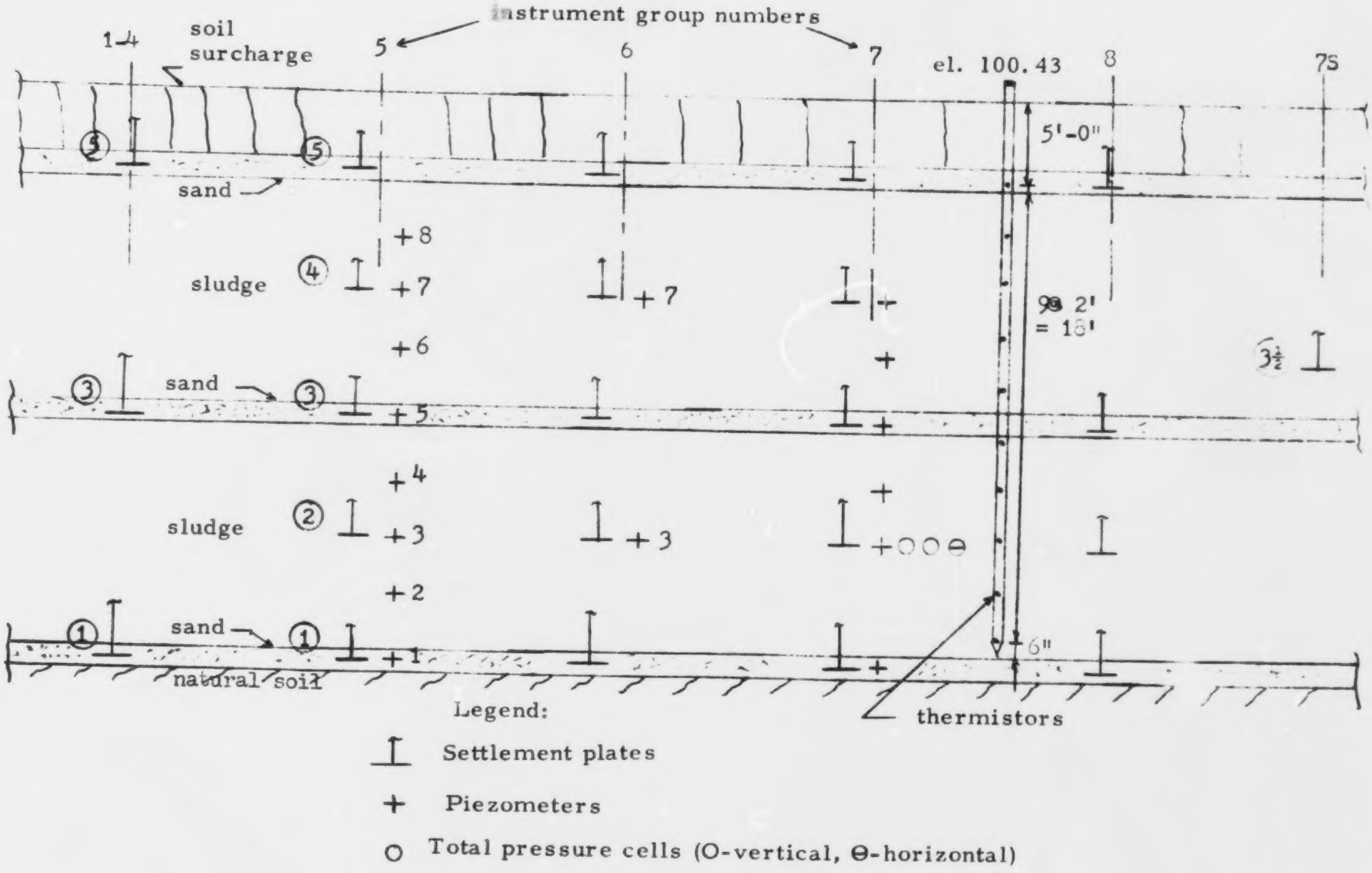
instrument group numbers
1-4
soil surcharge
5
6
7
el. 100.43
8
75
5'-0"
9@ 2' = 18'
6"
sand
sludge
sand
sludge
sand
natural soil
thermistors
①
②
③
④
⑤
+8
+7
+6
+5
+4
+3
+2
+1
3½
Legend:
Settlement plates
Piezometers
Total pressure cells (O-vertical, Θ-horizontal)

Figure 4.7. Distribution of settlement plates, piezometers, and total pressure cells in the instrument groups.

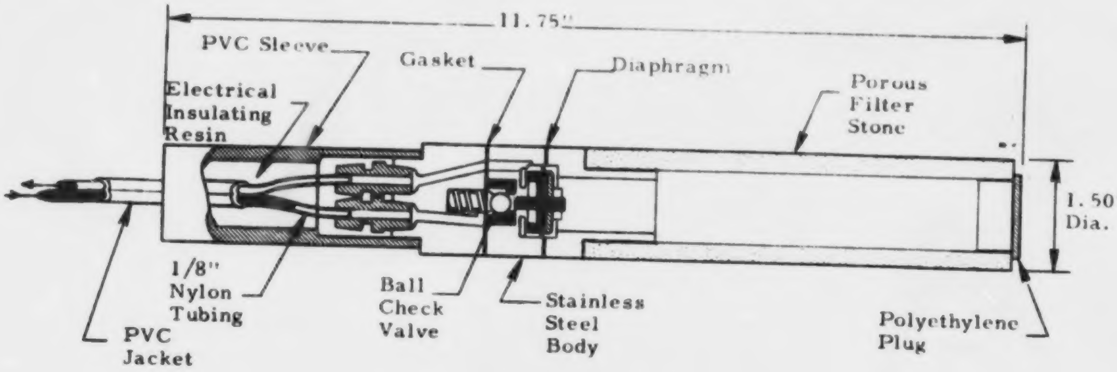
11.75"
PVC Sleeve
Gasket
Diaphragm
Porous Filter Stone
Electrical Insulating Resin
1.50" Dia.
1/8" Nylon Tubing
PVC Jacket
Ball Check Valve
Stainless Steel Body
Polyethylene Plug

(a) Pore pressure transducer.

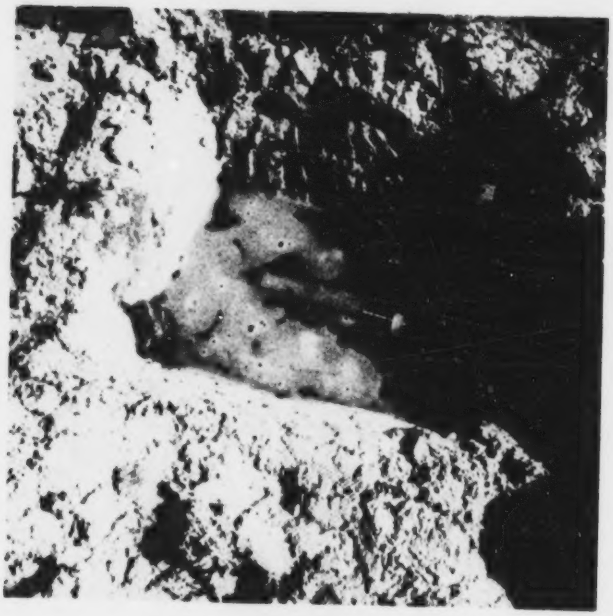

(b) Installation in a small sand pocket in the sludge.

Figure 4.8. Piezometer.

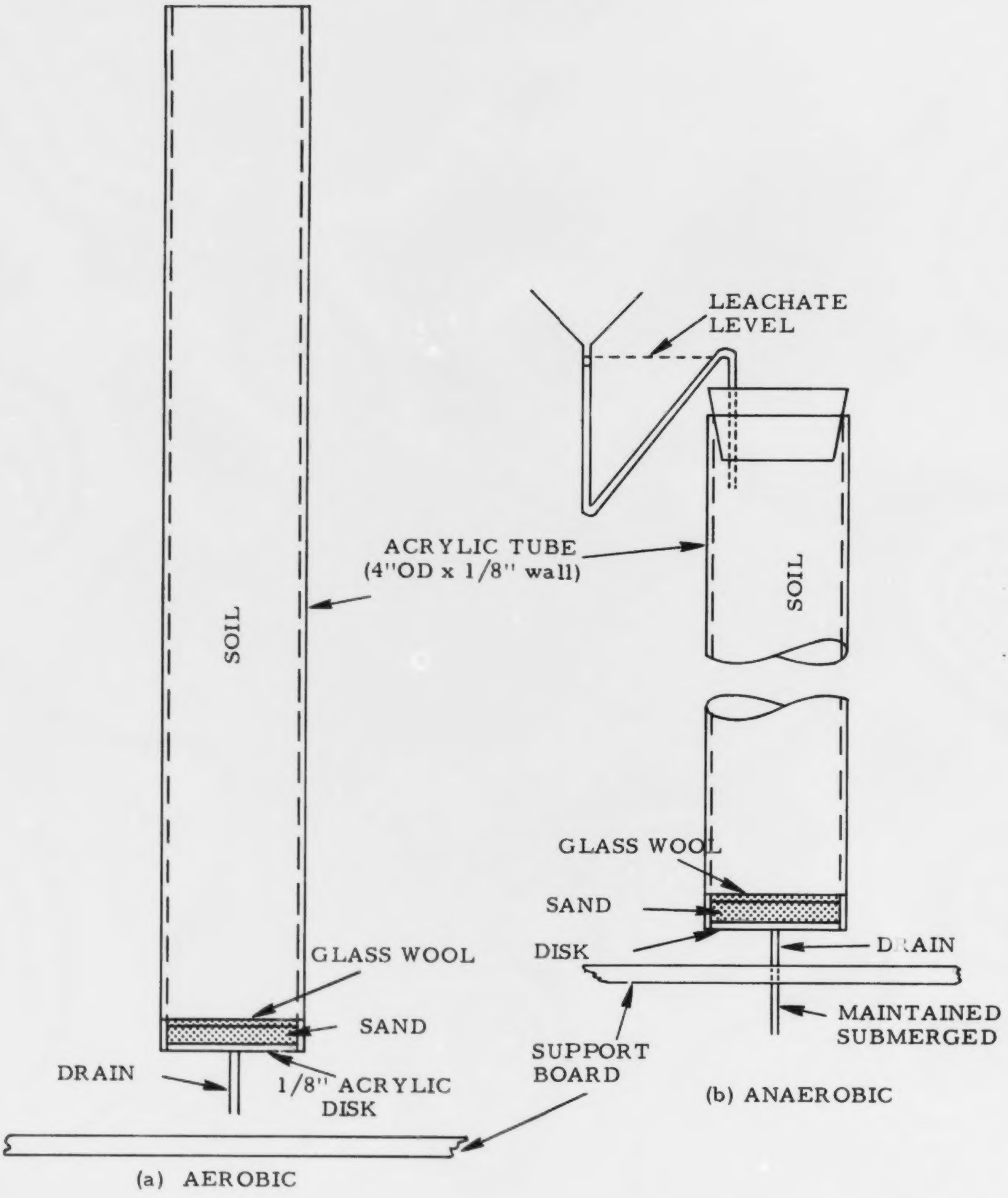
SOIL
ACRYLIC TUBE (4"OD x 1/8" wall)
GLASS WOOL
SAND
DRAIN
1/8" ACRYLIC DISK
(a) AEROBIC
LEACHATE LEVEL
SOIL
GLASS WOOL
SAND
DISK
DRAIN
SUPPORT BOARD
MAINTAINED SUBMERGED
(b) ANAEROBIC

Figure 4.9. Diagram of lysimeter.

FIGURE 4.10

SCHEMATIC OF ANALYSES CONDUCTED ON LEACHATE AND LYSIMETER PERCOLATES

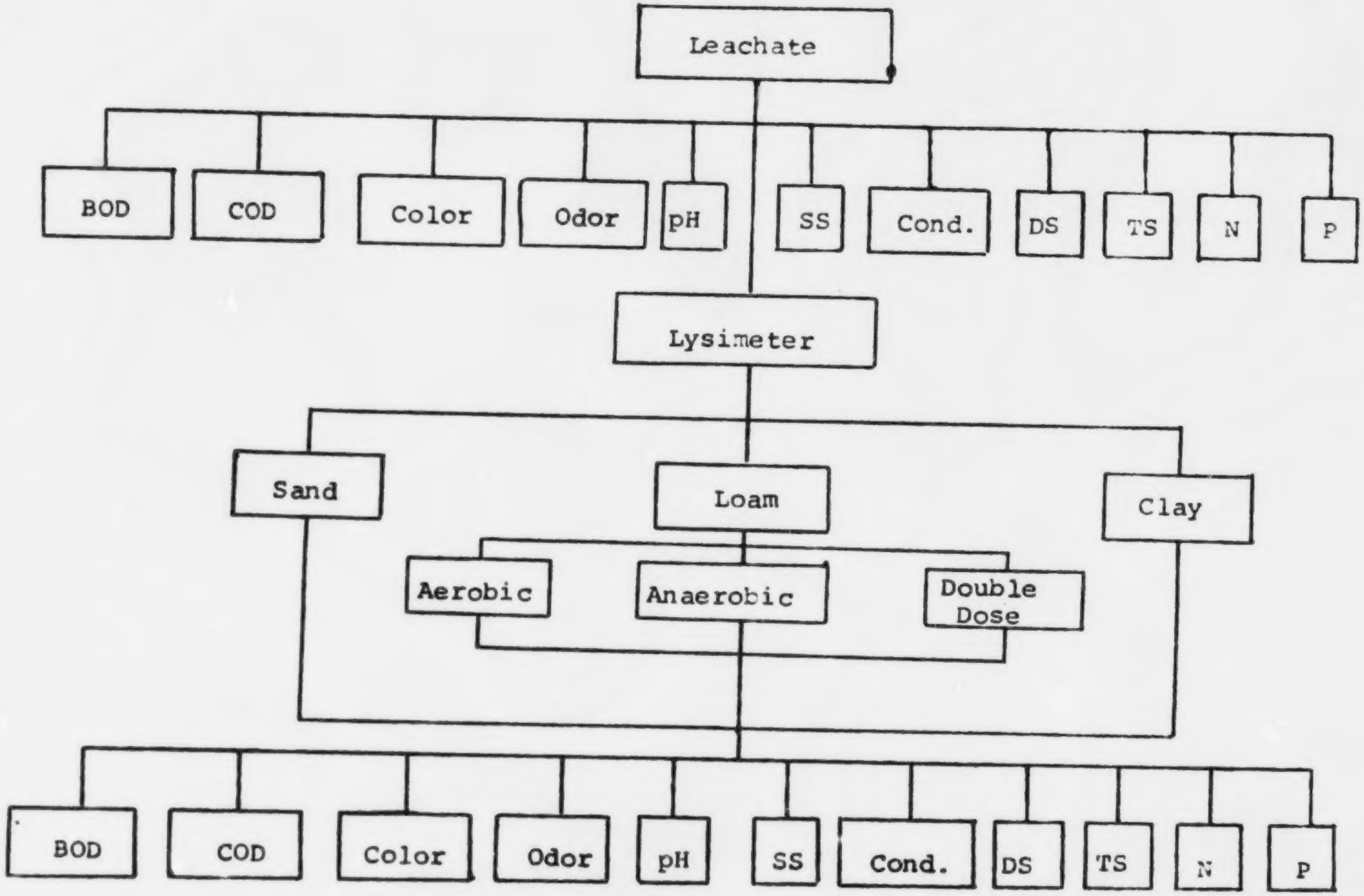
Leachate
BOD
COD
Color
Odor
pH
SS
Cond.
DS
TS
N
P
Lysimeter
Sand
Loam
Clay
Aerobic
Anaerobic
Double Dose
BOD
COD
Color
Odor
pH
SS
Cond.
DS
TS
N
P

Chapter V. EXPERIMENTAL RESULTS

The experimental results are presented under four headings: physical properties of the papermill sludge, stress-deformation behavior of the sludge, field monitoring, and leachate analysis and lysimeter study. Each section may include both laboratory test data and field observations.

Physical Properties of the Papermill Sludge

Physical properties of the papermill sludge used in the experimental landfill are summarized in Table 5.1. Properties given include the liquid and plastic limits, ash content, solids content, and specific gravity. Of the eight samples listed, data shown for samples L-1 and L-2 each represent the average of three different locations at the given elevation. Data shown for samples U-1 through U-5 represent the average of three tests on each sludge sample obtained from one given location. The sludge variability within the landfill is apparent for samples U-1 through U-5, although the average ash content (41.8 percent) is close to that for samples 2 and 3. The initial solids content shown in Table 5.1 range from 26.9 to 34.4 percent by weight. Using equation 3.1, the equivalent water contents range from 190.7 to 271.7 percent. Additional water content samples taken at several instrument group locations and elevations are summarized in Table 5.2. These water contents appear to fall in the vicinity of the liquid limit. Bulk unit weight of the papermill sludge was 69.7 lb/cu ft based on the weight and volume of a truck box full of sludge. Using a standard 1/10 cu ft bucket and careful hand placement, the observed bulk unit weight equals 69.0 lb/cu ft. For the soil surcharge material, the sand cone method gave a bulk unit weight of 130.4 lb/cu ft.

Stress-Deformation Behavior of the Sludge

Laboratory consolidation tests were run on samples of sludge to determine parameters needed for estimating settlement of the landfill. In-place vane shear tests provided data on the undrained shear strength of the sludge at various stages of consolidation.

Laboratory Consolidation. Results from one-dimensional consolidation tests on sludge samples from four different locations are summarized

Preceding page blank

in Table 5.3 in terms of the coefficient of consolidation c_v, primary compression ratio r, coefficient of secondary compression C_α, and the compression index C_c. Based on the average placement water contents (Table 5.2), sludge samples U-3 and L-2 (Table 5.1) appear to be reasonably representative of the sludge in the landfill. Data for several single increment tests, such as those recommended by MacFarlane (1969) for peat, are included. The earlier tests, including U-4-1, U-3-1 through U-3-9, and L-2-1 were run using the fixed ring container and the loading methods illustrated in Figures IX-5a and IX-4 in SOIL TESTING FOR ENGINEERS by T. W. Lambe (1951). The remaining tests, U-3-10 through U-3-12 and L-2-2, were run on the Bishop consolidation machine. The latter tests were less subject to minor equipment errors. Data from test U-3-10 are used in Figure 5.1 to show the consolidation characteristics of the sludge and include the void ratio, coefficient of consolidation, and primary compression ratio plotted against the logarithm of total effective stress. The high compression index, C_c, equal to 1.70 represents a highly compressible material. Coefficient of consolidation values from both the logarithm of time and square root of time fitting methods are included for comparison. The primary compression ratio shows a sharp drop after the first load increment followed by an increase with subsequent load increments. This initial drop in r for loads of 0.1 to 0.2 kg/cm^2 appears to be characteristic of the sludge. Two typical compression dial reading-logarithm of time curves are shown in Figure 5.2. The coefficient of secondary compression, C_α, shown in Figure 5.3a, increases slightly over the total effective pressure range of 0.1 to 3.2 kg/cm^2. Since stress appears to be a factor in determining the magnitude of secondary compression (MacFarlane, 1969; Leonards and Girault, 1961), the ratio of C_α to the load increment, Δp, is presented in Figure 5.3b. The ratio $C_\alpha / \Delta p$ decreases rapidly with increase in load increment.

In-Place Vane Shear Tests. Test procedures for measurement of the in-place vane shear strength of the sludge are given in chapter IV. Vane shear strengths taken after completion of each sludge layer and after partial consolidation are summarized in Figure 5.4. Some consolidation occurred during placement of each sludge layer, hence an increase in strength with depth was observed before placement of the second sludge layer and before placement of the surcharge load. The degree of sensitivity, defined as the ratio of the undisturbed to the remolded shear strength is small, ranging from about 1.5 to 2.5, very similar to many clays (Terzaghi and Peck, 1967). Both layers increased substantially in strength during consolidation, as shown by data taken on March 20, 1972 (Figure 5.4).

Field Monitoring

Field monitoring involved making observations of elevations from settlement plates, pore water pressures from piezometers, temperature from thermistors, and both horizontal and vertical pressures from total pressure cells. Figures and graphs are used to summarize the tabulated data which are given in Appendices A through D. The results are presented under headings including settlement, pore water pressures, temperatures, and lateral sludge pressures.

Settlement. Time-settlement curves for each instrument group are shown in Figure 5.5a through 5.5h for both the upper and lower sludge layers. The upper part of the figure shows the landfill surface elevation, both during construction and during consolidation, as a function of time. Also shown at different times are the vertical locations of the settlement plates and the relative thickness of each portion of the sludge landfill. Notation on Figure 5.5, such as ⑤ - ③ , indicates that the settlement of plate ③ has been subtracted from the total settlement of plate ⑤ , in this case giving the time-settlement curve for the upper sludge layer.

On completion of the upper sludge layer, rapid placement of the top sand drainage blanket and surcharge load (1-1/2 days) gave an approximation to instantaneous loading. The settlement versus square root of time curves for the top sludge layer are presented in Figure 5.6a and 5.6b for each instrument group. The initial point is not at zero since some compression of the layer occurred during placement of the sand blanket and surcharge load. The data plotted represent observations taken after completion of the surcharge placement, and give square root of time plots similar to those observed in the conventional consolidation test. Values for the coefficient of consolidation, c_v, backfigured from these plots, are fairly large and vary some for the different instrument group locations. Settlement-logarithm of time curves for the upper and lower sludge layers are shown in Figure 5.7 and 5.8 for each instrument group.

Pore Water Pressures. Piezometers used for measurement of pore water pressures gave the data summarized in Figure 5.9a through 5.9g. Pore pressures are plotted against time in the lower half of Figure 5.9, with the location of the piezometer in the landfill given in the upper half. Observed pore pressures in both layers show a consistent increase with time during placement of the sludge. An abrupt increase in pore pressure occurs during the rapid placement of the surcharge load followed by dissipation to some residual value, perhaps related to a threshold hydraulic gradient required for flow. In the upper sludge layer the observed pore pressure increase at the center of the layer is close in magnitude to the applied pressure due to placement of the top sand blanket and earth surcharge load. During the later stages of consolidation some fluctuations with time occur for piezometers in the upper sludge layer and middle sand blanket. High rainfall followed by seepage into the drainage blankets appears to be responsible for this pore pressure fluctuation. The pore pressure in the middle sand blanket (Figure 5.9g) is the result of a dish effect produced by greater consolidation in the central area of the sludge landfill. Field data are given in Appendix B.

Temperature. Thermistors used for temperature measurement gave the data summarized in Figure 5.10. An increase in temperature caused by biological activity is observed, with the higher values occurring in the lower sludge layer about 50 days after completion of the landfill. Subsequent temperatures show a pattern indicating that the sludge is responding to atmospheric and ground temperatures. Inconsistent temperatures for thermistor 2 indicate a malfunction or damaged unit. Field data are given in Appendix D.

Lateral Sludge Pressures. Total pressure cells installed in the lower sludge layer gave the data summarized in Figure 5.11 for both total lateral and vertical pressures. Pore water pressure data from an adjacent piezometer are included on Figure 5.11 so as to permit computation of effective lateral and vertical pressures. Total pressures increased gradually during sludge placement and increased sharply during placement of the earth surcharge load. Subsequently it required about 2 months for the lateral pressures to stabilize at a lower value. The total observed vertical pressure shows an additional unexplained increase after surcharge placement, opposite to what would be expected as leachate drained from the sludge landfill. Data for pressure cell G7-2 have been omitted from Figure 5.11 because instrument readings indicated a malfunction. Field data are given in Appendix C.

Leachate Analysis and Lysimeter Study

Leachate samples were obtained weekly, weather permitting, from the experimental papermill sludge landfill. The two sources were designated as pipe leachate (PL) and mid-depth well leachate (WL). Analyses shown on Figure 4.11 were conducted on the leachate with the remaining leachate applied to the lysimeter columns containing the organic loam, sand, and clay soils. Lysimeter columns are designated by the soil and the source of leachate being applied. Anaerobic and aerobic conditions are also specified where required.

The well leachate (WL) was applied to only one column of organic loam (topsoil) and has been designated as well topsoil (WT). The pipe leachate (PL) was applied to the remaining five lysimeter columns. The sand column was designated pipe sand (PS) and the clay column as pipe clay (PC). The organic loam column used to stimulate high flow rates was designated double dosage pipe topsoil (DPT). The remaining two organic loam columns were used for the aerobic and anaerobic conditions, one designated as pipe topsoil aerobic (PTA) and the other pipe topsoil anaerobic (PTAN).

Chemical oxygen demand (COD), biological oxygen demand (BOD), turbidity (Turb.), specific conductance (Spec. Cond.), total solids (TS), dissolved solids (DS), and suspended solids (SS) data from the analyses of of leachate and lysimeter percolate are plotted against time in Figures 5.12 through 5.36. Some curves for well and pipe leachate are shown with broken lines because changes in the leachate composition did not appear gradually for samples taken at certain intervals of time. Dilution of the pipe leachate after each rainfall was partly responsible for this. In most cases, only data for a particular sample are connected by a solid curve. Values for the various analyses on the well leachate are much higher for the first 20-30 days as compared to the remainder of the project. During installation, fiber and other solids perhaps were forced through the wellpoint giving a larger solids concentration to the initial well leachate samples. Most of the soil columns went through an acclimation period, during which less efficient results were obtained. The sand and clay columns exhibited slightly longer acclimation periods since they were not as biologically active as the organic loam.

TABLE 5.1 PHYSICAL PROPERTIES OF THE PAPERMILL SLUDGE

Sludge sample		Consistency limits[1]		Ash[2] content %	Solids[3] content % by wt.	Specific[4] gravity
No.	Elevation in layer, ft.	L_w	P_w			
L-0 8	5	325.4	141.6	35.7	28.5	2.01
L-1*	2.5	257.3	102.7	42.2	27.2	2.05
L-2*	7.5	247.7	105.6	43.3	28.2	2.07
U-1⁺	2.5	184.5	86.0	59.4	34.4	2.24
U-2⁺	4	218.5	101.6	46.5	31.9	2.07
U-3⁺	5	297.5	133.0	36.5	26.9	1.91
U-4⁺	7.5	287.4	122.1	34.2	29.0	1.87
U-5⁺	10	302.8	138.6	32.2	28.4	1.92

*Average of three samples. ⁺Average of 3 tests per sample location.

[1] L_w--liquid limit. P_w--plastic limit. ASTM test methods D 423-66 and D 424-59.

[2] ASTM test method D 586-63.

[3] Solids content of fresh sludge. Water content by dry weight given by the equation

$$w\% = 100 \left[\frac{100}{\%\ \text{solids by wt.}} - 1 \right].$$

[4] ASTM test method D 854-48.

Laboratory test sample locations.

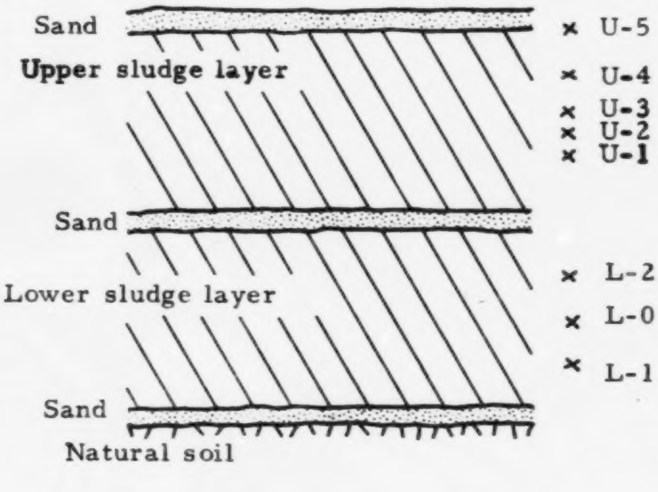
Sand
Upper sludge layer
Sand
Lower sludge layer
Sand
Natural soil
× U-5
× U-4
× U-3
× U-2
× U-1
× L-2
× L-0
× L-1

TABLE 5.2 SLUDGE PLACEMENT WATER CONTENTS

Elevation in layer (ft)	Group No.							
	1	2	3	4	5	6	7	8
		Lower	Sludge	Layer				
2.5	-	-	-	-	242 277	292	-	-
3.0	-	282	-	284	230 245	-	283	-
4.0	-	-	308	270	-	-	276	298
5.0	-	-	-	-	261 283 264	269 240 271 226	262 265 262	213 244 219 253
7.5	-	-	-	279 267	267 266 252 265 253 257	-	-	-
8.0	-	-	274 291	274	273 264	-	271 246 258 256	-
9.0	-	-	278 294	275	-	-	-	-
10.0	-	-	-	-	280 267 276 255	-	-	-
		Upper	Sludge	Layer				
2.5	262 260 262 262	-	-	-	268 248	-	270 270 270 290	-
3.0	-	-	-	-	251 262	-	-	-
6.0	-	-	-	-	251 284 264 276	279 264 278 277	244 262 271 261	-
7.5	-	-	-	-	235 256 257 232	254 237 234 269	232 234 224 212	-

Oven temperature 105°C.

Average initial water and solids content:

Lower sludge layer	265.1%,	27.4%
Upper sludge layer	257.3%,	28.0%

TABLE 5.3 SUMMARY OF CONSOLIDATION CHARACTERISTICS

Sludge		Load increment (kg/cm^2)	c_v $(in^2/min.)$		r	C_α	C_c or remarks	e_o
Sample No.	Test No.		log t	$\sqrt{t}$				
U-4	1*	0 - ¼	0.033	0.035	0.87	0.00737	1.73	4.67
		¼ - ½	0.028	0.030	0.79	0.0112		
		½ - 1	0.024	0.019	0.77	0.0136		
		1 - 2	0.0067	0.0067	0.74	0.0128		
		2 - 4	0.00826	0.0095	0.87	0.0144		
		4 - 8	0.00462	0.00538	0.79	0.0167		
		8 - 16	0.00162	0.00463	0.95	0.0102		
U-3	1*	0 - 0.1	0.0133	0.0134	0.86	0.00791	1.38	5.42
		0.1 - 0.2	0.0178	0.0228	0.76	0.00945		
		0.2 - 0.4	0.0211	0.0207	0.80	0.00768		
		0.4 - 0.8	0.0221	0.0180	0.84	0.00584		
		0.8 - 1.6	--	--	--	--		
		1.6 - 3.2	0.0164	0.0175	0.83	0.00932		
U-3	3*	0 - 0.1	0.0162	0.0160	0.74	0.00907	1.24	5.21
		0.1 - 0.2	0.0161	0.0174	0.71	0.00943		
		0.2 - 0.4	0.0216	0.0216	0.63	--		
		0.4 - 0.8	0.0348	0.0312	0.70	0.00572		
		0.8 - 1.6	0.0233	0.0266	0.87	0.00500		
		1.6 - 3.2	0.0183	0.0167	0.83	0.00947		
U-3	4*	0 - 0.239	0.0154	0.0185	--	0.00567	1 increment, 24-hr.	5.64
U-3	5*	0 - 0.239	0.0245	0.0187	--	0.00720	1 increment, 24-hr.	5.40
U-3	6*	0 - 0.239	0.0264	0.0215	--	0.0103	1 increment, 24-hr.	5.48
U-3	7*	0 - 0.1	0.0101	0.00985	0.80	0.00905	1.13	5.67
		0.1 - 0.2	0.0124	0.0166	0.82	0.00604		
		0.2 - 0.4	0.0121	0.0105	0.86	0.00361		
		0.4 - 0.8	0.0145	0.0128	0.83	0.00450		
		0.8 - 1.6	0.0216	0.0304	0.92	0.00375		

*Load frame similar to Figure IX-4, Lambe, 1951. +Bishop type consolidation machine, Figure 3.2.

c_v - coefficient of consolidation, t - time, r - primary compression ratio,

C_α - coefficient of secondary compression, C_c - Compression index, e_o - initial void ratio.

TABLE 5.3 SUMMARY OF CONSOLIDATION CHARACTERISTICS (cont'd.)

Sludge		Load increment	c_v (in^2/min.)		r	C_α	C_c or remarks	e_o
Sample No.	Test No.	(kg/cm^2)	log t	$\sqrt{t}$				
U-3	8*	0 - 0.1	0.0148	--	0.83	0.00780	1.24	5.26
		0.1 - 0.2	0.0244	0.0277	0.68	0.00928		
		0.2 - 0.4	0.0099	0.010	0.84	0.00642		
		0.4 - 0.8	--	--	--	--		
		0.8 - 1.6	0.0284	0.0317	0.80	0.00645		
		1.6 - 3.2	0.0194	0.0197	0.82	0.00960		
U-3	9*	0 - 0.1	0.00646	0.00584	0.88	0.0115	1.41	5.97
		0.1 - 0.2	0.00938	0.00846	0.74	0.0111		
		0.2 - 0.4	0.00537	0.00456	0.80	0.0114		
		0.4 -0.8	0.0265	0.0353	0.77	0.00551		
		0.8 - 1.6	0.0158	0.0168	0.84	0.00704		
		1.6 - 3.2	0.00882	0.00906	0.88	0.00827		
L-2	1*	0 - 0.1	0.00945	0.00860	0.86	0.0106	1.27	5.34
		0.1 - 0.2	0.0125	0.0191	0.78	0.00962		
		0.2 - 0.4	0.0136	0.0202	0.73	0.00803		
		0.4 - 0.8	0.0113	0.0106	0.92	0.00314		
		0.8 - 1.6	0.0143	0.0228	0.81	0.00815		
		1.6 - 3.2	0.0136	0.0180	0.86	0.00715		
U-3	10+	0 - 0.1	0.0151	0.0155	0.80	0.0128	1.70	5.35
		0.1 - 0.2	0.0135	0.0147	0.62	0.0167		
		0.2 - 0.4	0.0087	0.0130	0.69	0.0169		
		0.4 - 0.8	0.00643	0.00875	0.76	0.0182		
		0.8 - 1.6	0.00506	0.00718	0.77	0.0182		
		1.6 - 3.2	0.00336	0.00595	0.79	0.0171		
U-3	11+	0 - 0.25	0.0175	0.0149	0.83	0.0147	1 increment, 1-wk.	5.25
U-3	12+	0 - 0.1	0.0157	0.0153	0.83	0.0126	1.56	5.14
		0.1 - 0.2	0.0130	0.0127	0.59	0.0140		
		0.2 - 0.4	0.00994	0.0115	0.60	0.0195		
		0.4 - 0.8	0.00645	0.0117	0.74	0.0176		
		0.8 - 1.6	0.00500	0.00714	0.77	0.0202		
		1.6 - 3.2	0.00364	0.00613	0.77	0.0183		

TABLE 5.3 SUMMARY OF CONSOLIDATION CHARACTERISTICS (cont'd)

Sludge		Load increment (kg/cm^2)	c_v (in^2/min.)		r	C_α	C_c or remarks	e_o
Sample No.	Test No.		log t	$\sqrt{t}$				
L-2	2^+	0 - 0.1	0.00985	0.00853	0.86	0.00984	1.67	5.52
		0.1 - 0.2	0.00904	0.00894	0.62	0.0135		
		0.2 - 0.4	0.00622	0.00882	0.72	0.0162		
		0.4 - 0.8	0.00555	0.00906	0.75	0.0168		
		0.8 - 1.6	0.00495	0.00991	0.77	0.0161		
		1.6 - 3.2	0.00378	0.00660	0.78	0.0167		
L-2	3^+	0 - 0.1	0.0120	0.0115	0.86	0.00923	1.64	5.43
		0.1 - 0.2	0.0108	0.0141	0.61	0.0122		
		0.2 - 0.4	0.00788	0.0115	0.73	0.0143		
		0.4 - 0.8	0.00647	0.00920	0.77	0.0136		
		0.8 - 1.6	0.00482	0.00728	0.74	0.0158		
		1.6 - 3.2	0.00390	0.00583	0.74	0.0191		
U-4	2^+	0 - 0.1	0.0178	0.0173	0.80	0.0103	1.62	4.74
		0.1 - 0.2	0.0135	0.0180	0.61	0.0125		
		0.2 - 0.4	0.00973	0.0150	0.68	0.0166		
		0.4 - 0.8	0.00726	0.0127	0.76	0.0170		
		0.8 - 1.6	0.00510	0.00786	0.72	0.0190		
U-4	3^+	0.- 0.24	0.0161	0.0154	0.82	0.0151	1 increment, 24-hr.	4.43
L-2	4^+	0 - 0.63	0.0118	0.0103	0.90	0.0145	1 increment, 24-hr.	5.46
U-2	1^+	0 - 0.24	0.0170	0.0162	0.87	0.0106	1 increment, 24-hr.	4.38

*Load frame similar to Figure IX-4, Lambe, 1951. +Bishop type consolidation machine, Figure 3.2.

c_v - coefficient of consolidation, t - time, r - primary compression ratio,

C_α - coefficient of secondary compression, C_c - compression index, e_o - initial void ratio.

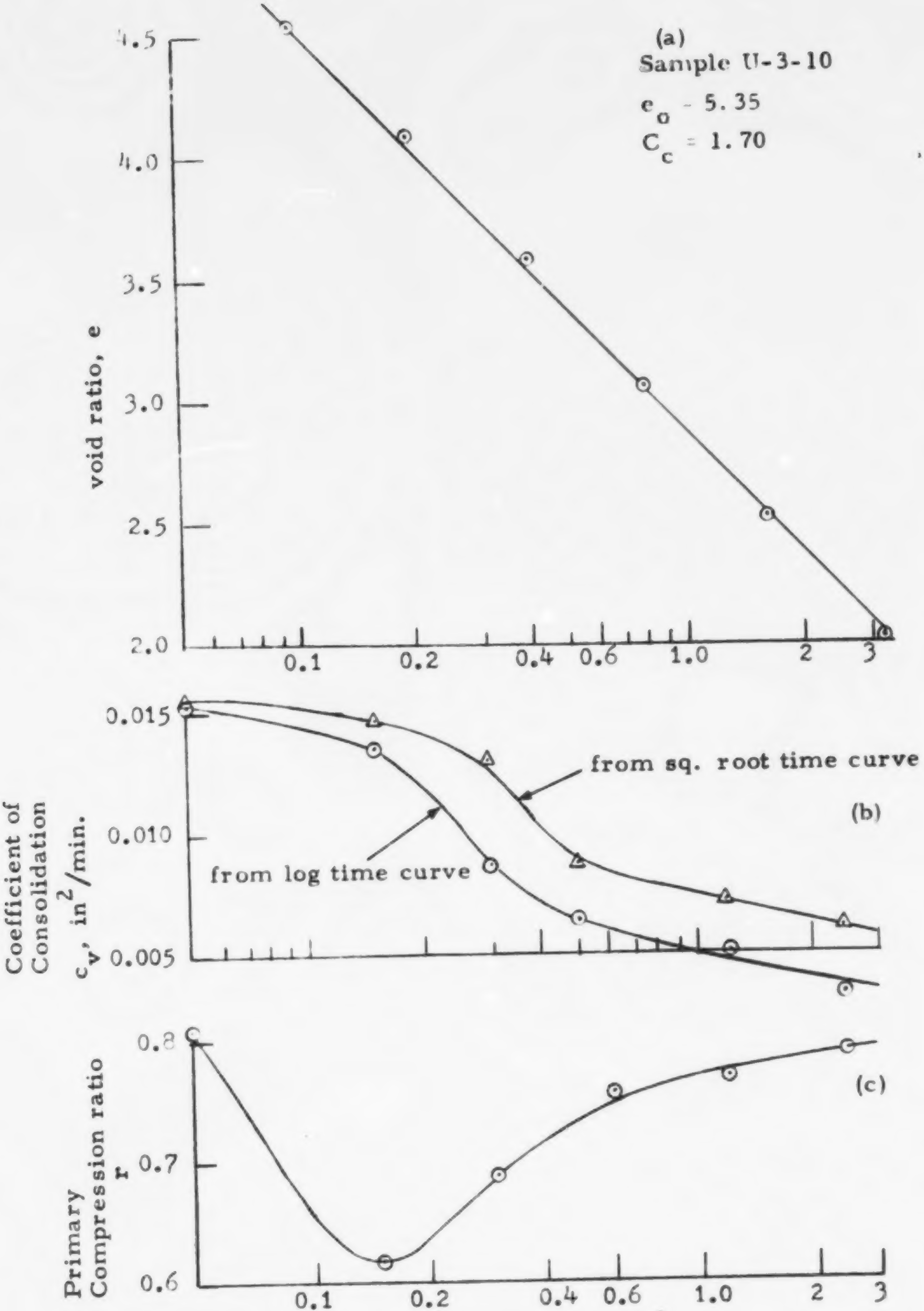

Figure 5.1. Consolidation characteristics for sludge sample U-3. (a) Void ratio. (b) Coefficient of consolidation, c_v. (c) Primary compression ratio, r.

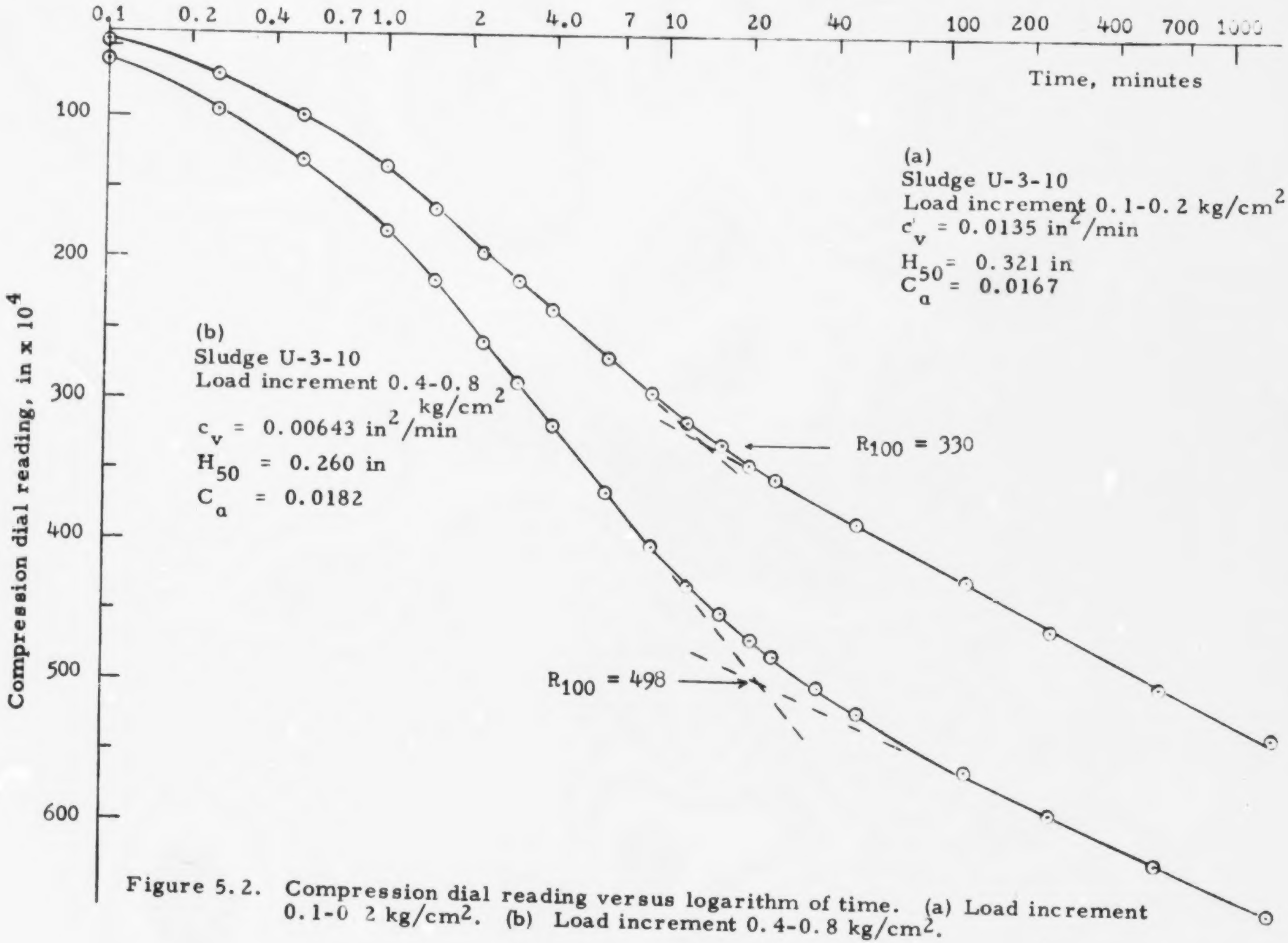

Figure 5.2. Compression dial reading versus logarithm of time. (a) Load increment 0.1-0 2 kg/cm^2. (b) Load increment 0.4-0.8 kg/cm^2.

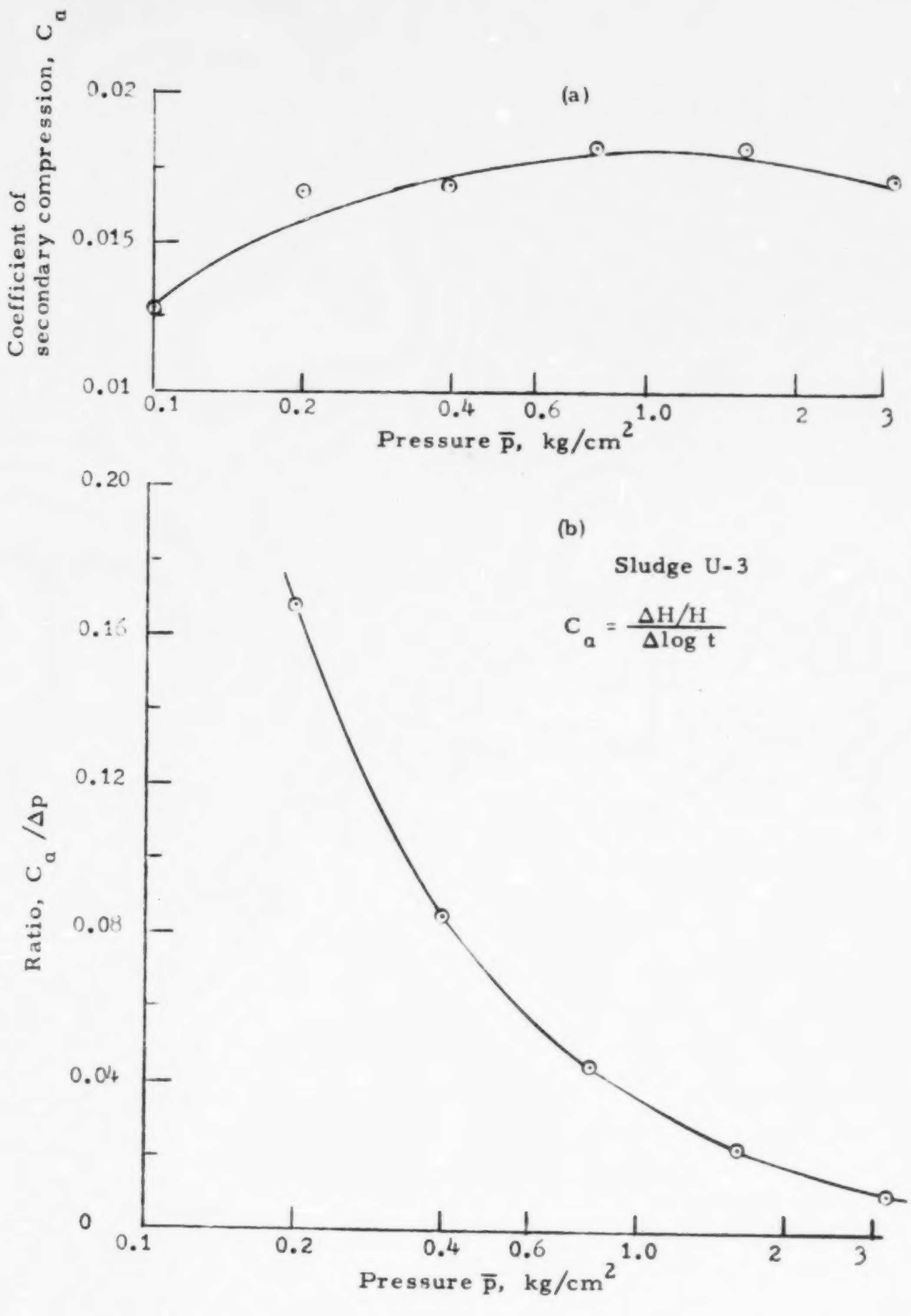

Figure 5.3. Coefficient of secondary compression C_a. (a) C_a versus log $\overline{p}$. (b) $C_a/\Delta p$ versus log $\overline{p}$.

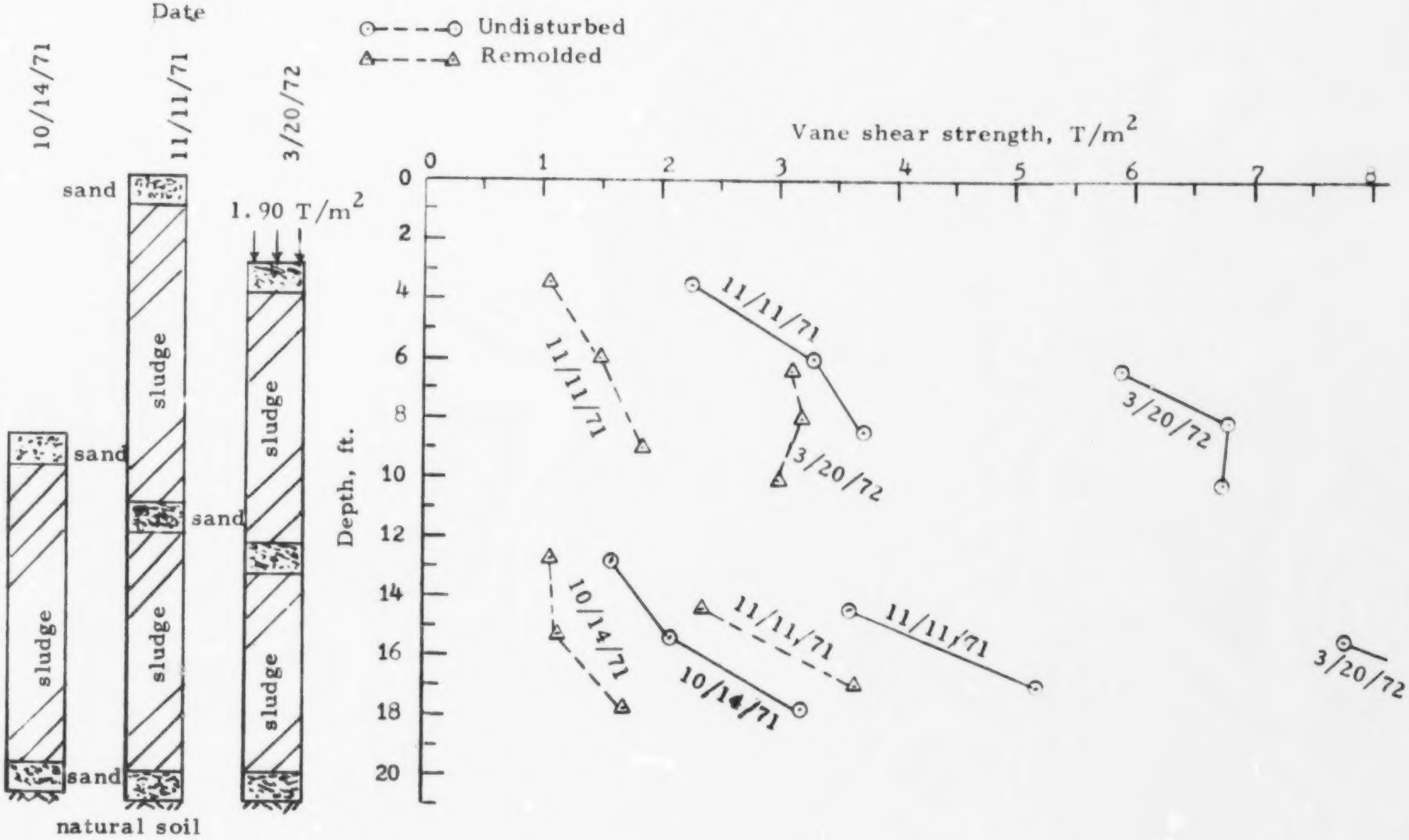

Figure 5.4. Vane shear strengths after completion of each sludge layer and after partial consolidation.

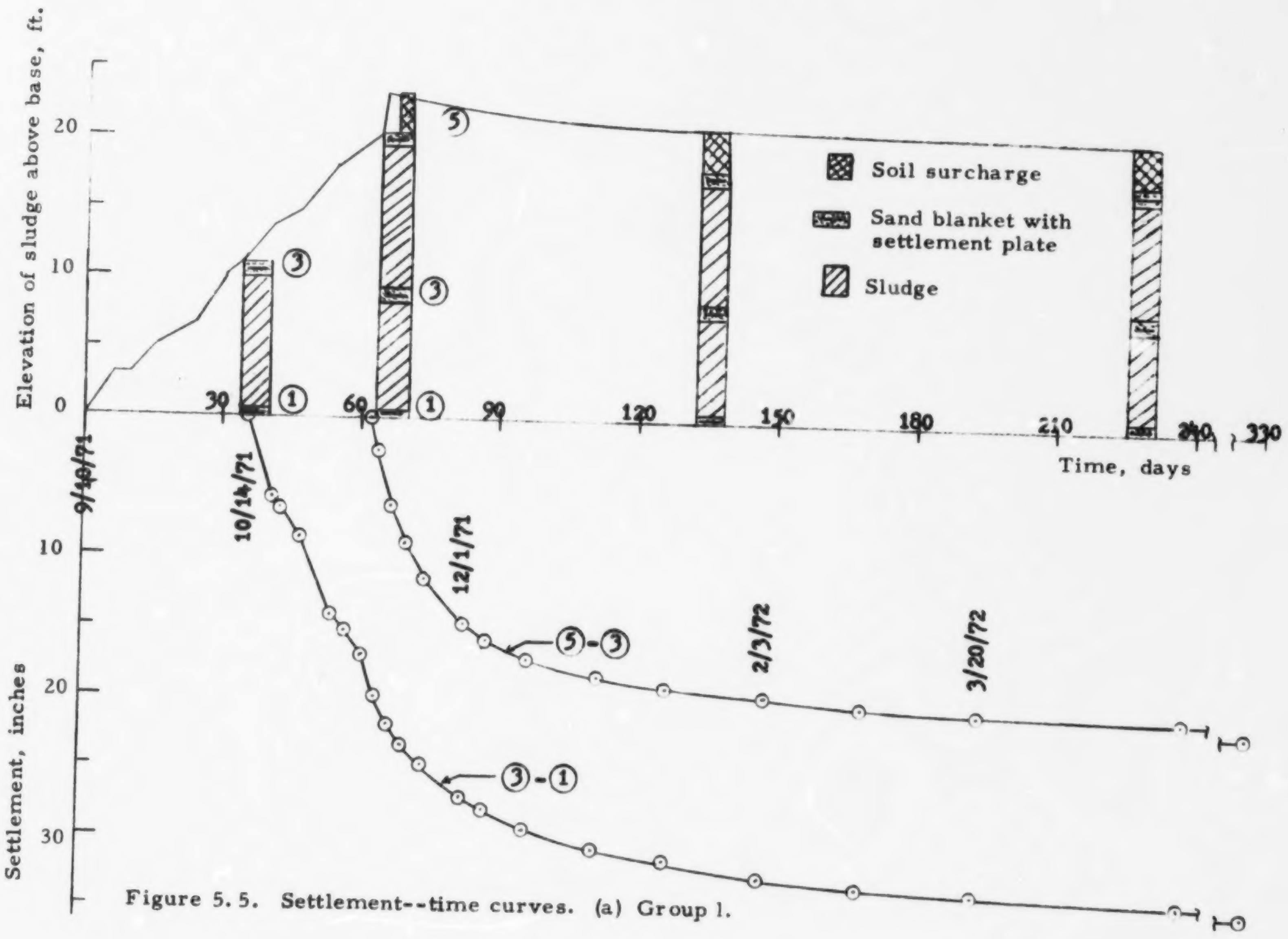

Figure 5.5. Settlement--time curves. (a) Group 1.

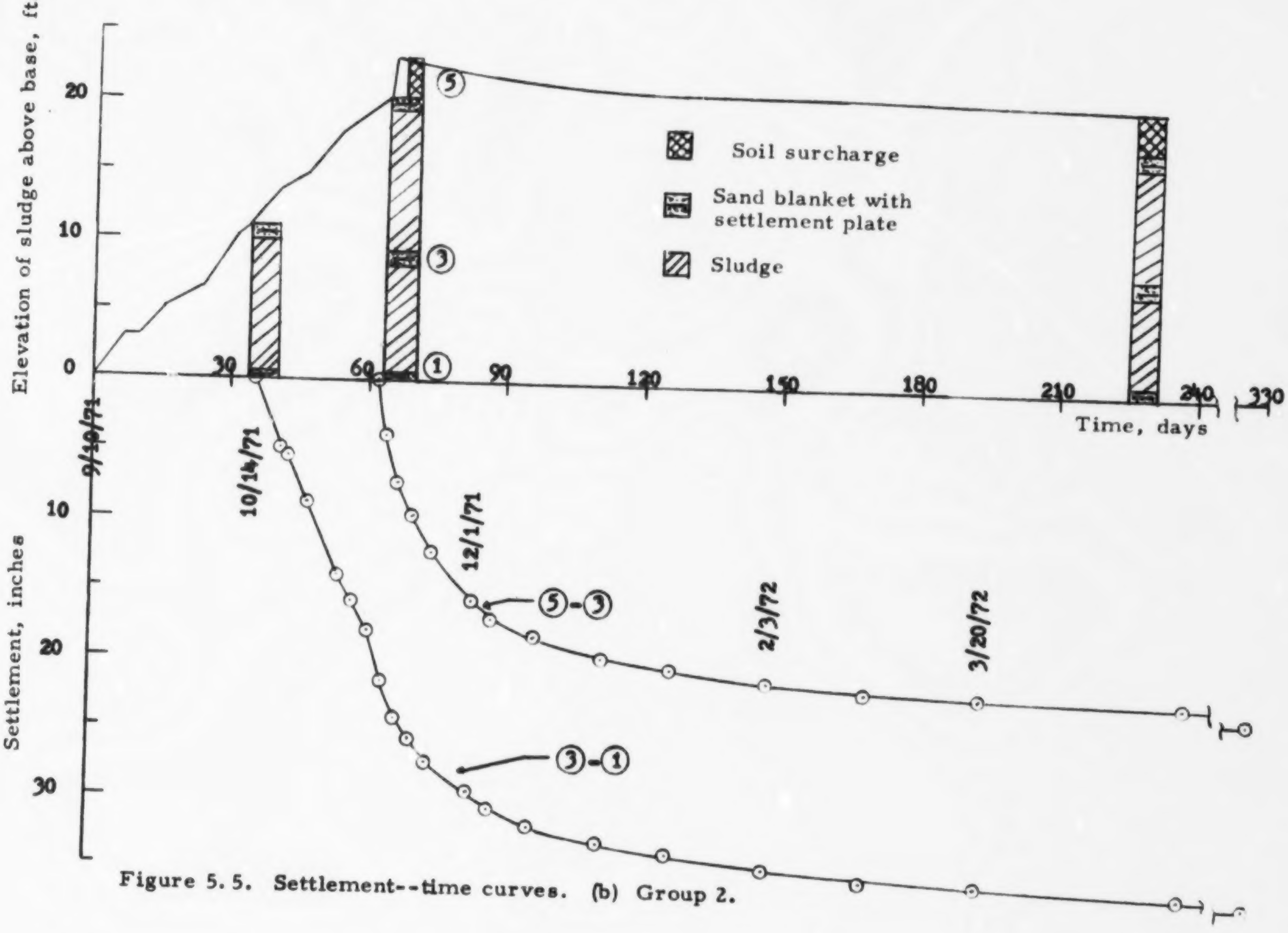

Figure 5. 5. Settlement--time curves. (b) Group 2.

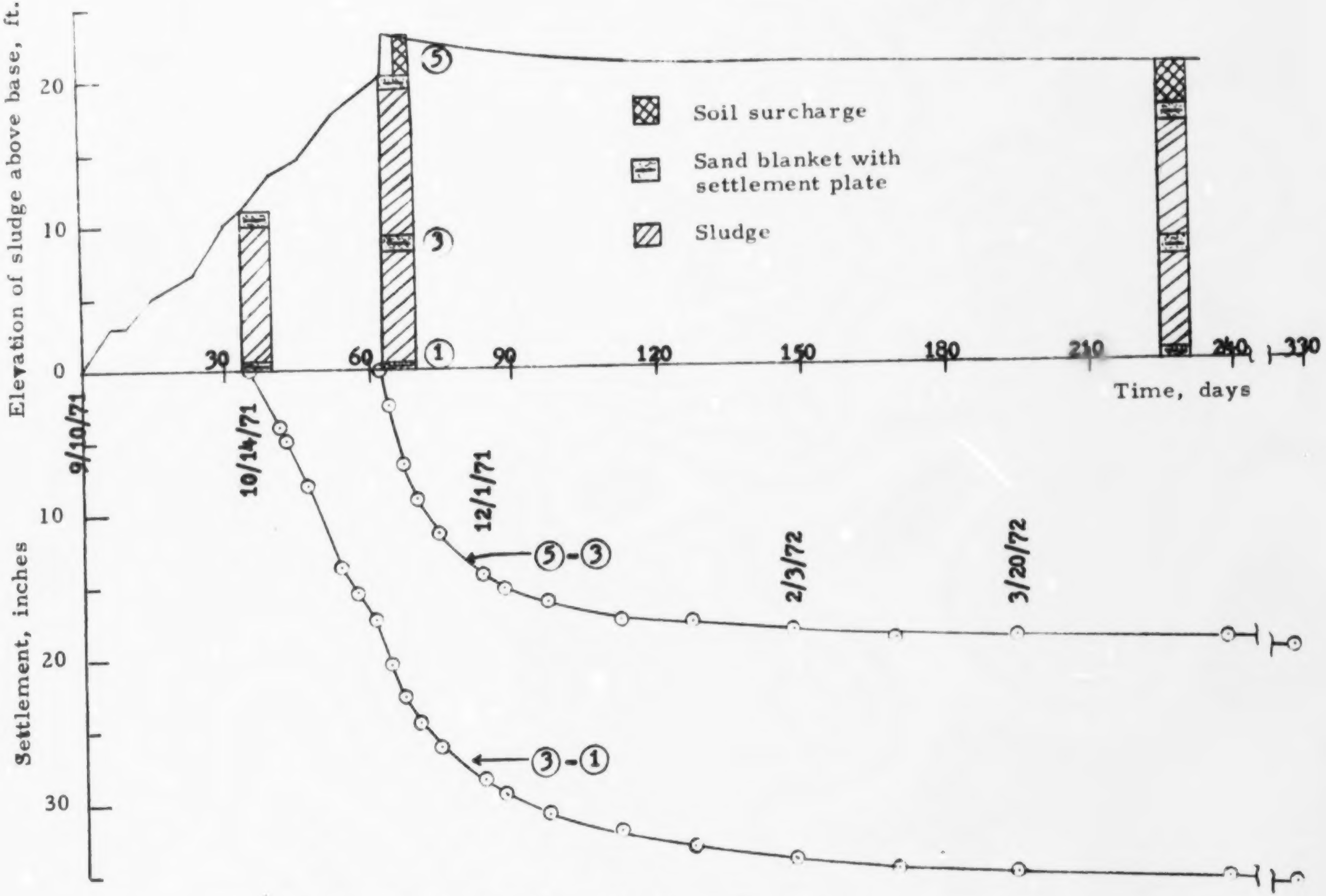

Figure 5.5. Settlement--time curves. (c) Group 3.

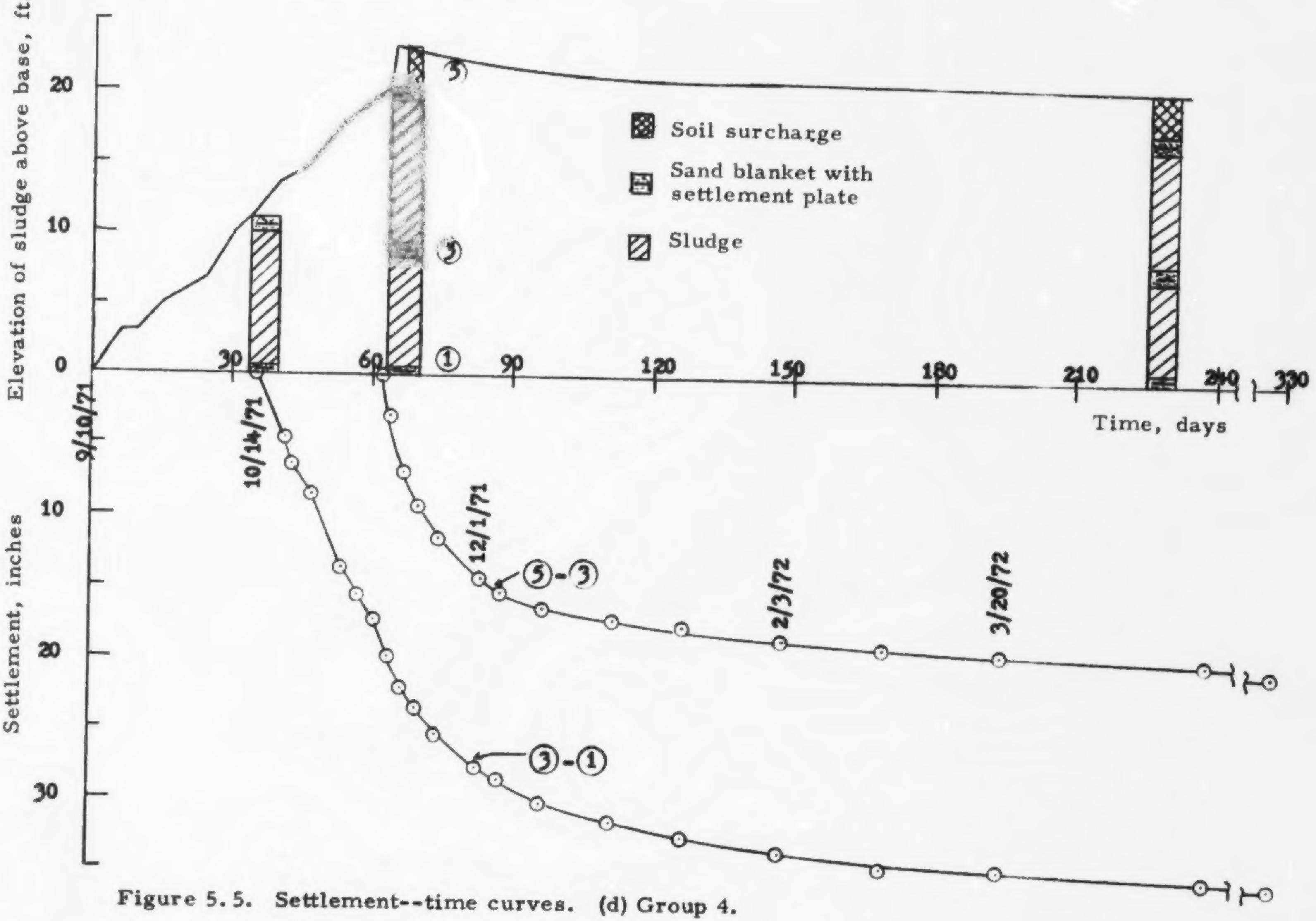

Figure 5.5. Settlement--time curves. (d) Group 4.

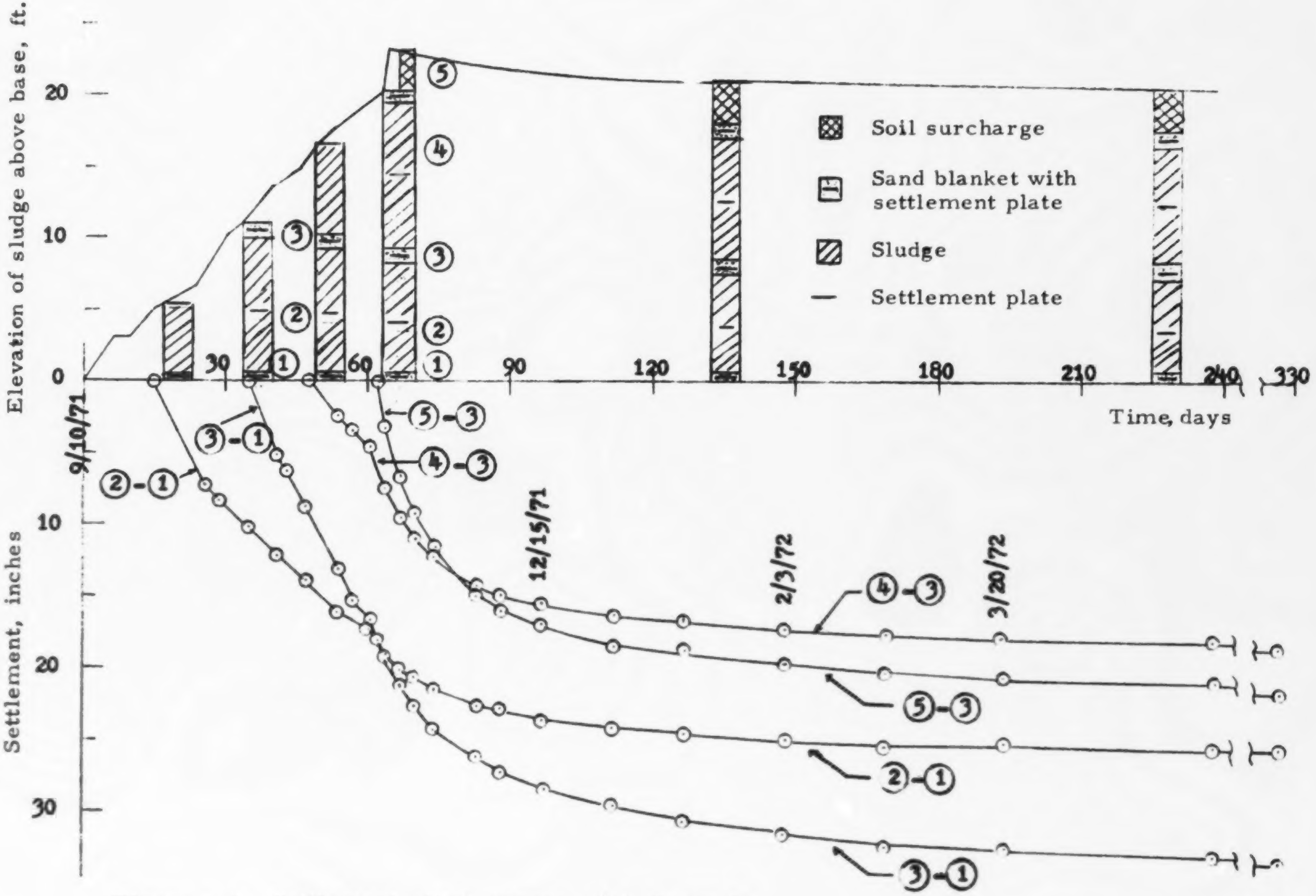

Figure 5. 5. Settlement--time curves. (e) Group 5.

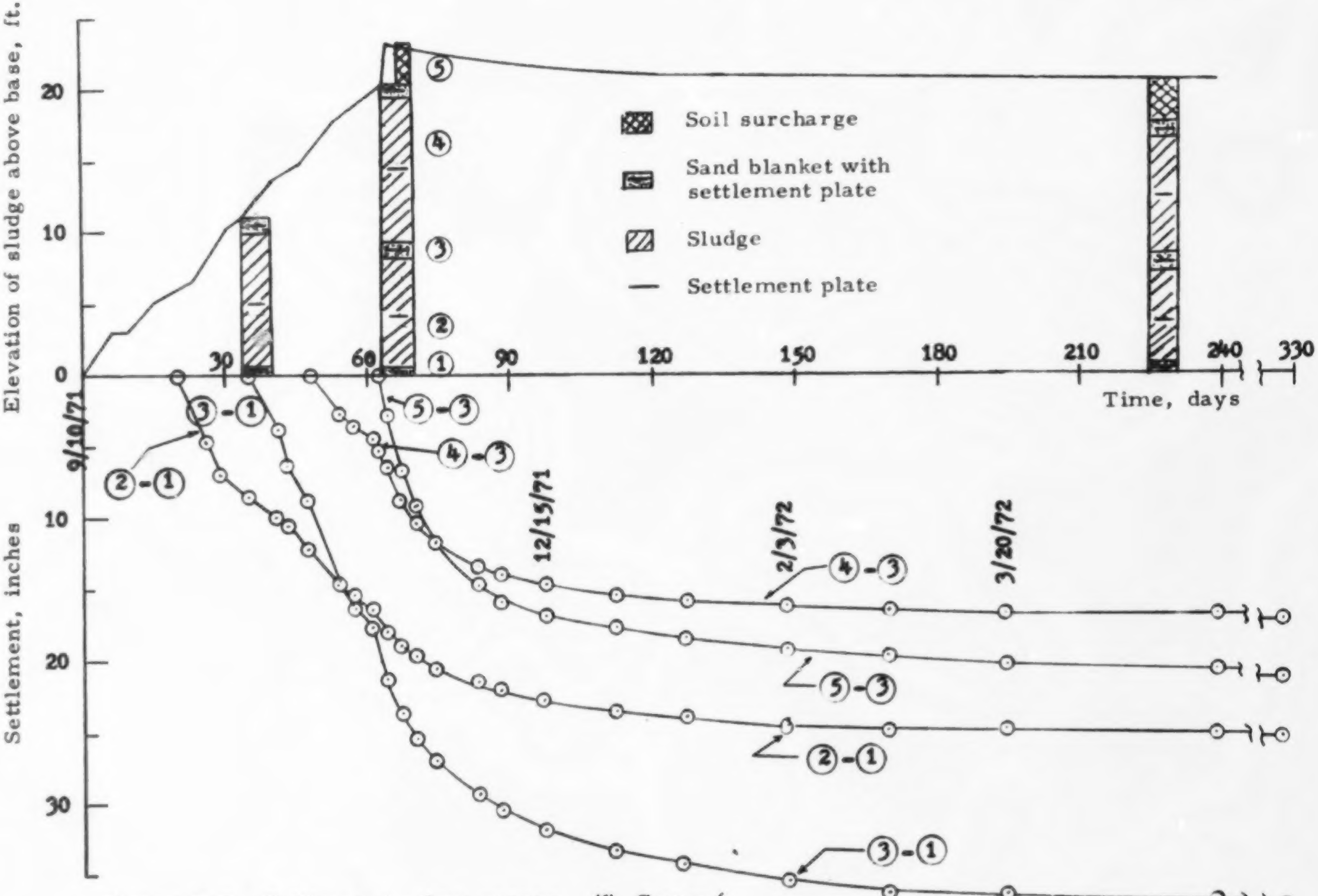

Figure 5.5. Settlement--time curves. (f) Group 6.

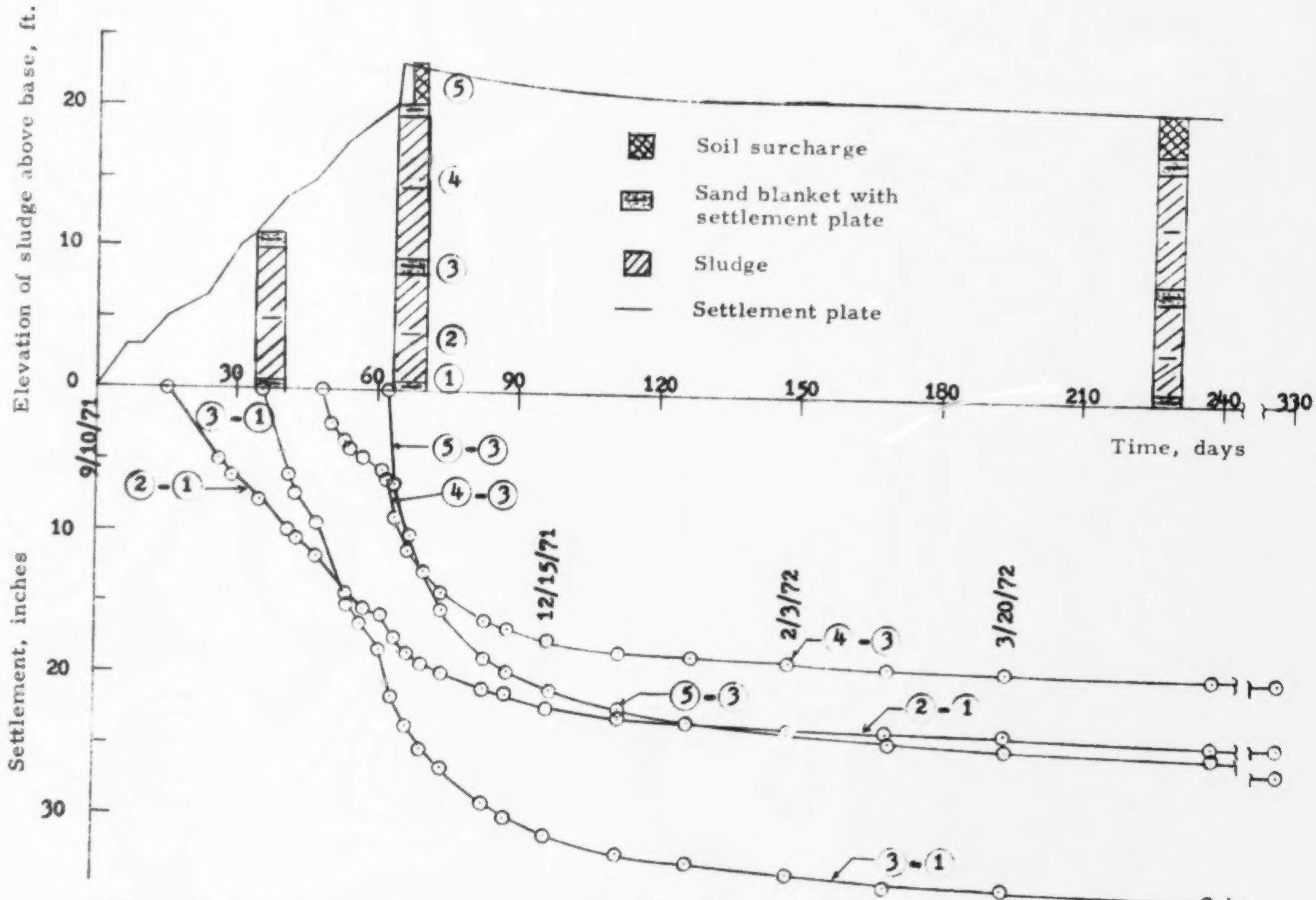

Figure 5.5. Settlement--time curves. (g) Group 7.

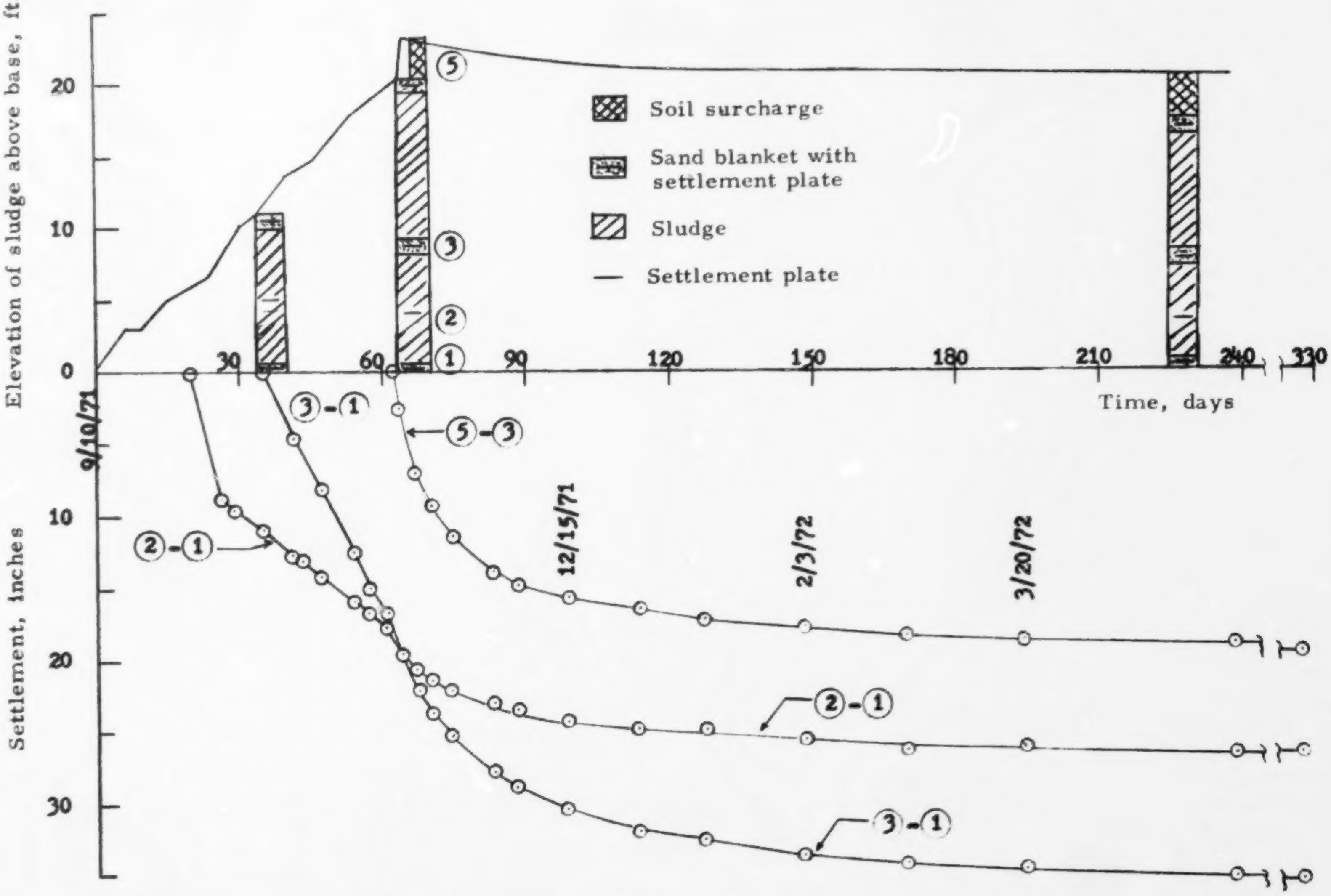

Figure 5.5. Settlement--time curves. (h) Group 8.

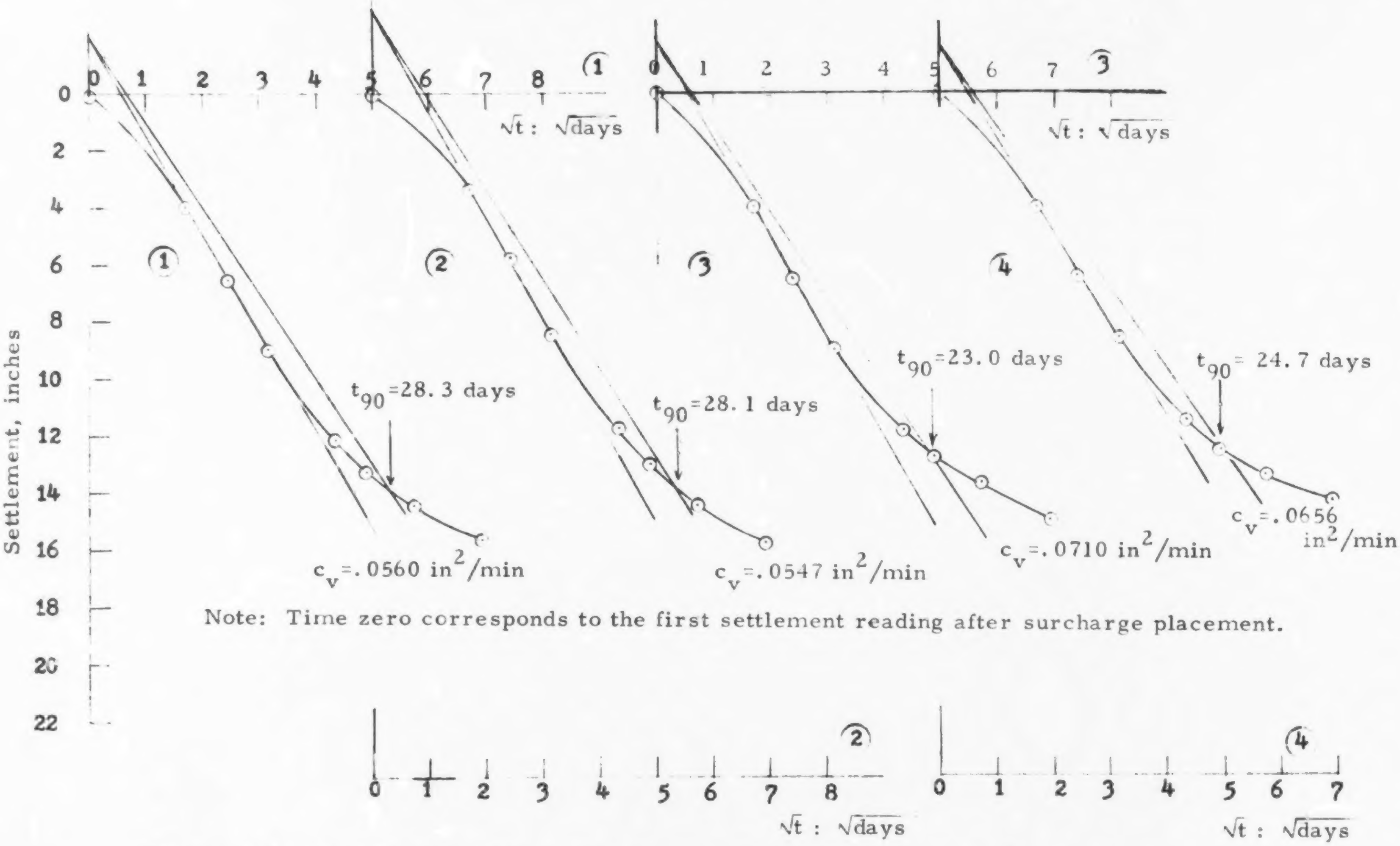

Note: Time zero corresponds to the first settlement reading after surcharge placement.

Figure 5.6. Settlement versus square root of time curves, upper sludge layer.
(a) Groups 1-4.

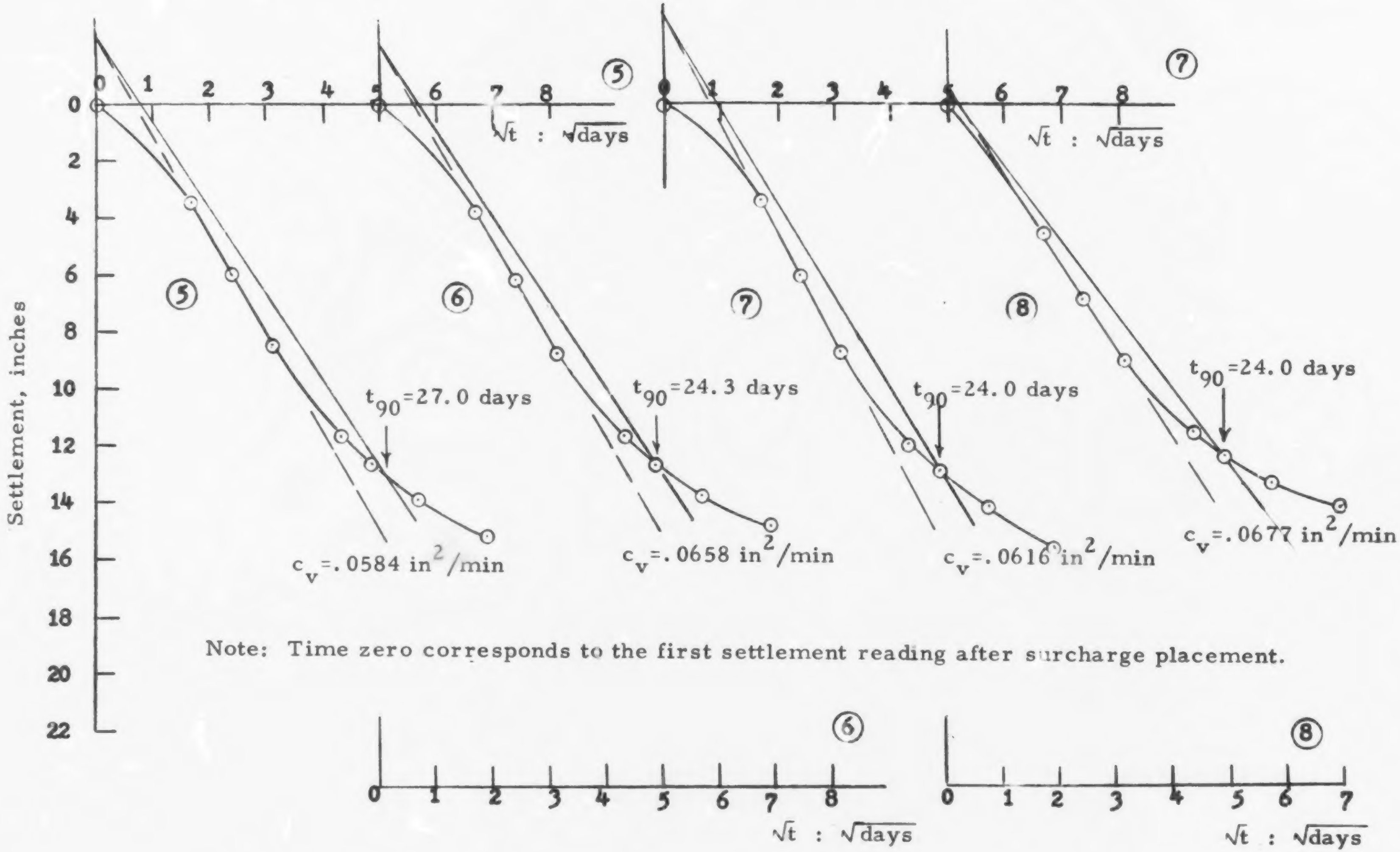

Note: Time zero corresponds to the first settlement reading after surcharge placement.

Figure 5.6. Settlement versus square root of time curves, upper sludge layer.
(b) Groups 5-8.

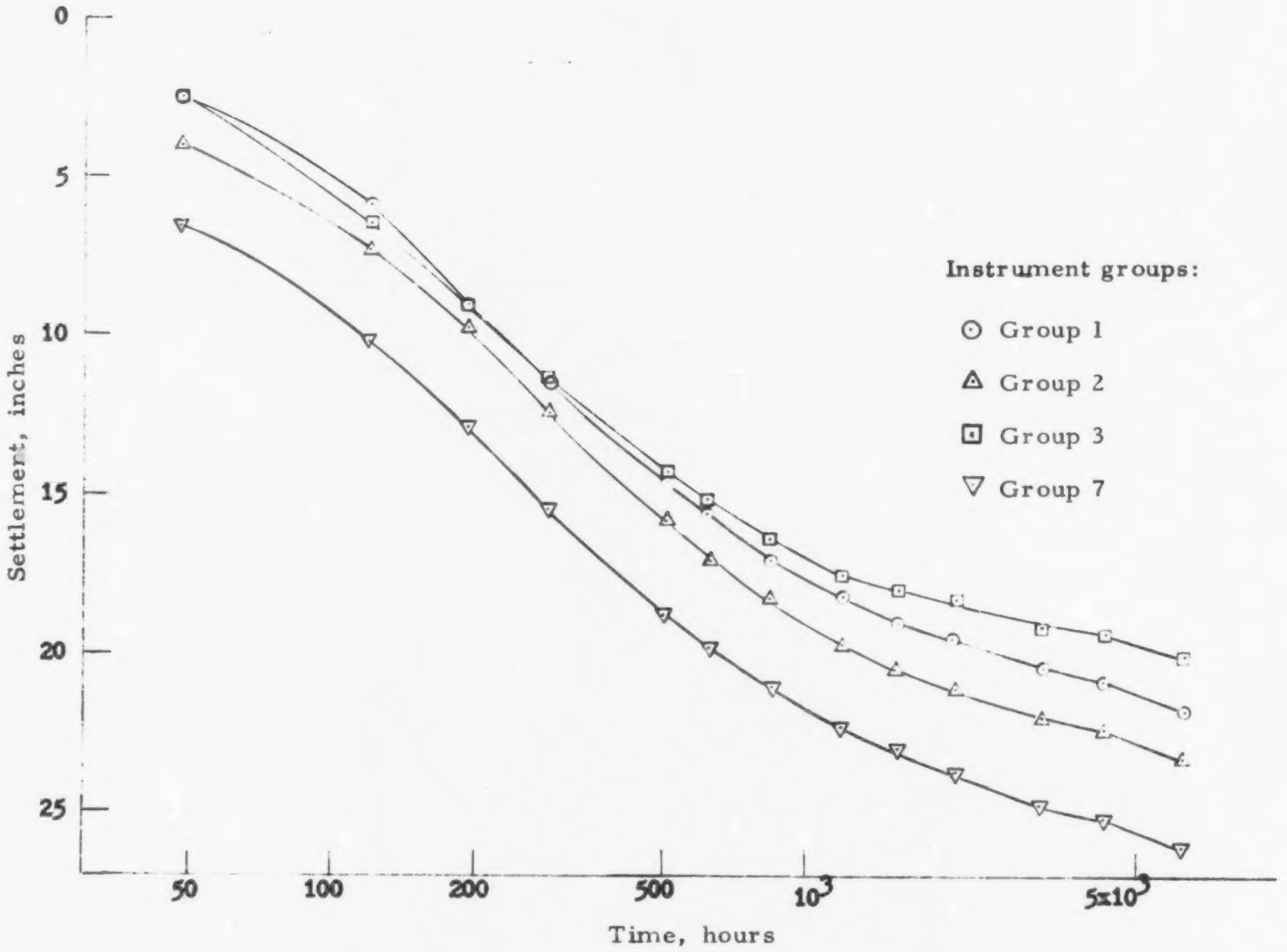

Figure 5. 7. Settlement--logarithm of time curves, upper sludge layer. (a) Groups 1, 2, 3, and 7.

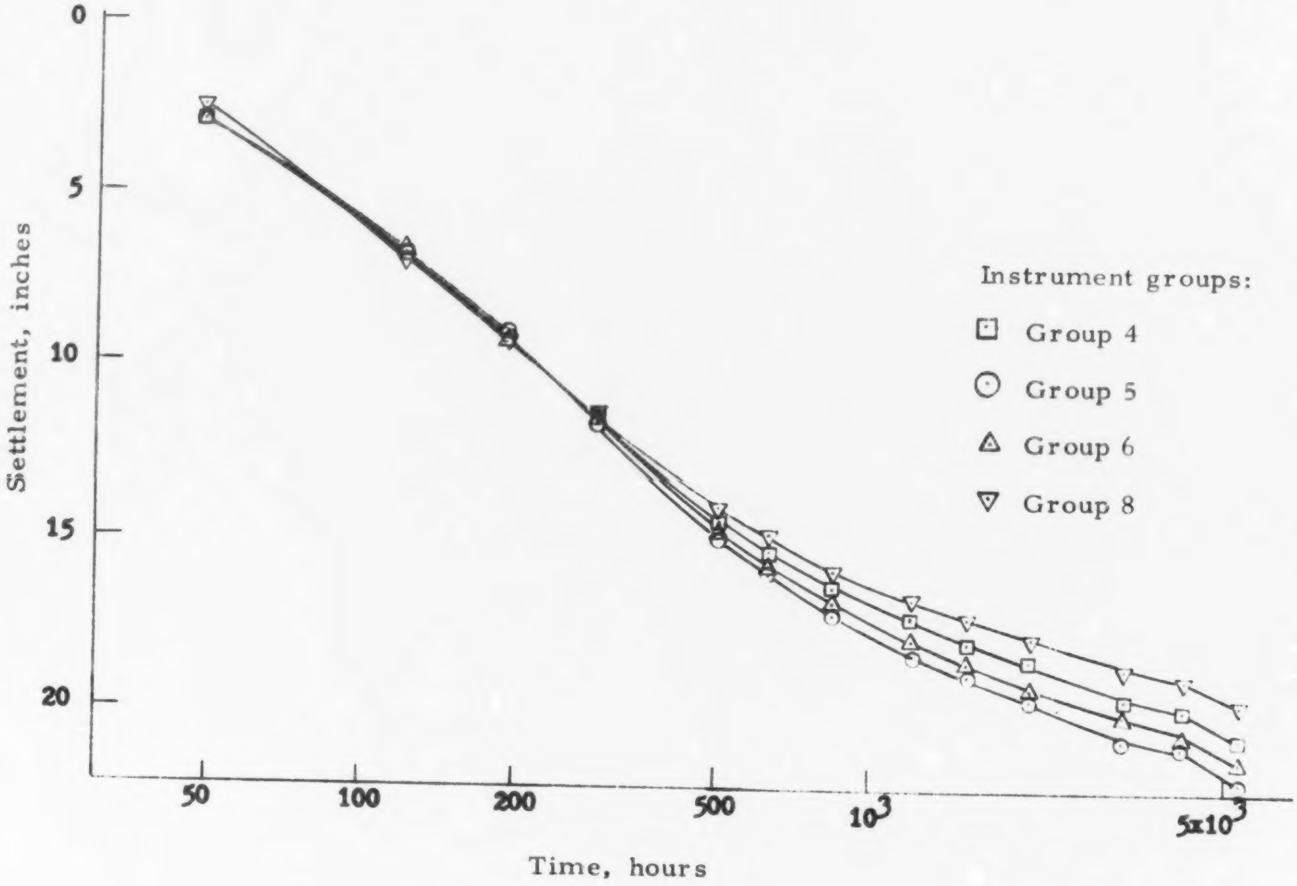

Figure 5.7. Settlement--logarithm of time curves, upper sludge layer. (b) Groups 4, 5, 6, and 8.

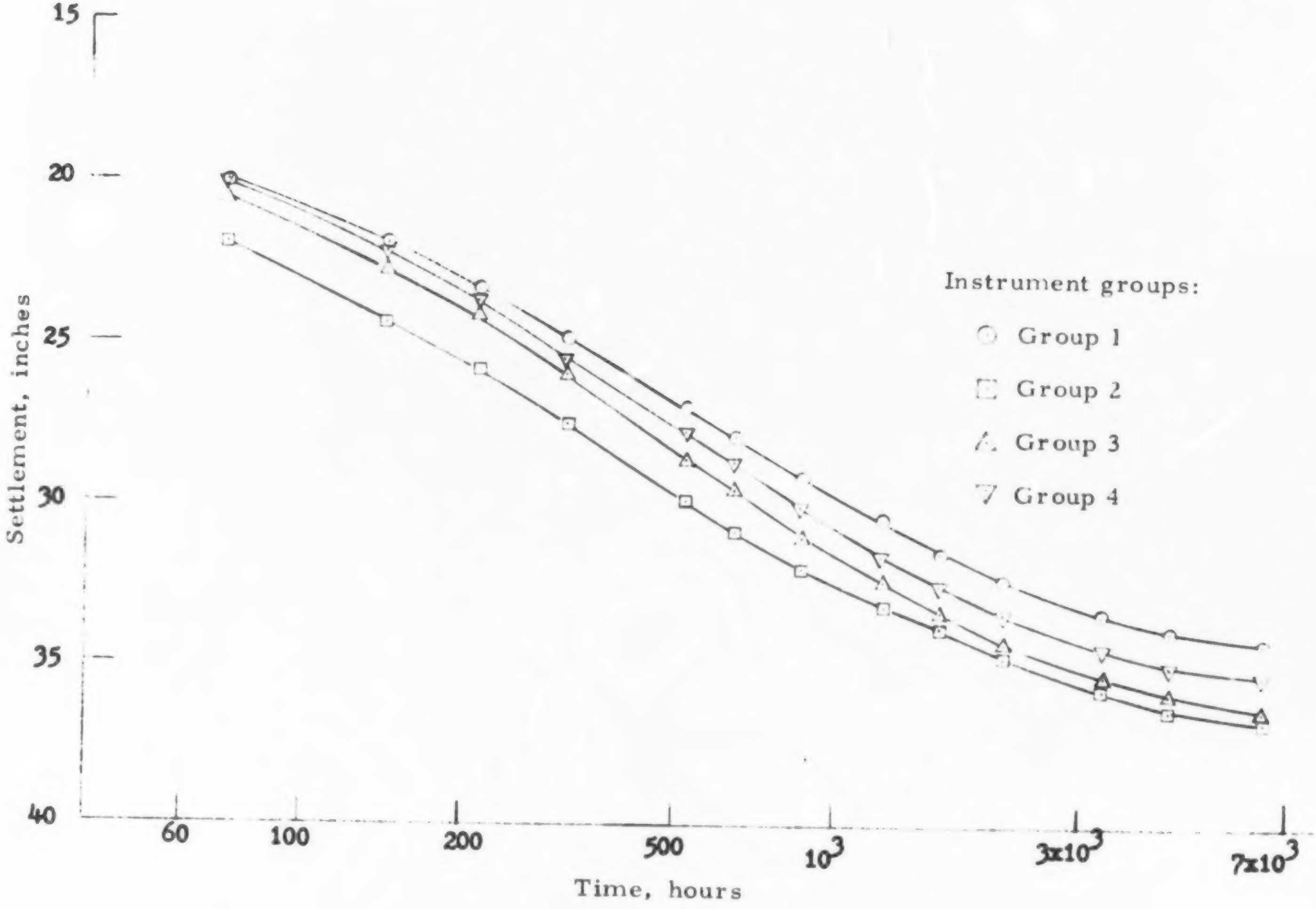

Figure 5. 8. Settlement--logarithm of time curves, lower sludge layer after surcharge placement. (a) Groups 1, 2, 3, and 4.

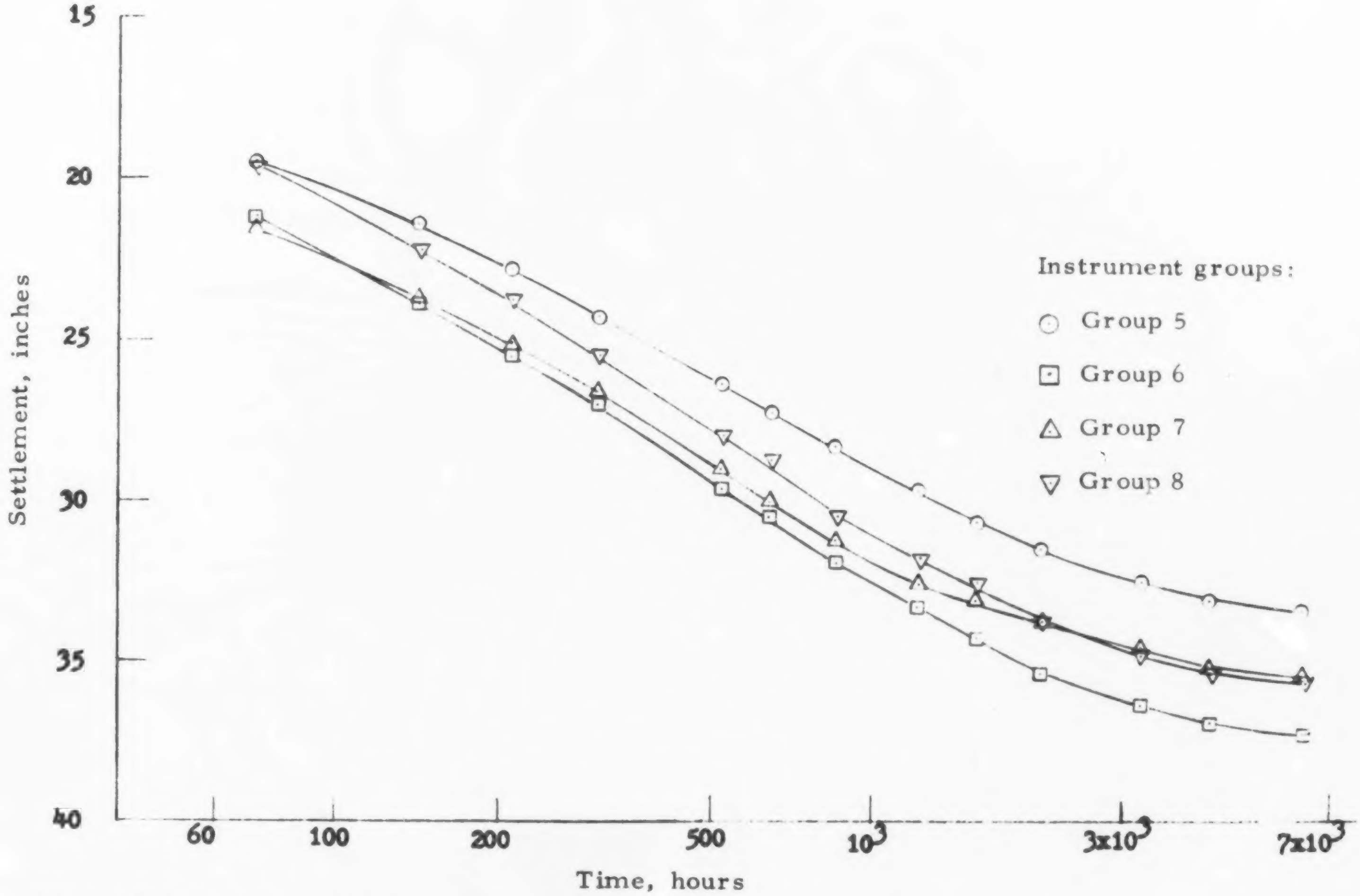

Figure 5.8. Settlement--logarithm of time curves, lower sludge layer after surcharge placement. (b) Groups 5, 6, 7, and 8.

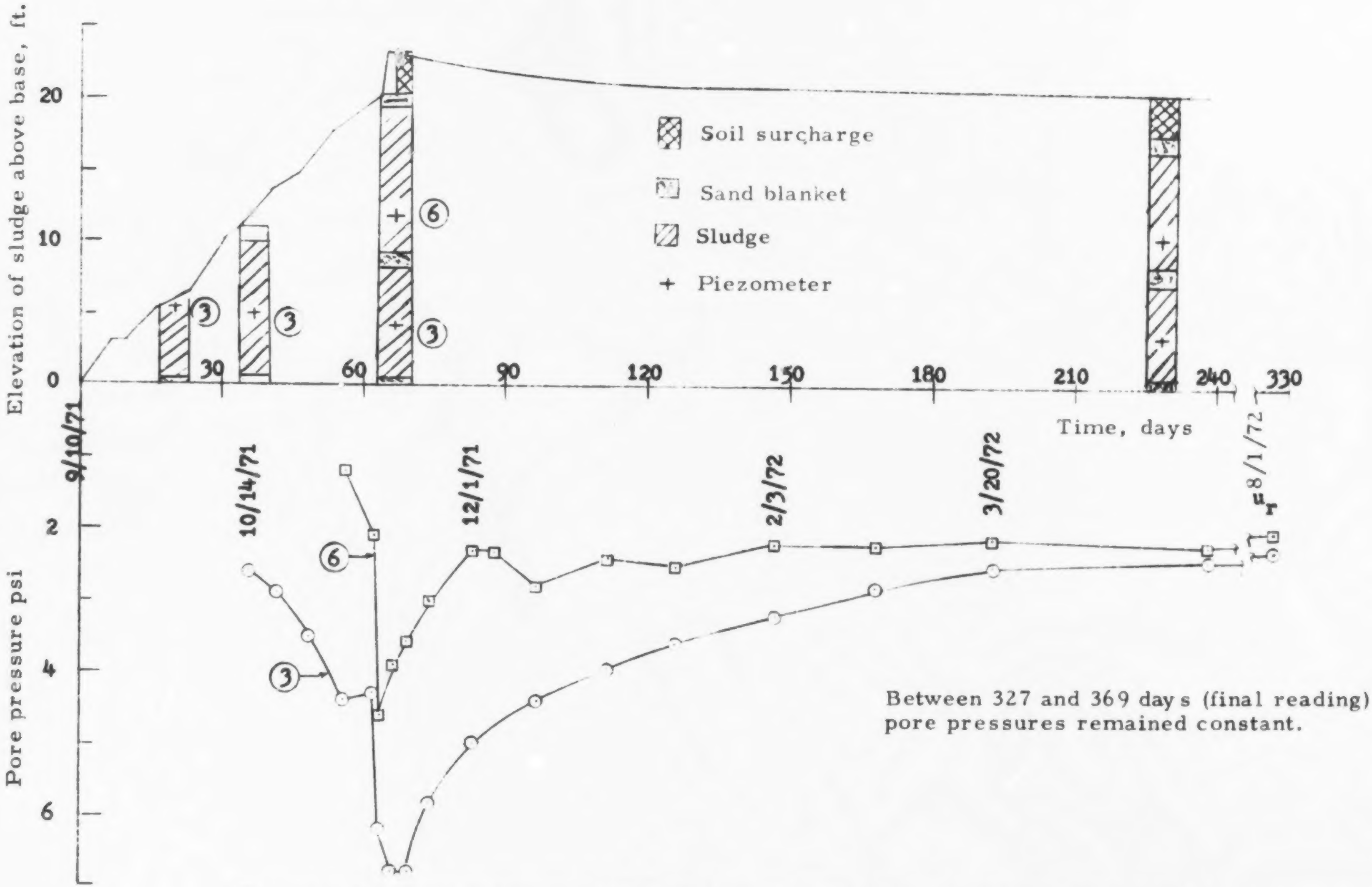

Between 327 and 369 days (final reading) pore pressures remained constant.

Figure 5.9. Pore pressure versus time curves. (a) Group 5 piezometers 3 and 6.

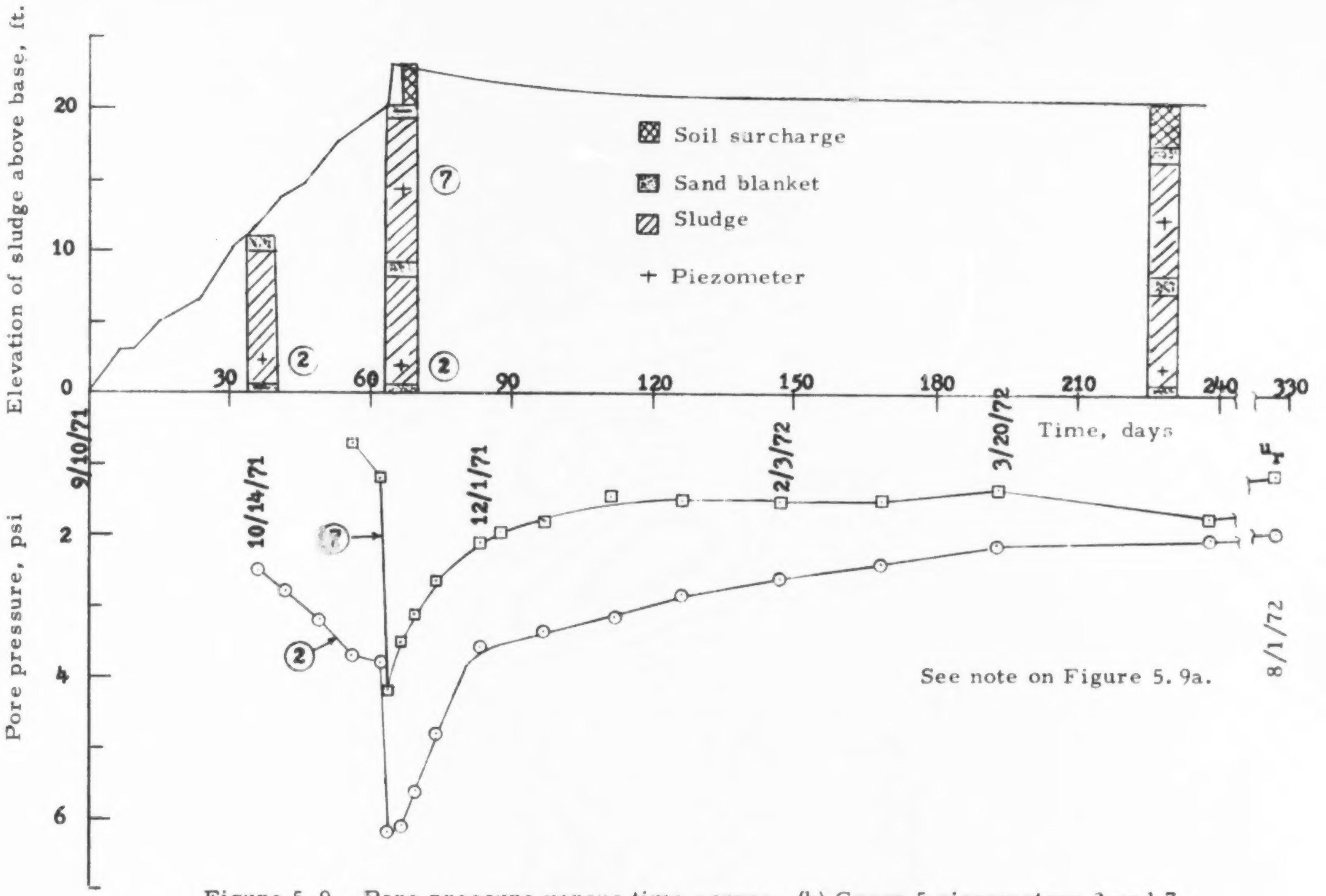

See note on Figure 5. 9a.

Figure 5. 9. Pore pressure versus time curves. (b) Group 5 piezometers 2 and 7.

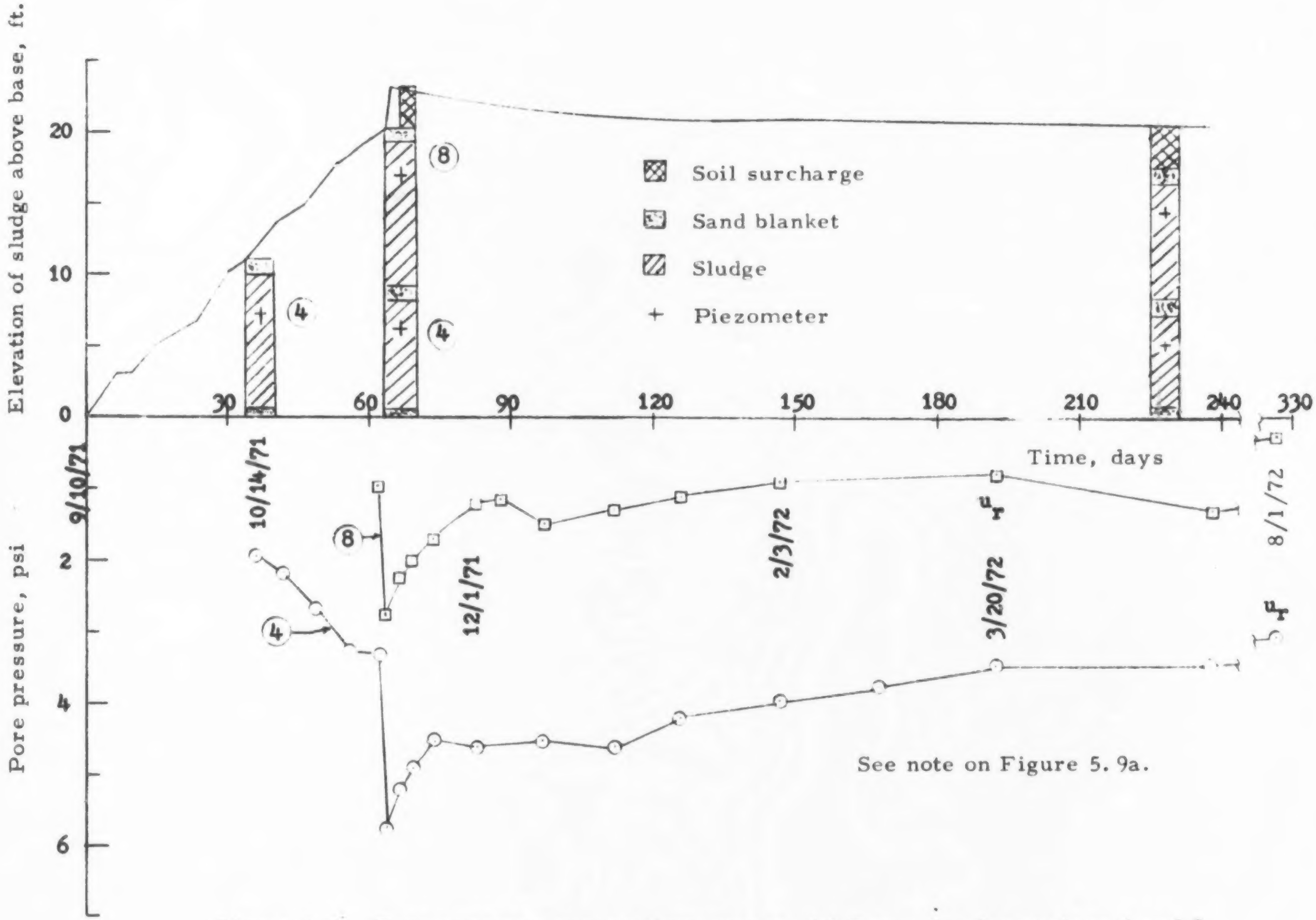

See note on Figure 5. 9a.

Figure 5. 9. Pore pressure versus time curves. (c) Group 5, piezometers 4 and 8.

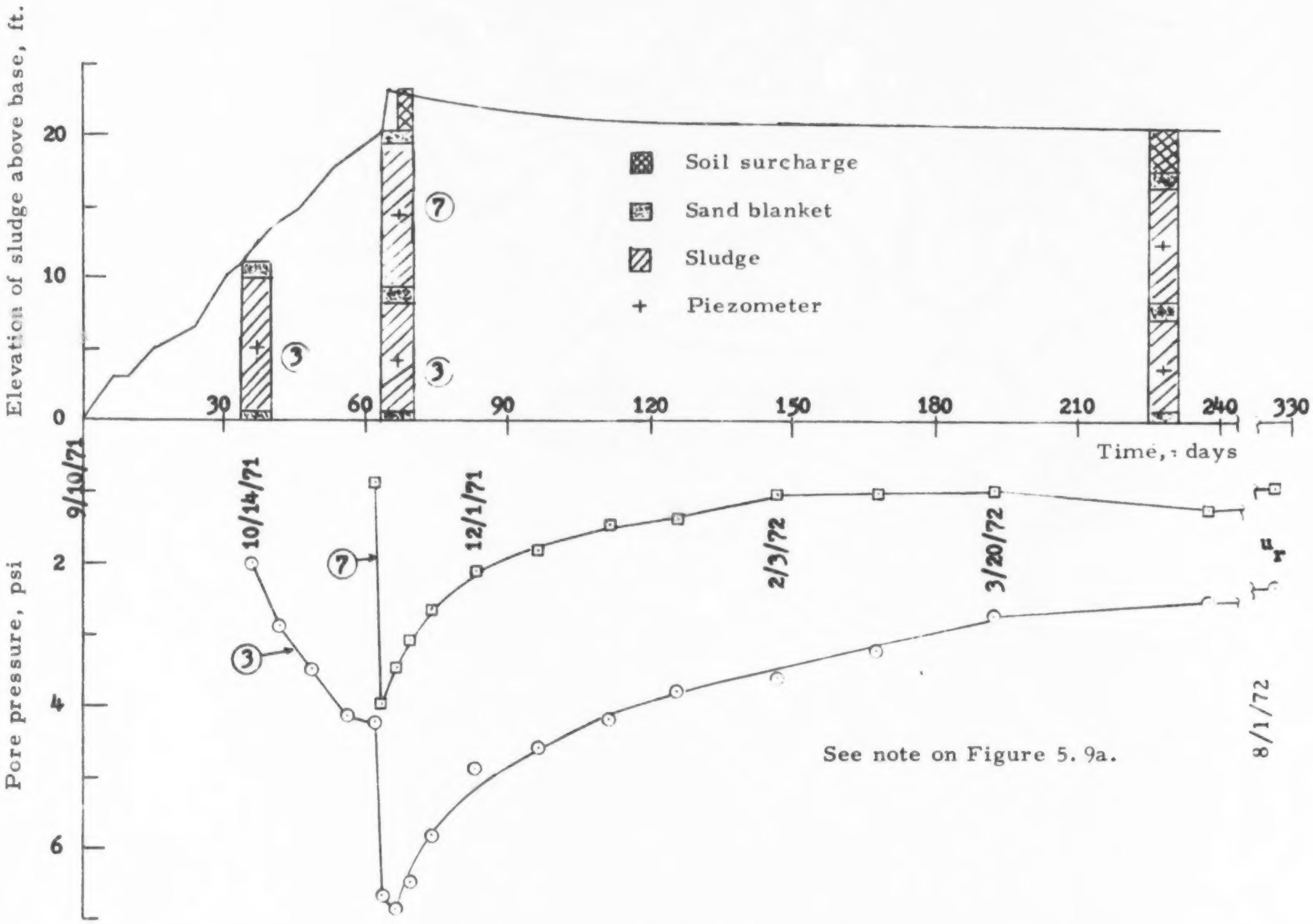

See note on Figure 5. 9a.

Figure 5. 9. Pore pressure versus time curves. (d) Group 6.

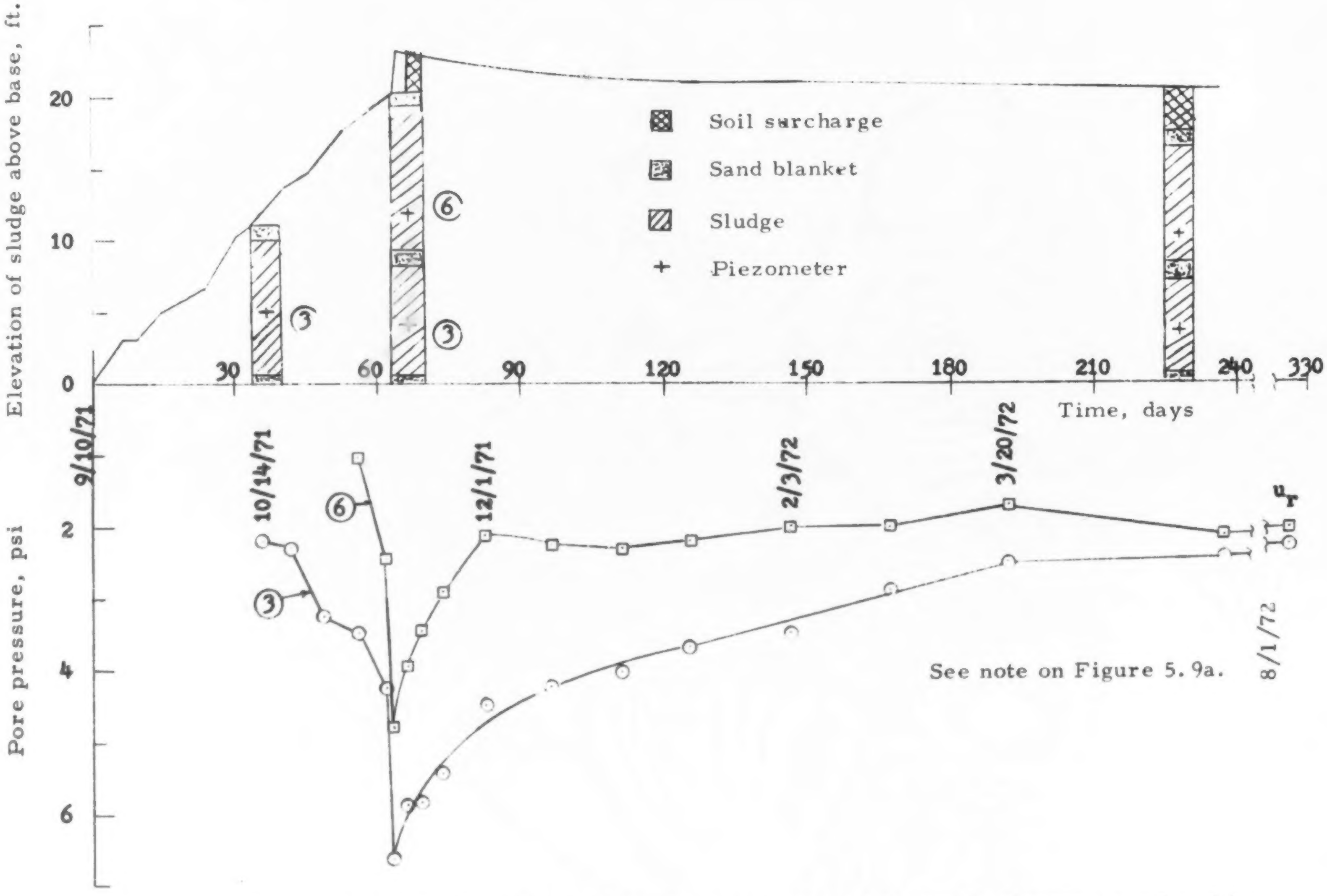

See note on Figure 5.9a.

Figure 5.9. Pore pressure versus time curves. (e) Group 7, piezometers 3 and 6.

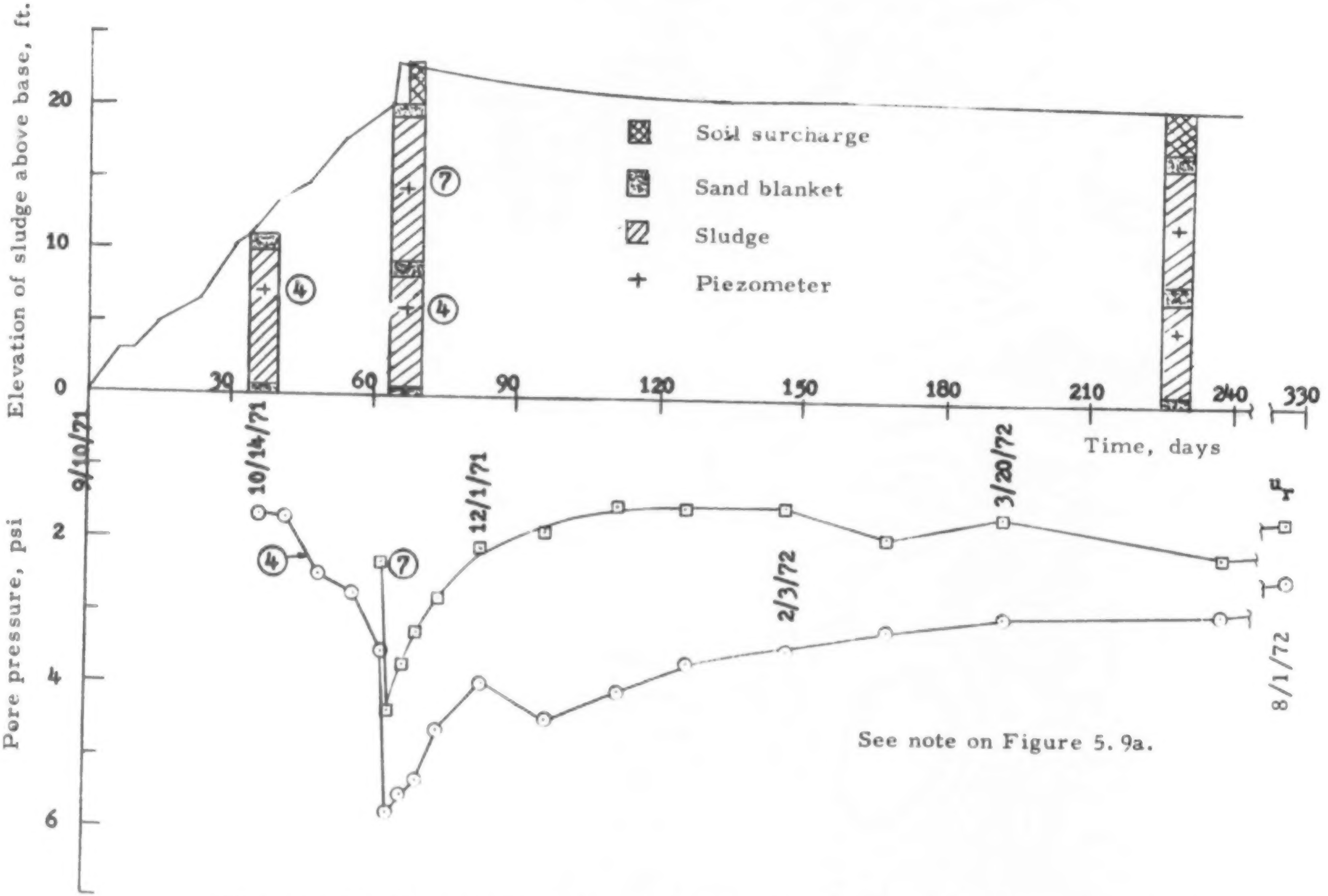

See note on Figure 5.9a.

Figure 5.9. Pore pressure versus time curves. (f) Group 7, piezometers 4 and 7.

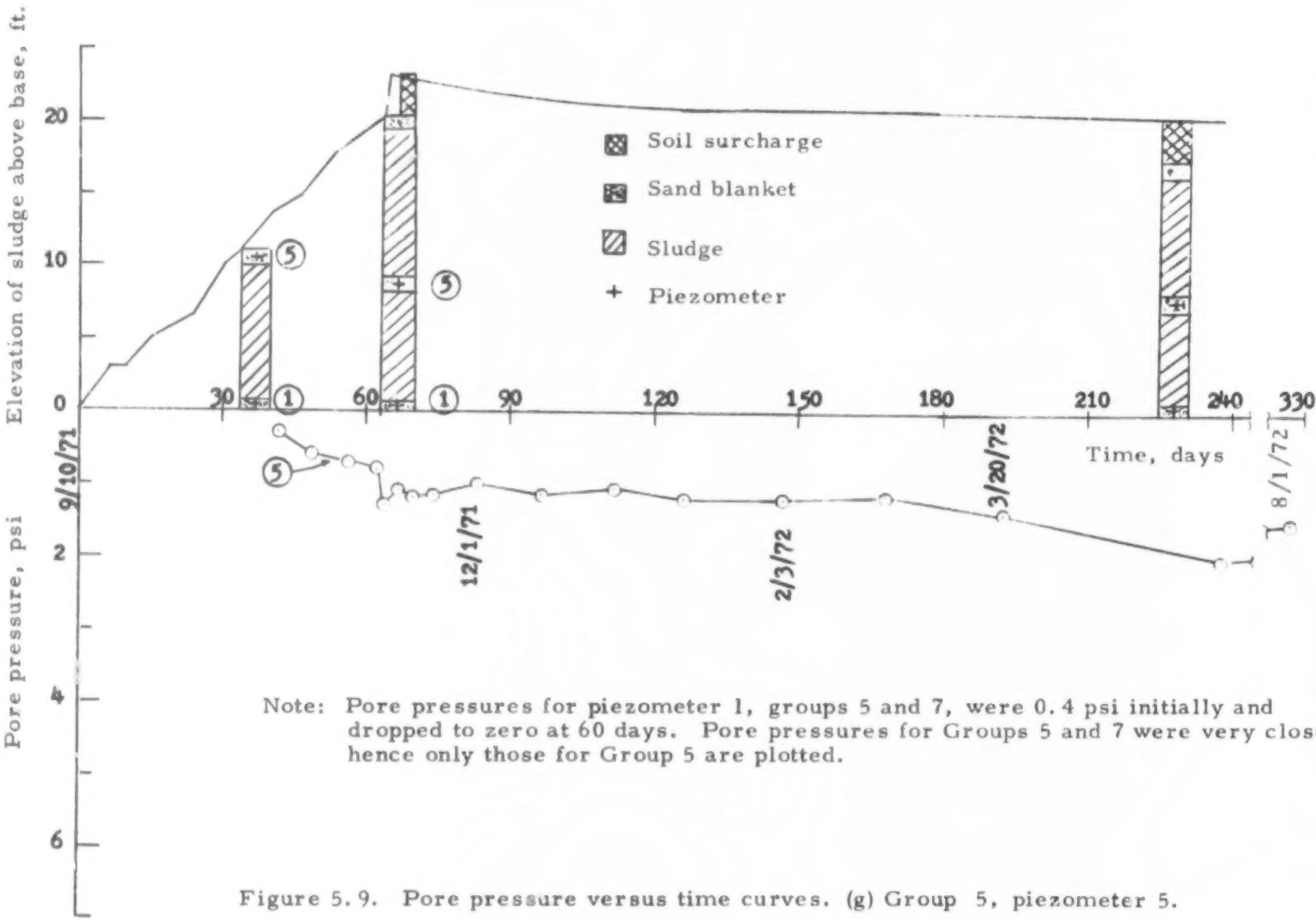

Note: Pore pressures for piezometer 1, groups 5 and 7, were 0.4 psi initially and dropped to zero at 60 days. Pore pressures for Groups 5 and 7 were very close, hence only those for Group 5 are plotted.

Figure 5.9. Pore pressure versus time curves. (g) Group 5, piezometer 5.

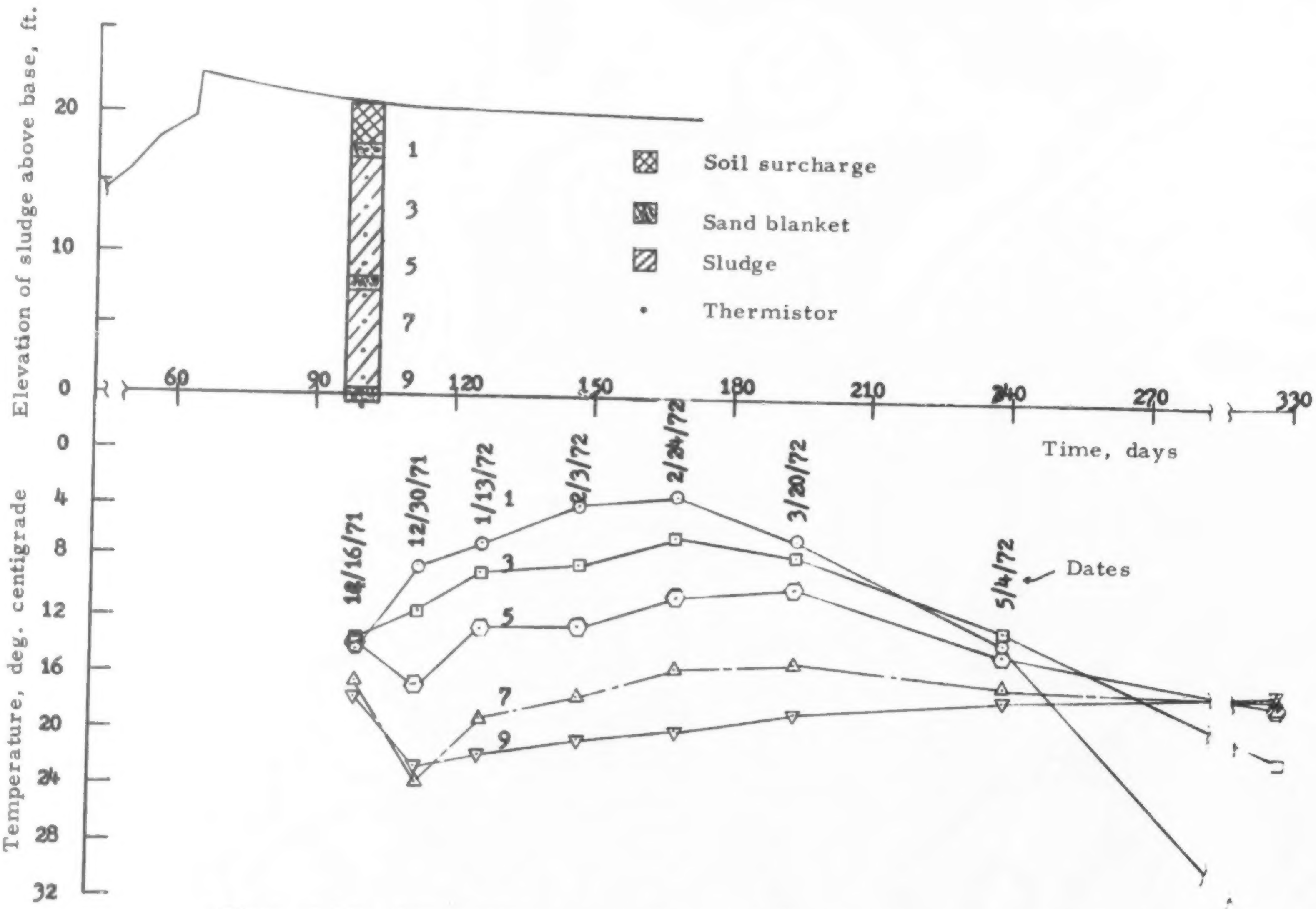

Figure 5.10. Temperature versus time. (a) Thermistors 1, 3, 5, 7, and 9.

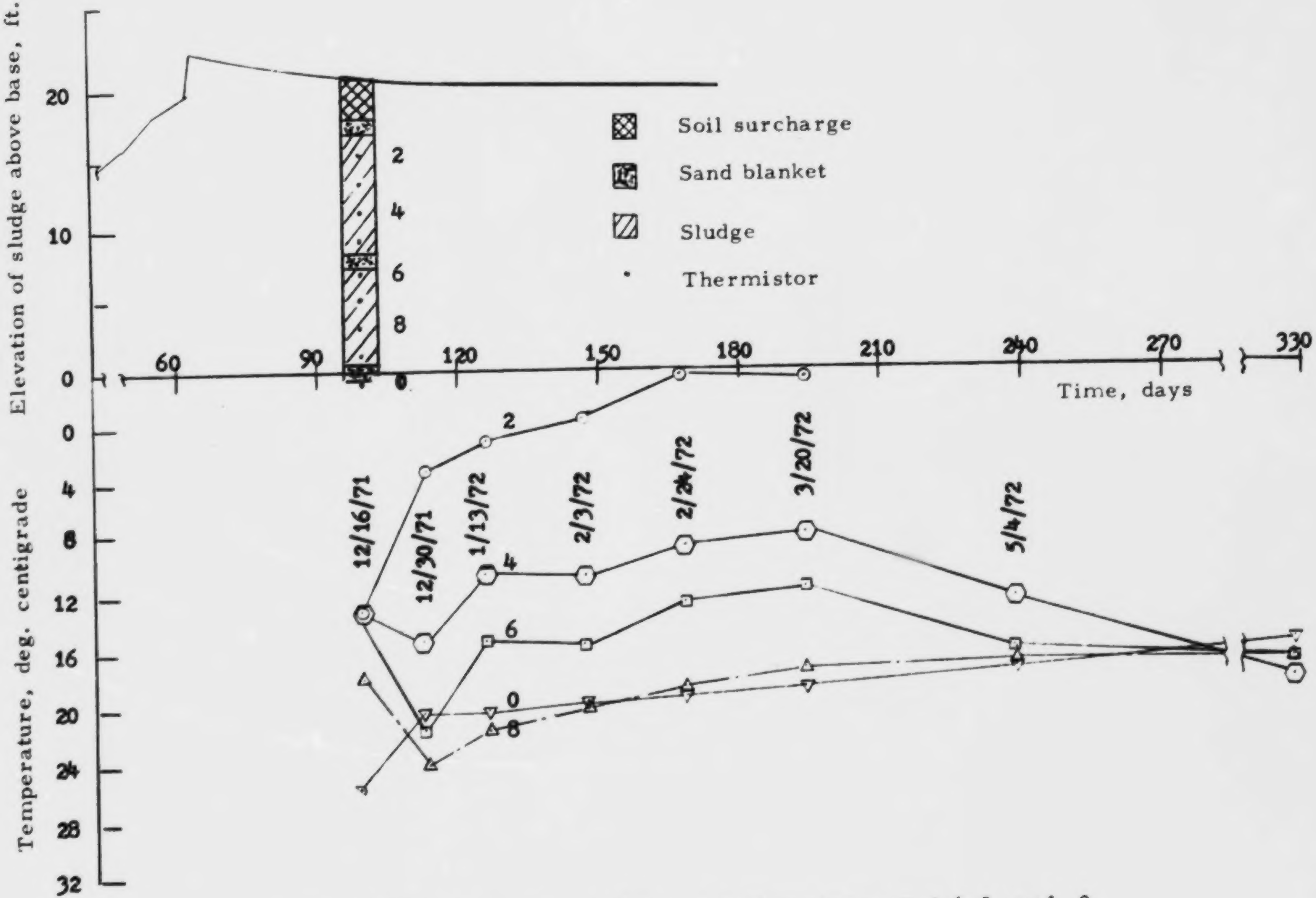

5.10. Temperature versus time. (b) Thermistors 2, 4, 6, 8, and 0.

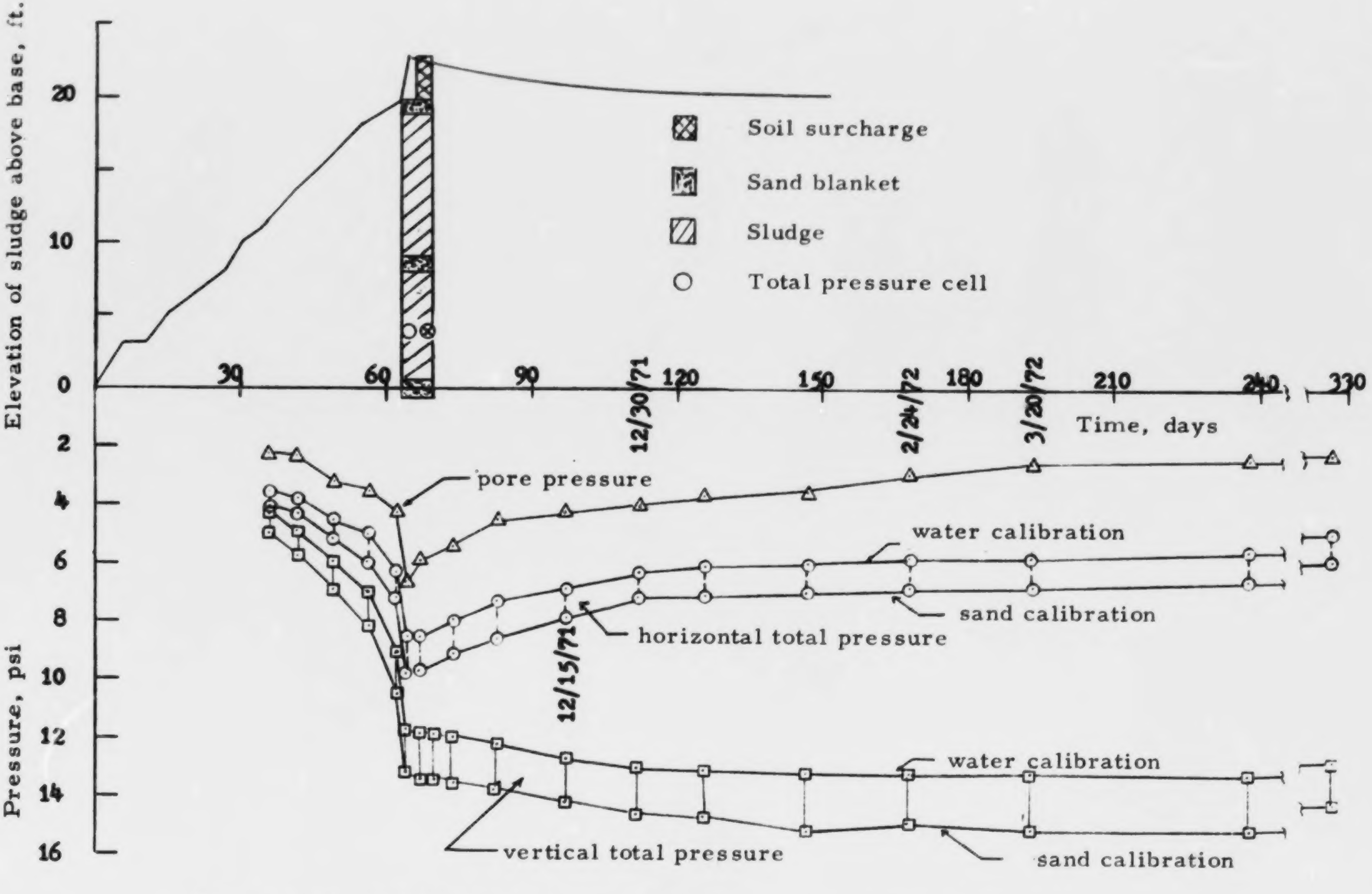

Figure 5.11. Horizontal and vertical total stresses, lower sludge layer.

Figure 5.12
COD Vs Time for Pipe Leachate (PL) and Well Leachate (WL)

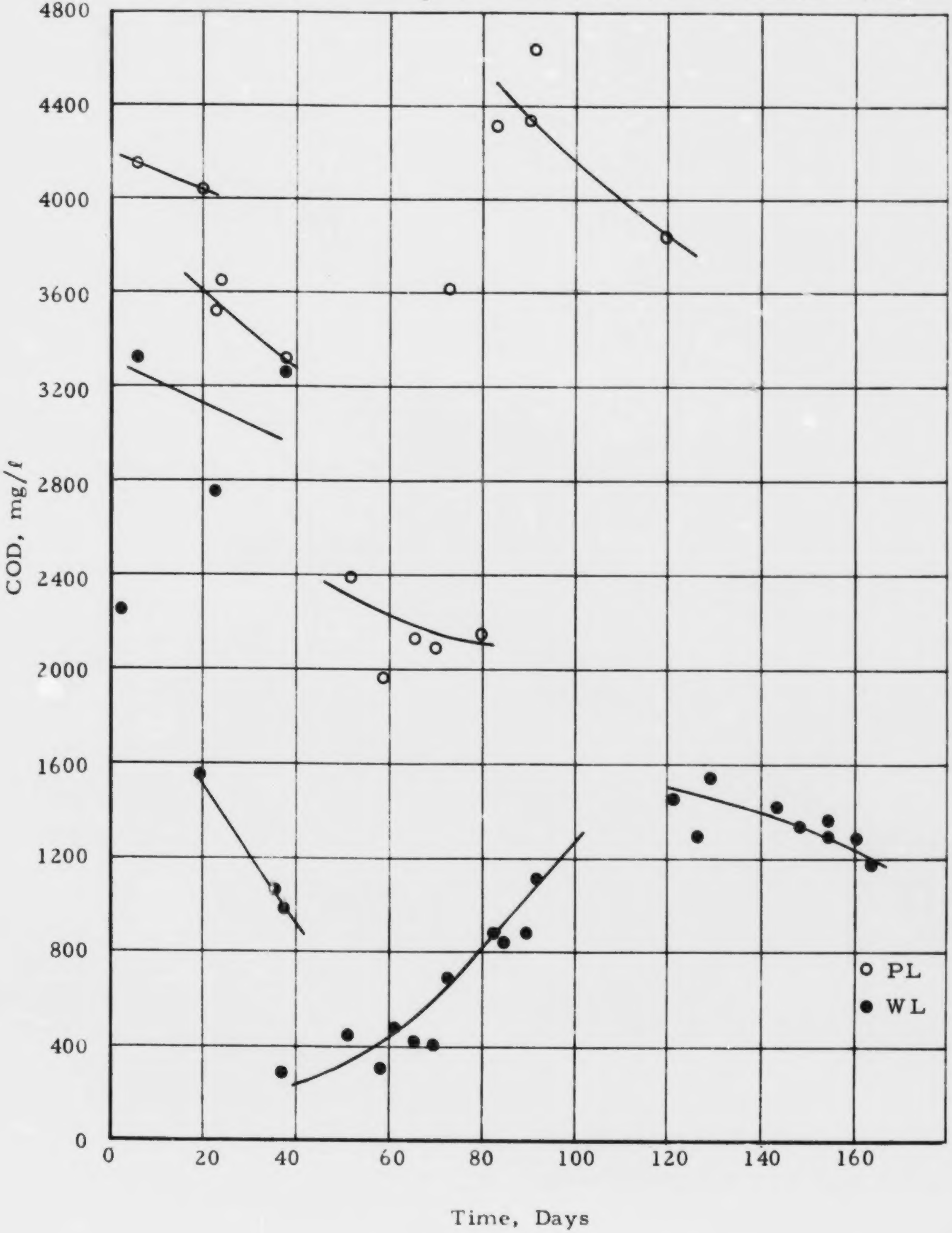

Figure 5. 13
BOD Vs Time for Pipe Leachate (PL) and Well Leachate (WL)

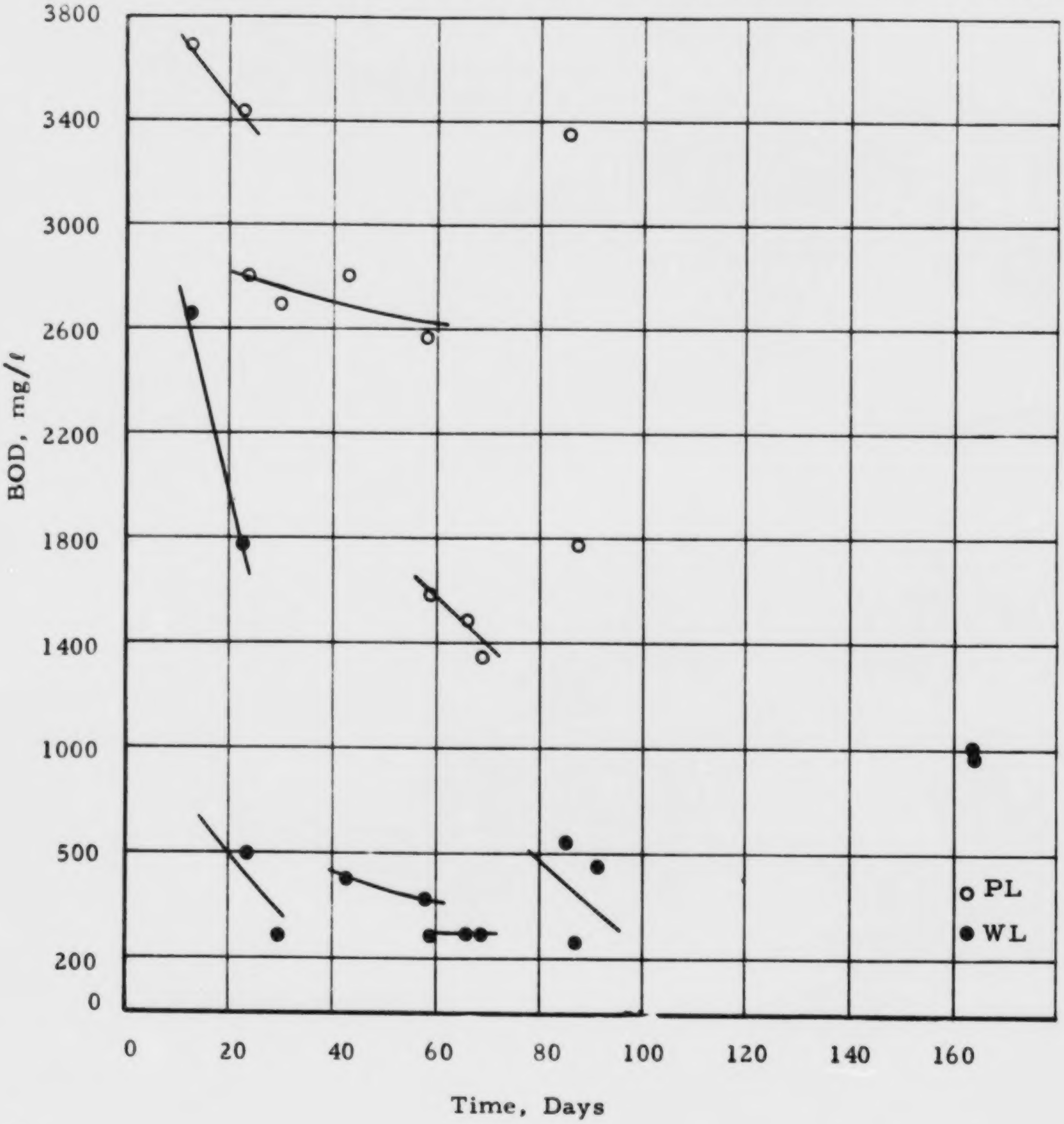

Figure 5. 14
Specific Conductance Vs Time for Pipe Leachate (PL) and Well Leachate (WL)

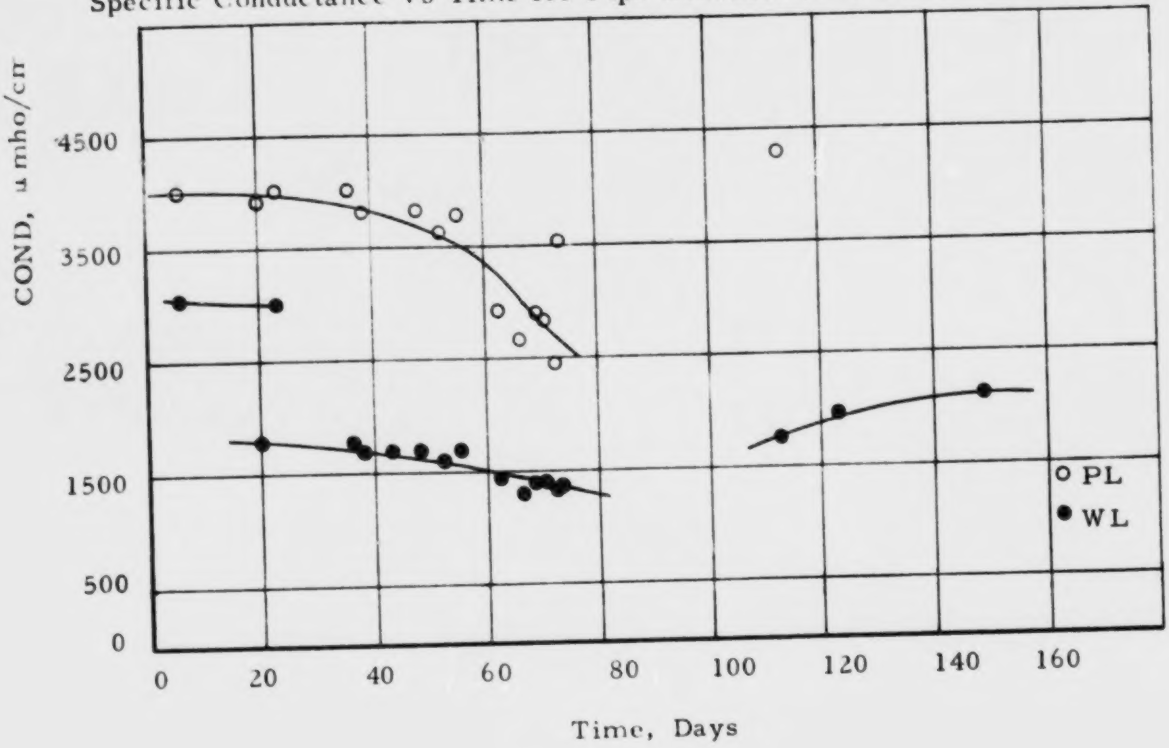

Figure 5. 15
Turbidity Vs. Time for Pipe Leachate (PL) and Well Leachate (WL)

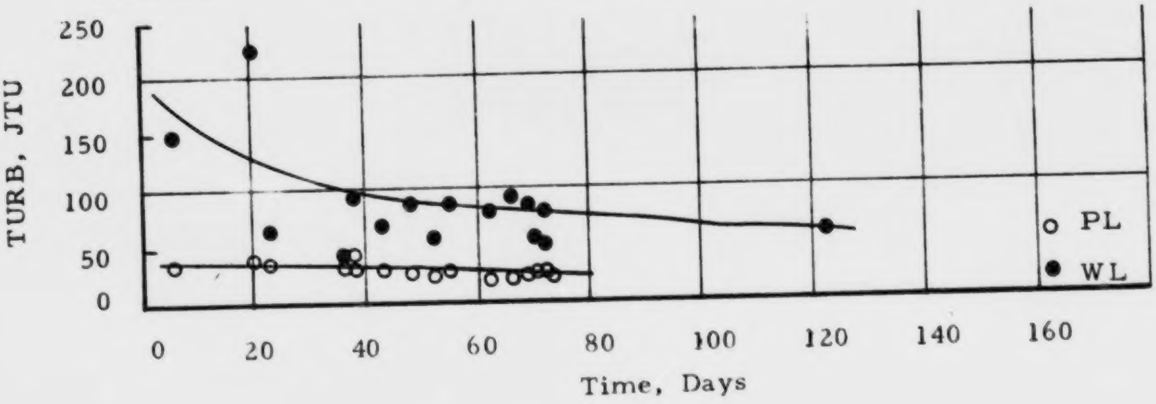

Figure 5.16.
Total Solids Vs Time for Pipe Leachate (PL) and Well Leachate (WL)

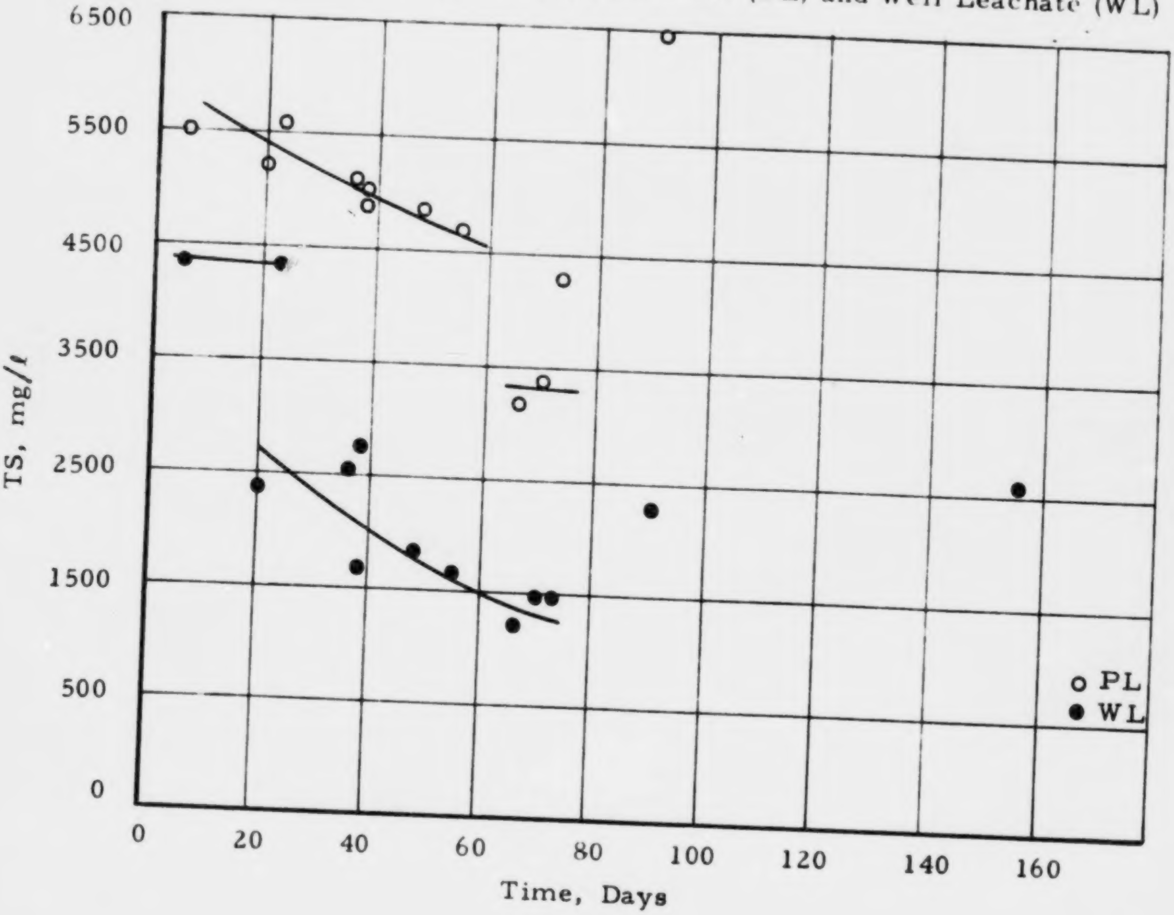

Figure 5.17.
Dissolved Solids Vs Time for Pipe Leachate (PL) and Well Leachate (WL)

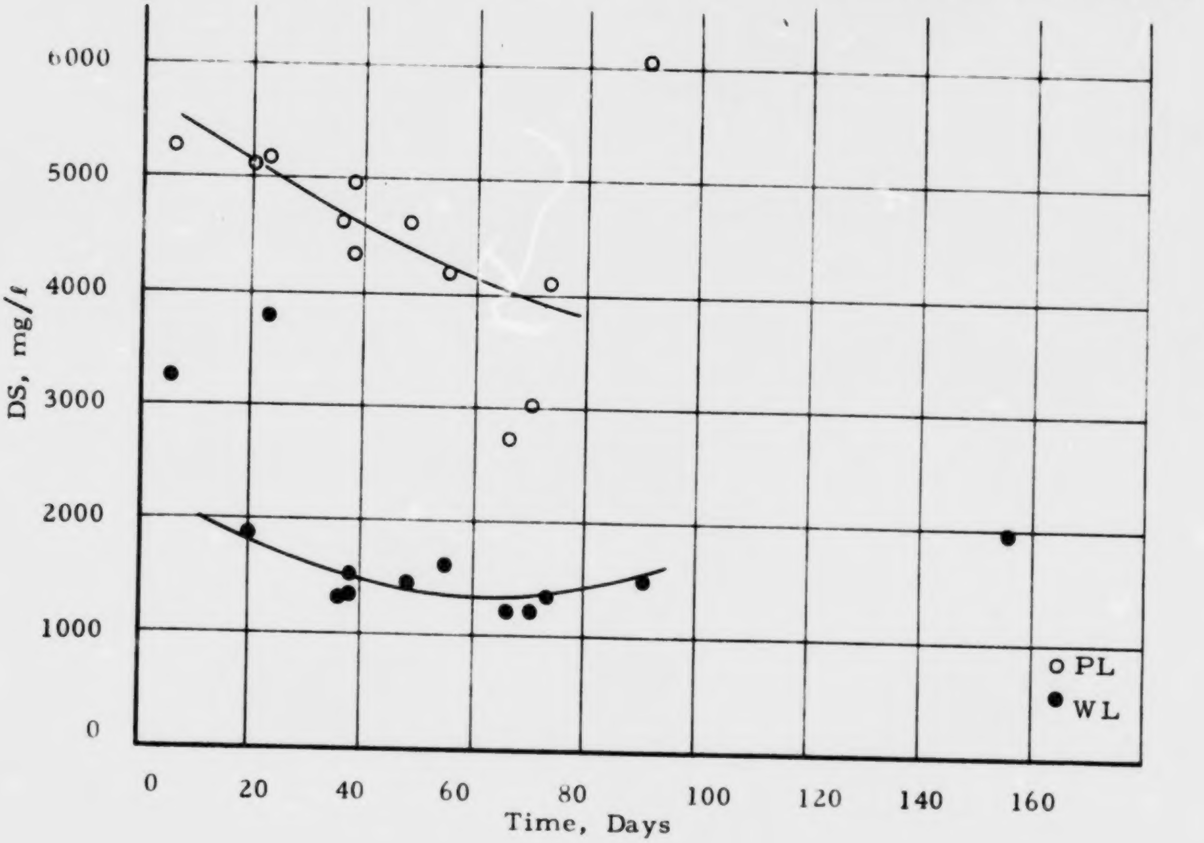

Figure 5.18.
Suspended Solids Vs Time for Pipe Leachate(PL) and Well Leachate (WL)

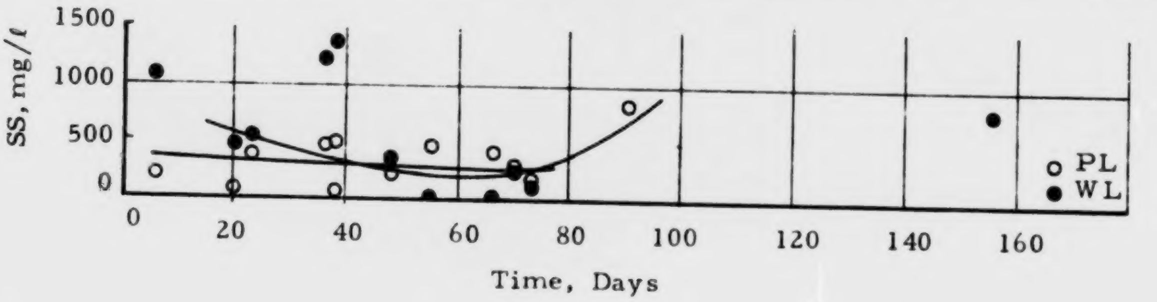

Figure 5.19.
COD Vs Time for Organic Loam Column-Well Leachate (WT) and Organic Loam Column-Aerobic-Pipe Leachate (PTA)

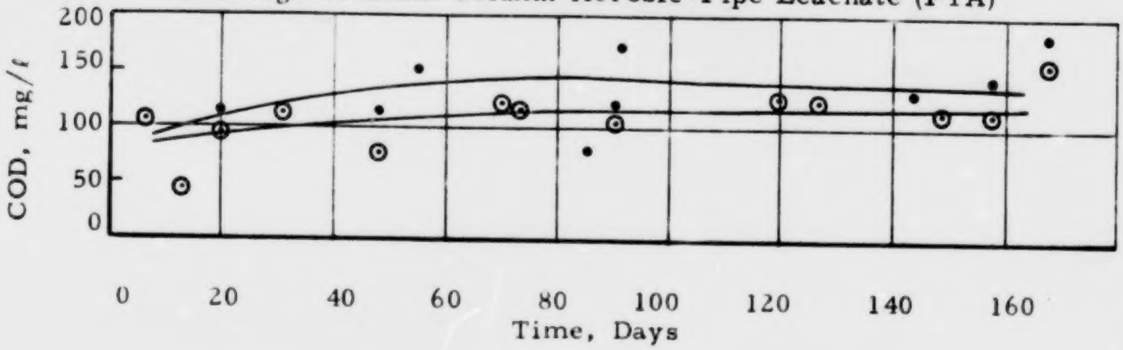

Figure 5.20.
COD Vs Time for Sand Column-Pipe Leachate (PS) and Clay Column-Pipe Leachate (PC)

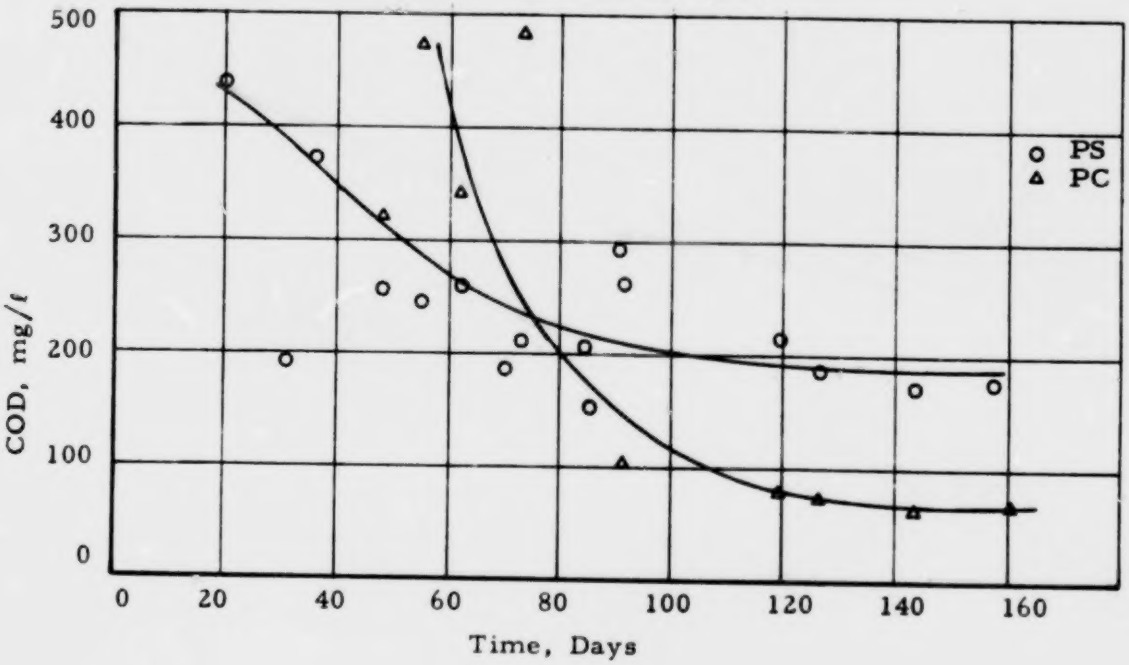

Figure 5.21.
COD Vs Time for Organic Loam Column-Anaerobic-Pipe Leachate (PTAN)

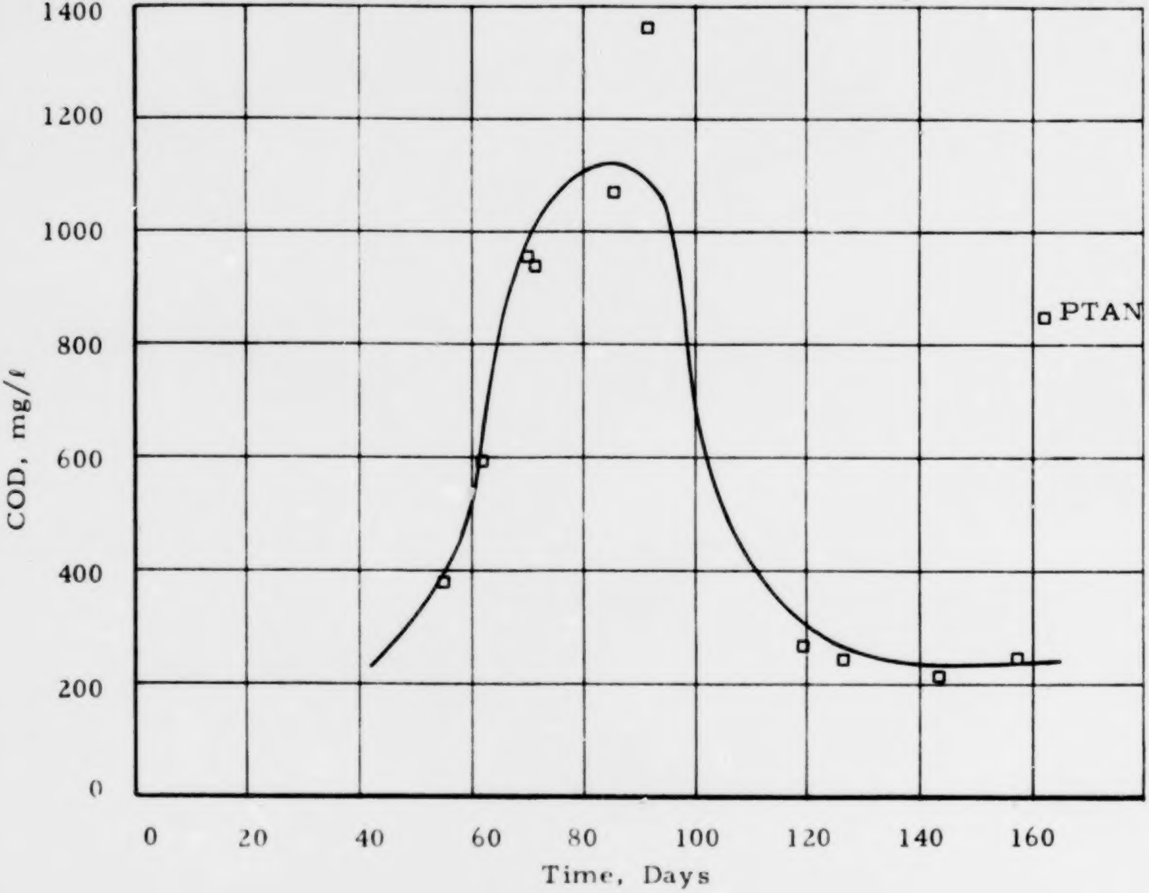

Figure 5.22.
BOD Vs Time for Organic Loam Column-Well Leachate (WT) and Organic Loam Column-Aerobic-Pipe Leachate (PTA)

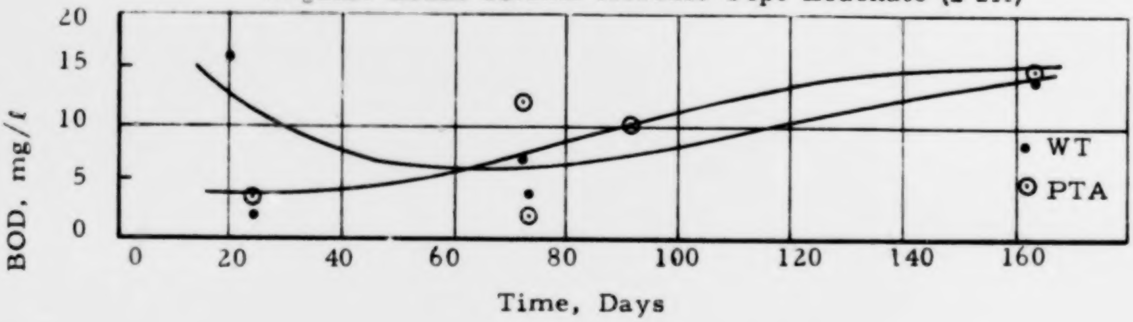

Figure 5.23
BOD Vs Time for Sand Column-Pipe Leachate (PS) and Clay Column-Pipe Leachate (PC)

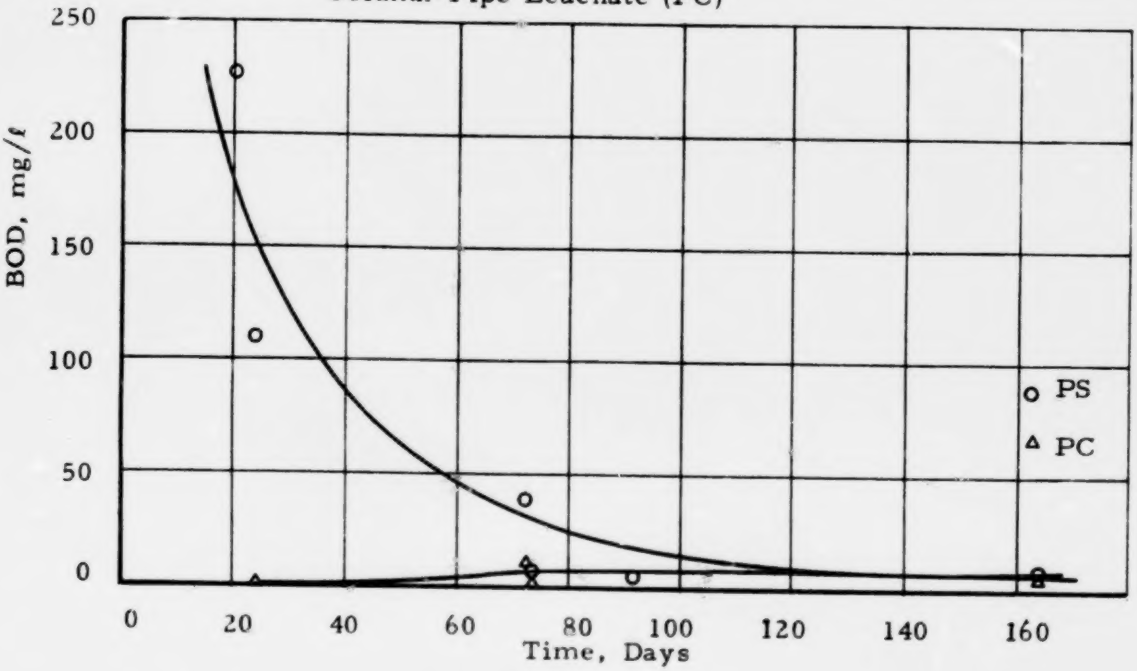

Figure 5.24.
BOD Vs Time for Organic Loam Column-Anaerobic-Pipe Leachate (PTAN) and Organic Loam Column-Double Dose-Pipe Leachate (DPT)

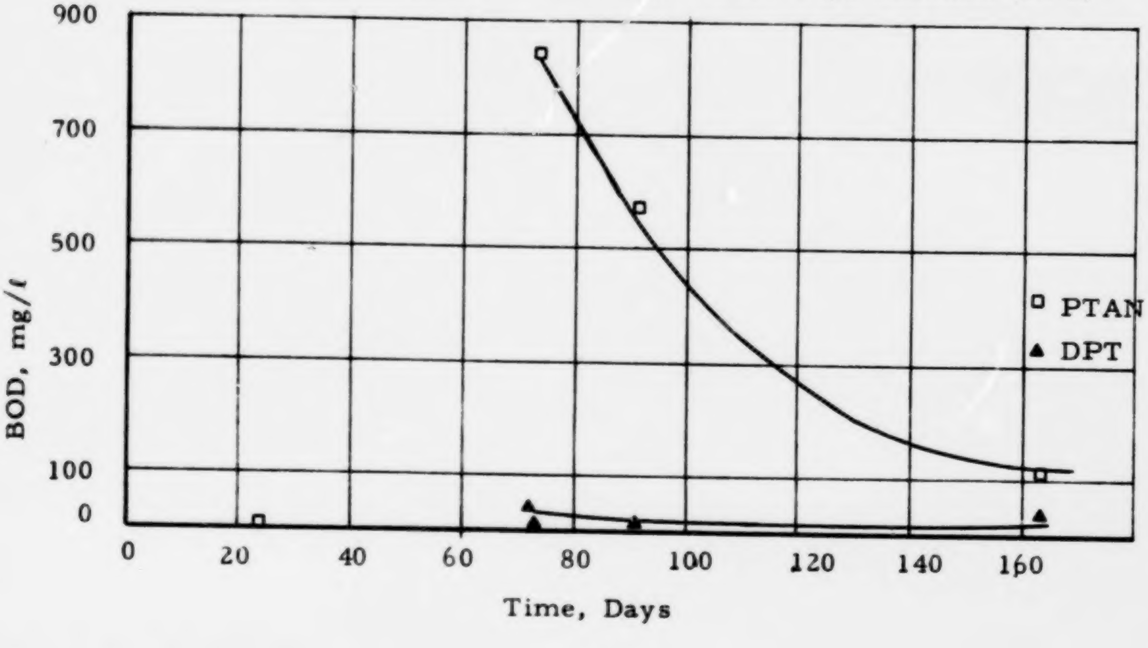

Figure 5.25.
Specific Conductance Vs Time for Organic Loam Column-Well Leachate (WT) and Organic Loam Column-Aerobic-Pipe Leachate (PTA)

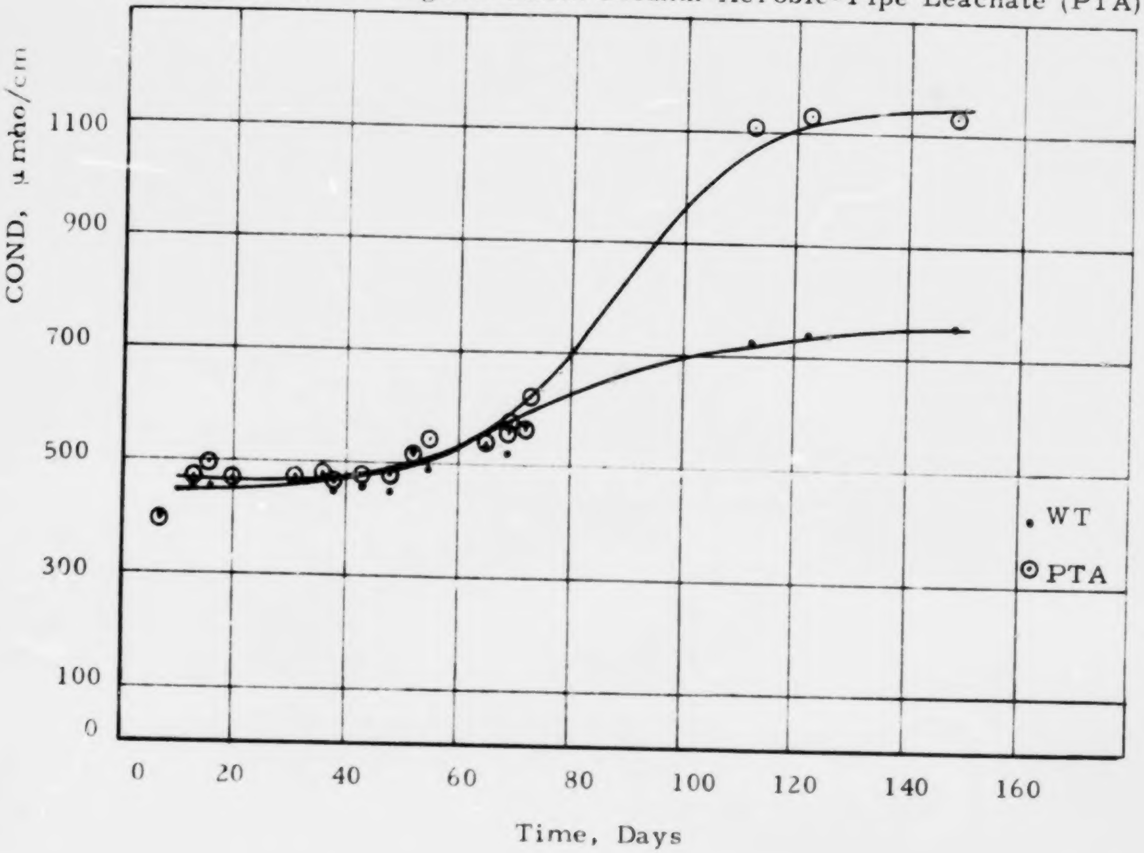

Figure 5.26.
Specific Conductance Vs Time for Sand Column-Pipe Leachate (PS) and Clay Column-Pipe Leachate (PC)

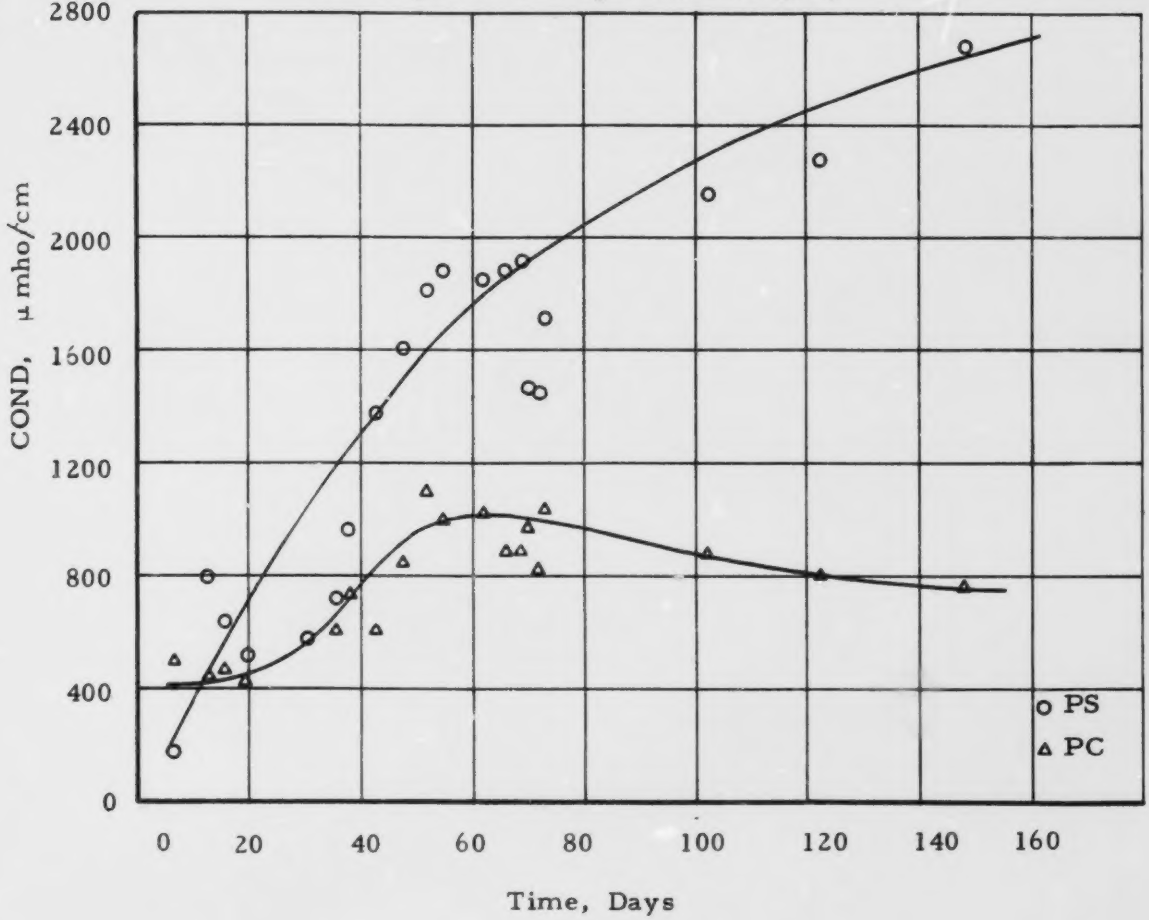

Figure 5. 27.
Specific Conductance Vs Time for Organic Loam Column-Anaerobic-Pipe Leachate(PTAN) and Organic Loam Column-Double Dose-Pipe Leachate(DPT)

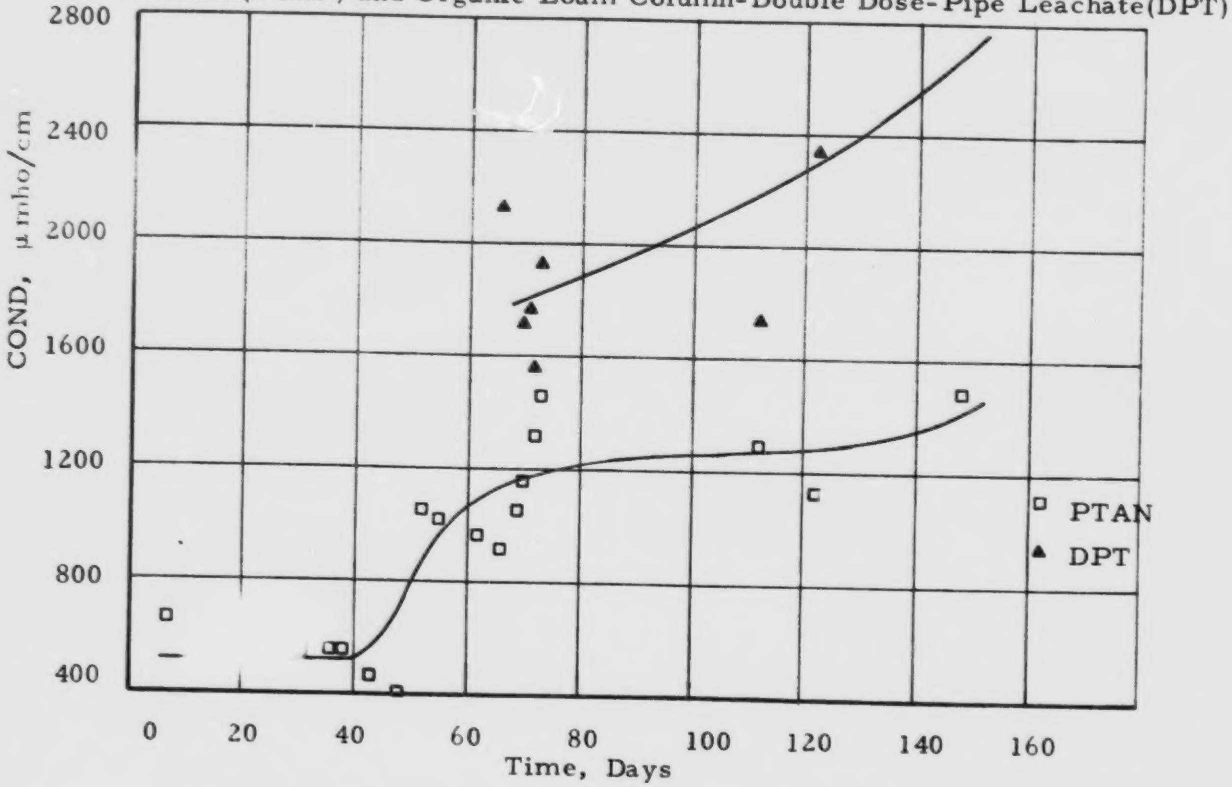

Figure 5. 28
Total Solids Vs Time for Organic Loam Column-Well Leachate (WT) and Organic Loam Column-Aerobic-Pipe Leachate (PTA)

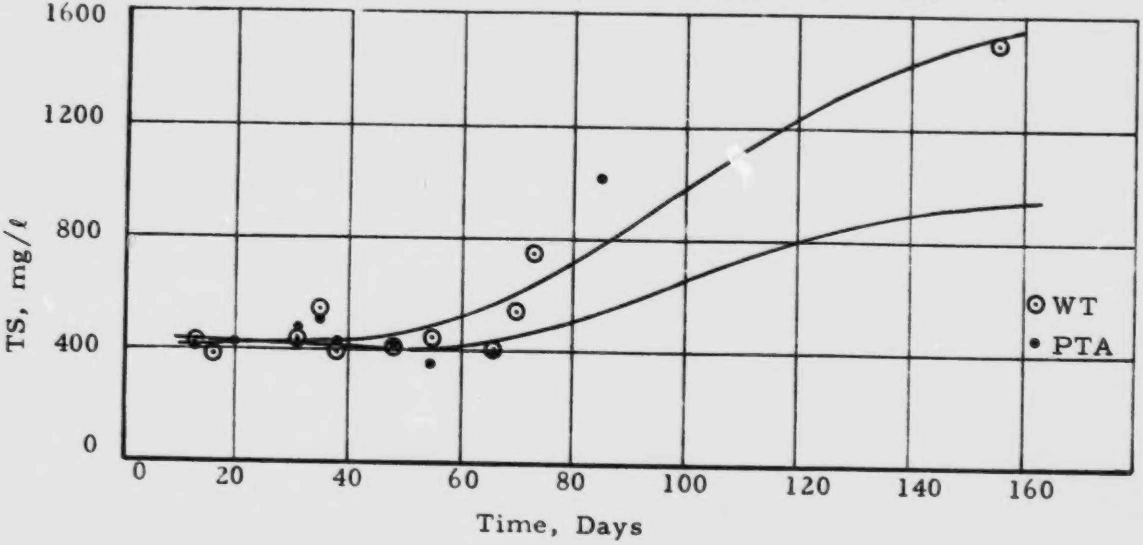

Figure 5. 29
Total Solids Vs Time for Sand Column-Pipe Leachate (PS) and Clay Column-Pipe Leachate (PC)

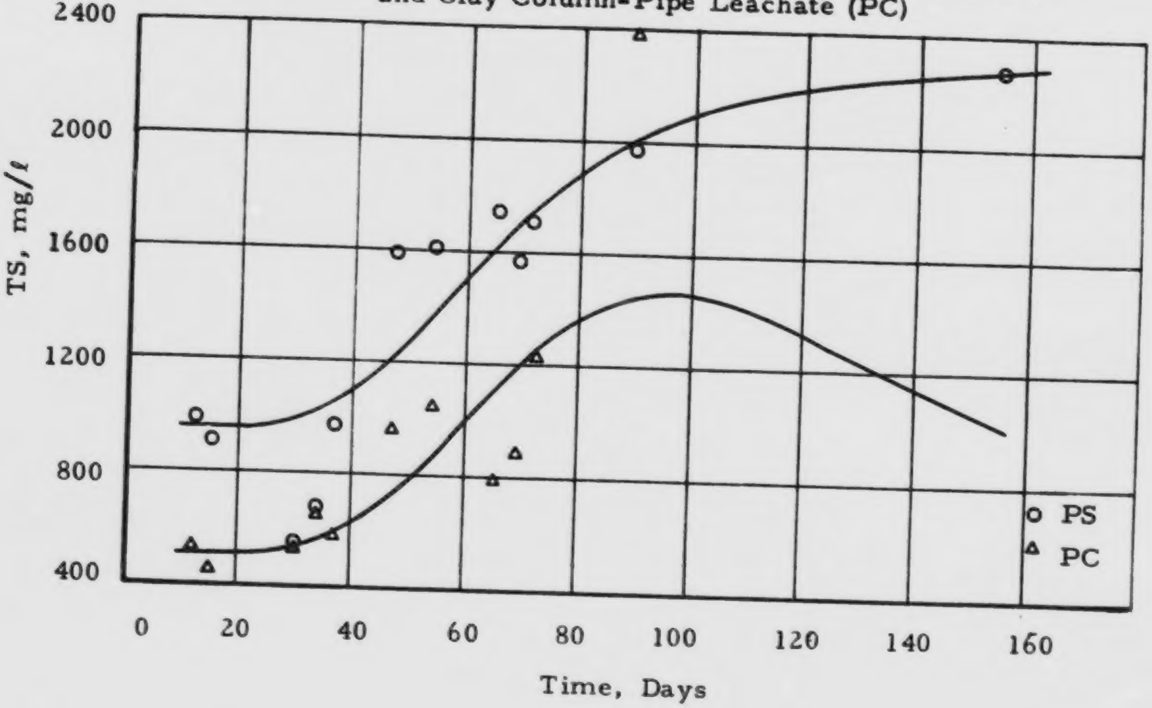

Figure 5. 30
Total Solids Vs Time for Organic Loam Column-Anaerobic-Pipe Leachate(PTAN) and Organic Loam Column-Double Dose-Pipe Leachate(DPT)

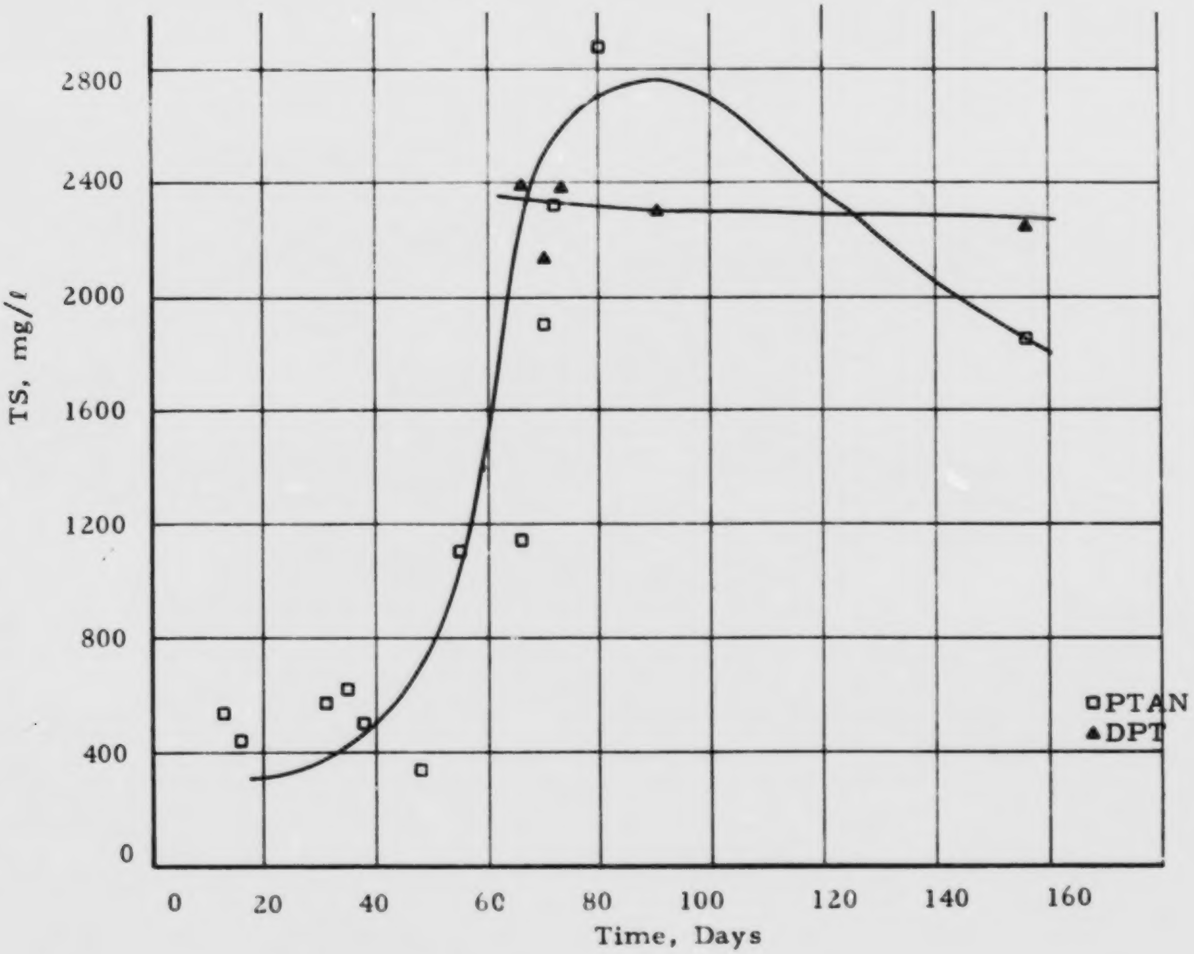

Figure 5.29
Total Solids Vs Time for Sand Column-Pipe Leachate (PS) and Clay Column-Pipe Leachate (PC)

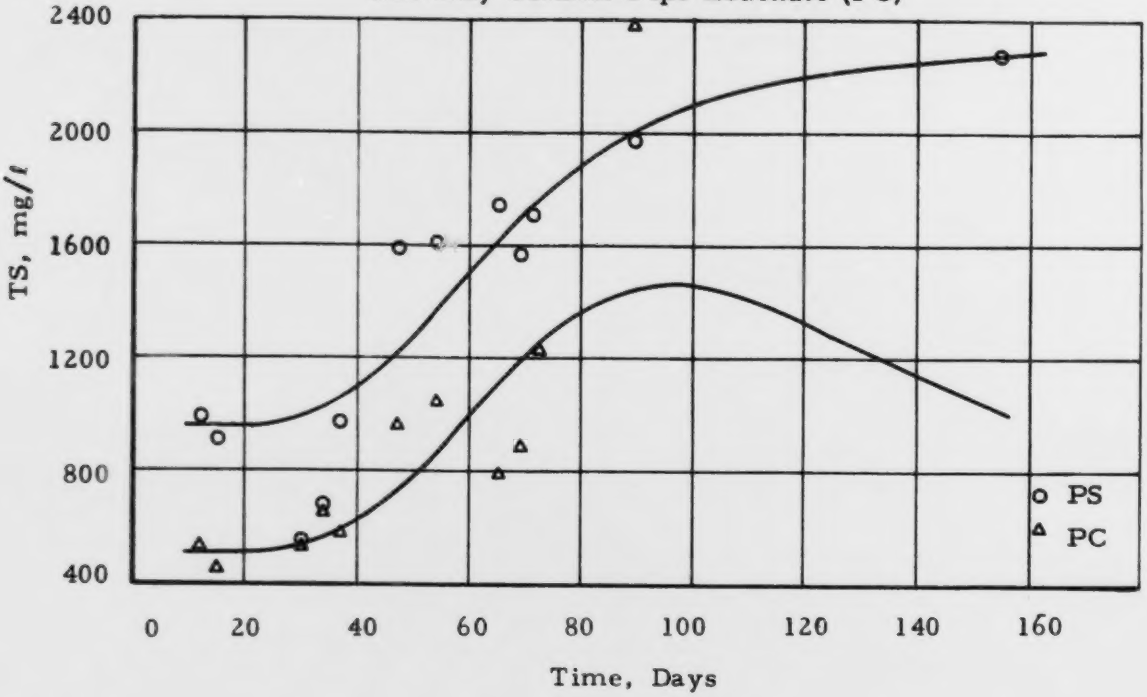

Figure 5. 30
Total Solids Vs Time for Organic Loam Column-Anaerobic-Pipe Leachate(PTAN) and Organic Loam Column-Double Dose-Pipe Leachate(DPT)

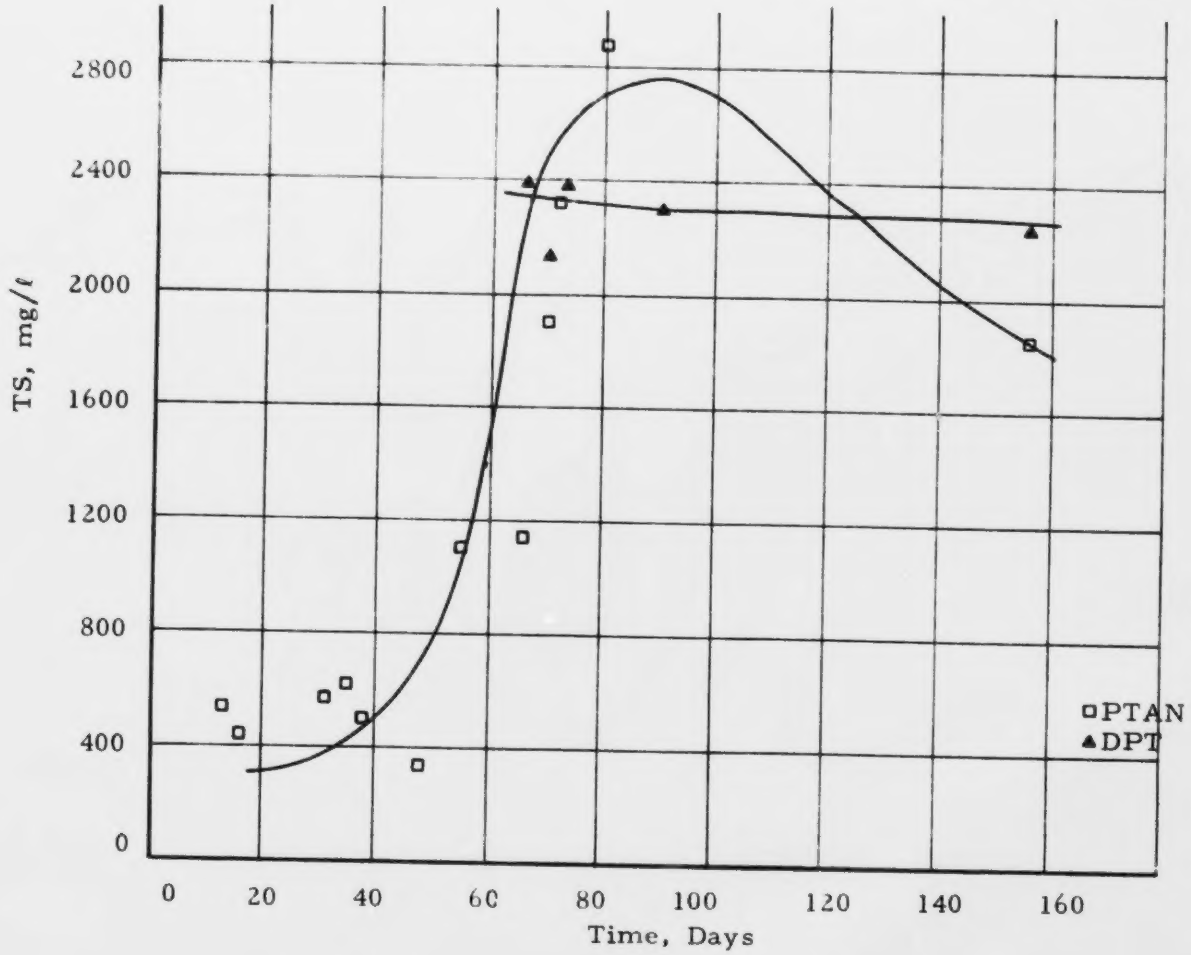

Figure 5. 31.
Dissolved Solids Vs Time for Organic Loam Column-Well Leachate(WT) and Organic Loam Column-Aerobic-Pipe Leachate (PTA)

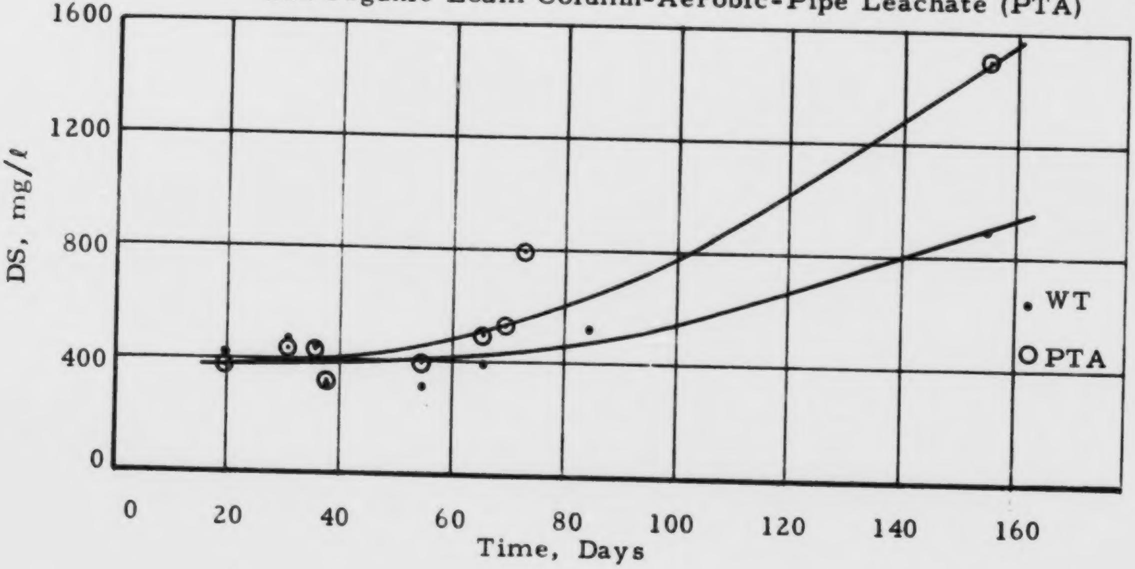

Figure 5. 32
Dissolved Solids Vs Time for Sand Column-Pipe Leachate (PS) and Clay Column-Pipe Leachate (PC)

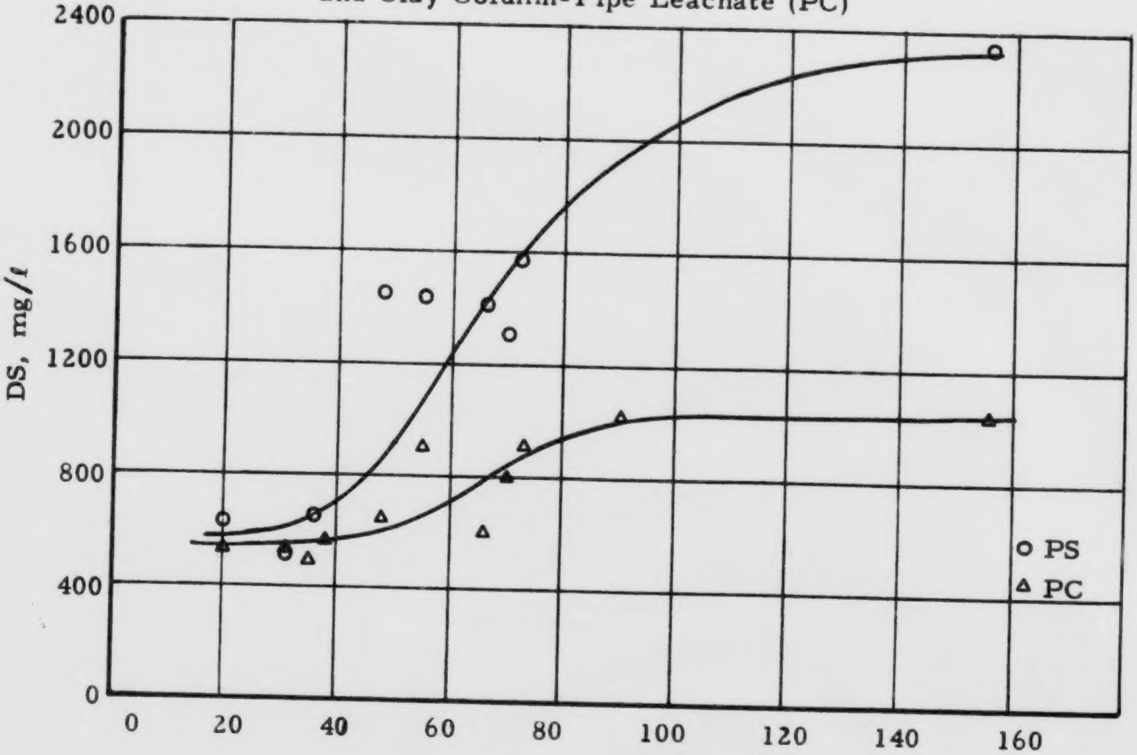

Figure 5.33.
Dissolved Solids Vs Time for Organic Loam Column-Anaerobic-Pipe Leachate(PTAN) and Organic Loam Column-Double Dose-Pipe Leachate(DPT)

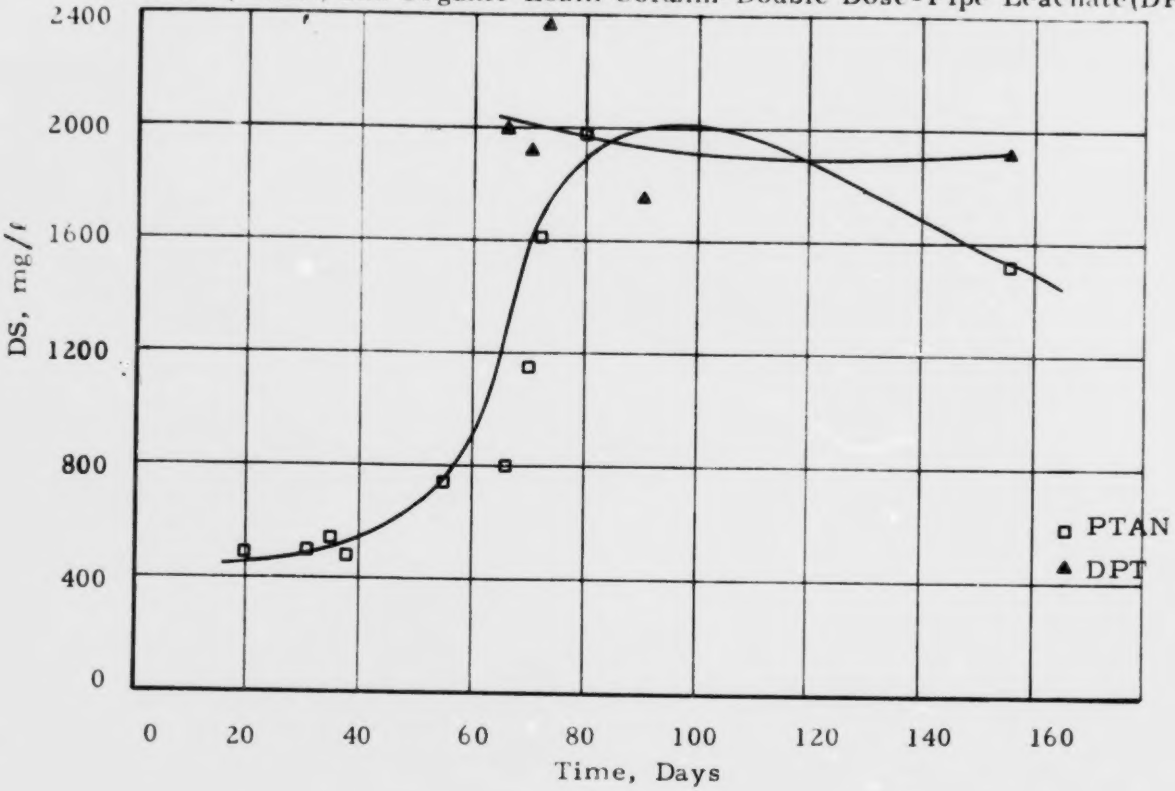

Figure 5.34.
Suspended Solids Vs Time for Organic Loam Column-Well Leachate (WT) and Organic Loam Column-Aerobic-Pipe Leachate (PTA)

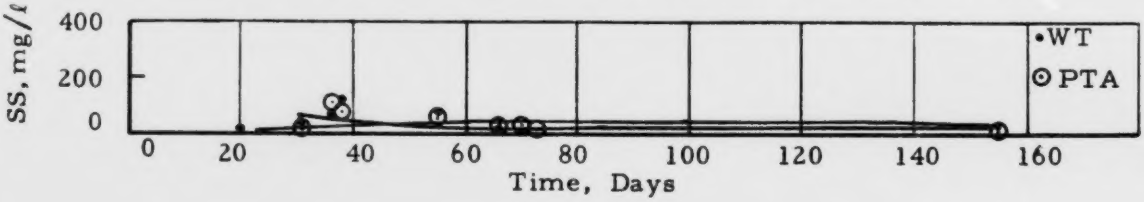

Figure 5. 35.
Suspended Solids Vs Time for Sand Column-Pipe Leachate (PS) and Clay Column-Pipe Leachate (PC)

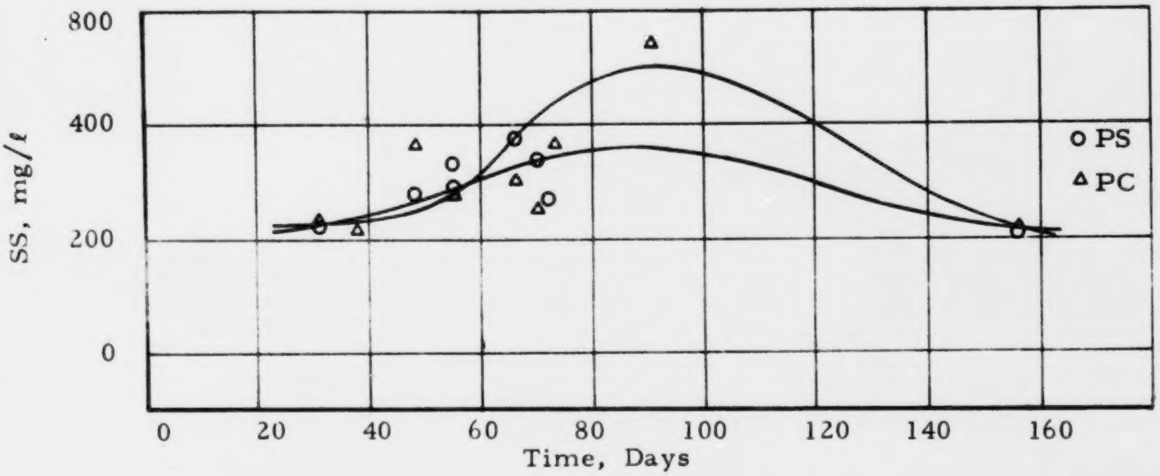

Figure 5. 36.
Suspended Solids Vs Time for Organic Loam Column-Anaerobic-Pipe Leachate(PTAN) and Organic Loam Column-Double Dose-Pipe Leachate(DPT)

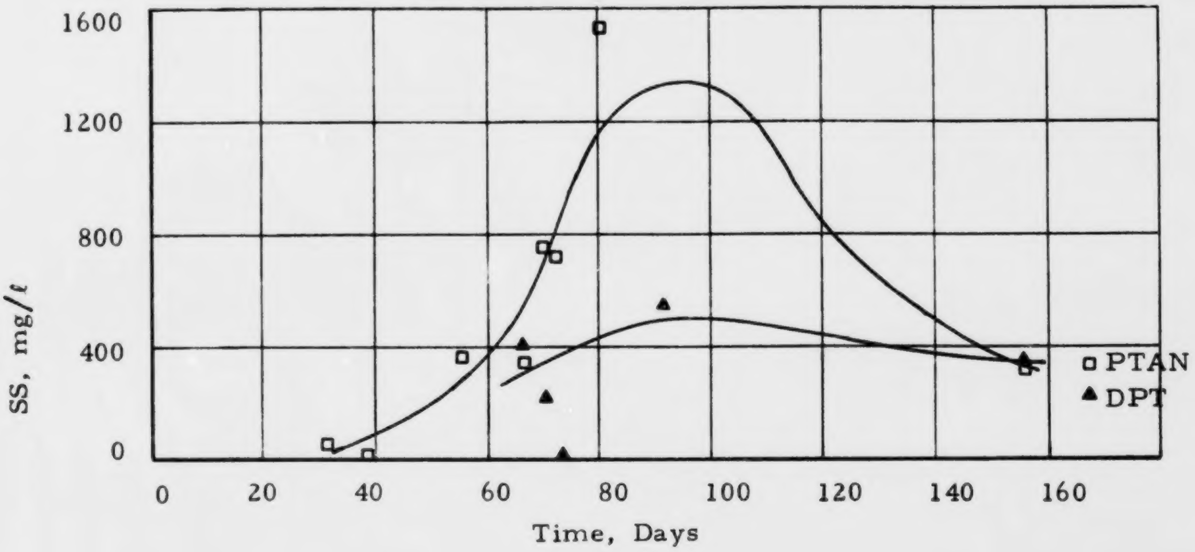

Chapter VI. DISCUSSION AND INTERPRETATION OF RESULTS

This discussion and interpretation includes laboratory and field results available in July, 1972, for the initial phase of the experimental papermill sludge landfill project. The material is presented in four sections including: (1) sludge placement, (2) engineering characteristics of the papermill sludge, (3) settlement behavior of the landfill, and (4) leachate analysis and lysimeter study.

Sludge Placement

A wide variety of equipment is available for papermill sludge landfill operations. Equipment selected for the project was based primarily on the contractor's experience with the sludge. Factors considered in selection included the cost and the ability of the equipment to meet the project needs. For example, placement of the sludge in 10-ft layers with reasonable uniformity required the use of a dragline that could reach to the central area of the landfill. The dragline was ideally suited to handle the loose bulk sludge where casting and placement were important, and the skill of the operator helped minimize hand shovel work adjacent to instrumentation. There was no problem of operating space requirements, and a firm support was provided by the earth dike surrounding the landfill. Sludge was delivered to the site from the dewatering facility by a large truck and was dumped either over the dike edge or adjacent to the site. Drainage blankets were placed by dumping sand from trucks on or adjacent to the site, followed by distribution with the dragline and/or dozer. For the top blanket, adequate support of the dozer was provided when sand was pushed ahead of the dozer. For the middle sand blanket, use of the dozer was avoided because of the possibility of its sinking into the soft sludge and the high dike walls shown in Figure 4.5. The sand was placed using the dragline and was leveled by pulling a makeshift drag (two telephone poles tied together) over the surface. Some hand shovel work was required next to instrumentation.

Preceding page blank

Engineering Characteristics of the Papermill Sludge

The engineering characteristics of the papermill sludge are discussed under headings which include (1) physical properties, (2) consolidation behavior, (3) undrained shear strength, (4) stress state in the sludge, and (5) temperature.

Physical Properties. The water content of the dewatered sludge is unusually high in comparison to inorganic soils normally encountered in engineering practice. Average water contents for the upper sludge layer were equal to 257 percent and for the lower layer equal to 265 percent for the data summarized in Table 5.2. Both the liquid and plastic limits shown in Table 5.1 tend to decrease for sludge samples with higher ash contents. This correlates with the decrease in water retention when organic content is reduced (Andersland and Laza, 1971). The presence of fibers in the sludge interfered with the mechanical test procedures used for the liquid and plastic limits, so that some error may have been introduced in the consistency limits. The volume change and settlement discussed in later sections involves a reduction in water content due to the weight of overlying sludge and surcharge loads.

Specific gravities of the sludge are directly related to the ash content, with the lower values shown in Table 5.1 corresponding to samples containing more organic material. Data in Table 5.1 show that the sludge composition will vary from day to day, with this variation dependent on operations at the papermill. The average specific gravity for the lower sludge layer, equal to 2.04, is not greatly different from the average for the upper layer, equal to 2.00. This small difference in average specific gravities, together with average water contents which are close for both sludge layers, indicates that initial unit weights should be about the same. The more accurate determination of sludge unit weight using the weight and volume of a truck load of sludge gave a value equal to 69.7 lb/cu ft.

Consolidation Behavior. The highly compressible nature of the papermill sludge is shown in Figure 5.1a, where the linear void ratio-logarithm of pressure curve gives a compression index, C_c, of 1.70. This high value for C_c is a result of the high organic and high water contents characteristic of fresh papermill sludge. Andersland and Paloorthekkathil (1972) have shown the dependence of C_c on these factors.

The nonorganic fraction, primarily kaolinite clay, has a compression index close to 0.25 and also contributes to the compressibility of the sludge.

The variation in the coefficient of consolidation, c_v, with each load increment is illustrated in Figure 5.1b. The square root of time fitting method gives the higher values for c_v as compared to the logarithm of time fitting method. The change in c_v during compression depends on the change in both the permeability and compressibility of the sludge, since c_v equals $\frac{k}{a_v \gamma_w}$ Here, k is the coefficient of permeability, a_v the coefficient of compressibility of the soil skeleton equal to $- \frac{1}{1 + e} \frac{\partial e}{\partial \bar{\sigma}}$, e the void ratio, $\bar{\sigma}$ the effectives stress, and γ_w the unit weight of water. It is apparent from Figure 5.1b that the coefficient of permeability for the sludge has decreased more rapidly than the compressibility. This reduces c_v for increasing effectives stress, as shown in Figure 5.1b.

The variation in primary compression ratio, r, with pressure is shown in Figure 5.1c. Compression can be separated into three parts such that $\frac{d_i}{D} + \frac{d_p}{D} + \frac{d_s}{D}$ equals unity, where D is the total compression experienced over the load increment and d_i, d_p, and d_s are the initial, primary, and secondary compression, respectively. In our case, r equals $\frac{d_p}{D}$ and is a measure of the amount of compression that occurs only as a result of pore water expulsion. The variation in r shown in Figure 5.1c is difficult to explain. Andersland and Paloorthekkathil (1972), for larger loads, obtain a fairly constant r with pressure, although there is considerable scatter in their results. The curve in Figure 5.1c shows results typical for all tests run with the Bishop consolidation machine with smaller loads. The drop in r with the second load increment could be due to a reduced hydrodynamic effect associated with the small amount of pressure added after the first increment (0.1 kg/cm^2). Since secondary compression is a function of stress level, its affect may increase slightly over the load increment. However, the load increment is so small that hydrodynamic compression due to pore water expulsion exhibits a reduced affect and secondary compression may become more prominent in the total compression over the load increment. This is shown by the flatter dial reading versus logarithm of time curve shown in Figure 5.2a. As the load increments increase in size, the hydrodynamic effect becomes more dominant and r increases. The high value of r for the first increment (0 to 0.1 kg/cm^2) may be due to the large amount of deformation occurring over the increment (e changes from 5.35 to 4.51). Figure 5.2b illustrates the curved shape of the logarithm of time curves associated with larger load increments.

Figure 5.3a shows the variation in the coefficient of secondary compression, c_{α}, with effective pressure. There is a slight increase in C_{α} with pressure, as might be expected because of the greater deviatoric stresses occurring at higher pressures. However, this is somewhat compensated for by the increased density and reduced compressibility of the sludge resulting from compression. Andersland and Paloorthekkathil (1972) show a fairly constant C_{α} with effective pressure. Figure 5.3b illustrates the reduction in the ratio $C_{\alpha}/\Delta p$ with increasing load increment.

Undrained Shear Strength. The undrained vane shear strengths summarized in Figure 5.4 show a very large dependence on the degree of consolidation. A slightly greater initial strength in the upper layer (11/11/71) as compared to the lower sludge layer (10/14/71) can be explained by the lower average initial water content (footnote, Table 5.2) in the upper layer. The increase in strength with depth shows up immediately with only partial consolidation. Laboratory data (Andersland and Laza, 1971) show a linear relationship between undrained strength and consolidation pressure. Sensitivity of the sludge in terms of the ratio of undisturbed to remolded strength is small, ranging from about 1.5 to 2.5. This is comparable to many inorganic clays (Terzaghi and Peck, 1967). Very significant increases in strength have occurred in 3-1/2 months, as shown by data obtained on 3/20/72. Most of this improvement in strength presumably occurred during primary consolidation. Final shear strengths, to be taken just prior to phase II of the project, are not available at this date.

According to recent data presented by Bjerrum (1972), the vane shear strengths summarized in Figure 5.4 do not represent the actual field undrained shear strengths needed in a slope stability analysis. Bjerrum (1972) recommends that the vane shear strengths be adjusted according to the relation

$$(s_u)_{field} = (s_u)_{vane} \cdot \mu \qquad (6.1)$$

where s_u is the undrained shear strength and μ a parameter which is dependent on the plasticity index. For the sludge plasticity index of about 150, Bjerrum's (1972) chart gives a value of $\mu = 0.6$. A comparison of $(s_u)_{vane} \cdot \mu$ values with preliminary laboratory undrained triaxial data gives reasonable agreement. More information will be available when phase II of the project is completed.

Stress State in the Sludge. Both the vertical and the lateral total stresses recorded on the total pressure cells (Terra Tec model T-9010) located near the middle of the lower sludge layer are summarized in Figure 5.11 for the period during sludge placement, surcharge loading, and consolidation. Values for the water calibration of the cells are probably on the low side, with the real pressures falling between the water and sand calibration. As consolidation proceeded, the horizontal pressures decreased while the vertical pressures increased. This increase is contrary to what would be expected because as water drains from the sludge and leaves the area, the total vertical pressure should decrease. It is presumed that this peculiar behavior is due to certain limitations of the total pressure cell.

Subtraction of pore pressures (piezometer G7-3) from total pressure values gives effective stresses. Taking the ratio of effective horizontal to vertical stresses gives an estimate of the coefficient of lateral earth pressure, K. Initial values for the ratio K are 0.63 for water calibration and 0.684 for sand calibration. Immediately after surcharge application these values were reduced to 0.386 and 0.481, respectively. For the final stages of consolidation the values for K dropped to 0.30 (water calibration) and 0.34 (sand calibration). These final values of K should approximate normal consolidation of the papermill sludge. Using a preliminary value for the angle of internal friction, $\overline{\phi}$, equal to 57 degrees at an organic content of 41 percent, it can be seen that the correlation between K_o and $\sin\overline{\phi}$ for normally consolidated inorganic clays (Lambe and Whitman, 1969) does not appear to hold for the papermill sludge (assuming that the data are accurate).

Temperature. Temperatures at various levels in the sludge landfill, with corresponding dates, are summarized in Figure 5.10. Difficulties with installation of thermistors delayed the initial temperature readings until about 1 month after placement of the surcharge load. The temperature rise due to increased biological activity appears to have peaked about 50 days after completion of the landfill. The maximum temperature rise of about 7°C occurred in the upper half of the lower sludge layer. Subsequent winter weather reduced the sludge temperatures at all levels until spring and summer, when the seasonal warming effects prevailed. During January and February, when average monthly air temperatures were close to zero degrees centigrade, sludge temperatures ranged from about 3°C near the surface to 20°C in the bottom sand blanket. Warmer spring air temperatures decreased this range in temperatures, and in the early part of August the colder temperatures were near the bottom of the landfill. The warmer summer temperature, plus a period of low rainfall, appeared to have influenced pore pressure readings shown in Figure 5.9 for the upper portion of the top sludge layer. This will be discussed in a later section on pore pressure dissipation.

Settlement Behavior of the Landfill

The settlement behavior of the landfill is discussed under two headings: the upper sludge layer and the lower sludge layer. Both sections include information on (1) loading and general field observations, (2) ultimate settlement, (3) time-rate of settlement, and (4) pore pressure dissipation.

Upper Sludge Layer.

Loading and Field Observations. The upper sand blanket and earth surcharge provided a total applied load of about 490 psf on the surface of the upper sludge layer. This load was applied in a period of about 4 days (Figure 5.5), with most of the surcharge placement occurring on the last day. This loading rate approximates an instantaneous loading condition. Considering the landfill area involved, the resulting settlement had to be due to drainage and compression only in the vertical direction. Similarity of time-settlement curves (Figure 5.5) between instrument groups supports this fact. Some difference in ultimate settlement between groups can be attributed to small differences in load application (maximum ±3 inches in surcharge thickness) and nonhomogenity of the sludge, with respect to water content, occurring during placement (Table 5.2). The major difference involved instrument group 7 where excess settlement occurred when soil for the surcharge was piled there prior to spreading with a dozer.

The square root of time and logarithm of time versus settlement curves (Figures 5.6 and 5.7) for the upper sludge layer provide information on the amount of primary and secondary compression, the coefficient of consolidation c_v, and the coefficient of secondary compression C_α. The square root of time curves in Figure 5.6 were prepared on the assumption that the initial point occurred at the completion of surcharge placement. About 3 inches of settlement occurred in most instrument groups during surcharge load placement. However, the assumed initial point gives an average c_v, equal to 0.0626 in^2/min for 90 percent consolidation, that is in agreement with the logarithm of time curves (Figure 5.7) and the pore pressure dissipation curves (Figure 5.9). The logarithm of time curve fitting method shows that primary settlement was complete after about 750 hours, and was then followed by secondary compression. Primary compression is rate controlling and determines the shape of the curve only during the initial stages of settlement because it occurs more rapidly than secondary compression. Using the time-settlement curves for instrument group 6 (Figure 5.5f) as representative of the sludge landfill, primary compression equaled about 16.7 inches and secondary compression about 4.1 inches (for a total $t = 238$ days). Pore pressure dissipation curves (Figure 5.8d) confirmed that primary compression is essentially complete at about 34 days.

The decreasing secondary compression rate, shown in Figure 5.7, is not in full agreement with the laboratory curves shown in Figure 5.2. The laboratory curves showed a linear relation between settlement and logarithm of time after a relatively short transition curve.

The settlement experienced over the last time interval shown on the settlement versus logarithm of time curves (Figure 5.7) was larger than expected. This is due to drying of the upper half of the layer as a result of higher summer temperatures and low rainfall. As shown in Figure 5.9c, piezometer G5-8 exhibited a large reduction in pore pressure over this time interval. Calculations showed that approximately 65 percent of the total settlement over this interval occurred in the upper half of the layer. Thermistors 1 and 3 (Figure 5.10a) showed higher temperatures in the upper half of the upper sludge layer at the time of the last reading (t = 327 days).

To illustrate the correlation between landfill settlement and leachate drainage, a comparison has been made in Figure 6.1 between the measured leachate flow rate, Q_m, at the drainage pipe outlet shown in Figures 4.1 and 4.3 and the calculated flow rate, Q_c, based on the slope of the time-settlement curves (Figure 5.5). All but one of the points shown give Q_c greater than Q_m. This would be expected because the drainage system was not constructed to be leakproof and leachate was undoubtedly lost into the dike and the material surrounding the pipe. The point shown of 11/12/71 was calculated from the slope of the time-settlement curve for the lower layer only, since the upper layer was not yet completed. Because leachate was draining from the upper layer also, the point should be displaced to the right to be more accurately located. It was assumed that for the upper layer one half of the flow went to the top of the layer and the other half to the drainage pipe. Despite the uncertainties involved in the flow rate measurements, the correlation to the settlements is fairly good. Heavy rain after December 1, 1971, caused infiltration of rainwater into the pipe and flow rates measured at the pipe outlet increased considerably.

Ultimate Settlement. For plastic clays and organic soils (including papermill sludge) the ultimate settlement estimate must include both primary and secondary compression. When data are not available from previous experience, the parameters needed for a settlement analysis are obtained from laboratory tests and extrapolated to field behavior. The following discussion reviews several procedures for estimating ultimate settlement and applies them to the experimental sludge landfill.

A common method for estimating ultimate primary settlement uses the stress-strain relation

$$\epsilon = \frac{C_c}{1 + e_o} \log_{10} \frac{\overline{\sigma}_f}{\overline{\sigma}_o} \qquad (6.2)$$

where $\epsilon = \frac{ds}{dz}$ is the vertical strain at a point, C_c the compression index, e_o the initial void ratio, $\overline{\sigma}_o$ the initial effective normal vertical stress, and $\overline{\sigma}_f$ the final effective normal vertical stress. Equation 6.2

is an extension of equation 2.1. The total or ultimate primary settlement, ΔH, for a sludge layer of initial thickness, H, can be found by integration.

$$S = \Delta H = \int_0^H \frac{C_c}{1 + e_o} \log_{10} \frac{\overline{\sigma}_f}{\overline{\sigma}_o} \, dz \qquad (6.3)$$

Application of this equation to in situ soil layers is straightforward, since the soil is in static equilibrium with a fixed groundwater table permitting computation of changes in effective vertical stresses. However, in the sludge landfill the presence of excess pore pressures both before loading, due to the weight of overlying sludge, and after completion of primary compression, a residual pore pressure assumed due to an insufficient gradient for flow, complicate computation of the effective stresses. The procedure followed in application of equation 6.2 is illustrated in Figure 6.2. The initial effective stresses in the sludge after placement of the upper sand blanket are given in Figure 6.2a. Pore pressures represent field data from instrument group 7 just prior to surcharge loading. The sand blanket was not yet placed at other instrument groups when these data were obtained. Total vertical stresses are computed using a constant sludge unit weight equal to 70 pcf. Initial void ratios are taken from a laboratory e log $\overline{p}$ curve at the effective stress $\overline{\sigma}_o$ shown. Final effective vertical stresses are given in Figure 6.2b. Final stresses due to the overburden weight of sludge and soil will be different because the sludge unit weight will have increased by an amount dependent on the decrease in water content. The effect would be to reduce the overburden weight. For this analysis it was assumed that this reduction in overburden weight would not greatly alter the results. Subtracting the residual pore pressure in Figure 6.5 from the total stresses in Figure 6.2b gave the final effective normal stresses. Substitution of the stresses from Figure 6.1a and 6.2b into equation 6.3 gave the strain values shown in Figure 6.2c. Integration of this strain over the thickness of the upper sludge layer provided an estimate of the ultimate primary settlement equal to 18.1 inches. Since this value was close to the observed primary settlement of 16.7 inches, use of equation 6.2 appeared to be justified. For design purposes the use of equation 6.2 will be somewhat limited, since no methods are available for predicting the residual pore pressure. Initial pore pressures generated during sludge placement can be estimated by the procedure discussed in the next section.

The accuracy of the analysis shown in Figure 6.2 and 6.12 can be seen from Table 6.1. Here the settlements calculated from the assumed strain distribution are compared to the actual settlement of the upper and lower halves of the two sludge layers. The end of primary compression for the field calculations was taken from the pore pressure dissipation curves (Figure 5.9), and the total primary settlement at this time was found from the settlement-time curves (Figure 5.5). Any settlement of the plates located at the mid-point of each layer that occurred prior to completion of the sludge layer had to be subtracted from the total primary settlement because the strain analyses of Figure 6.2 and 6.12 have initial conditions that occur after completion of the layer. The analyses appeared to underestimate the settlement of the lower half of each layer and overestimate the settlement of the upper half, with the actual settlement corresponding to a nearly constant strain condition.

MacFarlane (1969) has proposed that ultimate primary settlement in peat be computed on the basis of the equation

$$\Delta H_f = \frac{H_{o_f}}{H_{o_L}} \times \Delta H_L \qquad (6.4)$$

where ΔH_f is the total primary settlement of a peat layer in the field, H_{o_f} the initial thickness of the peat layer in the field, ΔH_L the initial compression of the laboratory sample, and H_{o_L} the initial thickness of the laboratory sample. This method requires that a representative laboratory sample be tested in an oedometer under an increment of load equal to the load applied in the field. The average unit strain in the laboratory specimen is then equated to the average unit strain in the field peat layer to obtain the settlement. An average primary settlement of 19.4 inches was obtained using average data from 5 laboratory tests with an applied load equal to 3.4 psi (weight of sand blanket plus soil surcharge). This method overestimates the actual primary settlement by about 2.7 inches. The validity of equation 6.4 is dependent on several factors including (1) difficulty in selecting a fully representative laboratory sample, (2) preparing the laboratory sample at a representative average initial void ratio for the layer, and (3) different strain rates for the laboratory sample as compared to the field.

Secondary compression may be estimated on the basis of the equation (MacFarlane, 1969)

$$\Delta H_s = H \; C_\alpha \; \log_{10} \frac{t}{t_p} \qquad (6.5)$$

where ΔH_s is the settlement due to secondary compression , C_α the coefficient of secondary compression equal to the strain occurring over one cycle of the secondary portion of the settlement-logarithm of time curve, t the field time considered, t_p the estimated field time for primary compression, and H the thickness of the sludge layer at time t_p. Using a laboratory value of c_v equal to 0.017 in^2/min to calculate t_p equal to 103 days, and using a laboratory value of C_α equal to 0.0150 gives an estimate of ΔH_s equal to 0.4 inch for t equal to 176 days. When a more realistic value of t_p equal to 34 days is used, the secondary compression becomes 1.0 inch. Since the actual secondary compression is close to 4.1 inches, the laboratory value of C_α is much too low.

A theory proposed by Gibson and Lo (1961) for estimation of ultimate settlement involves the representation of the soil skeleton by the mathematical model shown in Figure 6.3. In this model, primary compression is represented by the transfer of stress from the pore water to the soil skeleton resulting in an effective stress, $\overline{\sigma}$, which causes compression of the spring a. This effective stress is also initially carried by the viscous dashpot in the Kelvin element. As time passes, however, the stress is transferred to spring b, representing secondary compression. Mathematical details are omitted here but it can be shown (Gibson and Lo, 1961) that for a step loading and at large values of time the settlement S(t) is given by:

$$S(t) = q_o H \; [\, a + b \; (1 - e^{\lambda / b^{t}})\,] \qquad (6.6)$$

where q_o is the applied load, a represents primary compressibility, b represents secondary compressibility, $1/\lambda$ the viscosity, and H the layer thickness. At very large times $(t \rightarrow \infty)$ equation 6.6 becomes

$$S = q_o H (a + b) \tag{6.7}$$

which represents the ultimate settlement of the layer.

Application of this theory requires that the parameters a, b, and λ be determined for the papermill sludge. It appeared that the most representative values for the parameters could be obtained from an oedometer test where the single load increment was equal to the field load. A graph of $\log_{10} (\delta_2 - \delta_1)$ plotted against t_1 (Figure 6.4) provides information for determination of these parameters. Here δ_2 and δ_1 are settlements at times t_2 and t_1, respectively. Using the parameters shown in Figure 6.4, with q_o equal to 3.4 psi and H equal to 120 inches, gives an ultimate settlement of 22.4 inches for the upper sludge layer. Primary compression represented by $(a \cdot q_o \cdot H)$ equals 20.3 inches and secondary compression represented by $(b \cdot q_o \cdot h)$ equals 2.1 inches. Although the primary compression has been overestimated and the secondary compression underestimated, the total compression appears reasonable considering that infinite time has been used for computation. This method is subject to the same uncertainties in extending laboratory test data to field prediction of settlements as discussed earlier.

Time-Rate of Settlement. Time-rate of settlement predictions involving primary consolidation are generally based on the Terzaghi (1943) consolidation theory. This theory involves a solution of the differential equation (one-dimensional)

$$\frac{\partial u}{\partial t} = c_v \frac{\partial^2 u}{\partial z^2} \tag{6.8}$$

where u is the excess pore water pressure, t the time after application of load, z the distance from the mid-point of a doubly drained stratum, and c_v the coefficient of consolidation. The solution of equation 6.8 for various boundary conditions is given by Terzaghi (1943), Leonards (1962) and others. The degree of consolidation, U, for a given time, t, is commonly expressed as some function of the time factor, T_v, equal to $^{4c_v t}/_{H^2}$. The use of this theory in estimating the time settlement relation for the upper sludge layer is illustrated in Figure 6.6. Curve ② is based on c_v equal to 0.0170 in^2/min with an assumed uniform initial excess pore pressure.

Using MacFarlane's (1969) method, the total primary compression was taken equal to 19.4 in and the secondary compression equal to 0.4 in. This procedure relies on laboratory data and can be considered representative of a design estimate. Curve ① in Figure 6.6a shows the observed time-settlement relation for instrument group 6 in the landfill, and curve ② gives the time-settlement relation using Terzaghi's theory and parameters based on the field data. Curve ② considers primary compression equal to 16.7 in and secondary compression equal to 4.1 in ($C_\alpha = 0.0556$). The laboratory parameters give an underestimate of the time-rate of settlement. Part of the discrepancy between actual and calculated curves results from the assumption that the theoretical curves start after completion of surcharge placement whereas the field curve begins earlier. Settlement versus logarithm of time for curves ① and ② is shown in Figure 6.6b. This figure illustrates how the secondary portion of the field curve is concave upwards, as compared to the linear secondary portion of the theoretical curve. This would indicate that the field compression curve exhibits Type I (Lo, 1961) secondary compression. However, as mentioned earlier, the laboratory curves, even with one 3.4 psi load increment recorded for a week, did not indicate this behavior. The lower layer also exhibits this upward curvature in the secondary range. However, the field pore pressures indicate that slow pore pressure dissipation is still occurring in the layer, and so this curvature may be part of the transition zone between the primary and secondary compression regions.

Other assumptions in Terzaghi's theory which may cause deviation from the field results include (1) homogenous material, (2) constant consolidation parameters (c_v, k, m_v) during the load increment, (3) the time lag of the compression is caused exclusively by the low permeability of the material (the secondary compression effect is initially disregarded), (4) small strain-theory valid, and (5) fully saturated sludge. Gas present in the sludge prior to surcharge application would have been compressed on application of the load, giving an immediate settlement. This may be responsible for part of the 3 in of settlement which occurred during surcharge placement. Pore pressures generated upon loading (Figure 6.7) are less than the applied load, indicating partial dissipation during this loading period. Field samples to be taken during phase II of the project will provide additional information on water contents and densities after consolidation.

Pore Pressure Dissipation. Use of equation 6.2 for estimating total primary settlement requires information on initial pore pressures. The pore pressures shown in Figure 6.2a resulted from stresses induced by the sand blanket and weight of the sludge. Pore pressures resulting from a very rapid placement of the sand blanket were assumed equal to its load (100 psf) throughout the layer. Pore pressures resulting from the sludge layer increasing in thickness with time were estimated using a theory presented by Gibson (1958). Gibson solves the governing differential equation

$$c_v \frac{\partial^2 p_w}{\partial x^2} = \frac{\partial p_w}{\partial t} - \gamma \frac{dH}{dt} \qquad (6.9)$$

where c_v is the coefficient of consolidation, p_w the pore water pressure, x the distance from the bottom of the sludge layer, t the elapsed time since start of deposition, H equal to H(t) the height of sludge layer at time, t, and, γ, the unit weight of the sludge. Boundary conditions include a permeable base (sand blanket) where p_w equals zero at x equal to zero, and the sludge surface where p_w equals zero for x equal to H. Gibson's (1958) solution for the case of a layer increasing in thickness at a constant rate ($H = mt$) is presented as a series of curves of x/H versus $p_w/\gamma H$ for several values of m^2t/c_v. Using these curves, estimates of initial pore pressures for both laboratory and field values of c_v, along with the measured pore pressures, are presented in Figure 6.8. The observed pore pressures fall between the predicted values, with the exception of the 30-in depth. No duplicate piezometer readings are available for this depth, hence a recording error or malfunction is possible. The 115 psf pore pressure in the middle sand blanket may have influenced the value at the 90-in depth. Except for these factors Gibson's (1958) theory appears to predict pore pressures generated during sludge placement.

Pore pressure dissipation during placement of the sand and surcharge load appeared to be responsible for $\Delta u/\Delta p$ values less than unity, as shown in Figure 6.7. The pore pressure increase at the center of the layer ranged from 94 to 99 percent of the applied load, whereas at the 1/4 point pore pressures were about 85 percent of the applied load. The ▲ data point for group 7 in Figure 6.7b represents only the surcharge load, whereas for the other groups the pore pressures include application of the sand plus surcharge load. Adding a 100 psf load due to the sand layer for group 7 gives a point very close to $\Delta u/\Delta p$ equal to unity as shown by the second point.

Residual pore pressures summarized in Figure 6.5 represent data from the pore pressure versus time curves in Figure 5.9. The data in Figure 6.5 represent average values of u_r obtained from these curves. Piezometer 8 in group 5 appears to have a reduced pore pressure at 327 days due to drying of the earth surcharge and the upper portion of the upper sludge layer during a relatively dry summer. Fluctuation in pore pressures after 90 days appear to be due to measurement errors or environmental effects such as seasonal wetting and drying. Pore pressures in the middle sand blanket are the result of the sand forming a bowl shape because of less settlement along the periphery of the landfill, thus holding water up to a certain elevation.

The field pore pressure dissipation curve at the mid-point of the upper sludge layer in instrument group 6 is compared, in Figure 6.9, to computed curves based on Terzaghi's (1943) theory. The initial excess pore pressure used for computation was assumed equal to the difference between the maximum and residual pore pressures. The laboratory value of c_v (0.0170 in^2/min) gives pore pressures substantially higher than the observed pore pressures during the consolidation period. Using the c_v (0.0626 in^2/min) value based on field data, Terzaghi's (1943) theory slightly overestimates the pore pressures (curve 3) up to about 70 percent dissipation and thereafter gives an underestimate. The slower dissipation rate occurring after about 70 percent dissipation was also observed in the laboratory by Andersland and Paloorthekkathil (1972).

The decrease in pore pressure dissipation rate after 70 percent dissipation may be the result of non-Darcy flow in the sludge. Mitchell and Younger (1967) discussed this effect in detail and concluded that there are indications that deviations from Darcy's law exist in many fine-grained soils subjected to low hydraulic gradients but that not much direct field evidence is available concerning seepage or consolidation to corroborate this effect. The recorded field dissipation curves (Figures 5.9 and 6.9) indicate that non-Darcy flow does exist in the sludge landfill and that this flow precedes the formation of residual pore pressures in both sludge layers. These residual pore pressures imply the existence of a threshold gradient in the sludge below which no flow occurs. For a threshold gradient, i_o, drainage will occur only when

$$i > i_o = \frac{1}{\gamma_w} \frac{du_r}{dz} \tag{6.10}$$

where i is the existing hydraulic gradient, u_r the residual pore pressure at depth z, and γ_w the unit weight of water. If this gradient can be considered a constant property, then integration of equation 6.10 will give a theoretical distribution of the residual pore pressures shown in Figure 6.10. The observed residual pore pressure distribution summarized in Figure 6.5 is influenced by the pore pressures in the middle sand blanket. If the pore pressure in the sand blanket were reduced to zero, as it would be if complete drainage were possible, and if the value at the lower one-quarter point were reduced, the resulting distribution would likely agree with theory. Assuming that the theory represents the field conditions, using the maximum residual pore pressure at the center of the layer gives a value for i_o equal to 0.885. Below this gradient primary consolidation will cease, with no additional dissipation of pore pressures.

Reasons quoted by Mitchell and Younger (1967) for the development of non-Darcy flow and a threshold gradient include: (1) resistance to flow caused by cations in the electrical double layer surrounding the clay particles, (2) particle movements leading to reversible void plugging and unplugging, and (3) the existence of a quasi-crystalline adsorbed water structure. If any of these reasons apply to papermill sudge, the authors believe that (3) would best help explain the development of a threshold gradient. Since the existence of such a gradient implies a no-flow condition it would seem necessary for the water (or leachate) to develop a quasi-crystalline structure that could be considered as solid below the threshold gradient. Grim (1968) also favors this quasi-crystalline concept to explain the clay-water system. However, it should be noted that the chemical makeup of the leachate and the presence of large amounts of organic material in the sludge could have a marked effect on the leachate flow properties at low gradients. Andersland and Laza (1972) observed that a threshold gradient was required to initiate flow in the sludge only in the case of low backpressures, and that when the undissolved gas in the pore fluid was reduced to zero this gradient was not necessary. Such a result would indicate that gas generation in the sludge substantially contributes to the reduced leachate flow rate and residual pore pressure formation observed in the landfill.

The pore pressure dissipation and time-settlement curves predicted from Terzaghi's (1943) theory are based on the assumption of a uniform initial excess pore pressure. Because deviations from this assumption can cause changes in the dissipation-settlement relations, its validity is examined in Figure 6.11. From this figure it can be seen that the increase in pore pressures from their initial values to the maximum values generated under the applied loads is fairly uniform. Since the residual pore pressures are relatively close in magnitude to the initial pore pressures, the assumption of a uniform initial excess pore pressure in Terzaghi's theory appears to be valid. If the residual pressures were much different from the initial pressures, then the condition of one-dimensional consolidation would best be analyzed with water flow controlled by $v = k(i - i_0)$, where v is the velocity of flow and k is the coefficient of permeability. This condition is described by Mitchell and Younger (1967) and the inclusion of a threshold gradient in the consolidation process is covered by Janbu (1965).

Lower Sludge Layer.

Loading and Field Observations. The lower sludge layer supported an applied load of about 1290 psf from the weight of the middle and upper sand blankets, the upper sludge layer, and the earth surcharge. The upper sludge layer was placed at a fairly constant rate over a period of about 30 days. The settlement and pore pressure changes observed in the lower sludge layer are summarized in Figures 5.5 and 5.8. Pore pressures were generated in the lower sludge layer during placement of the upper sludge layer, however, some dissipation and settlement also occurred concurrently with this sludge placement. Surcharge placement induced an immediate increase in pore pressures throughout the lower sludge layer, followed by dissipation and the resulting curved time-settlement relation.

The logarithm of time and square root of time curve fitting methods used in settlement analysis assume an instantaneous application of load. In the case where loads are increased at some rate, such as for the lower sludge layer, these curves are of limited value. The logarithm of time versus settlement curves for the lower sludge layer in Figure 5.8 provides information on the secondary compression behavior of the sludge. The curve appears to show a decreasing secondary compression rate rather than a constant rate. The characteristic S-shape for the entire curve has been flattened due to the gradually increased load from sludge placement of the upper layer. Separation of the settlement into primary and secondary portions is more difficult for the lower sludge layer. The square root of time fitting method cannot be used.

Ultimate Settlement. The ultimate primary settlement of the lower sludge layer is computed to be 32.8 inches in Figure 6.12, using equation 6.2. The procedure is the same as described for the upper layer, with Figure 6.12a giving the stresses in the sludge after placement of the middle sand blanket and Figure 6.12b the stresses after application of the surcharge. Since the lower sludge layer has been subjected to larger effective stresses for a longer period of time than the upper layer, the amount of secondary compression should be greater. If 7 inches is assumed for secondary compression, based on the same primary compression ratio as for the upper layer, this leaves about 29 inches for primary compression. This means that equation 6.2 overestimates the primary settlement, but considering all the assumptions involved, this estimate appears reasonable.

A check on the total stresses calculated at the midpoint of the lower layer in Figure 6.12b can be made using the total pressure cell data from Figure 5.11. The calculated total vertical stress at the mid-point is 1740 psf (12.1 psi) whereas that shown in Figure 5.11 varies from 11.8 to 13.2 psi (water calibration). Since the slow increase in total vertical stress measured by the pressure cell cannot be explained, it is assumed that the actual stress falls between 11.8 and 13.2 psi giving support to the calculated value of 12.1 psi.

A consolidation test using a single load increment equal to 1290 psf (0.63 kg/cm^2) was carried out on a sludge sample from the lower layer to provide a basis for estimating the ultimate primary settlement by MacFarlane's (1969) method. Using data from test No. L-2-4 in equation 6.4 gives a value for primary settlement equal to 35.3 inches. This value is closer to the actual field settlement of 36 inches which includes both primary and secondary settlement. It is possible that the high initial void ratio of the laboratory sample, greater than the average initial in situ void ratio of the field layer permitted greater volume change than is representative for the sludge layer.

It is difficult to determine from the field data the exact amount of secondary compression in the lower sludge layer. For analysis purposes a value of C_α equal to 0.0556 and a t_p equal to 26 days (total $t = 60$ days) was used in equation 6.5. For H equal to 94 inches a value of 4.7 inches was obtained for the secondary compression. The value of C_α backfigured from the upper layer with t_p equal to 26 days appeared realistic in light of the high amount of primary consolidation that occurred throughout most of the loading period. The value of 4.7 inches of secondary compression appears low based on results from the upper sludge layer.

Time-Rate of Settlement. A theoretical estimate of the time-settlement relation for the lower sludge layer requires that the loading be represented by the numerical procedure shown in Figure 6.13. The placement of the upper sludge layer and upper sand blanket has been modeled as a linearly applied stress increasing with time and the surcharge has been represented as an instantaneously applied stress. Equation 6.8 is placed in finite difference form (Harr, 1966) with $\frac{\partial u}{\partial t}$ and $\frac{\partial^2 u}{\partial t^2}$ becoming

$$\frac{\partial u}{\partial t} = \lim_{\Delta t \to 0} \frac{u(z_i,\ t_{j+1}) - u(z_i,\ \overset{t^2}{t_j})}{\Delta t} = \frac{u_{i,\ j+1} - u_{i,j}}{\Delta t} \qquad (6.11)$$

and

$$\frac{\partial^2 u}{\partial z^2} = \frac{u_{i+1,j} - 2u_{i,j} + u_{i-1,j}}{(\Delta z)^2} \qquad (6.12)$$

Substituting these expressions in equation 6.8 gives

$$u_{i,j+1} = u_{i,j}(1 - 2\alpha) + (u_{i+1,j} + u_{i-1,j})\alpha \qquad (6.13)$$

where α is $\dfrac{c_v \, \Delta t}{(\Delta z)^2}$ and is assumed equal to 1/6 (Scott, 1963), Δt is the time increment, Δz equals $H/8$, with H the thickness of the layer, and c_v is the coefficient of consolidation. Using the time factor T_v equal to $c_v t/(H/2)^2$, and α equal to 1/6, results in a value for ΔT_v equal to 1/96. To model the linear stress, a unit initial pore pressure (stress) is first applied throughout the layer. This is allowed to dissipate over the interval ΔT_v equal to 1/96, at which time another unit of pore pressure is added to obtain a new pore pressure distribution. This process is repeated over the required number of increments (n) as shown in Figure 6.13, where n is defined as $t_s/\Delta t$ equal to $c_v(t_s)/\alpha\,(z)^2$, and t_s is the time at which the surcharge is applied. Since Δt is fixed, the number of increments n is dependent on the values of c_v and t_s. For the sludge landfill with $c_v = 0.063$ in^2/min, n was equal to 113. The percent consolidation, defined as

$$U(t) = 1 - \frac{1}{H}\int_0^H \frac{u(t)}{u_o}\, dz \qquad (6.14)$$

where u(t) is the excess pore pressure at any time t and u_o is the initial excess pore pressure, has been evaluated numerically, using the trapezoidal rule, for the finite difference formulation described.

For the linearly increasing load, u_o at any time t is equal to the total number of increments of pore pressure applied up to time t ($u_o = n$ at $t = t_s$). To obtain the settlement at time t it is necessary to determine the load acting on the lower layer at that time. The settlement of the lower layer then equals the ultimate settlement for that load multiplied by the percent consolidation based on the above consolidation theory. Estimates of the ultimate settlement of the lower sludge layer for three different elevations of the upper sludge layer (different loads) are given in Figure 6.14 for use in obtaining the theoretical time-settlement curve.

In the lower sludge layer it was assumed that the pore pressures measured in the field after application of the middle sand blanket acted as "static" pore pressures for analysis purposes. This means that they have been considered as both the initial and the residual pressures, and they must be added to the excess pressures calculated from the above theory to obtain the actual pore pressures. Since the actual residual pore pressures are slightly different from the above assumed values, the consolidation percentages calculated by the theory contain a small error. Gibson's (1958) theory would provide accurate values of pore pressures generated in the sludge due to its own weight if estimates of initial pore pressures were needed for design purposes.

Using a computer program written for the above analysis (Appendix I), two theoretical time-settlement relations for the lower sludge layer have been determined and are shown in Figure 6.15, along with the actual field settlement curve for group 3. The two theoretical curves occur after surcharge placement, one being calculated using c_v equal to 0.063 in^2/min and the other with c_v equal to 0.015 in^2/min. A c_v equal to 0.063 in^2/min was assumed during the linear loading range and was chosen based on the analysis of the upper sludge layer. Values of t_p equal to 26 days and C_α equal to 0.0556 (from the upper layer analysis) were used in calculating the secondary compression. The ultimate primary settlements used in the analysis are those shown in Figures 6.12 and 6.14. The three analyses shown in Figure 6.14 were used during linear loading and the 32.6 inches in Figure 6.12 was used after surcharge application.

The theoretical procedure above appears to give an adequate time-settlement relation for the lower layer. Although the occurrence of secondary compression has been poorly modeled, the governing factor affecting the time-settlement relation still appears to be the selection of a representative value of c_v. The fact that the actual settlement curve falls above the curve for c_v equal to 0.063 in^2/min would indicate that c_v has decreased during the settlement process. This would be in accordance with the laboratory data, which show a drop in c_v with increase in deformation and effective stress (Figure 5.1).

Pore Pressure Dissipation. A comparison between the predicted and measured pore pressures at the midpoint of the lower sludge layer is shown in Figure 6.16. The initial pore pressure was assumed equal to the residual value of 2.3 psi and was added to the excess pore pressure generated during loading. Pore pressures generated during the linear loading period were estimated using a value of c_v equal to 0.063 in^2/min and appear to give a reasonable approximation to the measured pore pressures. Two predicted curves are shown after surcharge application, one representing a c_v equal to 0.063 in^2/min and the other c_v equal to 0.015 in^2/min. The larger c_v value predicts pore pressure dissipation more rapidly than it occurs. This suggests that c_v decreases during consolidation under the linearly increasing load. The measured pore pressures fall between the two curves for a period of 30 days after surcharge placement, after which they dissipate more slowly. This would correlate with the decrease in rate of pore pressure dissipation which occurred after 70 percent dissipation in the upper sludge layer (Figure 6.9).

Initial pore pressures generated in the lower sludge layer due to its own weight are shown in Figure 6.17 and residual pore pressures remaining after consolidation are shown in Figure 6.5. The initial pore pressures were obtained by subtracting 100 psf (stress due to the middle sand blanket) from the pore pressure readings taken immediately after placement of the middle sand blanket. These pore pressures agree fairly well with those that would be predicted using Gibson's (1958) theory. Residual pore pressures shown in Figure 6.5 were obtained in a manner similar to the upper sludge layer. After 327 days (Figure 5.9) the pore pressures had stabilized sufficiently so that they would be labeled "residual" for analysis purposes. The values are somewhat higher than those measured in the upper sludge layer indicating that a higher threshold gradient exists in the lower layer. Higher sludge densities for the lower sludge layer and gas formation due to sludge decomposition may contribute to the formation of higher residual pore pressures. Using the maximum observed residual pore pressure at the midpoint of the lower layer gives a value of i_o equal to 1.63.

The $\Delta u/\Delta p$ ratios shown in Figure 6.7 are somewhat less for the lower sludge layer as compared to the upper layer. The lower ratios may be the result of partial drainage occurring during placement of the upper sand blanket and surcharge. The theoretical pore pressure increase shown in Figure 6.16 is consistent with the field measurements and would support this explanation. Because the surcharge covers a fairly large area it would appear that the reduction in the $\Delta u/\Delta p$ ratio is not due to reduced stresses in the lower sludge layer.

Table 6.1 COMPARISON OF ACTUAL AND CALCULATED PRIMARY SETTLEMENTS.

Location	Computed settlement from Fig. 6.2 or 6.12	Actual field settlement
Upper sludge layer		
Upper half	10.8 in	9.0 in
Lower half	7.3 in	8.0 in
Lower sludge layer		
Upper half	19.6 in	14.7 in
Lower half	13.2 in	14.3 in

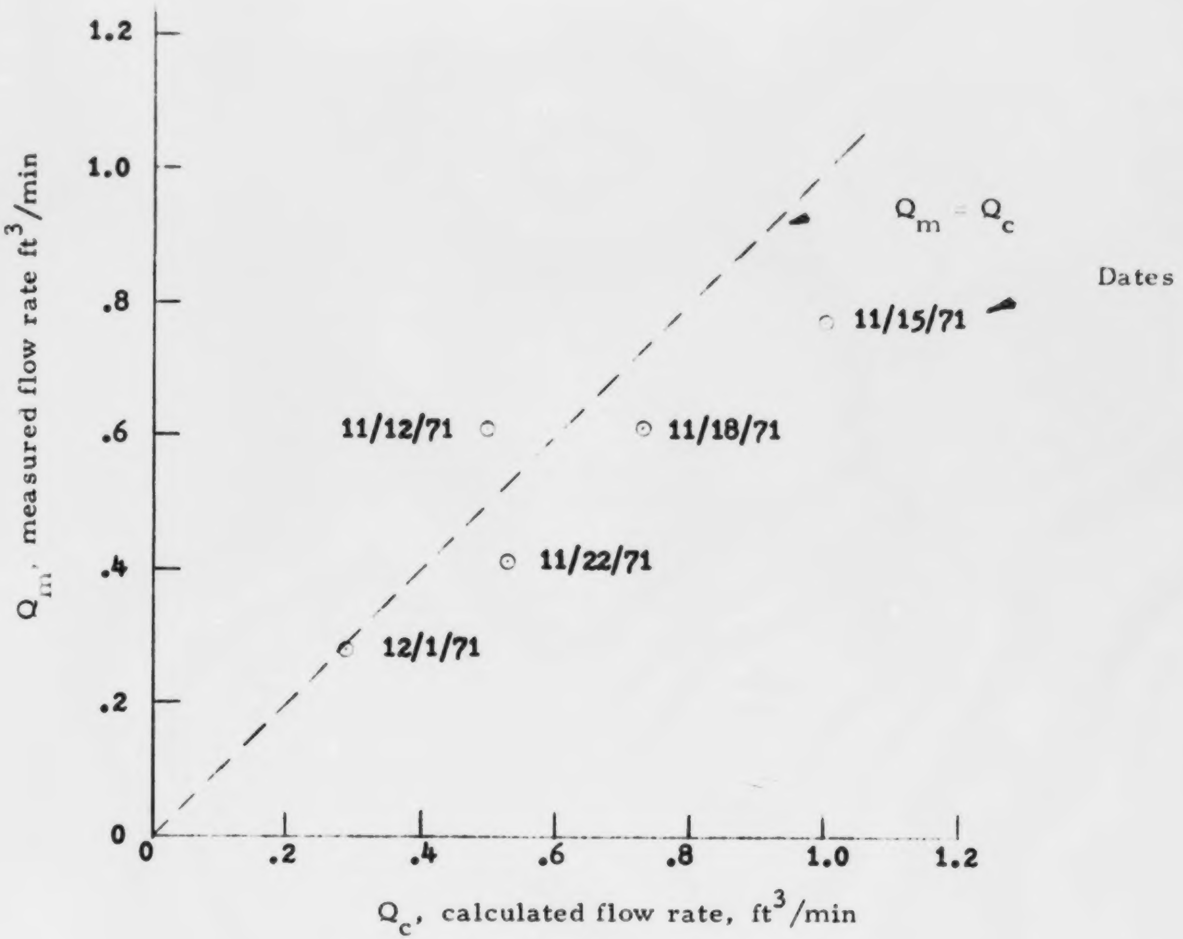

Figure 6.1. Comparison between the measured leachate flow rate and the flow rate calculated from the time-settlement curves.

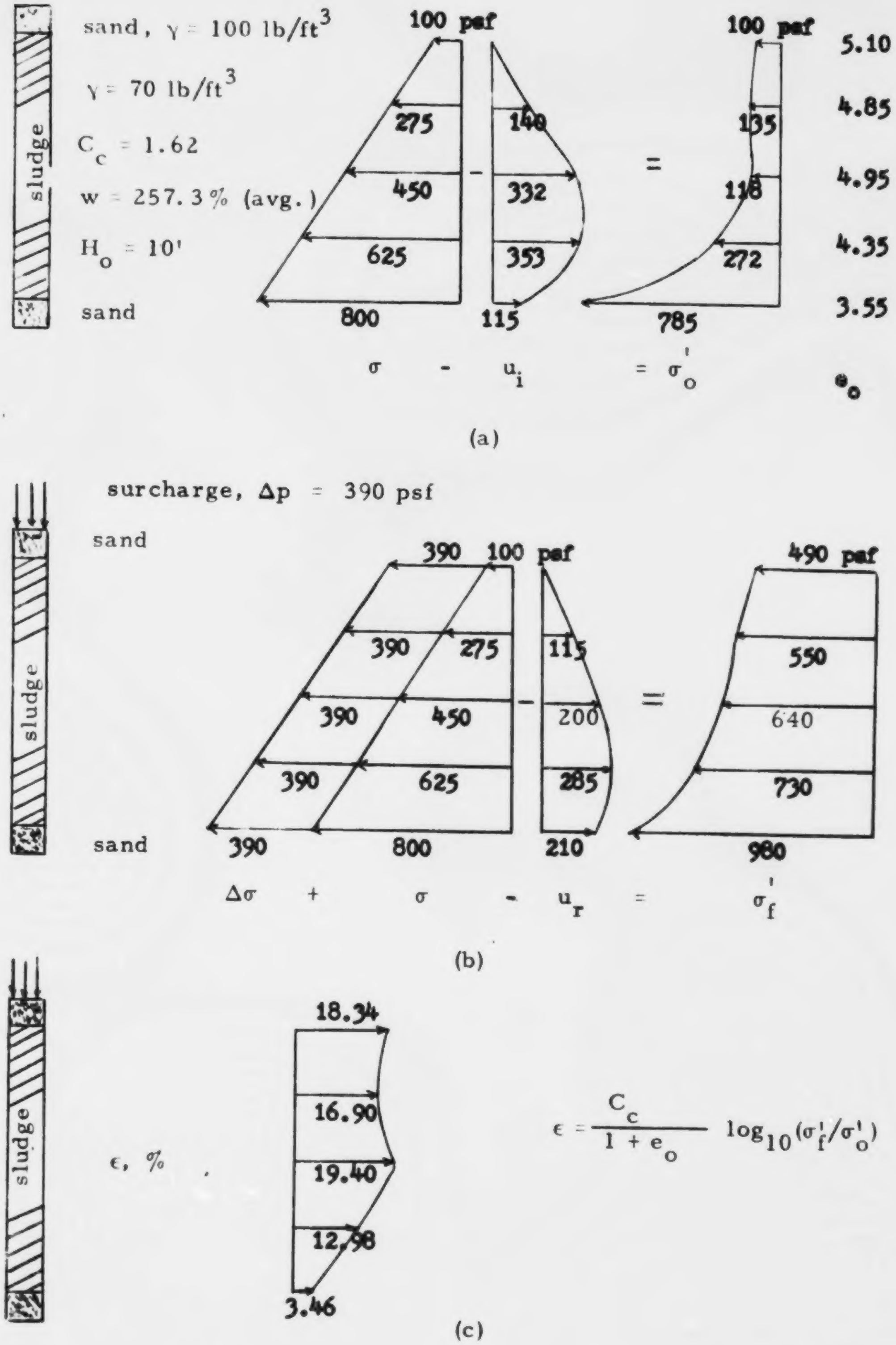
sand, γ = 100 lb/ft^3
γ = 70 lb/ft^3
C_c = 1.62
w = 257.3% (avg.)
H_o = 10'
sand
sludge
100 psf
275
450
625
800
140
332
353
115
100 psf
135
118
272
785
5.10
4.85
4.95
4.35
3.55
σ - u_i = σ'_o
e_o
(a)
surcharge, Δp = 390 psf
sand
sludge
sand
390 100 psf
390 275
390 450
390 625
390 800
115
200
285
210
490 psf
550
640
730
980
$\Delta\sigma$ + σ - u_r = σ'_f
(b)
sludge
ϵ, %
18.34
16.90
19.40
12.98
3.46
(c)

$$\epsilon = \frac{C_c}{1 + e_o} \log_{10}(\sigma'_f/\sigma'_o)$$

Figure 6.2. Estimated effective stress changes and strain distribution in the upper sludge layer. (a) Initial stresses. (b) Final stresses. (c) Strain distribution.

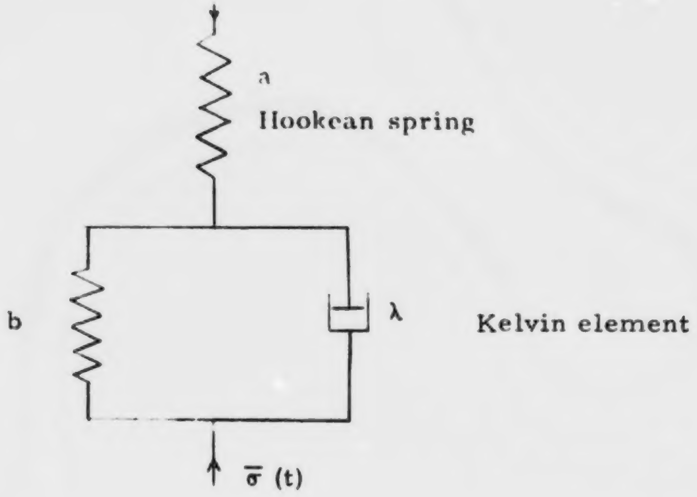
a
Hookean spring
b
λ
Kelvin element
$\bar{\sigma}$ (t)

Figure 6.3. Mathematical model of the soil skeleton. (Gibson and Lo, 1961).

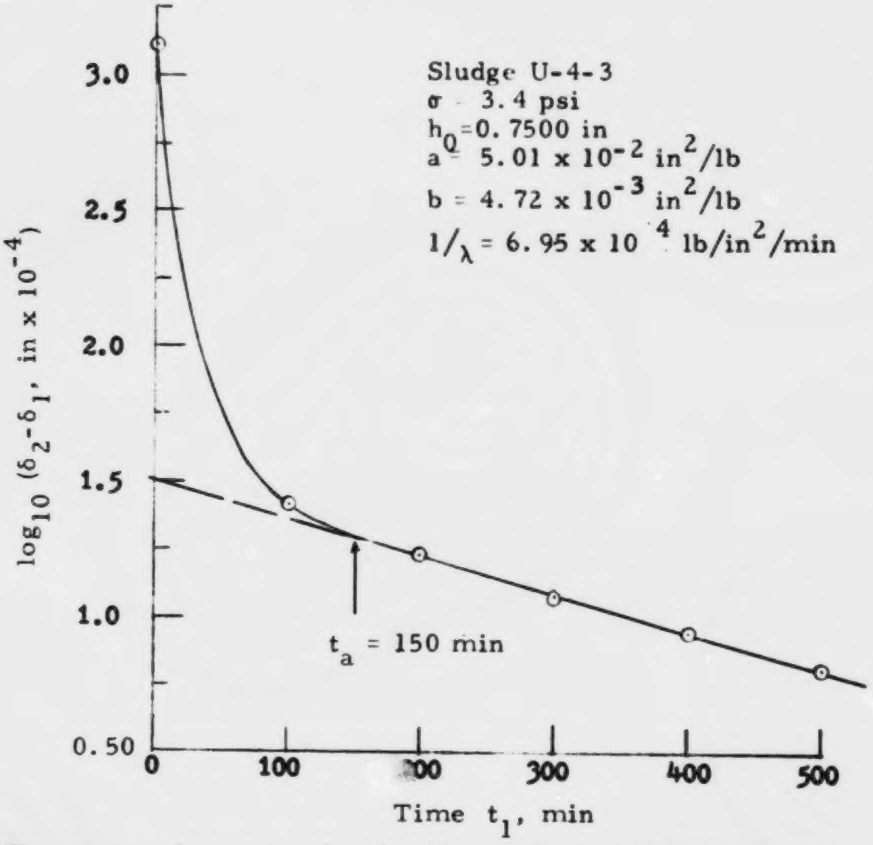

Figure 6.4. Parameter determination for the method of Gibson and Lo.

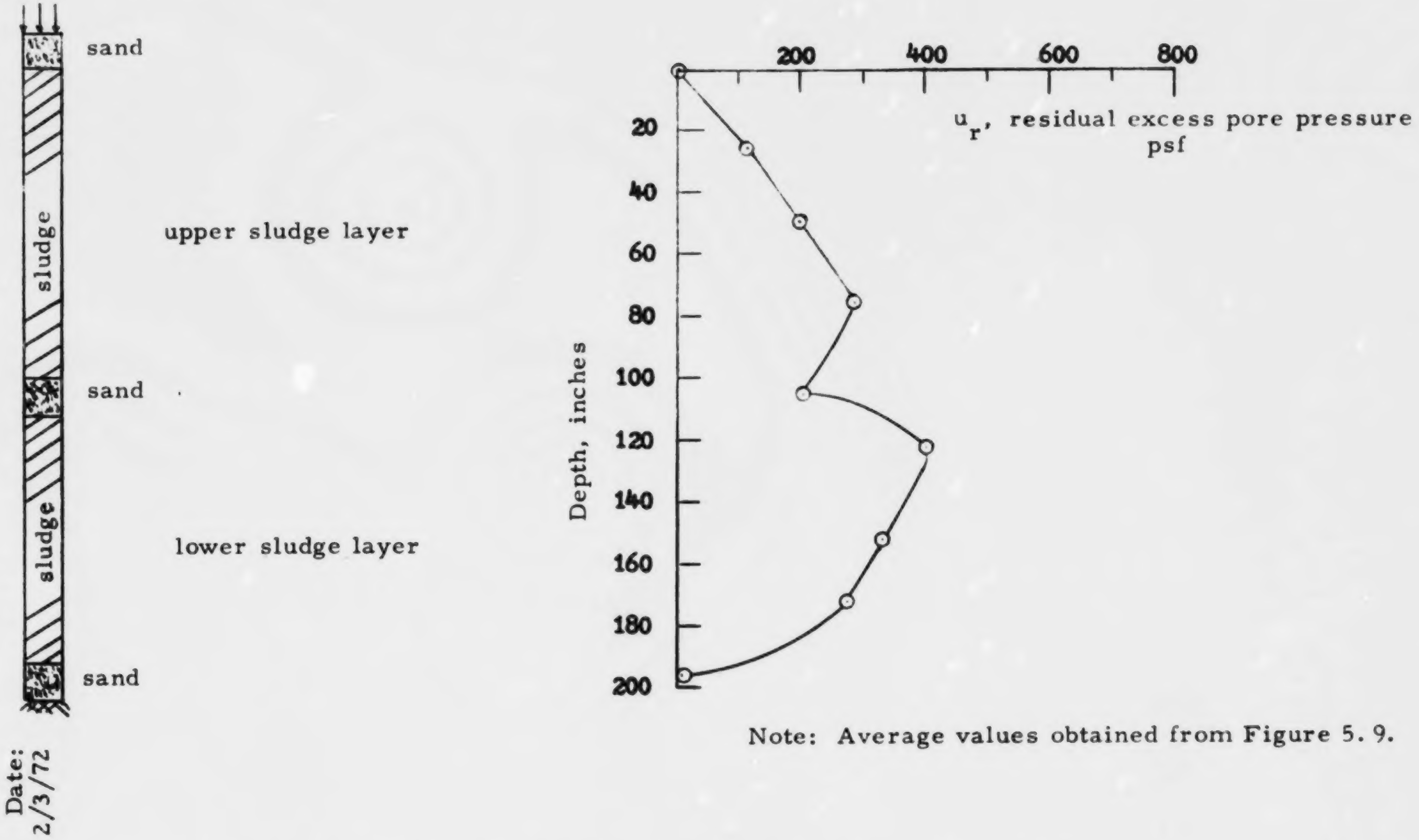

Note: Average values obtained from Figure 5. 9.

Figure 6. 5. Measured residual excess pore pressure versus depth.

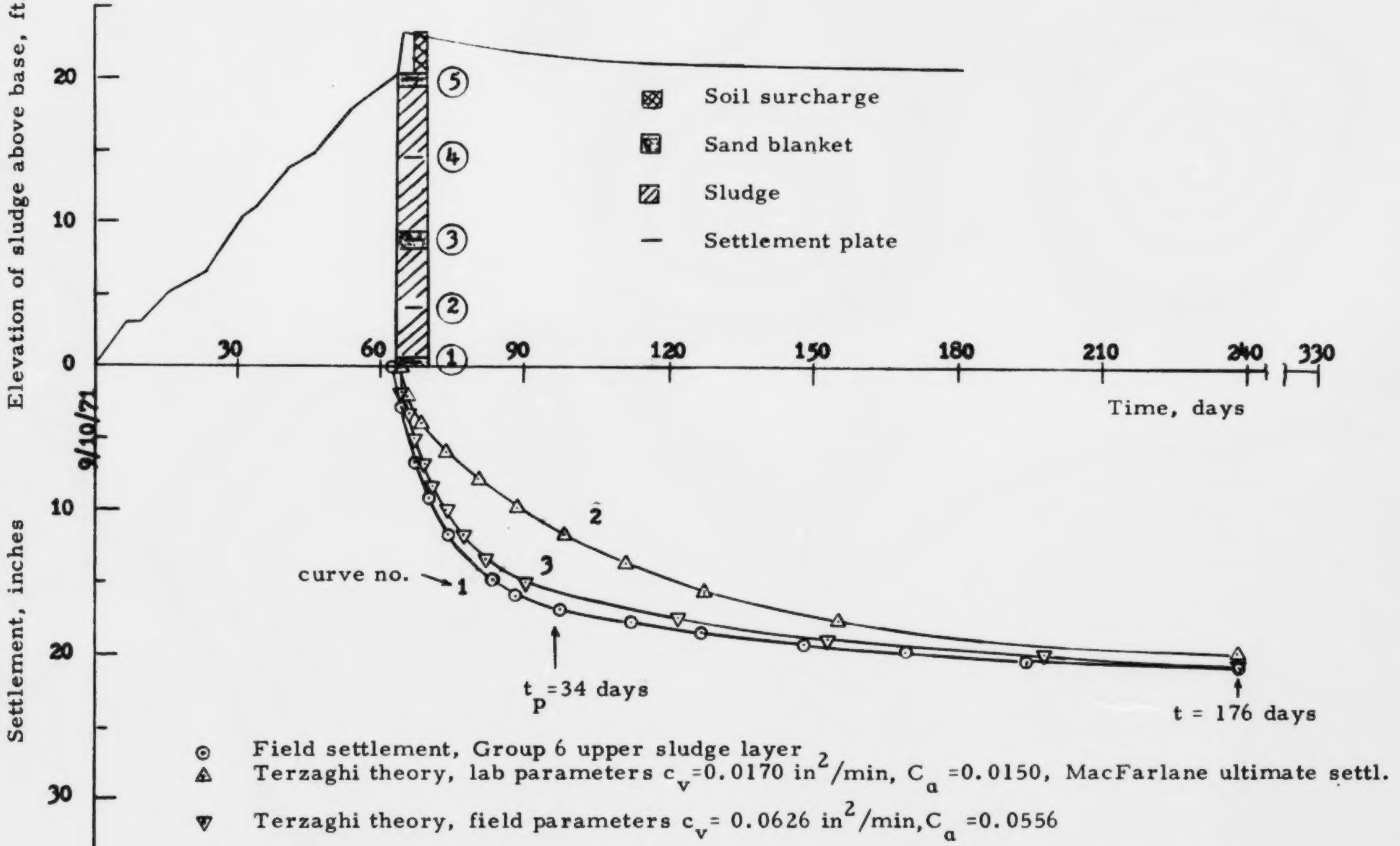

Figure 6.6. Comparison of actual and predicted time-settlement curves, upper sludge layer.
(a) Settlement versus time.

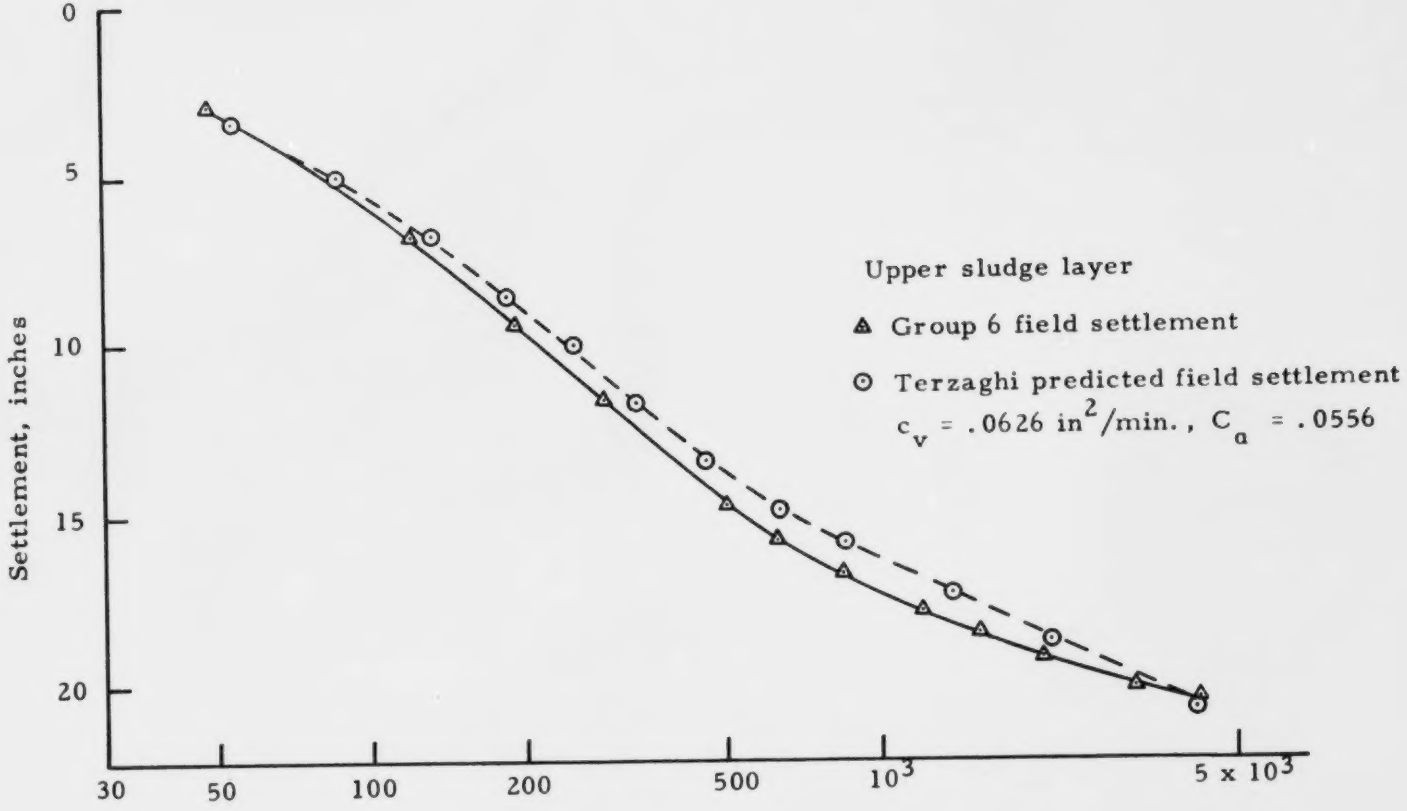

Figure 6.6. Comparison of actual and predicted time-settlement curves, upper sludge layer. (b) Settlement versus logarithm of time.

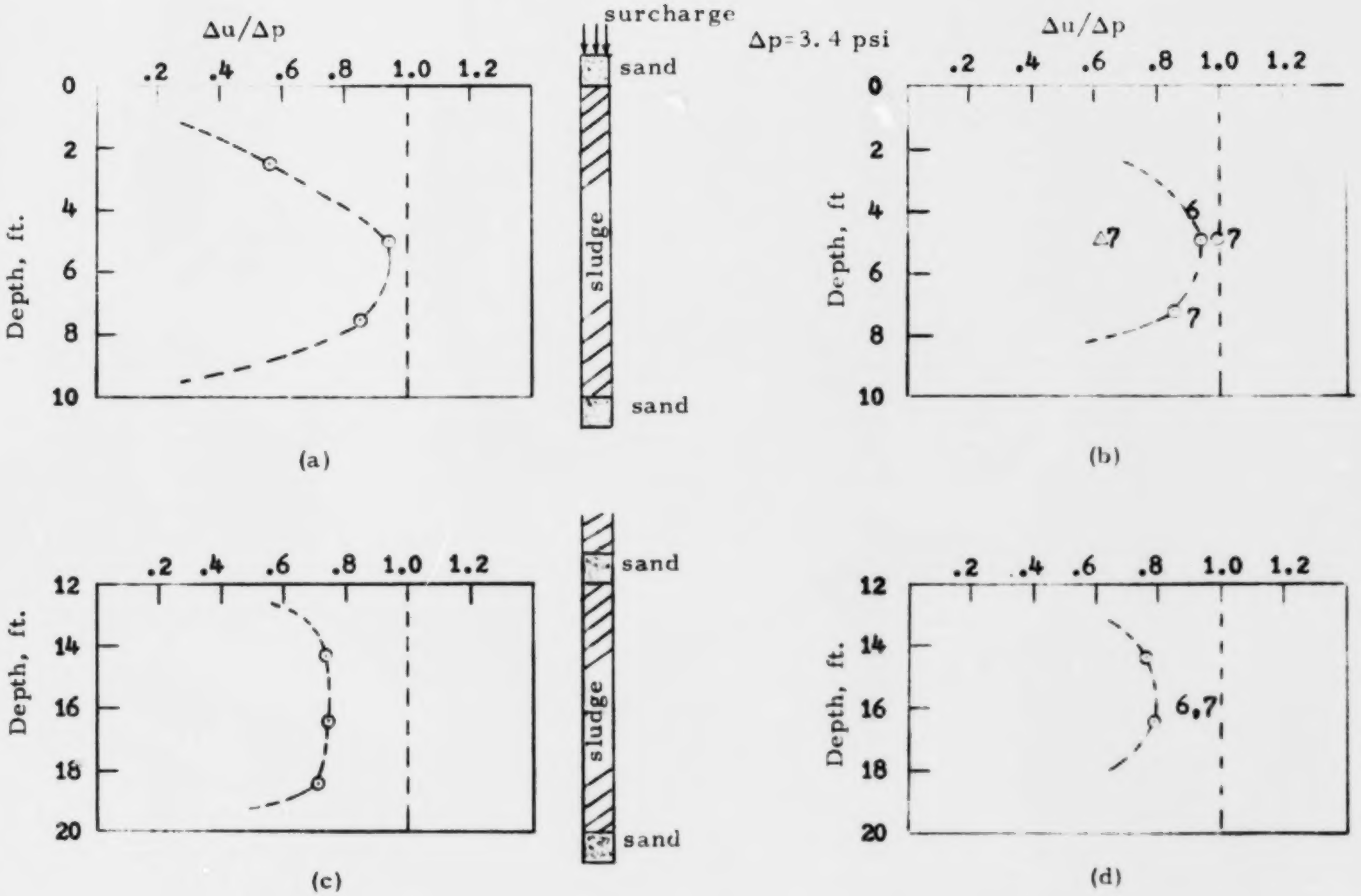

Figure 6. 7. Pore pressure increase due to the application of the upper sand blanket and surcharge. (a) Group 5, upper layer (b) Groups 6 and 7, upper layer (c) Group 5. lower layer (d) Groups 6 and 7, lower layer.

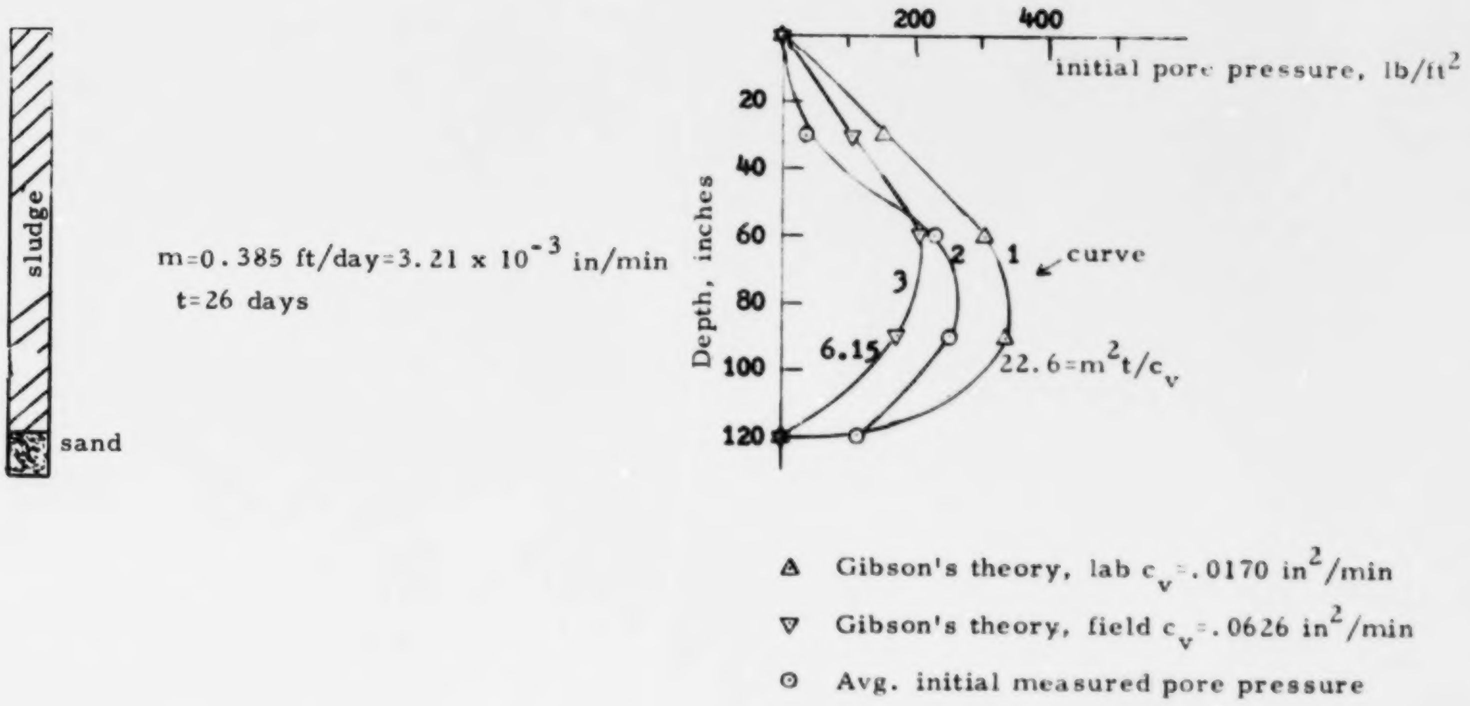

Figure 6.8. Comparison of measured and predicted initial pore pressures, upper sludge layer.

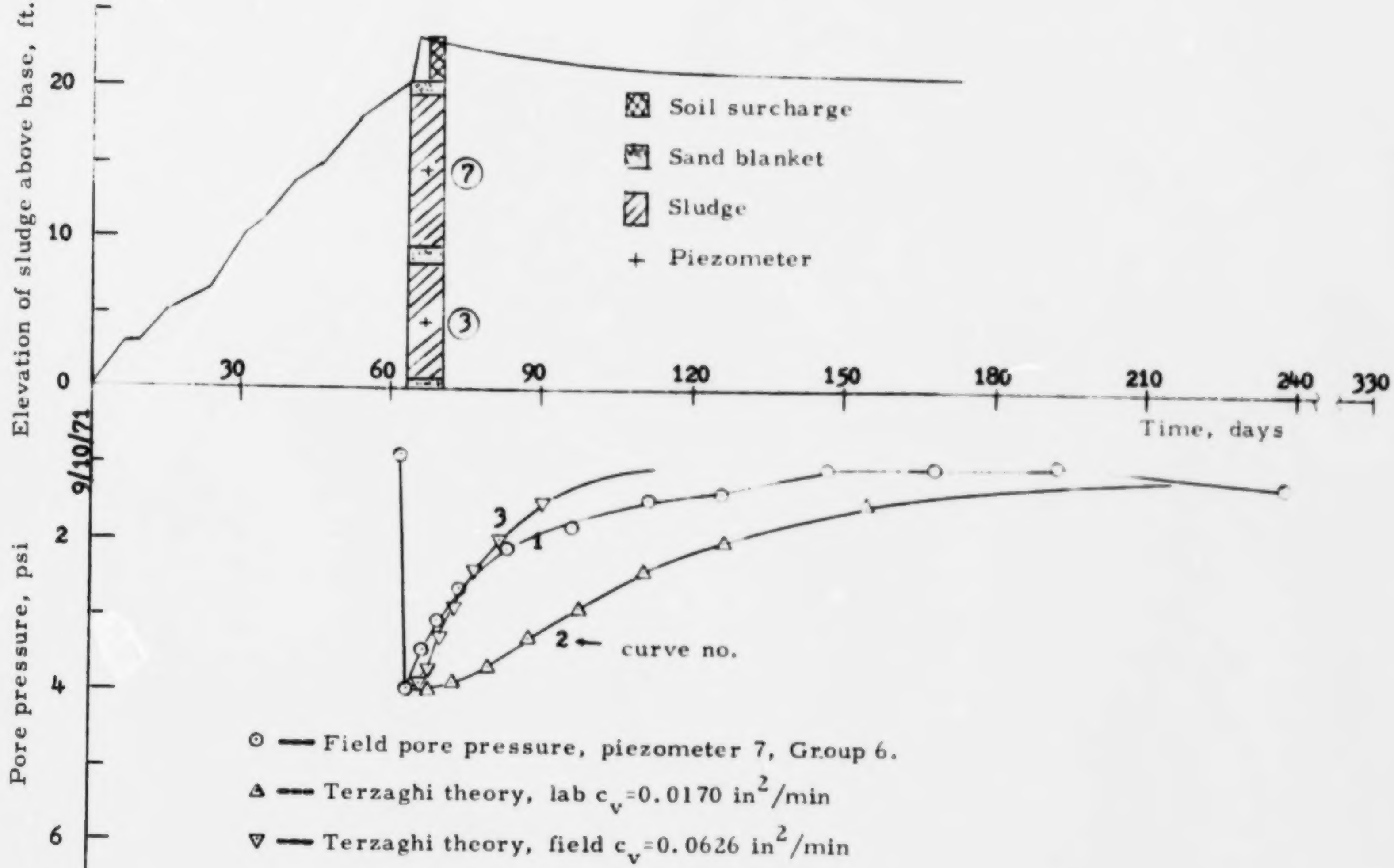

Figure 6.9. Comparison of measured and predicted pore pressure dissipation, midpoint of upper sludge layer.

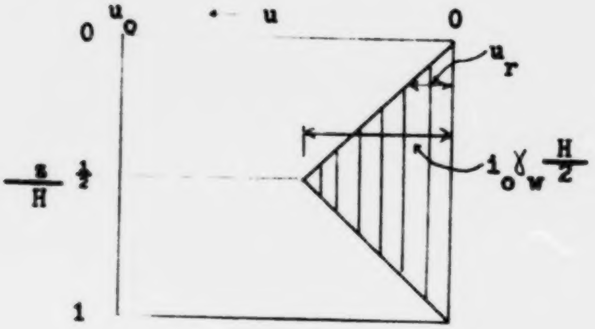
0
u_o
u
0
u_r
$\frac{z}{H}$ $\frac{1}{2}$
$i_o \gamma_w \frac{H}{2}$
1

Figure 6.10. Theoretical final pore pressure distribution at the end of consolidation if a threshold gradient exists.

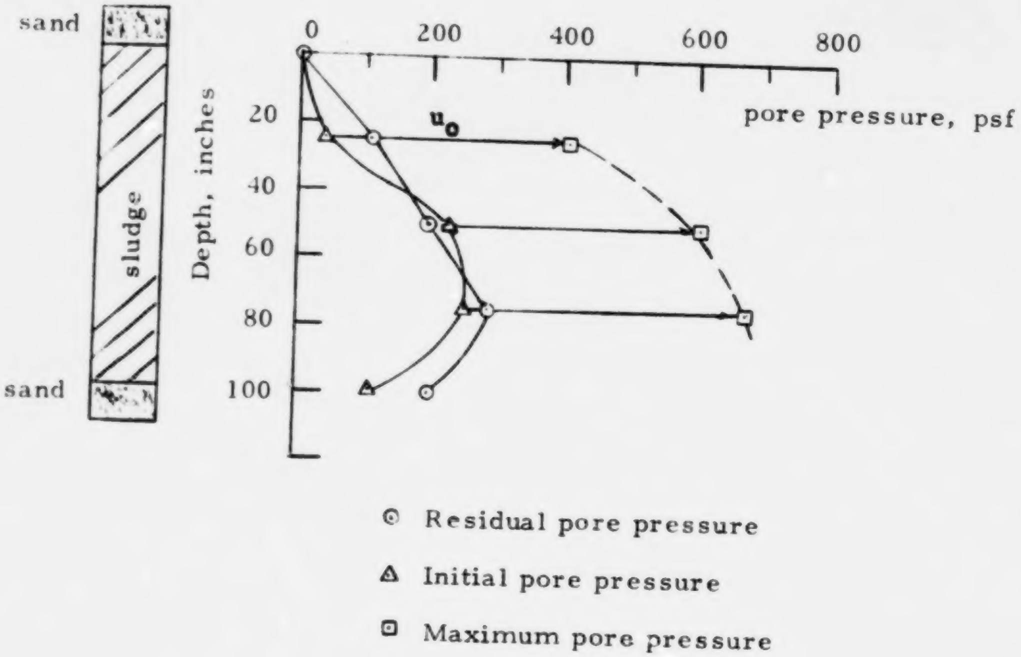

Figure 6.11. Comparison of initial, maximum, and residual pore pressures for the upper sludge layer.

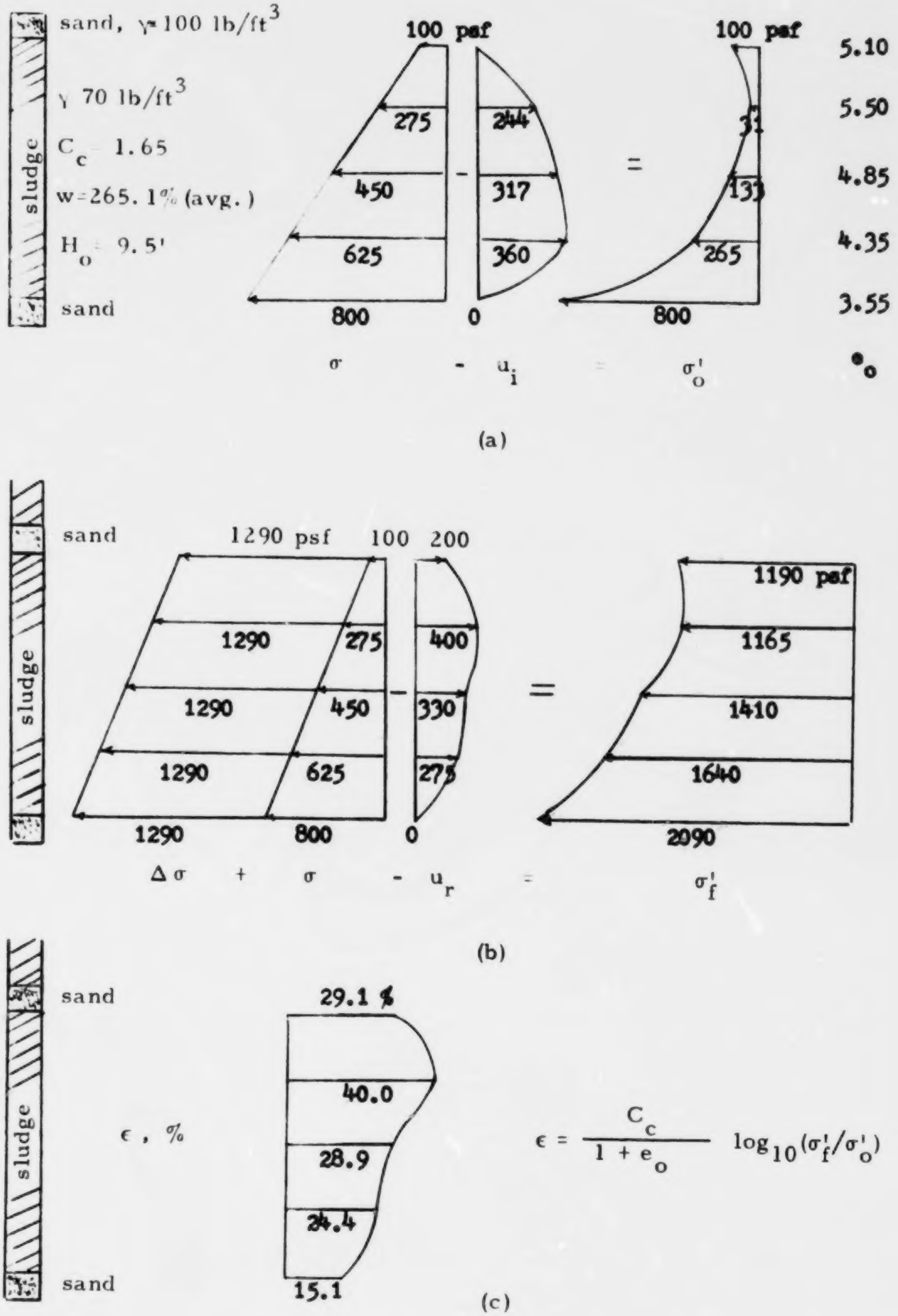
sand, γ = 100 lb/ft³
γ 70 lb/ft³
C_c 1.65
w = 265.1% (avg.)
H_o 9.5'
sludge
sand
100 psf
275
450
625
800
244
317
360
0
100 psf
51
133
265
800
5.10
5.50
4.85
4.35
3.55
σ
-
u_i
=
σ'_o
e_o
=
(a)
sand
sludge
1290 psf
100
200
1290
275
400
1290
450
330
1290
625
275
1290
800
0
1190 psf
1165
1410
1640
2090
Δσ
+
σ
-
u_r
=
σ'_f
(b)
sand
sludge
sand
ε, %
29.1 %
40.0
28.9
24.4
15.1
$\epsilon = \frac{C_c}{1 + e_o} \log_{10}(\sigma'_f/\sigma'_o)$
(c)

Figure 6.12. Estimated effective stress changes and strain distribution in the lower sludge layer. (a) Initial stresses (b) Final stresses (c) Strain distribution.

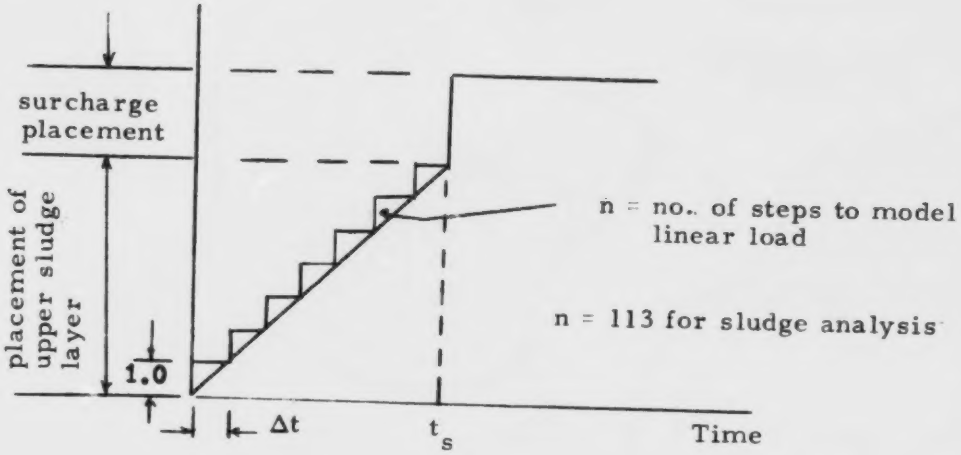
surcharge placement
placement of upper sludge layer
1.0
Δt
t_s
Time
n = no. of steps to model linear load
n = 113 for sludge analysis

Figure 6.13. Load increasing linearly with time followed by an instantaneous surcharge application.

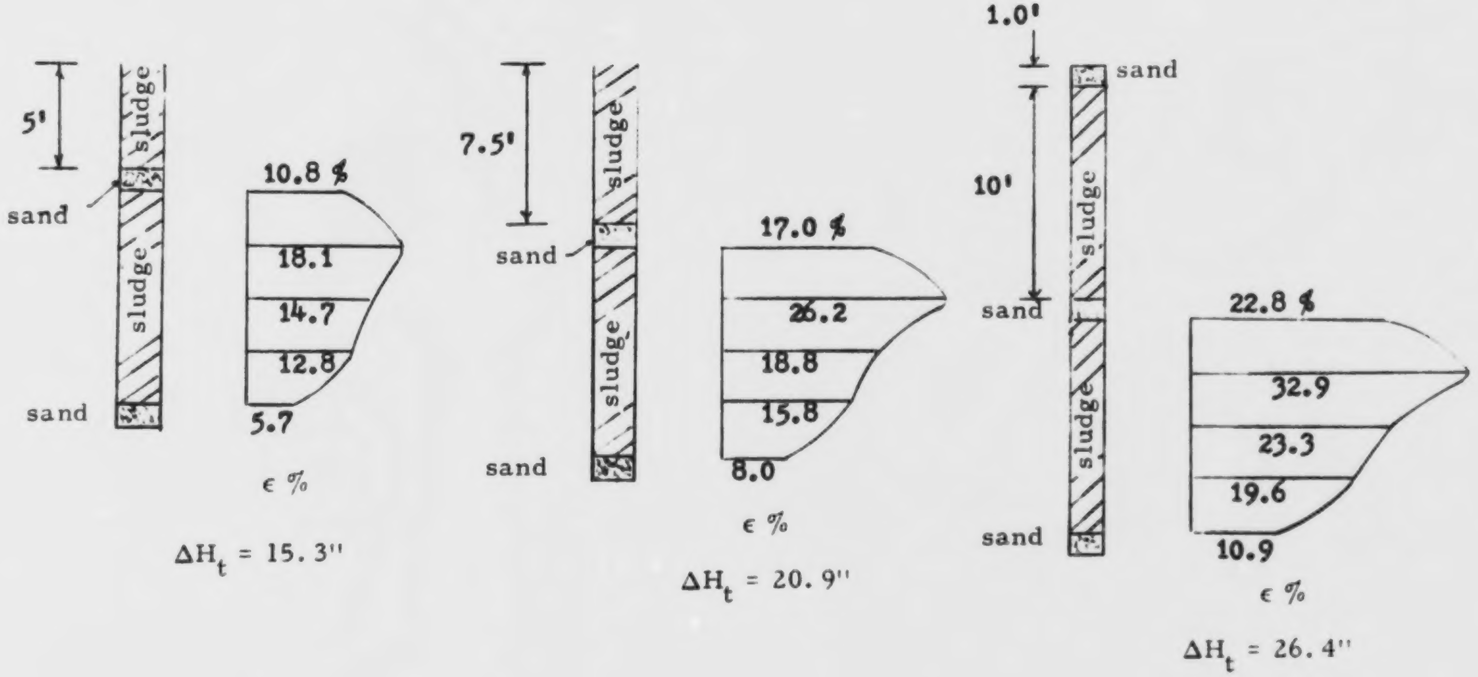
5'
sludge
sand
sludge
sand
10.8 $
18.1
14.7
12.8
5.7
ϵ %
ΔH_t = 15.3"
7.5'
sludge
sand
sludge
sand
17.0 $
26.2
18.8
15.8
8.0
ϵ %
ΔH_t = 20.9"
1.0'
sand
10'
sludge
sand
sludge
sand
22.8 $
32.9
23.3
19.6
10.9
ϵ %
ΔH_t = 26.4"

Note: The analyses shown here follow the same procedure as shown in Figure 6.12 except that $\Delta \sigma$ is different for each case.

Figure 6.14. Estimates of ultimate settlement of the lower sludge layer for different elevations of the upper sludge layer.

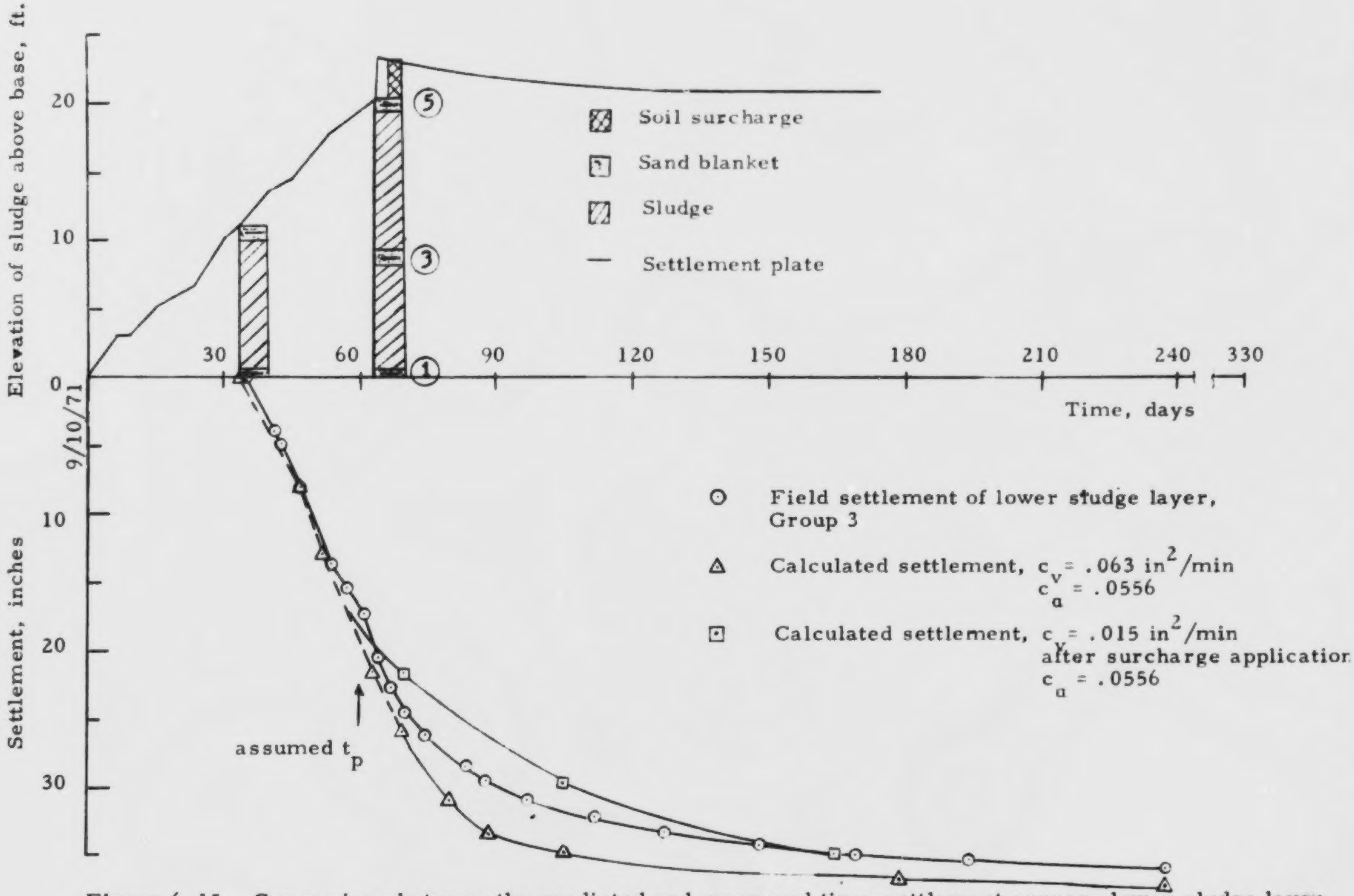

Figure 6.15. Comparison between the predicted and measured time-settlement curves, lower sludge layer.

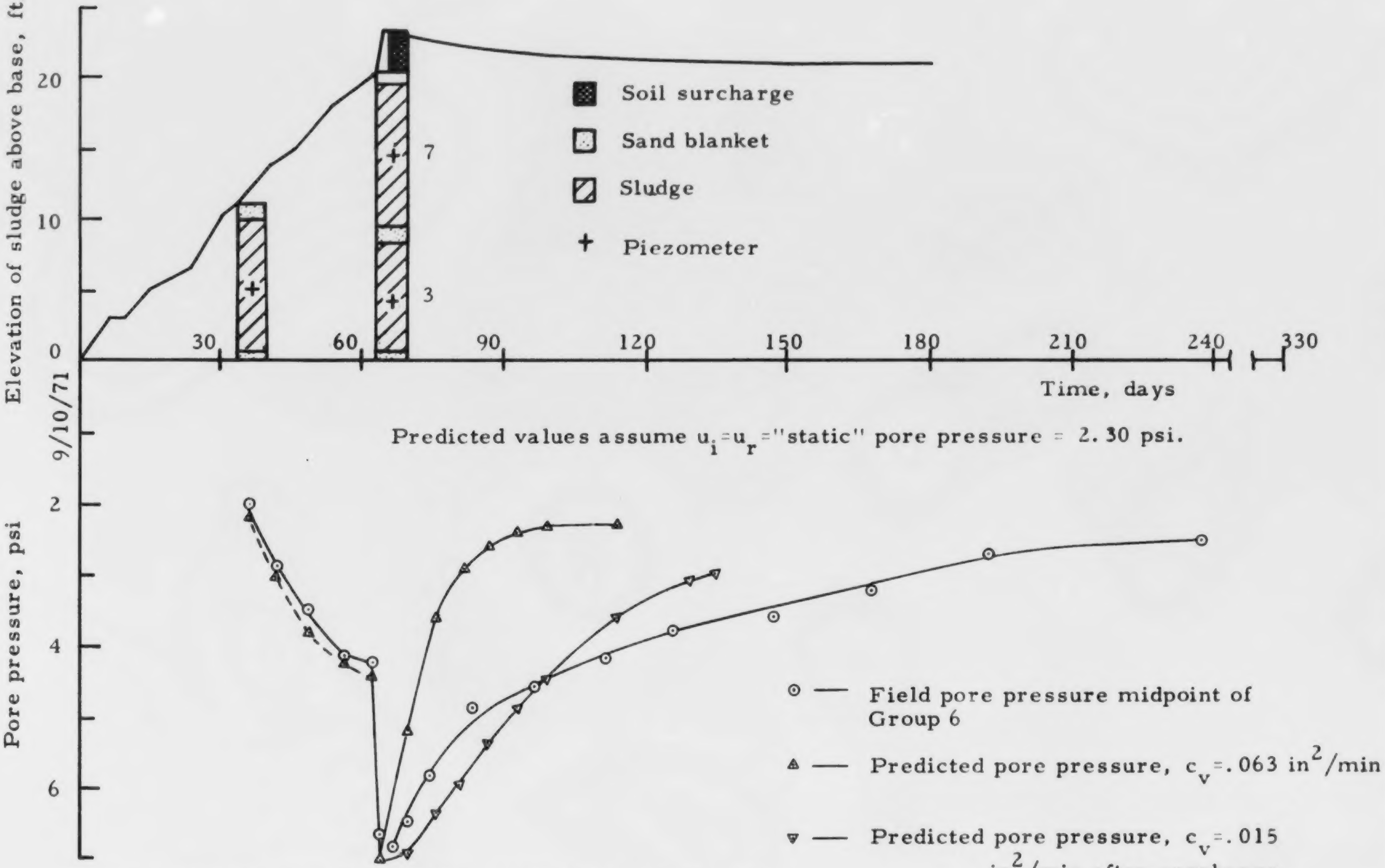

Predicted values assume u_i=u_r="static" pore pressure = 2.30 psi.

Figure 6.16. Comparison between predicted and measured pore pressures at the midpoint of the lower sludge layer.

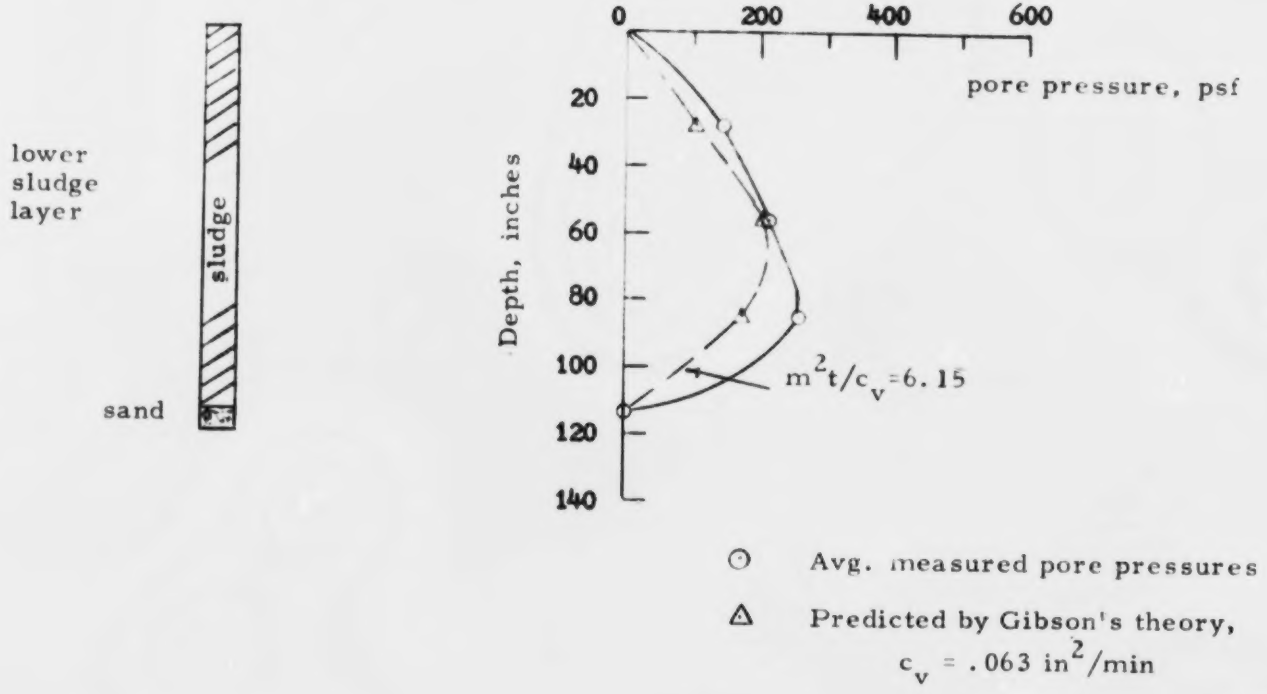

Figure 6.17. Measured and estimated initial excess pore pressures in the lower sludge layer.

Leachate Analysis and Lysimeter Study

The analysis conducted on the leachate and lysimeter percolates included chemical oxygen demand (COD), biological oxygen demand (BOD), specific conductance, total solids (TS), dissolved solids (DS), suspended solids (SS), turbidity, pH, color, odor, nitrogen and phosphorus concentration. The following discussion considers each item in the order listed.

The COD of the well leachate decreased from 3328 to less than 1200 mg/l at 163 days as shown in Figure 5.12. COD for the pipe leachate was higher and ranged from 1500 to 4600 mg/l. A significant reduction in COD was obtained by passage through the organic loam soil (WT). The percolate COD ranged from 40 to 190 mg/l, as shown in Figure 5.19. COD reduction of the pipe leachate (PL) by the sand and clay soils is shown in Figure 5.20. During an acclimation period for the soils, the COD ranged around 400 mg/l but dropped below 300 mg/l after 50 days. COD for the clay column dropped below 100 mg/l after 100 days. Significantly different changes in COD were found for the pipe leachate when comparing aerobic and anaerobic organic loam columns (PTA, Figure 5.19 and PTAN, Figure 5.21). During an acclimation period of about 90 days for the PTAN column, the percolate COD rose to 1360 mg/l followed by a drop to 250 mg/l after 110 days. The COD of the PTA column did not rise above 150 mg/l. The anaerobic environment is considered less efficient as compared to the aerobic environment, therefore less reduction would be expected. For the percolate from the organic loam column, and high flow rates (double dosage), the COD ranged from 175 to 510 mg/l.

Biological oxygen demand for the pipe leachate ranged from 1358 to 3675 mg/l and from 296 to 2660 mg/l for the well leachate, as shown in Figure 5.13. Significant BOD reductions were obtained in all soil columns, with the percolate from the WT column never exceeding 20 mg/l as shown in Figure 5.22. BOD of the percolate from the PTA and PC columns did not exceed 20 mg/l (Figures 5.22 and 5.23). For the DPT column, the BOD ranged from less than 20 mg/l to around 40 mg/l as shown in Figure 5.24. The PTAN column was less efficient, with a range of about 20 to 800 mg/l (Figure 5.24). BOD for the PS column ranged from less than 20 to about 230 mg/l (Figure 5. 23). All of the higher BOD values were obtained during the acclimation period.

The electrical conductance gives an indication of the total concentration of ionic solutes in the leachate or percolate. Specific conductance values for the leachate are shown in Figure 5. 14, with a range of 2440 to 4250 micromho/cm for the pipe leachate. Specific conductance values for the percolates increased with time but never reached the leachate values. The WT column had a range of 400 to 750 micromho/cm, with values increasing with time (Figure 5. 25). Percolate from the PTA column was similar to the WT column up to about 70 days when it continued to increase up to about 1100 micromho/cm at 110 days. The sand column (PS) showed the largest increase in conductance, going from 180 to 2650 micromho/cm (Figure 5. 26). Values for the clay column percolate increased up to about 1000 micromho/cm at 70 days followed by a decrease to 800 micromho/cm at 110 days. Specific conductance for the anaerobic percolate (PTAN) and high flow rate (DPT) columns showed steady increases (Figure 5. 27) with ranges of 400 to 1500 and 1580 to 2700 micromho/cm, respectively.

The total (TS), dissolved (DS), and suspended (SS) solids content of the leachate (Figures 5. 16, 5. 17, and 5. 18) appeared to decrease with time for the pipe leachate and to a lesser degree for the well leachate. For the percolates the solids content showed increasing trends in most cases. The TS, DS, and SS for the WT and the aerobic (DTA) column percolates are shown in Figures 5. 28, 5. 31, and 5. 34, respectively. Both TS and DS increased with time for the WT percolate. The SS remained less than 30 mg/l for about 20 days followed by an increase to 120 mg/l at one point. The PTA column gave the same performance as the WT column, with TS increasing from 390 to 1500 mg/l and the DS increasing from 330 to 1500 mg/l. The SS remained low except for one period (36 to 56th day) when it increased to a high value of 100 mg/l.

The TS, DS, and SS for the percolate from the sand (PS) and clay (PC) columns are shown in Figures 5. 29, 5. 32, and 5. 35. Both TS and DS for the sand column percolate increased throughout the project. The TS increased from about 600 to 2270 mg/l while the DS increased from 500 to 2200 mg/l. The SS increased to 350 mg/l around the 66th day but returned to a low value close to 10 mg/l. The TS for the clay column percolate increased from 480 to 2380 mg/l at about 90 days followed by a drop to about 1000 mg/l. The DS rose from 500 to 1000 mg/l at 90 days and leveled off, while the SS increased from 10 to 680 mg/l at 90 days followed by a decrease to about 10 mg/l.

The TS, DS, and SS for the percolate from the anaerobic (PTAN) and DPT columns is summarized in Figures 5.30, 5.33, and 5.36. The anaerobic column generated the highest total solids, but this included suspended solids of around 1500 mg/l. The TS increased from 350 to 2870 mg/l at 80 days followed by a decrease to around 1800 mg/l. The DS increased from 490 to 1970 mg/l at close to 80 days followed by a decrease to around 1500 mg/l. The SS increased from 10 to 1520 mg/l at 80 days followed by a decrease to 300 mg/l. Solids from the DPT column did not vary any great extent in comparison. TS values ranged from 2130 to 2384 mg/l while the DS ranged from 1750 to 2350 mg/l. The SS for the DPT column percolate ranged from 35 to 550 mg/l.

Turbidity values for the pipe and well leachate are summarized in Figure 5.15. The values for the pipe leachate remained relatively constant, with a range of 20 to 40 JTU. The turbidity of the well leachate decreased from a high of 225 to around 60 JTU. The higher initial values were due to fibrous particles in the well leachate. Turbidity of the percolates remained low throughout the project. The WT and PTA columns gave the lowest turbidity, with most values under 3 JTU. The sand (PS) column percolate ranged from less than 1 to 20 JTU, while the clay (PC) column ranged from about 2 to 34 JTU. The PS and PC columns gave higher values because of the nature of the soils and the fact that some colloidal particles washed through into the percolate. The anaerobic column (PTAN) gave a range from 10 to 39 JTU, while the DPT column gave a range from 3 to 30 JTU.

For the well leachate, pH values ranged from 6.4 to 8.0, with the lower values occurring during the latter half of the year. For the pipe leachate, pH values ranged from 7.6 to 8.1. pH values for the WT percolate ranged from 8.4 to 8.7 and for the PS percolate 6.6 to 9.4. The range of pH values for the remaining soil column percolates were:

8.4 to 8.8 for PTA, 7.2 to 8.9 for PTAN, 7.3 to 8.5 for PC, and 7.4 to 8.4 for DPT. Most of the higher values were obtained during the latter part of the year.

Color values for the well leachate averaged around 50 color units and for the pipe leachate 90 color units. The PS and PC percolates exhibited initial colors of 0 color units. After 160 days the color had increased to 200 color units for the PS and 26 for the PC percolates. All organic loam percolates exhibited high color, but during washings the color was reduced to the initial values. Less washing for the DPT percolate resulted in higher color. The color for the remaining percolates, initially and after 160 days, were as follows: 200 to 235 color units for WT, 135 to 244 color units for PTAN, 850 to 274 color units for DPT, and 0 to 200 color units for PS. The change in color appeared to result from end products of mechanisms active in the soil columns.

Odor for all of the percolates and the well leachate was similar to that of tap water, hence no odor tests were run. The pipe leachate exhibited a weak odor of sulfur. Preliminary analyses of the leachate for nitrogen and phosphorus yielded minimal concentrations. This is to be expected since pulp and paper wastes are nutrient deficient. For this reason only periodic tests were conducted.

Chapter VII. SUMMARY AND CONCLUSIONS

Field Consolidation

An experimental papermill sludge landfill was constructed and monitored to obtain engineering information essential to developing guidelines and recommendations for the design and operation of solid papermill waste landfills. The landfill consisted of 2 sludge layers, initially 10 ft thick, with sand drainage blankets at the top, middle, and bottom. An earth dike provided lateral confinement for the soft sludge during and after construction, and the surface load consisted of 3 ft of natural soil. The landfill was instrumented with 32 settlement plates, 16 piezometers, 3 total pressure cells, and 10 thermistors. Field data were obtained, during the year, on settlement, pore water pressures, vertical and lateral earth pressures, temperature, sludge unit weights, specific gravity, and water contents. Laboratory work included consistency limits, ash contents, and consolidation tests. Comparisons have been made between field settlement behavior and predicted behavior using laboratory test parameters, backfigured field parameters, and soil mechanics theories, including those on consolidation and pore pressure dissipation. Conclusions are given under the following headings: (1) settlement, (2) pore pressures, and (3) stress and temperature conditions.

Settlement.

1. Reasonable estimates of ultimate primary settlement for the sludge can be obtained using equation 6.2, provided that both the initial and residual pore pressures are used in computing effective stresses. A laboratory value for the compression index C_c appears to be appropriate, and the initial void ratio e_o for the field sludge layer may be taken from a laboratory void ratio-logarithm of pressure curve at the appropriate stress level.

2. MacFarlane's (1969) method, using data from a single increment laboratory consolidation test, overestimates primary settlement. Results for this method gave estimates of primary settlement that were closer to the actual total settlement of each sludge layer. This may be due to the high initial void ratio of the laboratory samples.

Preceding page blank

3. Gibson and Lo's (1961) theory provides an accurate estimate of total settlement under instantaneous loading conditions. Careful laboratory tests were required to determine the parameters used in this theory.

4. The field settlement versus logarithm of time curves exhibit a decreasing secondary compression rate with time. This behavior was observed for both the upper and lower sludge layers, although it was not experienced with any of the samples tested in the laboratory.

5. Estimates of secondary compression based on equation 6.5 are too low for laboratory values of the coefficient of secondary compression C_α. Backfigured field parameters yielded appropriate estimates for the upper sludge layer, while a somewhat arbitrary value of time t_p had to be assumed for the lower sludge layer.

6. Terzaghi's (1943) theory appears to adequately predict the time-settlement relation for the sludge, provided that an appropriate value for the coefficient of consolidation, c_v, is used in the theory. Satisfactory results were obtained for both the upper and lower sludge layers for different conditions of loading. The coefficient of consolidation appears to decrease with an increase in field consolidation similar to the decrease shown by laboratory tests. Environmental factors (surface drying, etc.) influenced the time-settlement relation for the upper sludge layer in the landfill.

7. Settlement rates for the landfill gave a good estimate of the flow rate for leachate draining from the papermill sludge.

Pore Pressures.

1. Gibson's (1958) theory gives estimates of pore pressures generated during sludge placement that are in accordance with field observations. Pore pressures in the sludge were influenced by excess pore pressures in the middle sand drainage blanket due to incomplete drainage caused by greater settlement in the test portion of the landfill.

2. Terzaghi's (1943) theory accurately predicted pore pressures in the sludge up to about 70 percent dissipation, provided that an appropriate value for the coefficient of consolidation was used. This was true for the different loading conditions experienced by the upper and lower sludge layers. After 70 percent dissipation, the pore pressures decrease at a slower rate and eventually appear to stabilize at some residual value.

This indicates that a threshold gradient exists for the sludge in the landfill, below which little or no flow of pore water can occur. Pore pressures may also be influenced by environmental factors, as demonstrated by the pore pressure fluctuations of the upper sludge layer with time.

3. The assumption of a uniform initial excess pore pressure for use with Terzaghi's theory appears to be reasonable because of the closeness in magnitude between the initial pore pressures generated during sludge placement and the residual pore pressures.

Stress and Temperature Conditions.

1. The undrained shear strength of the sludge increased considerably during consolidation and is greatest at points in the landfill that are under greater effective stress. A linear relationship between undrained strength and consolidation pressure was indicated by the data shown in Figure 5.4. Sensitivity of the sludge in terms of the ratio of undisturbed to remolded vane strengths was less than two.

2. The vertical stress measured close to the mid-depth of the lower sludge layer by the total pressure cells was in fair agreement with the stress calculated on the basis of material unit weights, indicating that the measured lateral stresses should be equally accurate.

3. The coefficient of lateral stress, K, based on total stress and pore pressure data, decreased from about 0.65 immediately after sludge placement to about 0.32 for the final stage of consolidation. This final value of K does not fit the empirical relationship between the lateral stress ratio at rest and the angle of internal friction associated with normally consolidated inorganic clays.

4. Temperature increase due to increased biological activity peaked about 50 days after completion of the landfill giving a maximum temperature rise close to $7^{\circ}C$ in the upper half of the lower sludge layer. Thereafter sludge temperatures were determined by ground and seasonal air temperatures.

Leachate Analysis and Lysimeter Study

Leachate from the experimental sludge landfill was collected via the drain pipe from the lower sand drainage blanket and from the middle sand blanket via a pipe and well point. Analyses conducted on the leachate included biological oxygen demand, chemical oxygen demand, color, odor, pH, suspended solids, specific conductivity, dissolved solids, total solids, nitrogen and phosphorus. The lysimeter study, which included both aerobic and anaerobic conditions and flow rates approximating field conditions, provided information on changes in quality of the leachate when passed through three natural soils. Conclusions based on this portion of the study are given below.

1. As shown by the results of BOD, COD, and color analyses, all soil columns exhibited excellent organic removal. Sand was slightly less efficient. The organic loam columns exhibited color of their own.
2. An adaptation period was necessary in all cases before peak efficiency of organic removal was obtained. The organic loam required less time for adaptation since it was biologically active in the beginning.
3. None of the three-foot soil columns showed any signs of having their organic removal capacity exhausted during the 160-day observation period.
4. Anaerobic conditions are less efficient than aerobic conditions in the removal of organics.
5. All soil columns showed some decrease in the level of inorganics as compared to the leachate.
6. Clay exhibited the best inorganic retention. This was probably due to greater ion exchange capacity for the clay.
7. With the exception of the clay column, all columns showed an increase of inorganic content in the percolate but none as high as the leachate. However, the increasing trends indicate the columns were slowly becoming exhausted in their ability to retain inorganics.
8. Nitrogen and phosphorus values for the leachate were very low. This was expected since paper wastes are nutrient deficient.
9. Turbidity for the leachate was not extremely high and all soil columns reduced turbidity to low values.
10. Leachate has a significant organic and inorganic content as it leaves the fill but this is an order of magnitude less than that expected from a sanitary landfill.
11. Results from the lysimeter study indicate that passage of leachate through a minimal depth of natural soil should render the percolate innocuous.

REFERENCES

1. American Society for Testing and Materials, Book of ASTM Standards, Parts 11 and 15, Philadelphia, Pennsylvania.

2. Andersland, O. B., and Laza, Robert W., "Peremability of high ash papermill sludge," Journal of the Sanitary Engineering Division, Proc. ASCE (In press), December 1972.

3. Andersland, O. B., and Laza, Robert W., "Shear strength and permeability of high ash pulp and papermill sludges," Tech. Rpt. 1 for the National Council of the Paper Industry for Air and Stream Improvement, Inc., Div. of Engineering Research, Mich. State Univ., E. Lansing, Mich., 1971.

4. Andersland, O. B., and Paloorthekkathil, John M., "Consolidation behavior of high ash pulp and papermill sludges," Tech. Rpt. 2 for the National Council of the Paper Industry for Air and Stream Improvement, Inc., Div. of Engineering Research, Mich. State Univ., E. Lansing, Mich., 1972.

5. Bishop, Alan W., and Henkel, D. J., The Measurement of Soil Properties in the Triaxial Test, Edward Arnold (Publishers) Ltd., London, 1962.

6. Bjerrum, Laurits, "Engineering geology of Norwegian normally-consolidated marine clays as related to settlements of buildings," Geotechnique, London, 17:81-118, 1967.

7. Bjerrum, Laurits, "Embankments on soft ground," Proc., Specialty Conf. on Performance of Earth and Earth-supported Structures, Am. Soc. of Civil Engrs., II:1-54, June, 1972.

8. Black, C. S., ed., Methods of Soil Analysis, No. 9 in the series Agronomy, Am. Soc. Agronomy, Inc., Part 2, 1965.

9. Blosser, Russell O., and Owens, Eben L., "Irrigation and land disposal," National Council of the Paper Industry for Air and Stream Improvement, Inc., Tech. Bull. No. 176, 1964.

10. County of Los Angeles and Engineering-Science, Inc., "Development of construction and use criteria for sanitary landfills," Interim Rpt., U. S. Dept. of Health, Education and Welfare, Cincinnati, 1969.

11. Davis, E. H., and Raymond, G. P., "A non-linear theory of consolidation," Geotechnique, London, 15:161-173, 1965.

12. Follett, Robert, and Gehm, Harry W., "Manual of practice for sludge handling in the pulp and paper industry," National Council of the Paper Industry for Air and Stream Improvement, Inc., Tech. Bull. No. 190, June, 1966.

13. Garlanger, John E., "The consolidation of soils exhibiting creep under constant effective stress," Geotechnique, London, 22:71-78, 1972.

14. Gibson, R. E., "The progress of consolidation in a clay layer increasing in thickness with time," Geotechnique, London, 8:171-182, 1958.

15. Gibson, R. E., and Lo, K. Y., "A theory of consolidation for soils exhibiting secondary compression," Norwegian Geotechnical Institute, Publication 41, Oslo, Norway, 1961.

16. Gibson, R. E., England, G. L., and Hussey, M. J. L., "The theory of one-dimensional consolidation of saturated clays," Geotechnique, London, 17:261-273, 1967.

17. Gillespie, W. J., "Summary Report--Questionnaire Survey--Sludge Cake Disposal on Land," National Council of the Paper Industry for Air and Stream Improvement, Inc., Unpublished, September 1969.

18. Gillespie, W. J., Gellman, I., Janes, R. L., "Utilization of high ash papermill waste solids," Proc. 2nd Mineral Waste Utilization Symposium, IITRI, Chicago, Ill., 1970.

19. Gillespie, W. J., Mazzola, C. A., and Gellman, I., "Landfill disposal of papermill waste solids," presented at the 7th TAPPI Air and Water Conf., Minneapolis, Minn., June 7-10, 1970.

20. Grim, R. E., Clay Mineralogy, McGraw-Hill Book Co., Inc., New York, 1953.

21. Grim, R. E., Applied Clay Mineralogy, McGraw-Hill Book Co., Inc., New York, 1962.

22. Harr, M. E., Foundations of Theoretical Soil Mechanics, McGraw-Hill Book Co., Inc., New York, 1966.

23. Hughes, G. M., Landon, R. A., and Farvolden, R. N., "Hydrogeology of solid waste disposal sites in Northeastern Illinois," Final Rpt. SW-12d, U. S. Environmental Protection Agency, 1971.

24. Janbu, N., "Consolidation of Clay Layers Based on Non-linear Stress-strain," Proc. 6th Internat. Conf. on Soil Mech. and Found. Engr., II:83-87, 1965.

25. Lambe, T. William, Soil Testing for Engineers, John Wiley and Sons, Inc., New York, 1951.

26. Lambe, T. William, and Whitman, Robert V., Soil Mechanics, John Wiley and Sons, Inc., New York, 1969.

27. Leonards, G. A., Foundation Engineering, McGraw-Hill Book Co., Inc., New York, 1962.

28. Leonards, G. A., and Girault, P., "A study of the one-dimensional consolidation test," Proc. 5th Internat. Conf. on Soil Mech. and Found. Engr., Dunod, Paris, I:213-218, 1961.

29. Lo, K. Y., "Secondary compression of clays," Journ. of the Soil Mech. and Found. Div., ASCE, 87:SM4:61-87, 1961.

30. MacFarlane, Ivan C., ed., Muskeg Engineering Handbook, Univ. of Toronto Press, 1969.

31. Mitchell, J. K., and Younger, J. S., "Abnormalities in hydraulic flow through fine-grained soils," STP No. 417, ASTM, pp. 106-139, 1966.

32. National Council of the Paper Industry for Air and Stream Improvement, Inc., "An investigation of improved procedures for measurement of mill effluent and receiving water color," Tech. Bull. No. 253.

33. Scott, R. F., Principles of Soil Mechanics, Addison-Wesley Publ. Co., Inc., Reading, Mass., 1963.

34. Standard Methods for the Examination of Water and Wastewater, American Public Health Association, Inc., New York, 13th ed. 1971.

35. Terzaghi, Karl, Theoretical Soil Mechanics, John Wiley and Sons, Inc., New York, 1943.

36. Terzaghi, Karl, and Peck, Ralph B., Soil Mechanics in Engineering Practice, 2nd ed., John Wiley and Sons, Inc., New York, 1967.

APPENDIX

Preceding page blank

TABLE A-1

SETTLEMENT PLATE ELEVATIONS AT THE BOTTOM SAND BLANKET

PLATE	ELEVATION, FT.							
Date	G1-1	G2-1*	G3-1	G4-1	G5-1	G6-1	G7-1	G8-1
9/10/71	78.50	78.30	78.00	77.70	78.00	78.20	78.50	78.00
10/5/71	78.31	78.09	77.79	77.46	77.76	78.00	78.31	77.73
10/8/71	78.31	78.08	77.79	77.46	77.75	77.99	78.31	77.73
10/14/71	78.31	78.09	77.78	77.45	77.75	77.99	78.30	77.75
10/20/71	78.30	78.10	77.80	77.46	77.74	77.98	78.32	77.75
10/22/71	78.33	78.10	77.81	77.47	77.76	78.00	78.32	77.77
10/26/71	78.31	78.11	77.80	77.45	77.75	77.99	78.31	77.75
11/2/71	78.27	78.07	77.76	77.43	77.73	77.96	78.27	77.74
11/5/71	78.30	78.07	77.79	77.44	77.69	77.97	78.29	77.74
11/9/71	78.31	78.08	77.80	77.42	77.72	77.97	78.27	77.74
11/10/71	78.28	78.07	77.75	77.43	77.70	77.95	78.28	77.73
11/12/71	78.27	78.03	77.73	77.44	77.67	77.95	78.25	77.72
11/15/71	78.38	78.04	77.73	77.43	77.67	77.94	78.26	77.73
11/18/81	78.27	78.03	77.71	77.42	77.67	77.93	78.25	77.73
11/22/71	78.26	78.03	77.70	77.42	77.65	77.93	78.28	77.73
12/1/71	78.27	78.04	77.71	77.44	77.67	77.93	78.26	77.74
12/6/71	78.26	78.04	77.70	77.43	77.65	77.93	78.25	77.73
12/15/71	78.27	78.04	77.71	77.42	77.65	77.91	78.25	77.72
12/30/71	78.28	78.05	77.71	77.41	77.66	77.92	78.26	77.72
1/14/72	78.28	78.05	77.72	77.43	77.67	77.92	78.26	77.73
2/3/72	78.25	78.03	77.70	77.41	77.64	77.90	78.24	77.70
2/24/72	78.23	78.01	77.68	77.39	77.62	77.87	78.21	77.68
3/20/72	78.26	78.04	77.70	77.41	77.64	77.91	78.24	77.71
5/4/72	78.25	78.02	77.69	77.40	77.64	77.90	78.24	77.70
8/1/72	78.27	78.05	77.71	77.43	77.65	77.92	78.26	77.72
9/11/72	78.27	78.04	77.70	77.42	77.65	77.91	78.26	77.71

*Note: G2-1 refers to group no. 2 settlement plate no. 1, etc.

Preceding page blank

TABLE A-2

SETTLEMENT PLATE ELEVATIONS AT THE MID-POINTS OF THE LOWER AND UPPER SLUDGE LAYERS

	ELEVATION, FT.							
PLATE	G5-2	G6-2	G7-2	G8-2	G7-3½	G5-4	G6-4	G7-4
Date								
9/27/71	83.51	——	83.92	——	——	——	——	——
9/29/71	——	83.63	——	83.11				
10/5/71	82.92	83.23	83.51	82.37				
10/8/71	82.81	83.04	83.40	82.29				
10/14/71	82.67	82.90	83.27	82.18				
10/20/71	82.49	82.78	83.08	82.03	91.01			
10/22/71	82.46	82.73	83.04	82.00				
10/26/71	82.35	82.62	82.93	81.90	90.64			
10/27/71	——	——	——	——	——	93.88	94.00	93.81
11/2/71	82.17	82.40	82.70	81.75	90.02	93.30	93.33	93.00
11/5/71	82.10	82.36	82.62	81.68	89.85	93.12	93.10	92.82
11/9/71	82.05	82.28	82.58	81.60	89.65	92.81	92.89	92.59
11/10/71	81.99	82.24	82.54	81.57	89.57	92.62	92.71	92.42
11/12/71	81.91	82.14	82.45	81.46	89.23	92.36	92.42	92.02
11/15/71	81.82	82.05	82.37	81.37	88.98	92.02	92.02	91.66
11/18/71	81.77	81.99	82.30	81.32	88.82	91.78	91.75	91.41
11/22/71	81.70	81.92	82.25	81.25	88.66	91.54	91.51	91.17
12/1/71	81.63	81.84	82.16	81.19	88.44	91.21	91.16	90.82
12/6/71	81.60	81.79	82.13	81.14	88.35	91.08	91.03	90.70
12/15/71	81.53	81.73	82.06	81.07	88.22	90.91	90.86	90.53
12/30/71	81.50	81.67	82.01	81.02	88.06	90.75	90.67	90.39
1/14/72	81.46	81.65	82.00	81.02	87.99	90.65	90.56	90.29
2/3/72	81.41	81.59	81.95	80.95	87.91	90.54	90.43	90.18
2/24/72	81.37	81.56	81.91	80.90	87.82	90.45	90.33	90.09
3/20/72	81.38	81.57	81.92	80.91	87.81	90.41	90.30	90.06
5/4/72	81.35	81.55	81.88	80.88	87.75	90.35	90.24	90.00
8/1/72	81.36	81.53	81.88	80.88	damaged	90.30	90.18	89.95
9/11/72	81.32	81.51	81.88	80.86	——	90.28	90.14	89.91

TABLE A-3

SETTLEMENT PLATE ELEVATIONS AT THE MIDDLE SAND BLANKET

	ELEVATION, FT.							
PLATE	G1-3	G2-3	G3-3	G4-3	G5-3	G6-3	G7-3	G8-3
Date								
10/14/71	88.47	88.95	88.58	88.64	88.46	88.82	88.66	88.49
10/20/71	87.98	88.52	88.25	88.25	88.03	88.51	88.15	88.10
10/22/71	87.93	88.48	88.17	88.10	87.94	88.29	88.09	87.99
10/26/71	87.75	88.20	87.91	87.92	87.72	88.08	87.87	87.80
11/2/71	87.29	87.77	87.44	87.49	87.36	87.63	87.40	87.43
11/5/71	87.19	87.61	87.29	87.33	87.18	87.47	87.29	87.23
11/9/71	87.05	87.43	87.13	87.20	87.06	87.35	87.12	87.08
11/10/71	86.96	87.33	87.03	87.14	86.98	87.73	87.02	86.97
11/12/71	86.80	87.12	86.88	86.97	86.84	87.04	86.84	86.84
11/15/71	86.64	86.92	86.68	86.79	86.67	86.83	86.67	86.64
11/18/71	86.52	86.79	86.54	86.66	86.56	86.69	86.55	86.50
11/22/71	86.40	86.66	86.40	86.52	86.43	86.56	86.43	86.37
12/1/71	86.21	86.47	86.20	86.33	86.26	86.36	86.24	86.16
12/6/71	86.14	86.39	86.11	86.25	86.18	86.28	86.16	86.08
12/15/71	86.03	86.28	85.99	86.13	86.06	86.16	86.16	85.96
12/30/71	85.92	86.19	85.89	86.01	85.97	86.04	85.97	85.82
1/14/72	85.86	86.12	85.80	85.93	85.89	85.97	85.90	85.76
2/3/72	85.77	86.03	85.72	85.85	85.82	85.87	85.83	85.66
2/24/72	85.70	85.96	85.65	85.78	85.75	85.80	85.76	85.60
3/20/72	85.69	85.95	85.63	85.76	85.74	85.79	85.76	85.58
5/4/72	85.64	85.90	85.58	85.71	85.68	85.74	85.70	85.53
8/1/72	85.61	85.87	85.54	85.69	85.67	85.71	85.69	85.51
9/11/72	85.60	85.85	85.52	85.67	85.65	85.69	85.67	85.48

TABLE A-4

SETTLEMENT PLATE ELEVATIONS AT THE TOP SAND BLANKET

	ELEVATION, FT.							
PLATE	G1-5	G2-5	G3-5	G4-5	G5-5	G6-5	G7-5	G8-5
Date								
11/10/71	98.32	98.35	98.23	98.01	98.10	98.15	98.32	97.84
11/12/71	97.87	97.81	97.88	97.59	97.69	97.72	97.58	97.49
11/15/71	97.38	97.33	97.33	97.07	97.23	97.19	97.12	96.92
11/18/71	97.04	96.99	96.99	96.74	96.91	96.85	96.78	96.59
11/22/71	96.71	96.64	96.65	96.42	96.58	96.50	96.44	96.27
12/1/71	96.25	96.16	96.20	95.99	96.73	96.05	95.97	95.85
12/6/71	96.09	95.98	96.04	95.83	95.96	95.87	96.81	95.69
12/15/71	95.88	95.77	95.84	95.63	95.75	95.68	95.60	95.50
12/30/71	95.67	95.55	95.63	95.43	95.54	95.47	95.40	95.30
1/14/72	95.54	95.43	95.52	95.31	95.42	95.34	95.27	95.18
2/3/72	95.41	95.28	95.38	95.16	95.27	95.19	95.13	95.04
2/24/72	95.29	95.16	95.27	95.05	95.16	95.08	95.02	94.93
3/20/72	95.25	95.13	95.23	95.00	95.11	95.03	94.98	94.88
5/4/72	95.17	95.05	95.16	94.93	95.04	94.95	94.90	94.81
8/1/72	95.06	94.94	95.06	94.83	94.94	94.84	94.80	94.73
9/11/72	94.98	94.87	94.99	94.72	94.88	94.75	94.73	94.64

TABLE B-1

PORE WATER PRESSURES FOR THE BOTTOM SAND BLANKET AND LOWER SLUDGE LAYER

	PORE PRESSURE, PSI							
PIEZOMETER	G5-1	G7-1	G5-2	G5-3	G6-3	G7-3	G5-4	G7-4
INITIAL EL.FT	78.0	78.5	81.0	83.5	83.6	83.9	83.0	86.4
Date								
10/15/71	.10	.30	2.50	2.65	2.00	2.15	1.95	1.65
10/21/71	.05	.45	2.80	2.90	2.90	2.30	2.15	1.70
10/28/71	0.0	.30	3.20	3.50	3.50	3.25	2.70	2.50
11/4/71	.10	.25	3.70	4.40	4.15	3.50	3.30	2.75
11/10/71	0.0	.20	3.80	4.30	4.25	4.20	3.35	3.55
11/12/71	0.0	.50	6.20	6.20	6.70	6.65	5.90	5.80
11/15/71	.10	.30	6.10	6.60	6.90	5.90	5.25	5.55
11/18/71	0.0	.30	5.60	6.60	6.50	5.85	4.90	5.35
11/22/71	0.0	.20	4.80	5.85	5.85	5.45	4.55	4.65
12/1/71	0.0	0.0	3.55	5.00	4.90	4.50	4.65	4.00
12/15/71	0.0	.10	3.35	4.45	4.60	4.25	4.55	4.50
12/30/71	0.0	.20	3.15	3.95	4.20	4.05	4.65	4.10
1/13/72	0.0	0.0	2.85	3.60	3.80	3.70	4.25	3.70
2/3/72	.10	0.0	2.60	3.20	3.60	3.50	4.00	3.50
2/24/72	.30	0.0	2.40	2.80	3.20	2.90	3.80	3.20
3/20/72	.30	0.0	2.10	2.50	2.70	2.50	3.50	3.00
5/4/72	.20	.10	2.00	2.40	2.50	2.40	3.50	2.90
8/1/72	.30	.30	1.90	2.25	2.30	2.25	3.10	2.40
9/6/72	.25	.40	2.00	2.25	2.25	2.25	3.25	2.60
9/11/72	.50	.35	2.00	2.30	2.45	2.35	2.15	2.65

TABLE B-2

PORE WATER PRESSURES FOR THE MIDDLE SAND BLANKET AND UPPER SLUDGE LAYER

	PORE PRESSURE, PSI							
PIEZOMETER	G5-5	G7-5	G5-6	G7-6	G5-7	G6-7	G7-7	G5-8
INITIAL EL. FT	88.1	88.3	91.3	91.4	93.9	93.8	94.0	95.5
Date								
10/21/71	.30	.20	--	--	--	--	--	--
10/28/71	.60	.50	--	--	--	--	--	--
11/4/71	.70	.75	1.20	1.00	--	--	--	--
11/10/71	.80	1.05	2.10	2.45	1.20	.85	2.35	.95
11/12/71	1.30	1.35	4.60	4.80	4.20	4.00	4.40	2.80
11/15/71	1.10	1.20	3.90	3.95	3.50	3.50	3.75	2.25
11/18/71	1.20	1.25	3.55	3.45	3.10	3.10	3.30	2.00
11/22/71	1.15	1.25	3.00	2.90	2.65	2.65	2.80	1.70
12/1/71	1.00	1.10	2.30	2.10	2.10	2.10	2.10	1.20
12/6/71	--	--	2.30	2.20	1.95	1.95	2.00	1.15
12/15/71	1.15	1.15	2.80	2.25	1.80	1.80	1.80	1.50
12/30/71	1.05	1.10	2.41	2.30	1.45	1.45	1.50	1.30
1/13/72	1.20	1.10	2.50	2.20	1.50	1.35	1.50	1.10
2/3/72	1.20	1.10	2.20	2.00	1.50	1.00	1.50	.90
2/24/72	1.30	1.00	2.20	2.00	1.50	1.00	1.90	--
3/20/72	1.40	1.30	2.10	1.70	1.30	1.00	1.60	.80
5/4/72	2.00	1.40	2.20	2.10	1.70	1.20	2.10	1.30
8/1/72	1.50	1.10	2.00	2.00	1.10	.90	1.60	.25
9/6/72	2.00	1.60	2.10	1.95	1.85*	.90	1.60	.05
9/11/72	1.90	1.50	1.80	2.00	1.25	1.00	1.70	.05

*Drilling rig near here at time of reading.

TABLE C-1 TOTAL PRESSURE CELL DATA

TOTAL PRESSURE CELL INITIAL ELEVATION	G7-Horiz. 83.60			G7-2 Vert. 83.78			G7-3 Vert. 83.48		
Date	I*	W†	S#	I	W	S	I	W	S
10/15/71	9.0	4.3	5.0	7.7	3.0	3.5	8.1	3.5	4.1
10/21/71	9.5	4.9	5.7	8.2	3.6	4.1	8.3	3.7	4.2
10/28/71	10.8	6.0	6.9	10.1	5.2	6.1	9.2	4.5	5.2
11/4/71	11.8	7.0	8.1	10.2	5.2	6.1	9.8	5.0	6.0
11/10/71	13.9	9.1	10.5	12.8	8.2	9.3	11.1	6.3	7.2
11/12/71	16.3	11.7	13.2	---	---	---	13.3	8.6	9.8
11/15/71	16.5	11.9	13.4	13.1	8.5	9.7	13.1	8.5	9.7
11/18/71	16.5	11.9	13.4	12.8	8.2	9.3	12.8	8.2	9.3
11/22/71	16.6	12.0	13.5	12.2	7.7	8.8	12.5	8.0	9.1
12/1/71	16.9	12.2	13.7	12.7	8.1	9.2	12.0	7.3	8.6
12/15/71	17.2	12.7	14.2	13.9	9.1	10.5	11.4	6.9	7.9
12/30/71	17.7	13.0	14.6	---	---	---	11.1	6.3	7.2
1/13/72	17.8	13.1	14.7	15.0	10.2	11.8	10.7	6.1	7.1
2/3/72	18.0	13.2	15.1	15.8	Discontinued		10.5	6.0	7.0
2/24/72	17.9	13.2	14.9	15.9			10.3	5.8	6.8
3/20/72	18.0	13.2	15.1	16.3			10.3	5.8	6.8
5/4/72	18.0	13.2	15.1	16.6			10.2	5.5	6.5
8/1/72	17.3	12.7	14.2	---			9.5	4.9	5.8
9/6/72	17.3	12.7	14.2	---			9.7	5.1	6.0

* I - INSTRUMENT READING

† W - TOTAL PRESSURE, WATER CALIBRATION, Psi

# S - TOTAL PRESSURE, SAND CALIBRATION, Psi

NOTE: CELL G7-2 GAVE ERRATIC DATA (MALFUNCTIONED) AND THESE VALUES ARE AN AVERAGE OF FOUR DIFFERENT READINGS.

TABLE D-1

TEMPERATURE DATA FOR PAPERMILL SLUDGE LANDFILL

Thermistor no.	1		2		3		4		5	
Elevation, ft.	95.43		93.43		91.43		89.43		87.43	
Date	I*	T†	I	T	I	T	I	T	I	T
12/16/71	3.69	14.1	3.90	12.9	3.84	13.2	3.84	13.2	3.80	13.5
12/30/71	4.87	8.2	6.30	3.0	4.20	11.3	3.53	15.1	3.25	16.8
1/13/72	5.30	6.6	7.04	.9	4.75	8.8	4.43	10.2	3.95	12.6
2/3/72	6.05	3.8	7.62	-.7	4.95	8.0	4.34	10.7	4.00	12.4
2/24/72	6.30	3.0	9.07	-4.0	5.44	6.0	4.85	8.4	4.43	10.2
3/20/72	5.42	6.1	8.78	-3.5	5.16	7.1	5.00	7.7	4.60	9.4
5/4/72	3.81	13.4	--	--	4.04	12.2	3.99	12.5	3.71	14.0
8/1/72	1.99	34.7	--	--	2.65	21.3	3.04	18.2	3.15	17.5
9/6/72	2.16	26.0	--	--	2.36	23.9	2.72	20.7	2.90	19.3

Thermistor no.	6		7		8		9		0	
Elevation, ft.	85.43		83.43		81.43		79.43		77.43	
Date										
12/16/71	3.84	13.2	3.32	16.4	3.11	17.7	3.10	17.8	2.26	24.9
12/30/71	2.63	21.5	2.42	23.4	2.37	23.9	2.50	22.7	2.77	20.3
1/13/72	3.53	15.1	2.92	19.0	2.67	21.2	2.63	21.6	2.81	20.0
2/3/72	3.50	15.3	3.16	17.4	2.84	19.7	2.76	20.4	2.88	19.5
2/24/72	3.95	12.6	3.47	15.4	3.02	18.5	2.88	19.7	2.93	19.1
3/20/72	4.31	11.4	3.55	14.9	3.20	17.2	3.02	18.3	3.00	18.5
5/4/72	3.38	16.0	3.30	16.5	3.23	17.0	3.17	17.3	3.16	17.4
8/1/72	3.21	17.1	3.18	17.3	3.20	17.2	3.25	16.9	3.41	15.8
8/6/72	3.10	17.8	3.10	17,8	3.19	17.2	3.28	16.7	3.48	15.4

*I INSTRUMENT READING (K-OHMS)

†T TEMPERATURE (DEGREES CENTIGRADE)

TABLE E-1 UNDISTURBED VANE SHEAR STRENGTHS

	UPPER SLUDGE LAYER									
Elev. below sludge top	-2-1/2 ft.			-5 ft.			-7-1/2 ft.			Vane Size
Date	R*	M$^+$	S#	R	M	S	R	M	S	
10/14/71	0	245	1.23	0	240	1.70	0	570	2.85	LARGE
10/14/71	0	300	1.50	0	485	2.43	0	620	3.10	LARGE
10/14/71	0	175	1.75	0	230	2.30	0	330	3.30	INTER.
10/14/71	0	190	1.90	0	200	2.00	0	360	3.60	INTER.
11/11/71	0	255	2.55	20	320	3.00	62	395	3.33	INTER.
11/11/71	0	100	2.00	20	150	3.00	60	265	4.60	SMALL
Elevation	-25 in.			-50 in.			-75 in.			
3/20/72	35	330	5.90	60	400	6.80	130	465	6.70	SMALL
3/20/72	45	320	5.50	140	380	4.80	185	480	5.90	SMALL

*R ROD FRICTION READING

$^+$M MAX. READING

#S SHEAR STRENGTH, T/M^2

	LOWER SLUDGE LAYER									
Elev. below sludge top	-2-1/2 ft.			-5 ft.			-7-1/2 ft.			
11/11/71	170	480	3.10	220	670	4.50	TORQUE WRENCH CAPACITY EXCEEDED OFF SCALE			SMALL
11/11/71	155	360	4.10	250	545	5.90				SMALL
Elevation	-25 in.			-40 in.						
3/20/72	340	720	7.60	370	850	9.60				SMALL
3/20/72	560	~950	7.80	CAPACITY EXCEEDED						SMALL

TABLE E-2 REMOLDED VANE SHEAR STRENGTHS

	UPPER SLUDGE LAYER									
Elev. below sludge top	-2-1/2 ft.			-5 ft.			-7-1/2 ft.			Vane Size
Date	R*	M+	S#	R	M	S	R	M	S	
10/14/71	0	180	.90	0	135	.68	0	340	1.70	LARGE
10/14/71	0	210	1.05	0	260	1.30	0	340	1.70	LARGE
10/14/71	0	110	1.10	0	130	1.30	0	190	1.90	INTER.
10/14/71	0	120	1.20	0	120	1.20	0	150	1.50	INTER.
11/11/71	0	135	1.35	20	160	1.40	62	240	1.78	INTER.
11/11/71	0	40	.80	20	70	1.00	55	150	1.90	SMALL
Elevation	-25 in.			-50 in.			-75 in.			
3/20/72	25	180	3.10	25	185	3.20	90	240	3.00	SMALL
3/20/72	30	155	2.50	80	230	3.00	130	280	3.00	SMALL

	LOWER SLUDGE LAYER							
Elev. below sludge top	-2-1/2 ft.			-5 ft.			-7-1/2 ft.	
11/11/71	155	345	1.90	200	440	2.40	TORQUE WRENCH CAPACITY EXCEEDED	SMALL
11/11/71	140	280	2.80	205	330	2.50		SMALL
Elevation	-25 in.			-40 in.				
3/20/72	235	435	4.00	--	--	--		SMALL

*R ROD FRICTION READING

+M MAX. READING

#S SHEAR STRENGTH, T/M^2

TABLE F-1 CONVENTIONAL CONSOLIDATION DATA

Sludge U-4-1, initial water content 250%, wt. dry specimen 26.5 gms.
February 15, 1972

time min.	dial reading in. x 10^4	time min.	dial reading in. x 10^4	time min.	dial reading in. x 10^4
load kg/cm^2		load 1 kg/cm^2		load 4 kg/cm^2	
0.00	0	0.00	0	0.00	0
0.25	311	0.10	120	0.10	115
0.50	395	0.25	185	0.25	180
1.00	522	0.50	250	0.50	255
2.25	700	1.00	340	1.00	355
4.00	836	2.25	475	2.25	525
6.25	928	4.00	575	4.00	660
9.00	980	6.25	640	6.25	760
12.25	1006	9.00	675	9.00	845
16.00	1031	12.25	705	12.25	873
20.25	1048	16.00	720	16.00	903
25.00	1063	20.25	740	20.25	933
36.00	1082	25.00	750	25.00	950
49.00	1093	36.00	770	36.00	977
120.00	1128	49.00	785	49.00	993
240.00	1147	120.00	825	120.00	1043
580.00	1168	240.00	856	240.00	1074
1440.00	1200	580.00	890	580.00	1103
		1440.00	930	1440.00	1137
load kg/cm^2		load 2 kg/cm^2		load 8 kg/cm^2	
0.00	0	0.00	0	0.00	0
0.10	115	0.10	95	0.10	60
0.25	175	0.25	125	0.25	90
0.50	244	0.50	153	0.50	125
1.00	331	1.00	185	1.00	170
2.25	470	2.25	240	2.25	240
4.00	570	4.00	300	4.00	305
6.25	630	6.25	425	6.25	350
9.00	670	9.00	480	9.00	390
12.25	697	12.25	510	12.25	420
16.00	718	16.00	533	16.00	440
20.25	735	20.25	544	20.25	460
25.00	750	25.00	560	25.00	475
36.00	765	26.00	570	36.00	495
49.00	785	49.00	595	49.00	510
120.00	832	120.00	635	120.00	555
240.00	863	240.00	655	240.00	580
580.00	897	580.00	675	580.00	600
1440.00	937	1440.00	710	1440.00	640

TABLE F-2 CONVENTIONAL CONSOLIDATION DATA

Sludge U-3-1, initial water content 306%, wt. dry specimen 23.9 gms.
February 28, 1972

time min.	dial reading in. x 10^4	time min.	dial reading in. x 10^4	time min.	dial reading in. x 10^4
load .1 kg/cm^2		load .4 kg/cm^2		load 1.6 kg/cm^2	
0.00	0	0.00	0	0.00	0
0.10	130	0.10	65	0.10	70
0.25	175	0.25	105	0.25	110
0.50	215	0.50	145	0.50	153
1.00	275	1.00	210	1.00	210
2.25	390	2.25	300	2.25	283
4.00	505	4.00	373	4.00	337
6.25	605	6.25	423	6.25	380
9.00	690	9.00	460	9.00	409
12.25	755	12.25	480	12.25	455
16.00	805	16.00	495	16.00	483
20.25	835	20.25	510	20.25	500
25.00	855	25.00	515	25.00	512
36.00	885	36.00	530	36.00	525
49.00	905	49.00	540	49.00	537
120.00	945	120.00	565	120.00	565
240.00	965	240.00	590	240.00	583
580.00	995	580.00	610	580.00	605
1400.00	1025	1480.00	635	1450.00	635
load .2 kg/cm^2		load .8 kg/cm^2		load 3.2 kg/cm^2	
0.00	0	0.00	0	0.00	0
0.10	50	0.10	70	0.10	95
0.25	85	0.25	110	0.25	140
0.50	120	0.50	155	0.50	192
1.00	175	1.00	220	1.00	262
2.25	260	2.25	320	2.25	360
4.00	330	4.00	410	4.00	428
6.25	380	6.25	465	6.25	475
9.00	420	9.00	485	9.00	507
12.00	450	12.25	495	12.25	325
16.00	470	16.00	500	16.00	540
20.25	490	20.25	505	20.25	550
25.00	500	25.00	515	25.00	560
36.00	520	36.00	520	36.00	570
49.00	535	49.00	525	49.00	578
120.00	575	120.00	545	120.00	603
240.00	600	240.00	560	120.00	620
580.00	630	580.00	570	580.00	640
1460.00	665	1440.00	585	1410.00	660
				load .8 kg/cm^2	
				720.00	190

TABLE F-3 CONVENTIONAL CONSOLIDATION DATA

Sludge u-3-3, initial water content 271%, wt. dry specimen 24.7 gms.
March 11, 1972

time min.	dial reading in. x 10^4	time min.	dial reading in. x 10^4	time min.	dial reading in. x 10^4
load .1 kg/cm^2		load .4 kg/cm^2		load 1.6 kg/cm^2	
0.00	0	0.00	0	0.00	0
0.10	70	0.10	43	0.10	87
0.25	105	0.25	72	0.25	135
0.50	145	0.50	105	0.50	195
1.00	200	1.00	150	1.00	280
2.25	290	2.25	227	2.25	420
4.00	375	4.00	290	4.00	498
6.25	455	6.25	337	6.25	550
9.00	510	9.00	372	9.00	587
12.25	555	12.25	400	12.25	600
16.00	585	16.00	420	16.00	605
20.25	610	20.25	433	20.25	610
25.00	620	25.00	448	25.00	615
36.00	655	36.00	468	36.00	622
49.00	665	49.00	485	49.00	628
120.00	700	120.00	540	120.00	640
240.00	725	240.00	568	240.00	650
580.00	760	580.00	583	580.00	662
1580.00	795	1460.00	606	1480.00	682
load .2 kg/cm^2		load .8 kg/cm^2		load 3.2 kg/cm^2	
0.00	0	0.00	0	0.00	0
0.10	30	0.10	62	0.00	75
0.25	53	0.25	93	0.25	126
0.50	80	0.50	127	0.50	185
1.00	120	1.00	173	1.00	263
2.25	187	2.25	242	2.25	378
4.00	247	4.00	286	4.00	464
6.25	293	6.25	307	6.25	520
9.00	327	9.00	320	9.00	551
12.25	350	12.25	330	12.25	570
16.00	373	16.00	337	16.00	580
20.25	388	20.25	342	20.25	583
25.00	400	25.00	348	25.00	590
36.00	415	36.00	357	36.00	602
49.00	428	49.00	365	49.00	610
120.00	468	120.00	382	120.00	627
240.00	492	240.00	392	240.00	642
580.00	520	580.00	412	580.00	658
1470.00	555	1450.00	460	1430.00	683
				load .8 kg/cm^2	
				1444.00	192

TABLE F-4 CONVENTIONAL CONSOLIDATION DATA

Sludge U-3-7, initial water content 299%, wt, dry specimen 23.0 gms.
March 27, 1972

time min.	dial reading in. x 10^4	time min.	dial reading in. x 10^4	time min.	dial reading in. x 10^4
load .1 kg/cm^2		load .4 kg/cm^2		load 1.6 kg/cm^2	
0.00	0	0.00	0	0.00	0
0.10	125	0.10	40	0.10	90
0.25	170	0.25	63	0.25	145
0.50	220	0.50	93	0.50	213
1.00	300	1.00	133	1.00	292
2.25	440	2.25	200	2.25	410
4.00	585	4.00	262	4.00	475
6.25	730	6.25	340	6.25	516
9.00	850	9.00	383	9.00	547
12.25	945	12.25	401	12.25	575
16.00	1020	16.00	414	16.00	594
20.25	1075	20.25	423	20.25	601
25.00	1110	25.00	430	25.00	610
36.00	1145.	36.00	440	36.00	622
49.00	---	49.00	448	49.00	---
120.00	1215	120.00	460	120.00	637
240.00	1235	240.00	468	240.00	643
580.00	1270	580.00	478	580.00	655
1660.00	1310	1430.00	500	1450.00	660
load .2 kg/cm^2		load .8 kg/cm^2		load 3.2 kg/cm^2	
0.00	0	0.00	0	0.00	0
0.10	35	0.10	50		
0.25	57	0.25	73		
0.50	83	0.50	103	lever hit floor increment no good	
1.00	122	1.00	140		
2.25	187	2.25	195		
4.00	241	4.00	250		
6.25	283	6.25	298		
9.00	315	9.00	322		
12.25	335	12.25	225		
16.00	354	16.00	345		
20.25	368	20.25	351		
25.00	380	25.00	355		
36.00	400	36.00	365		
49.00	410	49.00	373		
120.00	440	120.00	389		
240.00	460	240.00	398		
580.00	478	580.00	406		
1460.00	498	1420.00	422	1530.00	600

TABLE F-5 CONVENTIONAL CONSOLIDATION DATA

Sludge U-3-8, initial water content 272%, wt. dry specimen 24.5 gms.
April 3, 1972

time min.	dial reading in. x 10^4	time min.	dial reading in. x 10^4	time min.	dial reading in. x 10^4
load .1 kg/cm^2		load .4 kg/cm^2		load 1.6 kg/cm^2	
0.00	0	0.00	0	0.00	0
0.10	115	0.10	60	0.10	108
0.25	155	0.25	93	0.25	158
0.50	200	0.50	130	0.20	210
1.00	260	1.00	182	1.00	280
2.25	370	2.25	253	2.25	383
4.00	470	4.00	325	4.00	433
6.25	590	6.25	407	6.25	465
9.00	690	9.00	465	9.00	488
12.25	735	12.25	510	12.25	503
16.00	760	16.00	532	16.00	515
20.25	775	20.25	553	20.25	525
25.00	785	25.00	570	25.00	532
36.00	805	36.00	---	36.00	550
49.00	815	49.00	---	49.00	558
120.00	840	120.00	640	120.00	580
240.00	560	240.00	657	240.00	593
580.00	890	580.00	673	580.00	610
1465.00	925	1420.00	713	1440.00	630
load .2 kg/cm^2		load .8 kg/cm^2		load 3.2 kg/cm^2	
0.00	0	0.00	0	0.00	0
0.10	40			0.10	43
0.25	63			0.25	145
0.50	95	porous stone hung up on ring--reading of 340 obtained--new increment applied		150.00	210
1.00	138			1.00	295
2.25	205			2.25	428
4.00	253			4.00	515
6.25	290			6.25	570
9.00	315			9.00	600
12.25	333			12.25	622
16.00	345			16.00	637
20.25	358			20.25	648
25.00	368			25.00	657
36.00	325			36.00	670
49.00	397			49.00	678
120.00	430			120.00	705
240.00	453			240.00	722
580.00	480			580.00	743
1430.00	518			1425.00	770

TABLE F-6 CONVENTIONAL CONSOLIDATION DATA

Sludge U-3-9, initial water content 313%, wt. dry specimen 22.0 gms.
April 9, 1972

time min.	dial reading in. x 10^4	time min.	dial reading in. x 10^4	time min.	dial reading in. x 10^4
load .1 kg/cm^2		load .4 kg/cm^2		load 1.6 kg/cm^2	
0.00	0	0.00	0	0.00	0
0.10	90	0.10	53	0.10	115
0.25	130	0.25	77	0.25	158
0.50	175	0.50	108	0.50	208
1.00	240	1.00	150	1.00	275
2.25	355	2.25	215	2.25	378
4.00	505	4.00	270	4.00	465
6.25	660	6.25	320	6.25	512
9.00	795	9.00	405	9.00	532
12.25	925	12.25	472	12.25	550
16.00	1035	16.00	518	16.00	565
20.25	1125	20.25	550	20.25	580
25.00	1185	25.00	580	25.00	590
36.00	1255	36.00	610	36.00	602
49.00	1295	49.00	625	49.00	610
120.00	1365	120.00	655	120.00	632
240.00	1405	240.00	690	240.00	645
580.00	1435	580.00	715	580.00	660
1495.00	1495	1450.00	748	1430.00	682
load .2 kg/cm^2		load .8 kg/cm^2		load 3.2 kg/cm^2	
0.00	0	0.00	0	0.00	0
0.10	30	0.10	62	0.10	85
0.25	50	0.25	90	0.25	130
0.50	73	0.50	115	0.50	182
1.00	110	1.00	148	1.00	260
2.25	175	2.25	180	2.25	390
4.00	230	4.00	200	4.00	505
6.25	280	6.25	215	6.25	590
9.00	315	9.00	225	9.00	635
12.25	350	12.25	237	12.25	662
16.00	380	16.00	243	16.00	682
20.25	400	20.25	252	20.25	695
25.00	415	25.00	258	25.00	705
36.00	440	36.00	270	36.00	720
49.00	460	49.00	275	49.00	730
120.00	495	120.00	292	120.00	755
240.00	520	240.00	305	240.00	770
580.00	550	580.00	315	580.00	782
1460.00	595	1440.00	333	1480.00	802

TABLE F-7 CONVENTIONAL CONSOLIDATION DATA

Sludge L-2-1 bag 1, initial water content 256%, wt. dry specimen 26.2 gms.
April 18, 1972

time min.	dial reading in. x 10^4	time min.	dial reading in. x 10^4	time min.	dial reading in. x 10^4
load .1 kg/cm^2		load .4 kg/cm^2		load 1.6 kg/cm^2	
0.00	0	0.00	0	0.00	0
0.10	120	0.10	45	0.10	60
0.25	170	0.25	75	0.25	90
0.50	215	0.50	110	0.50	128
1.00	280	1.00	155	1.00	180
2.25	590	2.25	230	2.25	255
4.00	510	4.00	293	4.00	315
6.25	630	6.25	335	6.25	355
9.00	730	9.00	370	9.00	382
12.25	820	12.25	395	12.25	400
16.00	895	16.00	412	16.00	410
20.25	945	20.25	430	20.25	420
25.00	985	25.00	443	25.00	430
36.00	1030	36.00	465	36.00	445
49.00	1055	49.00	475	49.00	455
120.00	1105	120.00	515	120.00	480
240.00	1140	240.00	535	240.00	500
580.00	1170	580.00	557	580.00	518
1430.00	1210	1470.00	645	1480	540
load .2 kg/cm^2		load .8 kg/cm^2		load 3.2 kg/cm^2	
0.00	0	0.00	0	0.00	0
0.10	43	0.10	60	0.10	75
0.25	70	0.25	93	0.25	115
0.50	100	0.50	133	0.50	162
1.00	140	1.00	188	1.00	230
2.25	210	2.25	275	2.25	330
4.00	265	4.00	350	4.00	395
6.25	312	6.25	443	6.25	440
9.00	352	9.00	493	9.00	470
12.25	383	12.25	515	12.25	495
16.00	405	14.00	535	16.00	512
20.35	422	20.25	545	20.25	525
25.00	440	25.00	553	25.00	530
36.00	458	36.00	563	36.00	545
49.00	472	49.00	567	49.00	552
120.00	515	120.00	572	120.00	572
240.00	540	240.00	578	240.00	590
580.00	570	580.00	581	580.00	608
1450.00	595	1530.00	600	1445.00	620

TABLE F-8 BISHOP CONSOLIDATION DATA

Sludge U-3-10, initial water content 283%, wt. dry specimen 18.1 gms.
April 29, 1972

time min.	dial reading in. x 10^4	time min.	dial reading in. x 10^4	time min.	dial reading in. x 10^4
load .1 kg/cm^2		load .4 kg/cm^2		load 1.6 kg/cm^2	
0.00	0	0.00	0	0.00	0
0.10	220	0.10	55	0.10	65
0.25	270	0.25	80	0.25	95
0.50	330	0.50	110	0.50	132
1.00	420	1.00	155	1.00	182
2.25	560	2.25	225	2.25	255
4.00	670	4.00	275	4.00	315
6.25	745	6.25	315	6.25	365
9.00	800	9.00	345	9.00	395
12.25	840	12.25	365	12.25	420
16.00	860	16.00	385	16.00	442
20.25	875	20.25	400	20.25	458
25.00	885	25.00	410	25.00	470
36.00	905	36.00	435	36.00	490
49.00	920	49.00	450	49.00	505
120.00	950	120.00	495	120.00	545
240.00	975	240.00	525	240.00	570
580.00	1010	580.00	565	580.00	600
1440.00	1045	1460.00	600	1420.00	630
load .2 kg/cm^2		load .8 kg/cm^2		load 3.2 kg/cm^2	
0.00	0	0.00	0	0.00	0
0.10	45	0.10	60	0.10	55
0.25	70	0.25	95	0.25	85
0.50	100	0.50	130	0.50	120
1.00	135	1.00	180	1.00	165
2.25	195	2.25	258	2.25	232
4.00	235	4.00	318	4.00	288
6.25	270	6.25	365	6.25	332
9.00	295	9.00	402	9.00	362
12.25	315	12.25	430	12.25	388
16.00	330	16.00	450	16.00	405
20.25	345	20.25	468	20.25	420
25.00	355	25.00	480	25.00	430
36.00	370	36.00	502	36.00	450
49.00	385	49.00	520	49.00	465
120.00	425	120.00	560	120.00	505
242.00	460	240.00	590	240.00	528
580.00	500	580.00	625	580.00	548
1415.00	535	1450.00	660	1440.00	575

TABLE F-9 BISHOP CONSOLIDATION DATA

Sludge U-3-12, initial water content 278%, wt. dry specimen 18.7 gms.
May 16, 1972

time min.	dial reading in. x 10^4	time min.	dial reading in. x 10^4	time min.	dial reading in. x 10^4
load .1 kg/cm^2		load .4 kg/cm^2		load 1.6 kg/cm^2	
0.00	0	0.00	0	0.00	0
0.10	130	0.10	40	0.10	62
0.25	190	0.25	62	0.25	93
0.50	262	0.50	90	0.50	130
1.00	365	1.00	130	1.00	178
2.25	540	2.25	193	2.25	252
4.00	675	4.00	240	4.00	312
6.25	775	6.25	275	6.25	355
9.00	835	9.00	298	9.00	390
12.25	870	12.25	320	12.25	412
16.00	890	16.00	338	16.00	433
20.25	910	20.25	355	20.25	450
25.00	920	25.00	362	25.00	462
36.00	945	36.00	385	36.00	483
49.00	955	49.00	405	49.00	495
120.00	980	120.00	440	120.00	535
240.00	1005	240.00	472	240.00	562
580.00	1040	580.00	515	580.00	590
1440.00	1070	1470.00	560	1490.00	622
load .2 kg/cm^2		load .8 kg/cm^2		load 3.2 kg/cm^2	
0.00	0	0.00	0	0.00	0
0.10	35	0.10	555	0.10	55
0.25	55	0.25	90	0.25	85
0.50	78	0.50	123	0.50	115
1.00	110	1.00	175	1.00	162
2.25	160	2.25	248	2.25	230
4.00	203	4.00	308	4.00	280
6.25	225	6.25	355	6.25	328
9.00	245	9.00	387	9.00	355
12.25	262	12.25	412	12.25	380
16.00	275	16.00	532	16.00	400
20.25	285	20.25	448	20.25	412
25.00	295	25.00	462	25.00	428
36.00	313	36.00	482	36.00	448
49.00	325	49.00	495	49.00	458
120.00	358	120.00	540	120.00	493
240.00	385	240.00	572	240.00	518
580.00	412	580.00	608	580.00	540
1440.00	450	1440.00	640	1480.00	570

TABLE F-10 BISHOP CONSOLIDATION DATA

Sludge L-2-2 bag 1, initial water content 274%, wt. dry specimen 19.0 gms.
May 24, 1972

time min.	dial reading in. x 10^4	time min.	dial reading in. x 10^4	time min.	dial reading in. x 10^4
load .1 kg/cm^2		load .4 kg/cm^2		load 1.6 kg/cm^2	
0.00	0	0.00	0	0.00	0
0.10	195	0.10	38	0.10	60
0.25	265	0.25	62	0.25	90
0.50	340	0.50	88	0.50	125
1.00	445	1.00	125	1.00	175
2.25	625	2.25	187	2.25	243
4.00	800	4.00	235	4.00	300
6.25	945	6.25	272	6.25	338
9.00	1050	9.00	298	9.00	370
12.25	1110	12.25	320	12.25	395
16.00	1150	16.00	340	16.00	405
20.25	1175	20.25	350	20.25	421
25.00	1190	25.00	365	25.00	432
36.00	1210	36.00	385	36.00	458
49.00	1220	49.00	400	49.00	468
120.00	1255	120.00	940	120.00	505
240.00	1270	240.00	470	240.00	528
580.00	1290	580.00	500	580.00	550
1440.00		1440.00	535	1530.00	580
load .2 kg/cm^2		load .8 kg/cm^2		load 3.2 kg/cm^2	
0.00	0	0.00	0	0.00	0
0.10	25	0.10	62	0.10	60
0.25	45	0.25	90	0.25	90
0.50	63	0.50	123	0.50	122
1.00	90	1.00	170	1.00	167
2.25	135	2.25	240	2.25	234
4.00	175	4.00	298	4.00	285
6.25	205	6.25	342	6.25	327
9.00	225	9.00	372	9.00	353
12.25	242	12.25	400	12.25	373
16.00	255	16.00	418	16.00	390
20.25	263	20.25	432	20.25	400
25.00	273	25.00	448	25.00	412
36.00	285	36.00	470	36.00	435
49.00	300	49.00	485	49.00	450
120.00	330	120.00	522	120.00	478
240.00	355	240.00	550	240.00	498
580.00	383	580.00	578	580.00	520
1440.00	420	1440.00	610	1510.00	545

TABLE F-11 BISHOP CONSOLIDATION DATA

Sludge L-2-3 bag 1, initial water content 263%, wt. dry speciment19.4 gms.
June 5, 1972

time min.	dial reading in. x 10^4	time min.	dial reading in. x 10^4	time min.	dial reading in. x 10^4
load .1 kg/cm^2		load .4 kg/cm^2		load 1.6 kg/cm^2	
0.00	0	0.00	0	0.00	0
0.10	140	0.10	45	0.10	64
0.25	203	0.25	70	0.25	92
0.50	232	0.50	98	0.50	123
1.00	372	1.00	136	1.00	170
2.25	545	2.25	198	2.25	238
4.00	695	4.00	244	4.00	292
6.25	818	6.25	280	6.25	337
9.00	890	9.00	305	9.00	363
12.25	940	12.25	322	12.25	390
16.00	970	16.00	338	16.00	406
20.25	990	20.25	352	20.25	420
25.00	1042	25.00	363	25.00	430
36.00	1020	36.00	385	36.00	453
49.00	1032	49.00	---	49.00	480
120.00	1058	120.00	433	120.00	503
240.00	1075	240.00	463	240.00	525
580.00	1095	580.00	492	580.00	548
1440.00	1125	1400.00	522	1490.00	580
load .2 kg/cm^2		load .8 kg/cm^2		load 3.2 kg cm^2	
0.00	0	0.00	0	0.00	0
0.10	30	0.10	63	0.10	60
0.25	45	0.25	93	0.25	85
0.50	63	0.50	127	0.50	116
1.00	90	1.00	176	1.00	160
2.25	133	2.25	248	2.25	225
4.00	165	4.00	304	4.00	280
6.25	190	6.25	347	6.25	320
9.00	208	9.00	375	9.00	348
12.25	222	12.25	400	12.25	370
16.00	233	16.00	418	16.00	391
20.25	243	20.25	432	20.25	405
25.00	251	25.00	443	25.00	4.8
36.00	270	36.00	463	36.00	435
49.00	278	49.00	475	49.00	468
120.00	308	120.00	513	120.00	485
240.00	328	240.00	538	240.00	507
580.00	358	580.00	565	580.00	534
1460.00	390	1570.00	590	1270.00	560

TABLE F-12 BISHOP CONSOLIDATION DATA

Sludge U-5-2, initial water content 263%, wt. dry specimen 19.6 gms.
June 19, 1972

time min.	dial reading in. x 10^4	time min.	dial reading in. x 10^4	time min.	dial reading in. x 10^4
load .1 kg/cm^2		load .4 kg/cm^2		load 1.6 kg/cm^2	
0.00	0	0.00	0	0.00	0
0.10	89	0.10	50	0.10	65
0.25	150	0.25	75	0.25	100
0.50	210	0.50	105	0.50	135
1.00	290	1.00	150	1.00	187
2.25	420	2.25	215	2.25	265
4.00	527	4.00	265	4.00	325
6.25	595	6.25	303	6.25	377
9.00	630	9.00	330	9.00	413
12.25	660	12.25	350	12.25	442
16.00	678	16.00	366	16.00	463
20.25	690	20.25	382	20.25	480
25.00	700	25.00	393	25.00	495
36.00	715	36.00	418	36.00	520
49.00	725	49.00	428	49.00	535
120.00	753	120.00	473	120.00	575
240.00	773	240.00	502	240.00	600
580.00	798	580.00	538	580.00	633
1440.00	830	1430.00	580	1470.00	670

load .2 kg/cm^2		load .8 kg/cm^2		load .8 kg/cm^2	
0.00	0	0.00	0	0.00	0
0.10	35	0.10	64	1095.00	67
0.25	53	0.25	96		
0.50	77	0.50	134	load .1 kg/cm^2	
1.00	108	1.00	187		
2.25	156	2.25	265	0.00	0
4.00	192	4.00	328	245.00	377
6.25	220	6.25	375		
9.00	235	9.00	410		
12.25	253	12.25	438		
16.00	265	16.00	460		
20.25	272	20.25	474		
25.00	283	25.00	490		
36.00	295	36.00	510		
49.00	312	49.00	523		
120.00	342	120.00	570		
240.00	365	240.00	595		
580.00	398	580.00	628		
1430.00	435	1470.00	670		

TABLE F-13 SINGLE INCREMENT CONSOLIDATION DATA

Sludge U-3-4
initial water content 302%
initial void ratio 5.64
wt. dry specimen 23.1 gms.

load 0-.24 kg/cm^2 3/23/72

time min.	dial reading in. x 10^4
0.00	0
0.10	190
0.25	273
0.50	378
1.00	520
2.25	776
4.00	1018
6.25	1200
9.00	1328
12.25	1397
16.00	1448
20.25	1472
25.00	1490
36.00	1510
49.00	1518
120.00	1540
240.00	1558
580.00	1570
1312.00	1597

Sludge U-3-6
initial water content ?
initial void ratio 5.48
wt. dry specimen 23.7 gms.

load 0-.24 kg/cm^2 3/25/72

time min.	dial reading in. x 10^4
0.00	0
0.10	220
0.25	330
0.50	455
1.00	630
2.25	930
4.00	1185
6.25	1358
9.00	1470
12.25	1520
16.00	1550
20.25	1570
25.00	1585
36.00	1605
49.00	1620
120.00	1648
240.00	1678
580.00	1705
1440.00	1745

Sludge U-3-5
initial water content 291%
initial void ratio 5.40
wt. dry specimen 24.0 gms.

load 0-.24 kg/cm^2 3/24/72

0.00	0
0.10	265
0.25	380
0.50	500
1.00	680
2.25	993
4.00	1258
6.25	1448
9.00	1550
12.25	1610
16.00	1640
20.25	1660
25.00	1673
36.00	1705
49.00	1710
120.00	1737
240.00	1755
580.00	1783
1450.00	1805

TABLE F-14 SINGLE INCREMENT BISHOP CONSOLIDATION DATA

Sludge U-4-3
initial water content 246%
initial void ratio 4.43
wt. dry specimen 20.7 gms.
load 0-.24 kg/cm^2 7/5/72

time min.	dial reading in. x 10^4
0.00	0
0.10	200
0.25	290
0.50	390
1.00	530
2.25	755
4.00	940
6.25	1065
9.00	1135
12.25	1180
16.00	1208
20.25	1230
25.00	1245
36.00	1262
49.00	1277
120.00	1324
240.00	1340
580.00	1380
1630.00	1425

Sludge L-2-4
initial water content 266%
initial void ratio 5.46
wt. dry specimen 19.3 gms.
load 0-.63 kg/cm^2 7/26/72

time min.	dial reading in. x 10^4
0.00	0
0.10	350
0.25	490
0.30	670
1.00	930
2.25	1370
4.00	1750
6.25	2000
9.00	2160
12.25	2250
16.00	2295
20.25	2320
25.00	2340
36.00	2360
49.00	2380
120.00	2415
240.00	2440
580.00	2470
1510.00	2510

Sludge U-2-1
initial water content 216%
initial void ratio 4.38
wt. dry specimen 23.1 gms.
load 0-.24 kg/cm^2 7/11/72

0.00	0
0.10	190
0.25	280
0.50	380
1.00	520
2.25	760
4.00	945
6.25	1060
9.00	1120
12.25	1160
16.00	1173
20.25	1190
25.00	1200
36.00	1210
49.00	1225
120.00	1250
240.00	1275
580.00	1300
1500.00	1330

Sludge U-3-11
initial water content 284%
initial void ratio 5.25
wt. dry specimen 18.4 gms.
load 0-.24 kg/cm^2 5/8/72

0.00	0
0.10	250
0.25	370
0.50	500
1.00	690
2.25	990
4.00	1213
6.25	1360
9.00	1425
12.25	1475
16.00	1500
20.25	1520
25.00	1530
36.00	1555
49.00	1565
120.00	1590
240.00	1625
580.00	1655
1560.00	1659
2520.00	1715
4207.00	1745
5626.00	1765
6646.00	1785
9260.00	1805

Appendix G-1. WELL LEACHATE (WL) DATA

Date*of analysis	Day of project	COD (mg/ℓ)	BOD (mg/ℓ)	pH	Turbidity (JTU)	Spec. Cond. (μmho/cm)	TS (mg/ℓ)	DS (mg/ℓ)	SS (mg/ℓ)	Color (color units)
2/10/72										
2/18/72	3	2273								
2/21/72	6	3328					6185	2445	3740	
2/28/72	13		2662	7.6	150	3050	4334	3276	1058	
3/9/72	23	2769	1790							
3/20/72	34	2880		7.9	65	3000	4330	3800	530	
3/24/72	38	3267								
3/6/72										
3/10/72	24	1573	610							
3/16/72	30		300	7.2	225	1800	2375	1895	480	
3/20/72	34	1088								
3/22/72	36									
3/24/72	38	1000		7.9	45	1800	2520	1310	1210	
3/24/72	38	300					2740	1360	1380	
3/29/72	43		508	6.8	94	1700	1695	1535	160	
4/3/72	48			6.6	70	1700				
4/7/72	72	460		6.9	87	1700	1840	1480	360	
4/10/72	55			7.1	58	1600				
4/13/72	58	435		7.1	88	1700	1640	1630	10	
4/10/72										
4/12/72	58									
4/14/72	59	320	296	6.6						48
4/17/72	62	489								
4/21/72	66	436	301	6.9	80	1430				
4/24/72	69			7.5	93	1300	1220	1220		
4/25/72	70	420		7.3	86	1400				
4/27/72	72			7.4	57	1400	1470	1220	250	
4/24/72	69		300	7.5	40	1330				
4/28/72	73	708								
5/12/72	87		276	6.7	80	1370	1460	1360	100	
7/27/72	163	109	166							
5/3/72										
5/8/72	83	900								

*Underlined dates are date of shipment for leachate

Appendix G-1. WELL LEACHATE (WL) (cont.)

Date*of analysis	Day of project	COD (mg/ℓ)	BOD (mg/ℓ)	pH	Turbidity (JTU)	Spec. Cond. (μmho/cm)	TS (mg/ℓ)	DS (mg/ℓ)	SS (mg/ℓ)	Color (color units)
5/10/72	85	860	647							
5/15/72	90	904					2280	1510	770	
5/16/72	91	1132	560							
7/27/72	163	591	386							
6/2/72										
6/6/72	112					1760				
6/13/72	119	1188								
7/27/71	163	1013	706							
6/13/72										
6/15/72	121	1461								
6/16/72	122				60	1950				
6/20/72	126	1313								
7/12/72	148			6.9		2100				
7/27/72	163	1128	958							
6/20/72										
6/23/72	129	1559								
7/7/72	143	1436								
7/6/72										
7/12/72	148	1355		6.4		2200				
7/18/72	154	1315								
7/19/72	155						2760	1990	770	
7/27/72	163	1148	1007							
7/13/72										
7/18/72	154	1380								
7/19/72	155						2590	1950	640	
7/24/72	160	1301								
7/27/72	163	1198	983							

*Underlined dates are date of shipment for leachate

Appendix G-2. PIPE LEACHATE (PL) DATA

Date*of analysis	Day of project	COD (mg/ℓ)	BOD (mg/ℓ)	pH	Turbidity (JTU)	Spec. Cond. (μmho/cm)	TS (mg/ℓ)	DS (mg/ℓ)	SS (mg/ℓ)	Color (color units)
2/21/72	6	4160		7.8	36	4000	5490	5296	194	
2/28/72	13		3675							
3/9/72	23	3524	3426	7.9	36	4000	5550	5180	370	
3/20/72	34	4352								
3/24/72	38	3867								
3/6/72										
3/10/72	24	3650	3800	7.9	40	3900	5195	5115	80	
3/20/72	34	4032	2687							
3/22/72	36			7.9	34	4000	5070	4610	460	
3/24/72	38	3333		8.1	30	3800	4810	4330	480	
3/24/72	38	3200		8.0	43	3800	4990	4970	20	
3/29/72	43		2800	8.0	30	3800				
4/3/72	48			8.0	27	3800	4820	4620	200	
4/7/72	52	2400		8.0	25	3600				
4/10/72	55			8.0	29	3750	4650	4190	460	
4/13/72	58		2560							
7/27/72	163	2444	1993							
4/10/72										
4/13/72	58			7.6						91
4/14/72	59	1984	1586							
4/17/72	62			7.8	20	2900				
4/21/72	66	2147	1496	8.0	21	2650	3150	2750	400	
4/24/72	69			8.0	24	2870				
4/25/72	70	2106		8.1	25	2800	3320	3030	290	
4/27/72	72			8.0	28	2440				
6/15/72	121	1500								
6/20/72	126	1509	1358							
7/27/72	163	836	263							
4/24/72										
4/28/72	73	3616		7.5	23	3500	4260	4104	156	
5/5/72	80	2560								
5/12/72	87		1780							

*Underlined dates are date of shipment for leachate

Appendix G-2. PIPE LEACHATE (PL) (cont.)

Date*of analysis	Day of project	COD (mg/ℓ)	BOD (mg/ℓ)	pH	Turbidity (JTU)	Spec. Cond. (µmho/cm)	TS (mg/ℓ)	DS (mg/ℓ)	SS (mg/ℓ)	Color (color units)
5/3/72										
5/8/72	83	4300								
5/10/72	85	4400	3337							
5/15/72	90	4320					6450	6030	830	
5/16/72	91	4620								
6/6/72	112					4250				
6/13/72	119	3840								

*Underlined dates are date of shipment for leachate

Appendix H-1. ORGANIC LOAM COLUMN - WELL LEACHATE (WT)

Date of analysis	Day of project	COD (mg/ℓ)	BOD (mg/ℓ)	pH	Turbidity (JTU)	Spec. Cond. (μmho/cm)	TS (mg/ℓ)	DS (mg/ℓ)	SS (mg/ℓ)	Color (color units)
2/22/72	7	106		8.4	.9	404				200
2/28/72	13	42		8.5	1.0	460	410			
3/2/72	16			8.4	1.0	460	390			
3/6/72	20	115	16	8.6	2.0	460	430	430	0	
3/10/72	24		2							
3/17/72	31	115		8.4	1.0	470	490	480	10	
3/20/72	34			8.6	1.2					
3/21/72	35						510	450	60	
3/22/72	36	360				480				
3/24/72	38			8.7	1.0	450	440	320	120	
3/29/72	43			8.7	1.0	460				
4/3/72	48	116		8.7	1.5	450	420			
4/7/72	52			8.6	1.3	520				
4/10/72	55	150		8.7	2.0	490	360	320	40	
4/21/72	66			8.6	1.2	530	400	400	0	
4/24/72	69			8.5	1.3	520				
4/27/72	72	192	7	8.5	1.7	570				
4/28/72	73		4	8.6	1.3					
5/5/72	80						1120	530	630	
5/10/72	85	80								
5/15/72	90	121								
5/16/72	91	171								
6/6/72	112					720				
6/13/72	119	128								
6/16/72	122				1.5	740				
6/20/72	126	125								
7/7/72	143	131								
7/12/72	148			8.5		750				
7/19/72	155						930	900	30	
7/21/72	157	144								
7/27/72	163	125	14							
7/28/72	164			8.6	1.1					235

Appendix H-2. SAND COLUMN - PIPE LEACHATE (PS)

Date of analysis	Day of project	COD (mg/ℓ)	BOD (mg/ℓ)	pH	Turbidity (JTU)	Spec. Cond. (µmho/cm)	TS (mg/ℓ)	DS (mg/ℓ)	SS (mg/ℓ)	Color (color units)
2/22/72	7	10		7.1	.7	180				0
2/28/72	13			6.6	1.3	800	1010			
3/2/72	16			7.4	1.5	640	725			
3/6/72	20	438	226	8.0	2.0	520		630		
3/10/72	24		166							
3/17/72	31	192		7.6	20.0	590	570	520	50	
3/20/72	34			8.1	21.0					
3/21/72	35						700	650	50	
3/22/72	36	373				720				
3/24/72	38			8.4	13.0	960	990			
3/29/72	43			8.8	10.0	1380				
4/3/72	48	256		9.0	3.6	1600	1600	1440	160	
4/7/72	52			8.9	3.0	1800				
4/10/72	55	246		9.0	2.1	1875	1620	1430	190	
4/17/72	62	260		9.0	2.0	1840				
4/21/72	66			9.1	2.0	1870	1750	1400	350	
4/24/72	69			9.1	1.9	1900				
4/25/72	70	188		8.9	1.9	1460	1580	1300	280	
4/27/72	72		40	8.9	1.9	1440	1720	1580	140	
4/28/72	73	212	8	8.9	2.1	1700				
5/9/72	84	208								
5/10/72	85	152								
5/15/72	90	293					1970			
5/16/72	91	263	6							
6/6/72	112					2140				
6/13/72	119	212								
6/16/72	122				1.5	2250				
6/20/72	126	188								
7/7/72	143	171								
7/12/72	148			9.4		2650				
7/19/72	155						2270	2270		
7/21/72	157	176								
7/27/72	163	135	10							
7/28/72	164	135		9.4	1.1					200

Appendix H-3. ORGANIC LOAM COLUMN - AEROBIC - PIPE LEACHATE (PTA)

Date of analysis	Day of project	COD (mg/ℓ)	BOD (mg/ℓ)	pH	Turbidity (JTU)	Spec. Cond. (μmho/cm)	TS (mg/ℓ)	DS (mg/ℓ)	SS (mg/ℓ)	Color (color units)
2/22/72	7	106		8.5	1.5	402				161
2/28/72	13	46		8.5	1.0	475	435			
3/2/72	16			8.4	1.0	500	390			
3/6/72	20	96		8.7	1.0	470		395		
3/10/72	24		4							
3/17/72	31	111		8.6	1.0	470	450	450	0	
3/20/72	34			8.6	2.0					
3/21/72	35						550	450	100	
3/22/72	36	323				480				
3/24/72	38			8.7	1.5	470	400	330	70	
3/29/72	43			8.7	1.4	480				
4/3/72	48	76		8.8	1.4	480	420			
4/7/72	52			8.7	2.5	520				
4/10/72	55			8.7	3.2	545	450	400	50	
4/21/72	66			8.6	1.3	540	410	410	0	
4/24/72	69			8.7	1.5	555				
4/25/72	70	120		8.7	1.9	570	550	540	10	
4/27/72	72		12	8.5	1.5	560				
4/28/72	73	116	2	8.6	1.5	620	750	750	0	
5/2/72	77									
5/10/72	85	45								
5/15/72	90	104								
5/16/72	91		10							
6/6/72	112					1100				
6/13/72	119	128								
6/16/72	122				2.0	1120				
6/20/72	126	122								
7/12/72	148			8.6		1120				
7/19/72	155						1500	1500	0	
7/21/72	157	113								
7/27/72	163	133	15							
7/28/72	164			8.6	0.9					178

Appendix H-4. ORGANIC LOAM COLUMN - ANAEROBIC - PIPE LEACHATE (PTAN)

Date of analysis	Day of project	COD (mg/ℓ)	BOD (mg/ℓ)	pH	Turbidity (JTU)	Spec. Cond. (μmho/cm)	TS (mg/ℓ)	DS (mg/ℓ)	SS mg/ℓ)	Color (color units)
2/22/72	7	106		8.4	2.0	705				135
2/28/72	13	43		8.4	3.0	575	540			
3/2/72	16			8.4	1.5	610	450			
3/6/72	20	69		8.4	2.0	570		495		
3/10/72	24		2							
3/17/72	31	104		8.5	2.0	580	580	510	70	
3/20/72	34			8.4	1.8					
3/21/72	35						630	550	80	
3/22/72	36	276				590				
3/24/72	38			8.5	2.0	580	500	490	10	
3/29/72	43			8.6	2.0	500				
4/3/72	48	40		8.8	2.0	440	340			
4/7/72	52			7.2	11.0	1080				
4/10/72	55	384		7.4	20.0	1050	1110	740	370	
4/17/72	62	596		8.0	16.0	990				
4/21/72	66			8.0	25.0	940	1150	800	350	
4/24/72	69			7.8	28.0	1080				
4/25/72	70	952		8.0	36.0	1180	1900	1150	750	
4/26/72	71	936								
4/27/72	72			7.5	34.0	1340	2320	1600	720	
4/28/72	73		840	7.5	39.0	1480				
5/2/72	77									
5/10/72	85	1066								
5/15/72	90						2870	1970	1520	
5/16/72	91	1354	570							
6/6/72	112					1310				
6/13/72	119	272								
6/16/72	122				10.0	1150				
6/20/72	126	250								
7/7/72	143	224								
7/12/72	148			8.5		1500				
7/19/72	155						1850	1510	340	
7/21/72	157	257								
7/27/72	163	243	115							
7/28/72				8.9	9.0					244

Appendix H-5. CLAY COLUMN - PIPE LEACHATE (PC)

Date of analysis	Day of project	COD (mg/ℓ)	BOD (mg/ℓ)	pH	Turbidity (JTU)	Spec. Cond. (μmho/cm)	TS (mg/ℓ)	DS (mg/ℓ)	SS (mg/ℓ)	Color (color units)
2/22/72	7	96		8.2	21	500				0
2/28/72	13	15		8.4	30	450	550			
3/2/72	16			8.0	22	475	480			
3/6/72	20	23		8.3	20	430		540		
3/10/72	24		.7							
3/17/72	31	46		8.0	5	580	580	520	60	
3/20/72	34			8.1	15					
3/21/72	35						680	500	180	
3/22/72	36	242				610				
3/24/72	38			8.2	6	740	600	470	30	
3/29/72	43			8.4	4	610				
4/3/72	48	320		7.4	10	850	980	650	330	
4/7/72	52			7.3	24	1100				
4/10/72	55	472		7.9	24	1000	1060	900	160	
4/17/72	62	340		8.0	23	1020				
4/21/72	66			7.9	15	890	800	600	200	
4/24/72	69			7.8	14	880				
4/25/72	70			7.9	16	970	900	800	100	
4/27/72	72		12	7.9	23	820				
4/28/72	73	480	2	8.2	22	1030	1240	904	336	
5/2/72	77									
5/15/72	90						2380	1010	680	
5/16/72	91	105								
6/6/72	112					880				
6/13/72	119	80								
6/16/72	122				2.5	810				
6/20/72	126	76								
7/7/72	143	65								
7/12/72	148			8.5		770				
7/19/72	155						1050	1030	20	
7/24/72	160	70								
7/27/72	163	68	8							
7/28/72	164			8.5	4.5					26

Appendix H-6. ORGANIC LOAM COLUMN - DOUBLE DOSE - PIPE LEACHATE (DPT)

Date of analysis	Day of project	COD (mg/ℓ)	BOD (mg/ℓ)	pH	Turbidity (JTU)	Spec. Cond. (µmho/cm)	TS (mg/ℓ)	DS (mg/ℓ)	SS (mg/ℓ)	Color (color units)
4/21/72	66	566		7.9	6.7	2140	2390	1980	410	850
4/24/72	69			7.8	3.7	1730				
4/25/72	70	312		8.1	3.5	1780	2130	1900	230	
4/27/72	72	404	42	7.4	4.0	1580				
4/28/72	73		9	7.7	3.5	1940	2384	2352	32	
5/5/72	80	176								
5/8/72	83	200								
5/10/72	85	285								
5/15/72	90	345					2300	1750	550	
5/16/72	91	374	12							
6/6/72	112					1750				
6/13/72	119	892								
6/16/72	122				30.0	2350				
6/20/72	126	510								
7/7/72	143	275								
7/12/72	148			8.2		2700				
7/19/72	155						2250	1900	350	
7/21/72	157	193								
7/27/72	163	193	38							
7/28/72	164			8.4	21.0					274

APPENDIX I.

COMPUTER PROGRAM FOR LOAD INCREASING LINEARLY WITH TIME FOLLOWED BY AN INSTANTANEOUS SURCHARGE APPLICATION

```
      PROGRAM SLOPOE ( INPUT•OUTPUT)
      DIMENSION P(20•200)• TP(20•200)• U1(200)• U2(200)• PP(200)• T(200)
     1• TM1(200)•TM2(200)
C
C     EN = CONTROL CARD (IF=1.0 PROGRAM TERMINATES)
C     NCV = COFF. OF CONSOL. X 10**3 IN.**2/MIN. (CV1) INTEGER FORM
C     NH = AVG. THICKNESS OF LAYER (IN.) DURING LINEAR LOADING
C     NDT = TOTAL TIME OF LINEAR LOAD IN MIN.
C     I = INCREMENTS OF TIME SOLVED AFTER SURCHARGE APPLICATION
C     CV1 = COEF. OF CONSOL. OF LAYER DURING LINEAR LOADING
C     GAM1 TO GAM3 = UNIT WT. OF MATL≠S USED IN LINEAR LOAD SEGMENT
C     GAM4 = UNIT WT. OF SURCHARGE MAT≠L
C     H1 TO H3 = HT. OF MAT≠LS IN LINEAR LOAD SEGMENT
C     H4 = HT. OF SURCHARGE MAT≠L
C     CV2 = COEF. OF CONSOL. OF LAYER AFTER SURCHARGE LOADING
C     P(1•M) TO P(9•M) = INITIAL VALUES OF PORE PRESSURE
C     ULTS = ULTIMATE PRIMARY SETTLEMENT UNDER TOTAL LOAD (IN.)
C     HN1 = INITIAL THICKNESS OF LAYER (IN.)
C
   50 READ 3• EN
    3 FORMAT (F10.3)
      IF(EN.EQ.1.0)300•40
   40 READ 2•NCV•NH•NDT•I•CV1•GAM1•GAM2•GAM3•GAM4
    2 FORMAT(4I5•5F10.3)
      READ4•H1•H2•H3•H4•CV2
    4 FORMAT(5F10.3)
      M = 1
      READ 5• (P(L•M)•L=1•9)
    5 FORMAT(9F8.2)
      READ 69•ULTS•HN1
   69 FORMAT(2F10.0)
C
C     DETERMINE NO. OF INCREMENTS FOR STEP FUNCTION DETERMINED BY THE
C     VALUES OF CV•DT•AND H
C
      NXDT = (4*NCV*NDT*96)/(1000*NH*NH)
      XDT = NXDT
      HN=NH
      Y = GAM1*H1+GAM2*H2+GAM3*H3
      Z = GAM4*H4
      X = Y/XDT
C
C     SET BOUNDARY PORE PRESSURES = 0.00 FOR ALL TIMES
C
      DO 7 N = 1•200
      P(1•N) = 0.00
      P(9•N) = 0.00
      TP(1•N) = 0.00
      TP(9•N) = 0.00
    7 CONTINUE
```

```
C
C     CALCULATE PORE PRESSURES GENERATED BY UNIT INCREASES IN STEP LOAD
C     (LINEAR LOADING) FOR EACH TIME INCREMENT
C
      LXDT = NXDT-1
      DO 6 K = 1,LXDT
      DO 9 L = 2,8
      P(L,K+1) = P(L,K)*2./3.+(P((L+1),K)+P((L-1),K))*1./6.+1.00
    9 CONTINUE
    6 CONTINUE
C
C     CALCULATE ACTUAL PORE PRESSURES GENERATED AT END OF LINEAR LOADING
C     ( IN PSF )
C
      DO 10 L = 1,9
      PP(L) = X*P(L,NXDT)
   10 CONTINUE
C
C     CALCULATE PERCENT CONSOLIDATION UNDER THE EXISTING APPLIED STRESS
C     FOR THE LINEAR LOADING (USING TRAPEZOIDAL RULE)
C
      SUM = 0.00
      XT = 0.00
      DO 11 K = 1,NXDT
      XT = XT+1.00
      DO 12 L = 1,8
      R = ((2.*XT)-P(L,K)-P((L+1),K))/(16.0*XT)
      SUM = SUM+R
   12 CONTINUE
      U1(K) = SUM*100.0
      SUM = 0.00
   11 CONTINUE
C
C     SET INITIAL VALUES OF PORE PRESSURE FOR SURCHARGE INCREMENTAL
C     LOADING, HERE Z (OR TP(L,1)) COULD BE MADE EQUAL TO FIELD VALUES
C
      DO 13 L = 2,8
      TP(L,1) = PP(L)+Z
   13 CONTINUE
C
C     CALCULATE PORE PRESSURES, PERCENT CONSOLIDATION, AFTER SURCHARGE
C     APPLICATION
C
      J=I-1
      DO 15 K= 1,J
      DO 17 L = 2,8
      TP(L,K+1) = TP(L,K)*2./3.+(TP((L+1),K)+TP((L-1),K))*1./6.
   17 CONTINUE
   15 CONTINUE
      DSUM = 0.0
      DO 20 K = 1,I
      DO 21 L = 1,8
      D = ((Y+Z)*2.-TP(L,K)-TP((L+1),K))/(16.0*(Y+Z))
      DSUM = DSUM+D
   21 CONTINUE
      U2(K) = DSUM*100.
      DSUM = 0.00
   20 CONTINUE
      T(1) = 0.00
      TM1(1)=0.0
      TM2(1)=0.00
      DO 30 N = 2,200
      T(N) = T(N-1)+1./96.
      TM1(N)=(T(N)*HN*HN)/(4.0*CV1*1440.)
   30 CONTINUE
      DO 29 N=2,I
      H=HN1-(U2(N)+U2(N-1))/200.*ULTS
      TM2(N)=(T(N)*H*H)/(4.0*CV2*1440.)
   29 CONTINUE
C
C     PRINT OUT VALUES
C
      PRINT 39,NXDT,CV1,NH,X,Y,Z
   39 FORMAT(*1*,*NXDT = *,I3,2X,*CV1 = *,F5.3,1X,*SQ. IN./MIN.*,2X,*NH
     1= *,I3,1X,*IN.*,2X,*X = *,F5.2,1X,*PSF/INCREMENT*,2X,*Y = *,F6.1,1
     2X,*PSF(LINEAR STRESS)*,2X,*Z = *,F5.1,1X,*PSF(SURCHARGE)*)
      PRINT 31
   31 FORMAT(*0*,13X,*PORE PRESSURES, PERCENT CONSOLIDATION, DUE TO LINE
     1AR APPLIED STRESS*)
      PRINT 33
   33 FORMAT(*0*,18X,*H=0*,5X,*H/8*,5X,*H/4*,5X,*3H/8*,4X,*H/2*,5X,
     1*5H/8*,4X,*3H/4*,4X,*7H/8*,5X,*H*,8X,*U*,7X,*TIME,DAYS*)
      DO 100 K = 1,NXDT
      PRINT 35,K,T(K),(P(L,K),L = 1,9),U1(K),TM1(K)
   35 FORMAT(*0*,I3,1X,*T = *,F7.5,9F8.2,F8.1,F8.1)
  100 CONTINUE
      PRINT 41,(PP(L),L = 1,9),U1(NXDT)
   41 FORMAT(*0*,*PP ( IN PSF )*,1X,10F8.1)
      PRINT 80,CV2
   80 FORMAT(*0*,15X,*PORE PRESSURES, PERCENT CONSOLIDATION, DUE TO SURC
     1HARGE AND LINEAR LOAD*,5X,*CV2 = *,F5.3,1X,*SQ. IN. PER MIN.*)
      PRINT 33
      DO 101 K = 1,I
      PRINT 45,K,T(K),(TP(L,K),L = 1,9),U2(K),TM2(K)
   45 FORMAT(*0*,I3,1X,*T = *,F7.5,9F8.0,F8.1,F8.1)
  101 CONTINUE
      GO TO 50
  300 CONTINUE
      END
```